Effect of Surfactants on Oil Recovery in Water-Alternating-Gas Enhanced Oil Recovery An Investigation Into Important Factors

by

A thesis submitted to the

School of Graduate Studies

in partial fulfillment of the requirements for the degree of

Master of Engineering

The Faculty of Engineering and Applied Science

Memorial University of Newfoundland

May, 2016

St. John's Newfoundland and Labrador

ABSTRACT

Enhanced oil recovery techniques are used after primary (pressure depletion) and secondary (waterflooding) technique to increase oil recovery. One method of enhanced oil recovery uses surfactants. Surfactants have the potential to increase oil recovery through interfacial tension reduction and the possibility of creating foam. This investigation focuses on the surfactant assisted water-alternating-gas technique in a glass micromodel, investigating factors such as water-alternating-gas ratio (1:1, 1:1.5, and 1:2), surfactant concentration (one times CMC, 5.5 times CMC, and ten times CMC), gas type (air and propane), and surfactant type (Triton X-100 and Iveysol 106), and observing responses of oil recovery, breakthrough time, and fluid flow. Oil recovery data suggested that individual effects of surfactant concentration and gas type, and interaction effects of WAG ratio-surfactant concentration, WAG ratio-gas type, WAG ratio-surfactant type, and gas type-surfactant type were significant. Breakthrough time data suggested that the individual effects of WAG ratio, gas type, and surfactant type were significant. Additional experiments investigating interfacial tension and viscosity showed that surfactant concentration reduced both interfacial tension and viscosity, with Triton X-100 having lower interfacial tension and viscosity than Iveysol 106.

ACKNOWLEDGEMENTS

I would like to thank my supervisors Dr. Lesley James and Dr. Thormod Johansen for their guidance and support throughout my masters program. Without their insight and guidance this work would not be possible.

I would also like to thank the staff of the Hibernia Enhanced Oil Recovery Research group, Mr. Edison Sripal, Ms. Kimberly Power, Mr. Shervin Ayazi, and Ms. Mahsa Moayedi, who provided assistance in designing, ordering, and assembling the experimental equipment. I would also like to thank my colleagues Maziyar Mahmoodi and Ayub Khezrnejad for their assistance in designing, assembling, and operating the experimental setup and for their assistance in designing a set of experiments.

I gratefully acknowledge the support of the Hibernia Management and Development Company Ltd. (HMDC), Chevron Canada, the Research and Development Corporation (RDC), the Natural Sciences and Engineering Research Council of Canada (NSERC), and the Canadian Foundation for Innovation (CFI).

I would like to express my thanks to the Research and Development Corporation (RDC), the Natural Sciences and Engineering Research Council of Canada (NSERC), and the School of Graduate Studies at Memorial University of Newfoundland for their financial aid in the form of scholarships throughout this research.

Table of Contents

List of Tables

List of Figures

List of Symbols, Nomenclature or Abbreviations

Symbol	Description	Units
C	Concentration of surfactant as a multiple of the CMC	
G	Gas type (air or propane)	
GOR	Gas-Oil Ratio	
N_C	Capillary Number	
$P_{Capillary}$	Capillary Pressure	N/m^2
PV	Pore Volume	cm^3
R_{Oil}	Oil Recovery	%
S	Surfactant type (Triton X-100 or Iveysol 106)	
W	WAG Ratio, volumetric ratio of liquid slug to gas slug	
WAG	Water-Alternating-Gas	
CMC	Critical Micelle Concentration	Grams/Liter
mL	MilliLiter	MilliLiters
ppm	Parts Per Million	
r	Pore Radius	Meters
$t_{breakthrough}$	Breakthrough Time	Seconds
$\Upsilon_{l/g}$	Interfacial Tension between the liquid and gas phase	N/m
$\Upsilon_{l/o}$	Interfacial Tension between the liquid and oil phase	N/m
$\Upsilon_{o/g}$	Interfacial Tension between the oil and gas phase	N/m
θ	Contact Angle	^{o}
μ	Viscosity	Pa s or cP
σ_1	Interfacial Tension between Solid and Phase 1	N/m
σ_2	Interfacial Tension between Solid and Phase 2	N/m
σ_{12}	Interfacial Tension between Phase 1 and Phase 2	N/m

List of Appendices

Chapter 1: Introduction

1.1. Research Content

The object of reservoir engineering is to extract the greatest volume of hydrocarbons from the reservoir as is economically viable. Fluids in a reservoir are under pressure, therefore at the beginning of production, the expansion of the fluids when exposed to a decrease in pressure from the reservoir to the well bore is enough for many light oils to begin to flow, and this is termed primary recovery. Once the reservoir pressure is depleted, flow may decrease or cease entirely. Primary recovery is responsible for recovering approximately 25% of the oil originally in place for light oils, 5% for heavy oils, and 0% for very heavy oil sands oils (Thomas 2007). Secondary recovery consists of injecting water or gas into the reservoir to increase the pressure and extract additional oil. Secondary recovery is responsible for recovering an additional 30% of oil originally in place for light oils, 5% for heavy oils, and 0% for heavy oil sands oils. This means that 45% of oil originally in place for light oils remains in the reservoir after primary and secondary recovery (Thomas 2007). Therefore tertiary recovery techniques are required to extract the remaining oil from the reservoir by altering the fluid-fluid and/or fluid-rock properties. Surfactant based enhanced oil recovery is an example of chemical tertiary recovery techniques, where chemical additives are injected to extract additional oil from the reservoir by various mechanisms such as reducing the interfacial tension between the injected water and the residual oil.

Surfactants are surface active molecules with a hydrophilic head and a hydrophobic tail, meaning that they tend to congregate at the water/oil interface. If surfactants are present in high enough concentrations, the surfactant molecules will group together in a certain way to make surfactant micelles, where the hydrophobic tails are towards the centre and the hydrophilic heads are facing out, contacting the water molecules. Surfactant based enhanced oil recovery techniques operate by reducing the interfacial tension between the injection liquid and oil phases, which decreases the capillary pressure in the pores. If the local reservoir pressure is large enough to overcome the capillary pressure then the oil can be extracted from the pores. In some situations, when the surfactants are injected in conjunction with a gas phase, a foam phase may be created with the liquid and gas phases. This foam phase has the added benefits of increasing the sweep efficiency by blocking high permeability areas and forcing the injection fluids into lower permeability areas. Challenges associated with surfactants include; cost of the surfactant, adsorption of the surfactant onto the reservoir pore walls, and the surfactants' ability to also decrease the liquid viscosity, which may lead to a decrease in oil recovery instead of an increase. The generation and propagation of a stable foam phase is another challenge if foam is desired. To generate foam, the liquid must have a sufficient surfactant concentration and the injection parameters and schemes need to be carefully designed. It is known in literature that surfactants have the ability to decrease interfacial tension, thereby increasing oil recovery (Schramm 2000). It is also known that above the critical micelle concentration the surfactant molecules congregate together to form spherical micelles, with the hydrophobic tails pointing inward while the hydrophillic heads point outward to contact the water molecules.

There are several methods used to apply surfactants in enhanced oil recovery. Surfactants can be flooded into the reservoir by injection with a gas phase concurrently or alternating, with a polymer, or with an alkali and polymer solution.

Surfactant Flood

In surfactant floods, an aqueous solution of surfactant is injected into the reservoir in one of three main methods. First, the surfactant can be injected into an injection well as a slug of aqueous highly concentrated surfactant followed by injecting water to drive the surfactant through the reservoir (Johnson 1957). Second, the surfactant can be continuously injected into an injection well in a low concentration aqueous solution (Johnson 1957). Third, the surfactant can be injected into a production well in high concentrations, followed by shutting in the well for a period of time allowing the surfactant to “soak” into the reservoir (Manrique et. al 2004).

The second method is not widely used due to the large amount of surfactants required to continuously inject a low concentration surfactant aqueous solution (Johnson 1957). Surfactant floods typically loose large amounts of surfactant to adsorption. It has also been reported that in surfactant only floods, the surfactant tends to channel through the reservoir following the same path as a primary waterflood (Oil Chem Technologies 2010).

Surfactant-Gas Flood

Surfactants can also be injected in the presence of a gas phase. In this method, an aqueous solution of surfactant is injected into the reservoir along with a slug of gas. There are several methods to inject the surfactant solution and gas into the reservoir, which are described below.

When an aqueous surfactant solution is injected concurrently or alternatively with gas, the gas disperses into small bubbles within the liquid to create foam. Foam generation, propagation, and stability are further discussed in Section 2.3. The surfactant and gas can either be injected at the same time in different wells (co-injection), or in alternating slugs of surfactant and gas in one or more wells. The following are the various ways in which surfactant and gas separately, or a premade foam can be injected into a reservoir:

- Simultaneous Co-Injection

  In co-injection, the surfactant slug and gas phase are injected simultaneously into the reservoir either through the same injection well or through different injection wells (Al-Mossawy et. al 2011).

- Pre-made Co-Injection

  For pre-made co-injection, the surfactant and gas are mixed before being injected into the reservoir. This will create a foam substance that is injected into the reservoir (Al-Mossawy et. al 2011).

- Alternating Co-Injection

  The alternating method consists of injecting a slug of aqueous surfactant solution followed by a slug of the gas phase, either in two different wells or the same well. In this method foam may be created. This can be termed surfactant-alternating-gas (SAG) or surfactant assisted water-alternating-gas (WAG).

Surfactant-Polymer Flood

Surfactant/Polymer flooding utilizes two chemical formulations, a surfactant and a polymer. The surfactant is mixed in an aqueous solution and injected as one slug, with the polymer chemical injected as another slug. Both slugs are driven through the reservoir using brine. This method lowers the interfacial tension between water and oil and lowers the mobility ratio, which is the ratio of velocity of water to oil in the reservoir in this area. High mobility ratios mean the water is moving much faster than the oil, possibly causing earlier water breakthrough, therefore lower mobility ratios are desired. Mobility ratios are dependent on viscosity, as injection fluids with a low viscosity will yield a high mobility ratio. Surfactant/polymer floods have been found to be inefficient due to the loss of surfactant to the porous medium through adsorption (Somasundaran & Hanna 1979).

Alkali/Surfactant/Polymer Flood

Alkali/Surfactant/Polymer flooding utilizes three chemical formulations, an alkali caustic chemical, a surfactant, and a polymer. The three chemicals can be premixed and injected into the reservoir as a single slug, or each chemical can be injected individually as a separate slug. The alkali reacts with the acidic components of the crude oil to produce surfactant in-situ, increasing the amount of surfactant. This method lowers the interfacial tension between water and oil and improves the mobility ratio (Krumrine 1983).

1.2. Research Activities and Thesis Organization

This thesis will deal with the investigation of how several factors, pertaining to the surfactant assisted water-alternating-gas technique, affect both the oil recovery and breakthrough time in a two-dimensional glass micromodel. The factors investigated are the water-alternating-gas ratio (volume of water slug to the volume of gas slug), the concentration of the surfactant in the liquid phase, the type of gas phase used (air and propane), and the type of surfactant used (Triton X-100 and Iveysol 106). The use of a glass micromodel also allows the direct observation of the fluid flow through the porous media.

This thesis will first present a comprehensive literature review on the surfactant assisted water-alternating-gas enhanced oil recovery technique, including an overview of surfactants, mechanisms by which surfactants can increase oil recovery, and mechanisms of foam generation and how foam can increase oil recovery. The literature review will also discuss previous micromodel studies involving surfactants and their findings.

Following the literature review, the experimental system, design, and method will be presented. A complete overview of the experimental micromodel system which was designed as part of this research will be discussed, with the procedures available in Appendix B. The experimental design and method is also discussed, outlining the factors investigated and responses observed for the three different types of experiments conducted. The micromodel experiments vary the WAG ratio, surfactant concentration, gas type, and surfactant type, while the quantitative responses of oil recovery and breakthrough time, and qualitative response of fluid flow are observed.

Interfacial tension experiments are also conducted, varying surfactant type and concentration while measuring the interfacial tension between the injection liquid and oil phases. Finally, viscosity experiments are conducted, varying surfactant type and concentration while measuring the viscosity of the injection liquid. The set of micromodel experiments was designed using Stat-Ease Design of Experiments 9.0 optimal response surface methodology. The Design of Experiments software uses statistical design to determine the experimental runs to be conducted and also analyzes the results (through the analysis of variance technique) to identify the factors which significantly influence the response variable being observed. The optimal design response surface methodology was chosen to limit the number of experimental runs required. The Design of Experiments software also allows for the identification of any non-linearity in the factor effects, and is capable of identifying interaction effects between two or more individual factors.

The water-alternating-gas (WAG) ratio was chosen for investigation as it is an important parameter in the water-alternating-gas technique, with research being conducted on WAG ratios to determine the optimum WAG ratio to use to improve oil recovery. The published literature covers investigation over a wide range of WAG ratios including 3:1, 2:1, 1:1, 1:2, 1:3, and 1:0.5 which found that a WAG ratio of 1:1 was optimal (Salehi et. al 2013; Salehi et. al 2014; Motealleh et. al 2012; Shokrollahi et. al 2014; Feng et. al 2014). However no research has been published on WAG ratios between 1:1 and 1:2. Therefore the lower limit of the WAG ratio was set at 1:1 and the higher limit of the WAG ratio was set at 1:2, with a centre point at 1:1.5 to both investigate the WAG ratio of 1:1.5 and to identify and non-linearity in the oil recovery or breakthrough time effect between WAG ratios of 1:1 and 1:2.

The surfactant concentration was investigated as it is another main parameter of the use of surfactants in any industry. The published literature on the use of surfactants for improving oil recovery investigated the surfactants at the critical micelle concentration (CMC), and/or varied the surfactant concentration by weight percent in the solution (Shokrollahi et. al 2014; Moayedi et. al 2014; Chang et. al 1990; and Sagar and Castanier 1997). This research varies the surfactant concentration by multiples of the CMC, as each surfactant has a different CMC and the behavior of the surfactant is different at concentrations above and below the CMC. No research varying the surfactant concentration by multiples of the CMC rather than by weight percent could be found. It has also been suggested that surfactants should be injected around the CMC value for nonionic surfactants (Gurgel et. al 2008), while Schramm (2000) suggests that surfactants must be present at a concentration higher than the CMC value to achieve the greatest effect in lowering interfactial tension or promoting foam stability. Therefore it was decided to experiment with surfactants at and above the CMC value to take full advantage of the surfactants ability to lower interfacial tension and create a stable foam. Therefore the lower limit for the surfactant concentration was set at the CMC and the higher limit of the surfactant concentration was set at ten times the CMC, with a centre point at five-and-a-half times the CMC to investigate any non-linearity between the lower and higher limits of the surfactant concentration used.

The gas type was also chosen to determine if one gas performed better than another gas. Published literature on the gas phase for water-alternating-gas techniques include air, nitrogen, carbon dioxide, and reservoir gas (Hornbrook et. al 1991; Chang et. al 1994; Farajzadeh et. al 2009; Motealleh et. al 2012; Shokrollahi et. al 2014; Xu and Rossen 2003, Sohrabi et. al 2000; Feng et. al 2014; and Moayedi et. al 2014). Air and propane were chosen as the gas phases based on air being a readily available immiscible gas source, while propane was a readily available hydrocarbon gas. Air was a possible gas source due to the high auto-ignition temperature of oil at ambient conditions. At reservoir conditions air may pose an auto-ignition hazard, therefore at reservoir conditions air may not be a suitable gas choice. As the conditions investigated (ambient pressure and temperature) are unable to take advantage of any pseudo-miscible properties of propane, the two gas phases were chosen to investigate how physical gas properties (compressibility, viscosity, etc) may affect the recovery of oil.

The surfactant type was chosen to determine which, if any, of the two surfactants investigated performed better to increase oil recovery. Nonionic, cationic, and anionic surfactants have been investigated (Rao et. al 2006; and Shokrollahi et. al 2014), with non-ionic surfactants being found to produce a higher oil recovery (Rao et. al 2006). Due to this, two nonionic surfactants were investigated, Triton X-100 and Iveysol 106. Triton X-100 has limited published research for oil recovery available (Abdi et. al 2014; Moayedi et. al 2014), while no published research investigating the use of Iveysol 106 for oil recovery could be found.

The Design of Experiments Optimal Design Response Surface Methodology method resulted in 23 required experiments. However, these core experiments did not include certain baseline experiments with which to compare the results, therefore additional micromodel experiments were conducted to determine when or if enhanced oil recovery techniques should be implemented. Experiments consisting of waterflooding, water-alternating-gas flooding, surfactant flooding and surfactant assisted water-alternating-gas flooding as the secondary recovery phase will be compared with waterflooding followed by water-alternating-gas and surfactant assisted water-alternating-gas experiments. The difficulties encountered in the micromodel experiments will then be discussed, including either fixes used or possible fixes for future experiments.

The results from these three different types of experiments are then analyzed and discussed. The micromodel results for fluid flow are first presented, discussing the observation or lack of observation of phenomena such as foam, viscous fingering, gravity segregation, oil displacement mechanisms, and the wettability of the micromodel. The interfacial tension experimental results discuss the reduction in liquid/oil interfacial tension with increasing surfactant concentrations, with Triton X-100 reducing the interfacial tension to a greater degree than Iveysol 106. The viscosity experimental results discuss the reduction in liquid viscosity with increasing surfactant concentrations, with Triton X-100 reducing the viscosity to a greater degree than Iveysol 106.

For the micromodel experiments, the oil recovery results are then presented, followed by the breakthrough time results. For oil recovery, the individual effects of WAG ratio, surfactant concentration, gas type, and surfactant type, along with the interaction effects of WAG ratio-surfactant concentration, WAG ratio-gas type, WAG ratio-surfactant type, and gas type-surfactant type are discussed in detail, drawing on the interfacial tension and viscosity experiments to better explain the results. Additional experiments that were conducted outside of the core set of experiments are then presented, showing the benefit of using surfactants in a water-alternating-gas method over methods such as waterflooding, surfactant flooding, or water-alternating-gas flooding without surfactants. For the breakthrough time, the individual effects of WAG ratio and gas type are discussed.

Chapter 2: Literature Review

This section details the literature review conducted on surfactant and foam assisted enhanced oil recovery. The basics of surfactants, the physical mechanisms of surfactants and the foam they create, the impact on oil recovery of surfactants and foam, experimental methods and techniques for micromodels, surfactant and foam field trials, and an overview of the design of experiments method will be presented in this section. This will provide a detailed overview of surfactants and foam, how they are used in enhanced oil recovery, and how they can be investigated.

2.1. Oil Recovery Mechanisms

This section will discuss the processes by which oil can become trapped in the pore spaces of a hydrocarbon reservoir. First the concept of interfacial tension will be introduced; this concept is used in both of the following mechanisms of capillary pressure and wettability. This will be followed by discussions on both capillary pressure trapping and wettability trapping. The effect of surfactants on these two mechanisms will be discussed in Section 2.2.3.

Between two immiscible fluids there exists a thin boundary region termed an interface. The interface is caused by an imbalance of intermolecular attractive forces. These forces are discussed below.

Cohesive Forces

The molecules of one liquid all experience the same intermolecular forces; however the forces at the interface only experience the intermolecular forces from the molecules to the side of and behind the interface. The molecules at the interface will also experience intermolecular forces from across the interface, from the molecules of the other phase. If the two liquids are identical, the intermolecular forces will be identical and no interface will exist. However if the two liquids consist of different molecules, the intermolecular forces will be different and an interface may exist. The imbalance between the intermolecular forces of both fluids is termed the cohesive force (Bird 2001). Figure 2-1 below provides a schematic of the cohesive forces in a liquid and at an interface. As shown, the molecules in the centre of the liquid are acted on by identical molecules in every direction; therefore the net sum of all the forces on these molecules would be zero, since the force directly to the left is balanced by the force directly to the right, which is repeated for every direction. The molecules at the interface however are not acted on by identical molecules in every direction, since these molecules are at the boundary there are no identical molecules across the boundary. Therefore in this case, the boundary molecules bulge in the centre of the boundary. In the centre there are molecules acting on the boundary molecules in every direction except for directly above the boundary molecules. The right and left forces are balanced, however the forces acting up and down are not balanced. The boundary molecules feel a greater force pushing on them from below than they feel pushing on them from above, and therefore there exists an imbalance in forces which results in the upwards bulge seen in the centre.

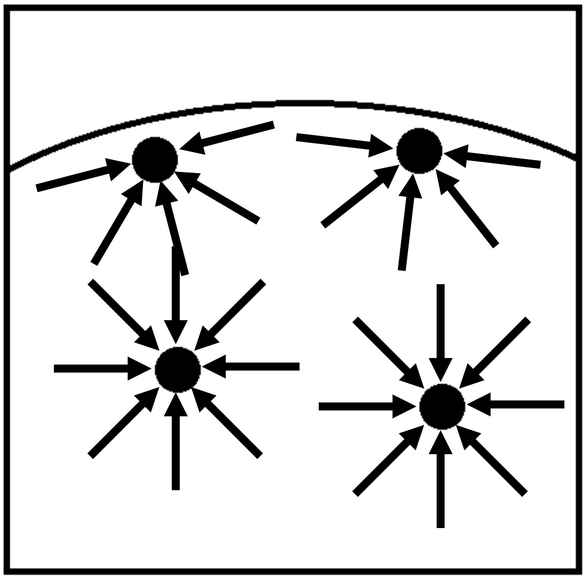

Figure 2-1. Cohesive Forces

Adhesive Forces

The forces of attraction between a fluid and a solid surface are termed adhesive forces. The imbalance between adhesive forces and cohesive forces (termed the interfacial tension) determines the behavior that a fluid will exhibit when in contact with a solid surface (Bird 2001).

In the case of two immiscible fluids and a solid, the wetting phase will occupy as much of the solid surface as is required to balance the adhesive and cohesive forces. This causes the wetting phase to "climb" either up or down the solid surface, as shown in Figure 2-2, wetting phases will be discusses in detail below. In Figure 2-2, the dark liquid is the wetting phase of the solid surface on the left, and is the non-wetting phase of the solid surface on the right. We get these concave down and concave up menisci due to the wetting or non-wetting nature of the liquid. When the liquid is wetting the solid, the liquid will "climb" up the side of the solid. While when the liquid in not wetting the solid, the liquid will try to avoid contacting the solid, resulting in the concave up meniscus.

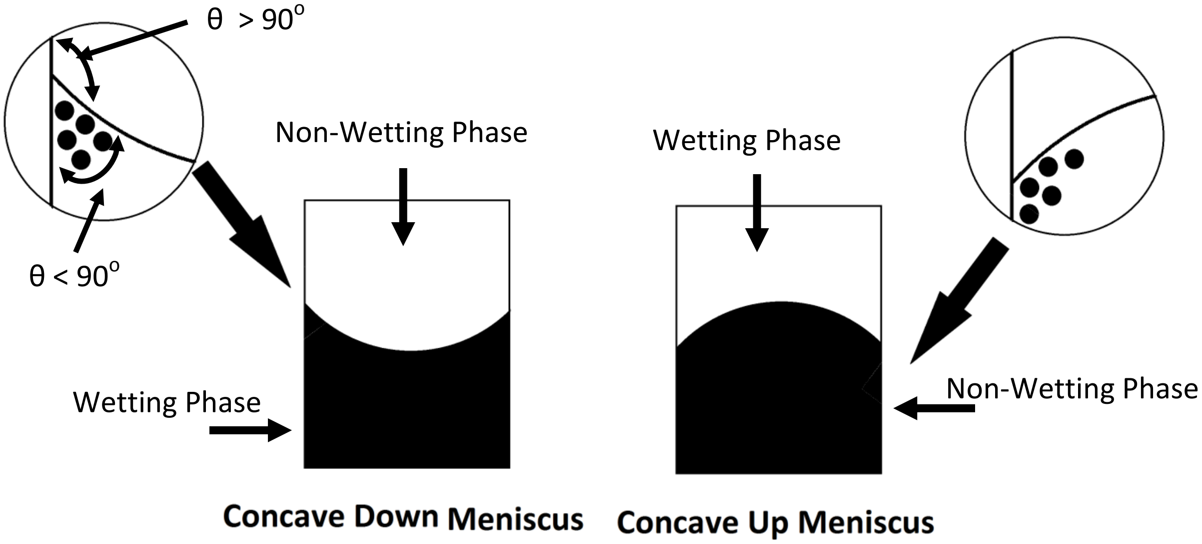

Figure 2-2. Adhesive Forces

The interfacial tension, or interfacial tension, can be best illustrated by observing a single droplet of one phase adhering to a solid substance in the presence of a second phase. Figure 2-3 is an illustration of this, showing the interfacial tension between the two phases.

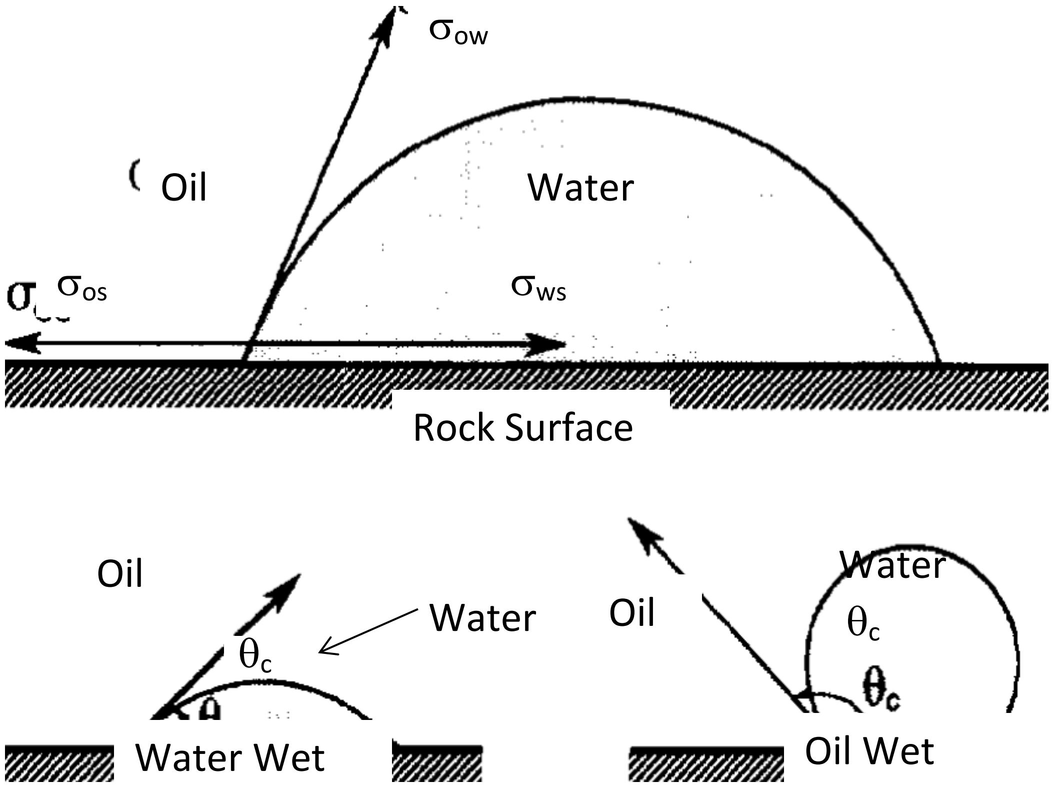

Figure 2-3. Interfacial Tension (AAPG 2014)

where:

σ_{OS} = Interfacial Tension between surface and oil (N/m),
σ_{WS} = Interfacial Tension between Surface and water (N/m),
σ_{OW} = Interfacial Tension between oil and water (N/m), and
θ_c = Contact Angle between Phases.

A convenient way to discern between the two fluids in Figure 2-3 is to term one fluid the wetting fluid, while terming the other fluid the non-wetting fluid. A fluid is considered to be wetting if the internal contact angle is less than 90^o. A contact angle less than 90^o will result in the fluid spreading over the surface (wetting the surface). Fluids with contact angles of greater than 90^o do not spread over the surface, and in fact attempt to reduce the interfacial area between the fluid and the surface, often forming droplets on a surface which will not spread over the surface.

2.1.1. Capillary Pressure

The interfacial tension between two fluids will result in an additional pressure, meaning there will be a pressure differential across the interface. The non-wetting phase will have a higher pressure than the wetting phase due to the contact angle. This pressure can be calculated using Equations (1) (Muskat 1949) and (2) (Laplace 1805).

$$P_{Capillary} = P_{Non-Wetting} - P_{Wetting} \quad and \tag{1}$$

$$P_{Capillary} = \frac{2\sigma_{12} cos(\theta)}{r} \tag{2}$$

where:

σ_{12} = Interfacial Tension between Phase 1 and 2 (N/m),
$P_{Capillary}$ = Capillary Pressure (N/m^2),
θ = Contact Angle, and
r = Pore Radius (m).

As shown in Equation (2), the capillary pressure increases with an increase in interfacial tension. This is because as the interfacial tension increases, the molecular forces underlying the fluid-fluid interfacial tension (cohesive bonds) create more of a force imbalance at the interfaces. These forces thereby require even greater forces to overcome them, increasing the capillary pressure. The capillary pressure decreases with increases in the contact angle of pore radius. This is due to the contact angle being closely associated with the interfacial tension of fluid-solid surfaces. The contact angle is a measurement of the adhesive forces which determine whether a fluid is wetting or non-wetting. Large contact angles result from large adhesive forces pushing away from the solid interface, while low contact angles result from the adhesive forces pushing towards the solid interface. Therefore non-wetting fluids will have a larger capillary pressure than wetting fluids to enter the pore. The increasing capillary pressure-decreasing pore radius relationship is due to the area over which the imbalance of forces is acting. For example, if the force imbalance is kept constant, smaller pores will exhibit a larger capillary pressure than larger pores. The cross-sectional area in small pores is very small, and since pressure is a measurement of force per unit area, the capillary pressure is large. Oppositely, in larger pores, the radius is also larger; therefore the capillary pressure is smaller.

The pressure difference between the injection fluid and the fluid in the pore must be equal to or greater than the capillary pressure in order to displace the oil. This is a key aspect to oil recovery, as natural reservoirs are made up of a porous network with varying sizes of pores. The main difficulty encountered therefore is the very small pores which require very large injection pressures to cause flow of displacing fluids into the pores.

In reservoirs, there are many interconnected pore channels of varying length. The Capillary Number, Equation (3) (Melrose and Brandner 1974), is the ratio of viscous forces to capillary forces and is used to determine which path the injection fluid will take.

$$N_c = \frac{\mu v}{\sigma_{12}} \quad , \tag{3}$$

where:

N_c = Capillary Number,
μ = Viscosity of the liquid (Pas),
v = Flow rate per unit cross sectional area (m/s), and
σ_{12} = Interfacial Tension between Phases 1 and 2 (N/m).

It necessary to determine which force dominates the flow. If viscous forces dominate flow, the trapping mechanism will be dictated by viscosity. When viscosity forces dominate, frictional losses to the pore walls will greatly affect flow, with frictional losses being larger in small-diameter channels compared to large-diameter channels. Therefore when viscous forces dominate, the fluid will follow the path of least resistance which will be the path with the lowest frictional losses, which would be the larger diameter channels. Therefore when viscous forces dominate the injection fluid will move through the larger pores faster and cause breakthrough, trapping oil in the smaller pores.

When the capillary number is low then capillary forces dominate, which are dependent on the radius of the pores. Larger pores have larger radii, and therefore lower capillary forces, while smaller pores have larger capillary forces. Therefore the capillary forces are larger in the small diameter pores, which causes the fluid to travel at a greater rate in the small diameter pores, causing breakthrough in the small pores and trapping oil in the larger pores.

Looking at the capillary number in conjunction with the mobility ratio can be beneficial. The mobility ratio (M) is the ratio of the mobility of an injected fluid to the mobility of the displaced fluid which is oil in this case, and is given in Equation (4). Mobility ratios of 1.0 or greater indicate that the injection fluid is moving at a greater velocity than the fluid being displaced. In this case, this would cause the injection fluid (water or gas) to finger through the oil phase.

$$M = \frac{K_{ri}}{K_{ro}} \frac{\mu_o}{\mu_i} \quad , \tag{4}$$

where:

$M =$ Mobility Ratio,
$\mu_o =$ Oil Viscosity,
$\mu_i =$ Injected Fluid Viscosity,
$K_{\mathrm{ro}} =$ Oil Relative Permeability, and
$K_{\mathrm{ri}} =$ Injected Fluid Relative Permeability.

For two injection fluids of different viscosities, the fluid with the lower viscosity will have a higher mobility ratio. The amount of oil trapped by the lower viscosity injection fluid will be greater than for the higher viscosity injection fluid since the low viscosity fluid will be able to finger through the oil phase to a greater extent in the large or small pores, causing an earlier breakthrough and increasing the amount of trapped oil.

2.1.2. Wettability

When water is injected into a water-wet reservoir (imbibition), the water will imbibe in films along the pore wall surrounding the oil in the pore volume. The adhesive forces of the water to the pore walls will be greater than the adhesive forces of the oil to the pore wall; therefore the water will creep along the pore walls. If the water pressure is high enough, it may have the necessary force to push the oil from the pore body as well, however the adhesive forces present creeping along the pore walls as the path of least resistance to the water.

When the water reaches the next small pore throat, it will cause the oil to “snap off” disconnecting it from the oil in the other pore body. This effectively traps globules of oil in the pore bodies because additional waterflooding will not remove the trapped oil (Roof 1970; Chatzis et. al 1983). Figure 2-4 gives a schematic of an oil globule being trapped in a water-wet porous media during an imbibition process. The flow is from the left to the right and each consecutive figure is an instant ahead in time.

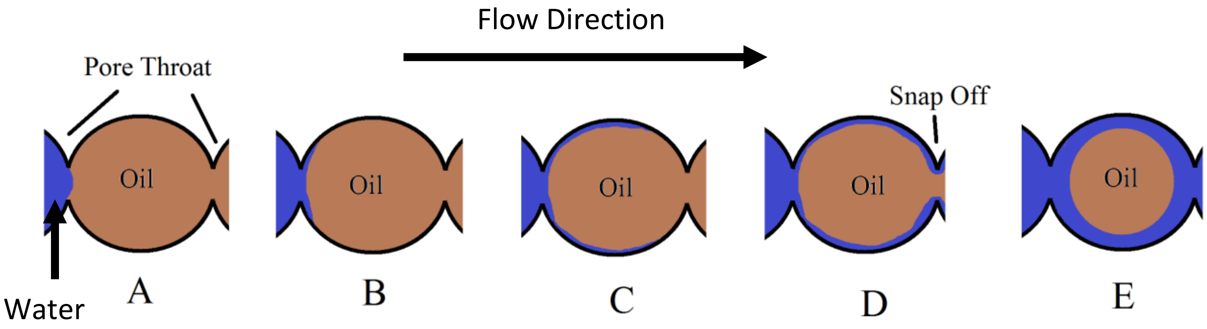

Figure 2-4. Wettability Trapping Mechanism

2.2. Physical Mechanisms of Surfactants

This section will discuss the surfactant molecule and the physical mechanisms that surfactant molecules undergo when injected into a hydrocarbon reservoir. Background information for interfacial tension, capillary pressure, and wettability is discussed to explain the effect of surfactants on oil recovery.

2.2.1. Surfactants

Surfactant molecules are composed of a "head" molecule attached to a "tail" molecule. These two sections are chemically different and therefore do not behave the same. The tail is composed of a hydrocarbon molecule which is hydrophobic, while the head is composed of a polar or ionic group which is hydrophilic, and therefore interacts strongly in an aqueous environment via dipole-dipole or ion-dipole interactions. Figure 2-5 presents a typical anionic surfactant molecule; the anionic nature of the molecule can be seen by the negative electrical charge of the surfactant head. Note the different chemical structure of the tail vs. the head. The carbon atoms are shown in a zigzag orientation because carbon molecules have a tetrahedral configuration which requires the bonds to be separated by 109.5^{o} (Reusch 2013).

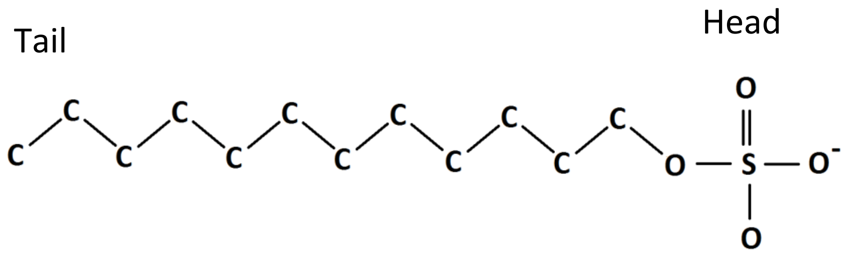

Figure 2-5. Typical Anionic Surfactant Monomer

When surfactant molecules are present they will migrate to the fluid interface to decrease the potential energy of the system. The scenario with the lowest potential energy is the equilibrium state of the system. Various surfactant orientations are shown in Figure 2-6.

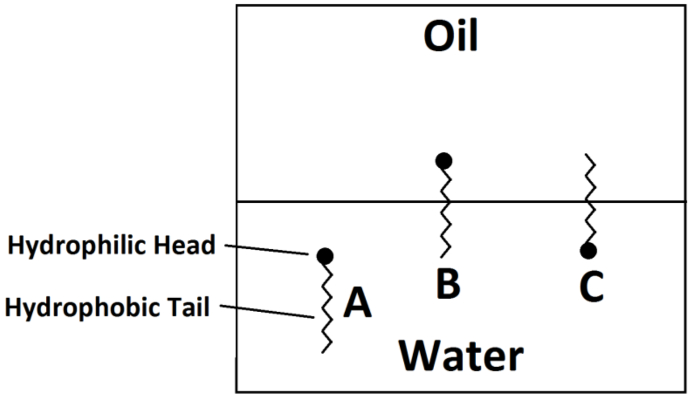

Figure 2-6. Surfactant Orientations in Liquid

In Figure 2-6, molecule C is in the lowest state of potential energy. This is because the hydrophilic head is within the water phase and the hydrophobic tail is within the oil phase. The hydrophilic head is polar, meaning that there is a difference in charge from one side of the molecule to the other. The polar head can bond more easily with the polar water molecules, which is why the head is hydrophilic. The surfactant tail is non-polar, meaning that is does not have any change in charge from one side of the molecule to the other. Non-polar molecules have difficulty bonding with polar water molecules, which is why they are termed hydrophobic. The non-polar parts of the molecule prefer to be in solutions of non-polar molecules. Therefore in cases A and B, either the hydrophilic head is in a non-polar solution, or the hydrophobic tail is in a polar solution, which are both non-ideal cases. In case C, the hydrophilic head is in the water phase while the hydrophobic tail is in the oil (non-polar) phase.

Without this orientation, the hydrophobic and/or hydrophilic parts of the molecule will not be in contact with the fluid that it has an affinity for (the hydrophobic part in contact with water or the hydrophilic part not in contact with water) (Schramm 2000).

2.2.2. Surfactant Types

Surfactants are categorized based on the molecular structure of the hydrophilic “head” part of the surfactant molecule. The following are the four main classifications of surfactants (Schramm 2000). Figure 2-7 provides an overview of the different surfactants based on “head” electrostatic charge.

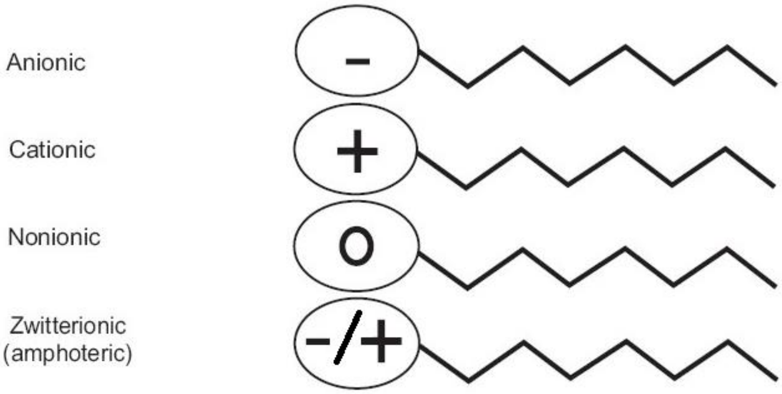

Figure 2-7. Classification of Surfactants (Som et. al 2012)

There are different categories of surfactants. These include cationic, anionic, nonionic, and zwitterionic surfactants. All of these categories are discussed below.

Cationic

A surfactant with a head consisting of a positively charged group is termed a cationic surfactant. An example of a cationic surfactant head is quaternary ammonium (Schramm 2000).

Anionic

A surfactant with a head consisting of a negatively charged group is termed an anionic surfactant. Examples of anionic surfactant heads are sulphonates, sulphates, or carboxylates (Schramm 2000).

Nonionic

A surfactant with a non-charged hydrophilic molecule is termed a nonionic surfactant (Schramm 2000).

Zwitterionic

A surfactant with a head consisting of a negatively charged atom and a positively charged atom on different locations of the hydrophilic head is termed a zwitterion surfactant. Zwitterion surfactants can act as an anionic surfactant in an alkali solution and a cationic surfactant in an acidic solution (European Textile Services Association 2013).

2.2.3. Surfactant Chemistry

The dual hydrophilic/hydrophobic nature of surfactants causes the molecules to exhibit a unique behavior. In low concentrations, the surfactant molecules are dispersed, with ionic surfactants acting much like normal electrolytes. At higher concentrations, the molecules begin to congregate into large molecules called micelles. The micelle consists of the hydrophobic tails gathering in the middle of the molecule and the hydrophilic heads gathering on the outside of the molecule, creating a spherical molecule (Schramm 2000). This occurs to reduce the potential energy of the molecule by allowing the hydrophilic heads to be in contact with the water phase, while the hydrophobic tails are grouped in the middle to be farther away from the water phase. Figure 2-8 below shows this behavior.

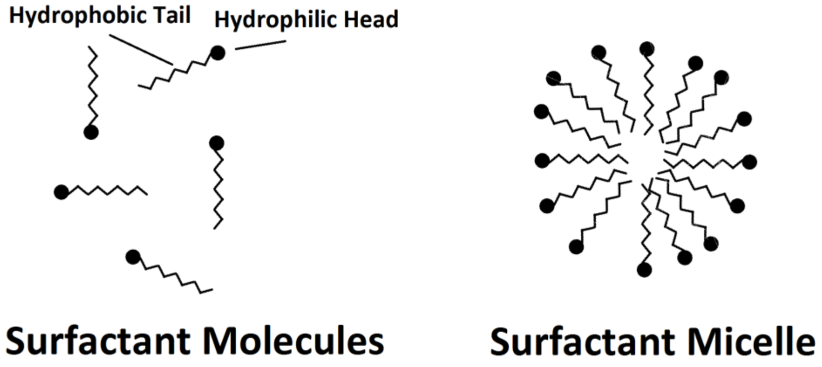

Figure 2-8. Surfactant Monomers and Micelle

The concentration at which the surfactant molecules begin to form micelles is termed the critical micelle concentration (CMC). Many of the physio-chemical properties of the surfactant will be significantly different above and below the critical micelle concentration. This is because the surfactant molecules are involved in a cooperative association process when congregated in a micelle and do not exhibit the properties associated with single surfactant molecules (Schramm 2000).

Due to the hydrophilic “head” and hydrophobic “tail” components of a surfactant molecule, the surfactant molecule can adsorb onto the reservoir rock. There are several mechanisms for surfactant adsorption, including electrostatic attraction/repulsion, ion-exchange, chemi-sorption, chain-chain interactions, hydrogen bonding, and hydrophobic bonding. The characteristics of the surfactant, along with the solution conditions and the mineralogical composition of the reservoir rock determine the mechanism that causes adsorption (Somasundaran and Zhang 2006). The adsorption of the surfactant molecule onto the reservoir rock can alter the wettability of the rock, thereby altering the relative permeability of the reservoir fluids.

There are different adsorption mechanisms depending on the surfactant concentration. At low concentrations, the surfactant adsorbs mainly due to electrostatic interactions between the surfactant head and the ionic mineral sites on the reservoir rock, this leads to a very sparsely covered reservoir rock, termed Region 1 by Somasundaran and Zhang (2006). As the concentration of surfactant increases (while still being far below the CMC value), there is an increase in adsorption resulting from the interaction of the hydrophobic chains of new surfactants with the hydrophobic chains of previously adsorbed surfactants, forming microstructures termed solloids (surface colloids or hemimicelles), termed Region 2. This continues until the surface is electrically neutralized, after which time the interactions are purely chain-chain interactions. As surfactant concentrations increase (while still below the CMC value), more surfactant adsorbs due to chain-chain interactions until the surface begins to take on the same electric charge as the adsorbing molecules, termed Region 3. At this point, electrostatic repulsion begins to repel any additional adsorption. As the surfactant concentration increases to and above the CMC value, the adsorption rate stays constant with chain-chain and electrostatic repulsive forces balanced, termed Region 4. These Regions and the surface density of surfactants are shown in Figure 2-9 (Somasundaran and Zhang 2006).

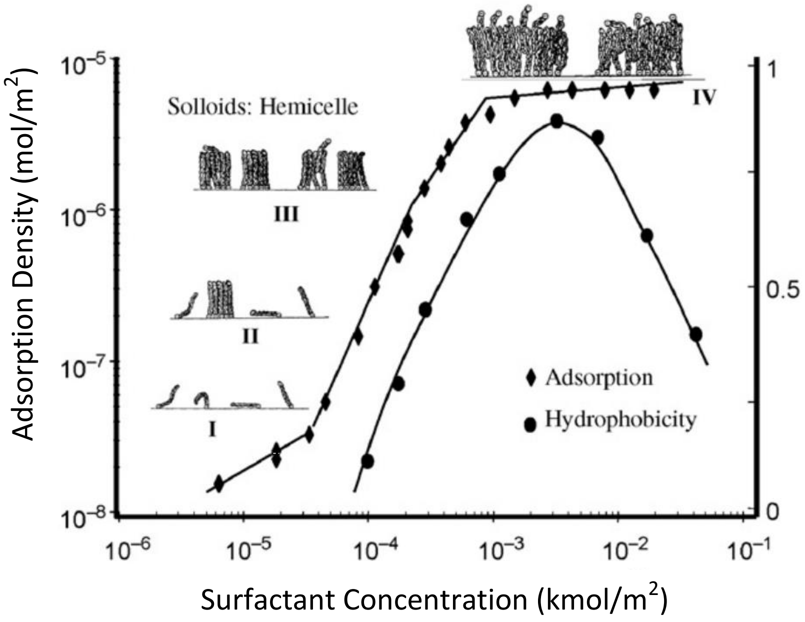

Figure 2-9. Surfactant Concentration vs. Adsorption (Somasundaran and Zhang 2006)

With the hydrophilic “head” adsorbing onto the reservoir rock surface, the hydrophobic “tail” is exposed into the pore space. Due to the hydrophobic characteristic of the molecule “tail”, the reservoir rock will have a weaker affinity for water as more surfactant is adsorbed onto the reservoir rock. In Region 1, the surface is water wet, while in Region 2, the surface becomes oil wet. In Regions 3 and 4, the surface becomes less oil wet, approaching a mixed wet condition (Somasundaran and Zhang 2006).

The trapping mechanisms of both wettability and capillary pressure were discussed in Section. The effect of surfactants on both of these trapping mechanisms are discussed below.

Wettability

The literature on the effect of surfactants on enhanced oil recovery mainly focuses on the reduction in interfacial tension, leaving the effect of wettability alteration relatively unexplored (Rao et. al 2006). However, as discussed above, the adsorption of surfactant onto the reservoir rock can alter the wettability of the rock, and thereby alter the relative permeabilities of the reservoir fluids. It has been shown (Rao et. al 2006; Schramm 2000) that the non-ionic surfactants perform better in altering the wettability of the reservoir rock to a mixed-wet state (Moayedi et. al 2014). The oil recovery from a mixed-wet state is higher than the recovery from either a purely water-wet or purely oil wet state.

As discussed in Section 2.2.1, the surfactant molecules will migrate to the interface to minimize the potential energy of the system, the hydrophilic head will be on the aqueous side of the interface, while the hydrophobic tail will be on the non-aqueous (in this case, hydrocarbon or rock) side of the interface. The surfactant molecules provide an expanding force at the interface, pushing the water molecules further apart. The expanding force acts opposite to the intermolecular attractive forces, thereby decreasing the overall intermolecular forces, and decreasing the imbalance between the intermolecular forces of both fluids. This leads to a decrease in the interfacial tension between the two fluids. With a decrease in interfacial tension, the capillary pressure will also decrease, potentially allowing for the recovery of previously unrecoverable oil (Schramm 2000).

Capillary Pressure

Water-oil systems have a low capillary number due to high interfacial tensions, therefore in waterflooding the oil will be displaced in an imbibition process, where the oil will be trapped in the large pores as is shown in Figure 2-10. Gas-oil systems have a small capillary number; therefore in gas flooding the oil will be displaced in a drainage process, where oil is the wetting fluid and will be trapped in the smaller pore as shown in Figure 2-10 (Chatzis et. al 1983) as the drainage mechanism is controlled by the smallest pore throats. This implies that more oil will be trapped with waterflooding compared to gasflooding. In Figure 2-10, the darker spot in the capillaries is trapped oil, while the white colour is the injected fluid (water or gas).

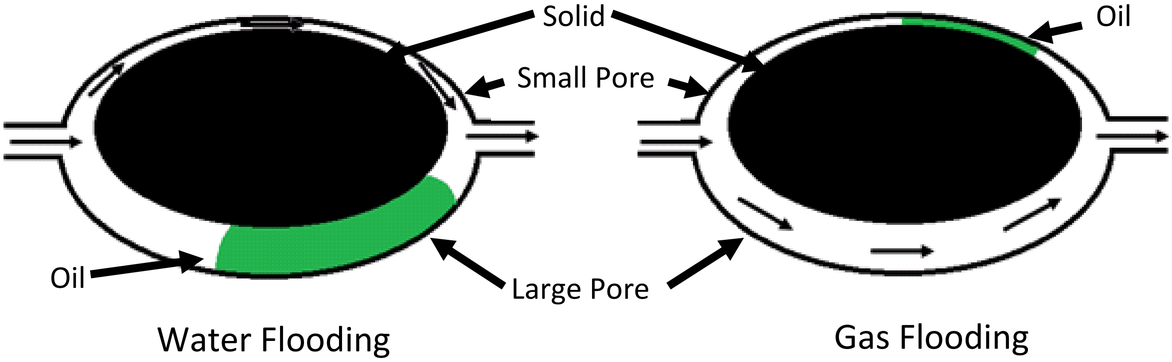

Figure 2-10. Capillary Pressure Trapping Mechanism

2.3. Physical Mechanisms of Foam

This section will discuss the physical mechanisms of foam. First, foam characteristics will be discussed, followed by the mechanisms of foam generation and propagation. Finally, theories on foam destruction will be presented.

2.3.1. Foam Characteristics

Foam is a mixture of water, gas, and a foaming agent (surfactant). The gas bubbles are separated by a film of liquid called a lamallae. The point where three lamallae connect is termed a plateau border (Al-Mossawy et. al 2011; Schramm 2000). Figure 2-11 shows an illustration of a foam structure.

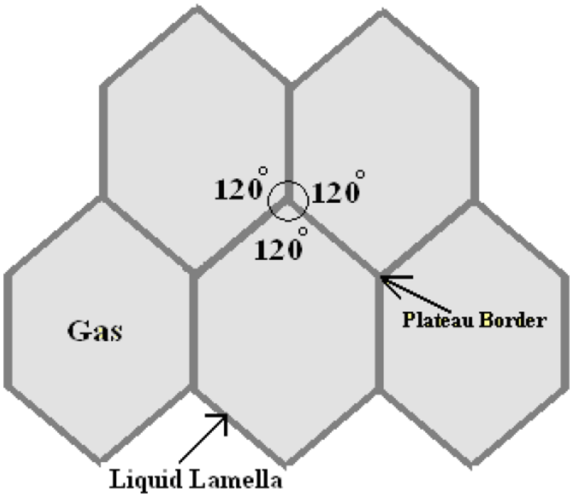

Figure 2-11. Diagram of Foam Structure (Al-Mossawy et. al 2011)

2.3.2. Foam Formation and Propagation

There are three known methods of foam generation: snap-off, leave-behind, and lamella division. These three methods will be discussed in detail in this section to provide an understanding of how a foam structure can be generated.

2.3.2.1. Lamella Division Mechanism

The lamella division mechanism occurs when pre-existing lamellae encounter branches in the porous network. When a moving lamella encounters a branch in the flow path, it may split into two lamellae, one traveling in each branch. Lamella division is believed to be the primary method of foam generation for steady gas-liquid flow regimes (Tanzil et. al 2002; Al-Mossawy et. al 2011).

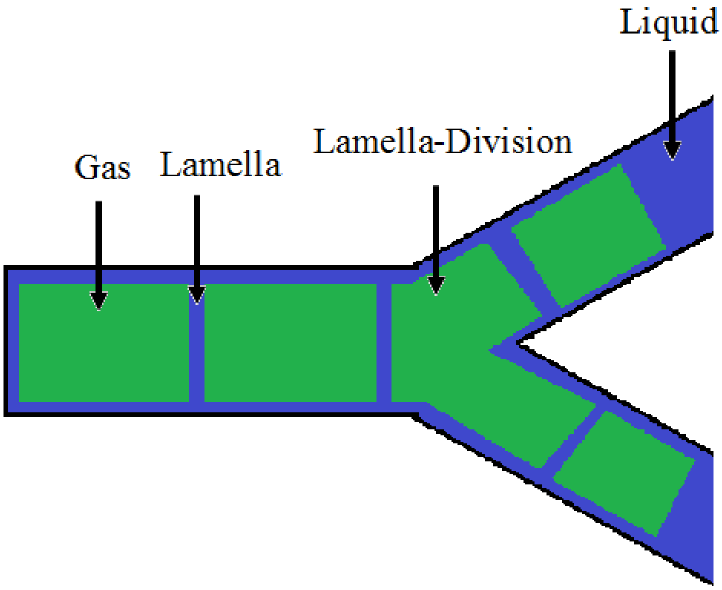

Figure 2-12. Lamella Division Mechanism of Foam Creation

2.3.2.2. Snap-Off Mechanism

The snap-off mechanism occurs when the gas phase invades porous media that is currently liquid filled. The pressure of the gas phase at the pore throat must exceed the entry capillary pressure of the pore throat for the gas to invade the pore body. Once the gas has invaded the pore body, the pressure must fall below the critical capillary pressure for snap-off, which for cylindrical pore throats is half the entry pressure of the pore throat. The snap-off pressure is less than the entrance pressure because typically the liquid is more wetting than the gas; therefore the gas requires a much larger pressure to invade the pore throat than the liquid. This causes the liquid to re-fill the pore throat, effectively "snapping" the gas bubble from the continuous gas phase. Figure 2-13 illustrates this mechanism (Roof 1970; Kovscek and Radke 1993; Li 2006).

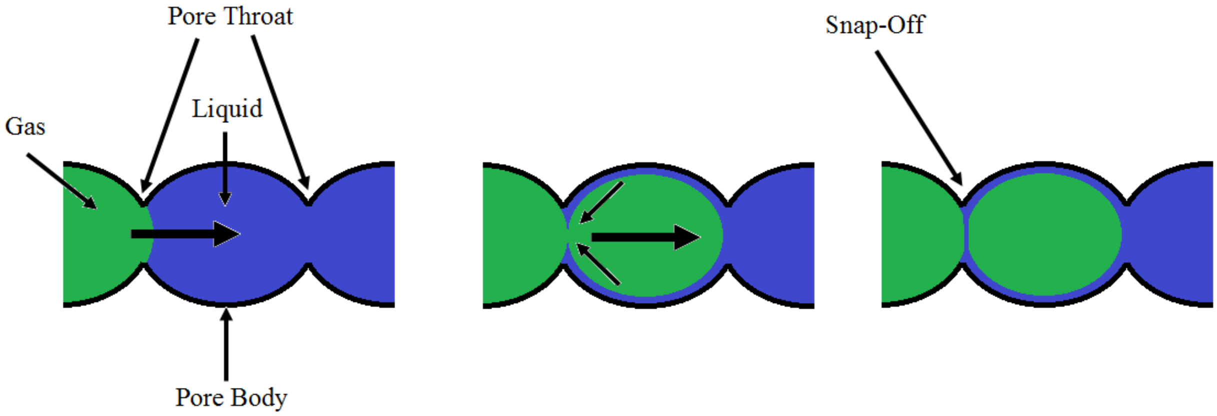

Figure 2-13. Snap-Off Mechanism of Foam Creation

Snap-off requires the non-wetting phase pressure to be sufficient enough to enter the pore, and then drop by at least a half to allow the snap-off mechanism to occur. According to Li (2006), there are eight documented ways that this reduction in capillary pressure may occur:

- Macroscopic imbibition: Injecting gas and liquid slugs alternatively, the capillary pressure may fall during the liquid injection because the gas does not have the pressure backing that it would if it was being injected (Falls et al. 1988; Chambers and Radke 1990).
- Lamallae Movement: As lamallae move through the pore network, the curvature of the lamella change, creating fluctuations in capillary pressure. This is due to the heterogeneous nature of the porous network, with varying pore sizes (Rossen 1990).
- Pressure Gradients: If gas and liquid are injected at different pressures, the capillary pressure may be different (lower) at the rear of sufficiently long bubbles due to pressure gradients (Huh and Handy 1989).
- Shifts in permeability: Capillary pressure is low in high permeability regions; therefore a transition between a low permeability zone and a high permeability can decrease the capillary pressure (Yortsos and Chang 1990; Van Duijn et. al 1995).
- Imbibition: In instances where the gas pressure is insufficient to penetrate the pore throat, the liquid at the pore throat may infiltrate the gas bubble through film flow and snap-off a portion of the gas immediately adjacent to the pore throat (Ransohoff et. al 1987; Chambers and Radke 1990).

- Density differences: Due to gravity, pressure is highest in the lower end of a liquid or gas phase. However, density differences cause the liquid pressure to be higher than the gas phase pressure (Falls et. al 1988; Tanzil et. al 2002)
- Lamallae mobilization: If strong foam forms inside a porous media and the lamallae are mobilized, the gas mobility increases and reduces the gas pressure gradient, causing the pressure to drop suddenly at the inlet of the porous media (Chen et. al 2005).

The snap-off mechanism occurs with or without surfactant. However if the surfactant foaming agent is not present, the gas bubbles coalesce.

2.3.2.3. Leave-behind Mechanism

The leave-behind mechanism occurs only during drainage when the gas phase invades porous media that is currently liquid filled. The gas flows through the pore network, but leaves behind liquid in some pore throats due to the wetting nature of the liquid and high capillary pressures required to drain the liquid from small pores (Ransohoff and Radke 1988; Kovscek and Radke 1993; Al-Mossawy et. al 2011). This is shown in Figure 2-14.

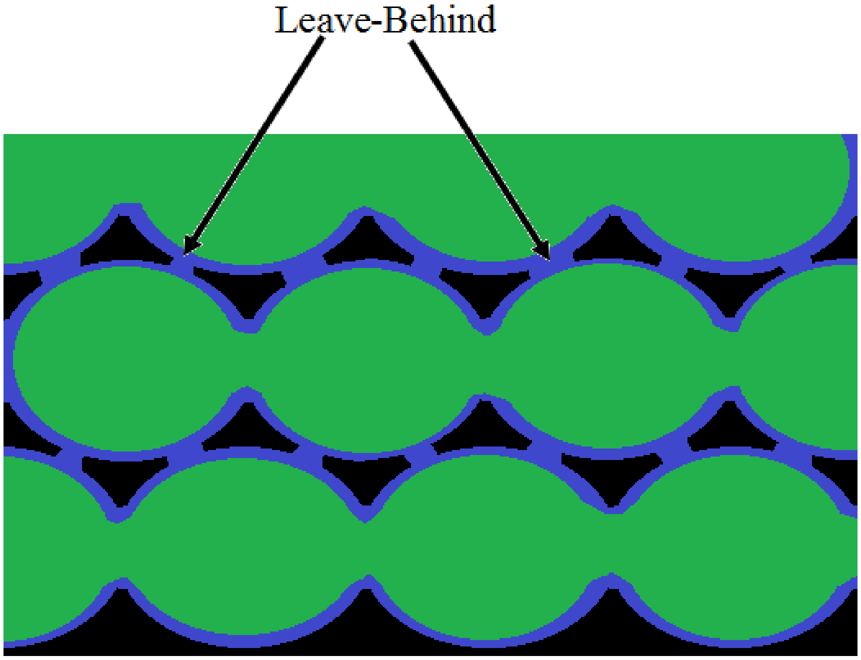

Figure 2-14. Leave-Behind Mechanism of Foam Creation

2.3.3. Types of Foam Films

The lamellae are thin films of liquid separating the gas bubbles. The films present in foam can be described as either symmetrical (gas bubble-lamallae film-gas bubble), or asymmetrical (gas bubble-lamallae film-container surface or gas-bubble-lamallae film-other liquid film). The ultimate stability of a foam depends on the stability of these thin films (Aveyard and Clint 1996)

2.3.3.1. Symmetrical Films

In bulk foam, the lamellae films separating gas bubbles are symmetrical films. The gas bubbles are in contact with the lamellae film, and the film is always in contact with another gas bubble. This type of film would only be possible within the bulk of the foam, and is not possible at the extremities of the foam as they do not interact with the reservoir rock or the hydrocarbon which exists in the reservoir. If they did interact with the pore channel walls of any other fluid within the reservoir, they would no longer be symmetrical films and would be termed asymmetrical film (Aveyard and Clint 1996).

2.3.3.2. Asymmetrical Films

Asymmetrical films exist when the bulk foam encounters another phase at an interface, whether it is the solid surface of the pore channel (wall-lamellae-gas bubble) or another liquid phase (liquid-lamellae-gas bubble). For the lamellae to be in direct contact with the pore channel wall the lamellae must be the wetting phase. If the lamellae are not the wetting phase, a separate liquid phase (oil or water) will exist between the lamellae and the pore channel wall. In this case the film is asymmetrical due to it being a liquid-lamellae-gas bubble film (Aveyard and Clint 1996).

2.3.4. Foam Stability and Destruction

This section presents the theories which exist on the stability of a foam phase. Generally a foam is considered stable if the rate of foam generation is equal to or greater than the rate of foam destruction.

2.3.4.1. Disjoining Pressure

If two film surfaces are brought into close proximity of each other, repulsive positive electrostatic and attractive negative van der Waals forces create pressures within the film, termed disjoining pressures. These forces interact to balance the capillary pressure in the film.

Positive pressures imply repulsive forces, thickening and stabilizing the film, while negative pressures imply attractive forces, thinning and destabilizing the film. With asymmetric films, the van der Waals forces may be attractive or repulsive (Israelachvilli 1991; Hirasaki 1991; and Farajzadeh et. al 2012).

As foam consists of multiple gas bubbles in a liquid, there is always a meniscus present for every foam gas bubble. This meniscus creates capillary pressures in the gas bubble. The van der Waals and electrostatic forces attempt to balance the capillary forces to create stable foam.

The foam is stable as long as the film surfaces are not brought into close proximity. If two film surfaces are in close proximity they will interact in the form of repulsive positive electrostatic and attractive negative van der Walls forces (Farajzadeh et. al 2012). The unbalanced forces can rupture the films and coalesce the gas bubbles, leading to the collapse of the foam. The attractive van der Waals forces depend mostly on the densities of the neighboring phases, while the repulsive electrostatic forces depend on the charge density on the film interface and the concentration of electrolytes in the aqueous phases (Farajzadeh et. al 2012).

The factors affecting disjoining pressure include (Farajzadeh et. al 2012):

- Surface Charge Density:

  Surface Charge Densities increase the repulsive electrostatic forces. Therefore an increase in charge density is ideal.

- Phase Densities:

The densities of the neighboring phases influence the van der Waals forces.

- Interfacial Tension:

Interfacial tension is the main contributing factor to capillary pressures, and therefore has an effect on the disjoining pressure. Low interfacial tensions decrease the capillary pressure and produce a more stable foam.

2.3.4.2. Limiting Capillary Pressure

The size of the gas bubbles in the foam has an effect on the pressure gradient of the foam. Smaller gas bubbles generate a higher pressure gradient than larger gas bubbles. Ideally, the rate of foam generation will increase until the rate of foam coalescence equals the rate of foam generation. Foam generation increases the number of gas bubbles per unit volume of foam, which gives the foam a finer texture. Smaller gas bubbles reduce the gas mobility, as the gas mobility is reduced, the gas phase will displace the water phase, resulting in a lower water saturation. As the water saturation decreases, the gas/water capillary pressure increases (Farajzadeh et. al 2012).

As discussed in Section 2.3.4.1, the capillary pressure balances the disjoining pressure. If the capillary pressure increases beyond a value, termed the limiting capillary pressure, the foam will become unstable and will collapse.

The factors affecting the Limiting Capillary Pressure include (Farajzadeh et. al 2012):

- Surfactant Concentration:

Increasing surfactant concentration decreases the interfacial tension, which decreases the capillary pressure.

- Surfactant Type:

Different surfactants affect the interfacial tension to different degrees, which affect the capillary pressure.

- Foam Flowrate:

The foam flowrate affects the pressure gradient; a larger flowrate produces a larger pressure gradient.

- Porous Media Permeability:

The permeability of the porous media directly affects the pressure gradient.

- Electrolyte Concentration:

Electrolyte concentrations affect the interfacial tension, and thereby affect the capillary pressure.

2.3.4.3. Drainage

Initially as foam is produced, gas bubbles are dispersed in a large volume of liquid. This causes the gas bubbles to be separated by thick foam films, causing them to take on a spherical shape (Pugh 1996). As the foam progresses, the gas bubbles come in closer contact, either through both the foam generation mechanisms described in Section 2.3.2 or from liquid drainage around the gas bubbles. As the liquid drains away from the gas bubble, the foam films separating gas bubbles decrease and the gas bubbles take on a polyhedral shape with plateau borders forming between multiple gas bubbles (Pugh 1996).

The interface between the gas bubbles and the liquid at the plateau border takes on a curved shape due to interfacial tension, and this curvature causes the plateau border to have a thicker film and a lower pressure when compared to the foam films outside of the plateau borders. This gives rise to a capillary suction effect, which causes the liquid to flow from the foam films between gas bubbles to the plateau borders.

In vertical foams, gravity acts on the foam. The liquid phase experiences a stronger force of gravity than the gas phase, resulting in the liquid flowing through the foam films and plateau borders vertically down the foam. This results in the highest foam height being more susceptible to rupture, as this area will be drained first by gravity (Pugh 1996).

The factors affecting drainage include (Pugh 1996):

- Surfactant Concentration:

  Increasing surfactant concentration increases the surface viscosity and surface elasticity, thereby decreasing the drainage rate. Increasing surfactant concentration increases adhesive and cohesive bonding.

- Liquid Phase Composition:

Using a mixture of different types of surfactants can also increase adhesive forces. Nonionic surfactants tend to increase the foam stability of ionic surfactant foams.

- Liquid Viscosity:

The liquid viscosity directly affects the rate of drainage. Higher liquid viscosities produce lower drainage rates, while lower liquid viscosities produce higher drainage rates. It has been found that foams with the same viscosities have the same lifetime, even with differing interfacial tensions. Several solutes, such as glycerol, may be added to increase viscosity and thereby decrease drainage.

Bulk liquid viscosity tends to decrease the thinning of thick films; surface viscosity tends to decrease the thinning of thin films.

- Gravity:

Gravity has a direct effect on drainage as gravity is the main force driving drainage. Gravity acts directly on the foam films and indirectly through the capillary suction effect in the Plateau borders.

- Interfacial Tension:

Interfacial tensions between the liquid and gas phases control the shape of the gas bubbles and plateau borders. The interfacial tension can be used to oppose the gravity and slow drainage.

2.3.4.4. Disproportionation

Disproportionation is a diffusion mechanism whereby the gas molecules diffuse through the liquid films from smaller bubbles into larger bubbles. Smaller bubbles have a higher pressure than large bubbles, driving the diffusion (Pugh 1996). As larger bubbles are unfavorable, this process is detrimental to the quality of the foam. This diffusion mechanism is highly dependent on the gas composition and only causes a major effect if the gas is very soluble in the liquid phase (Pugh 1996). Therefore, for strong foams that resist this diffusion mechanism in a WAG technique, gases which are not soluble in the water/brine phase would be ideal.

The main factor affecting disproportionation is gas solubility in liquid. The driving force for disproportionation is diffusion, and the diffusion mechanism is dependent on the solubility of the gas phase in the liquid phase, lower gas solubility's decrease disproportionation (Pugh 1996).

2.3.4.5. Surfactant Depletion

As described in Section 2.2.3, the surfactant molecules can adsorb onto the reservoir rock. This adsorption may change the surface chemistry of the rock. The impact of this adsorption on the foam stability of the asymmetrical films on the reservoir rock is not known, however the impact on the symmetrical foam films and the asymmetrical foam films between the foam and oil can be implied from the decrease in surfactant molecules in the liquid phase. As more surfactant molecules adsorb to the rock wall, the surfactant concentration in the liquid phase of the foam will decrease. As surfactant concentration is important in the disjoining pressure and drainage, a decrease in surfactant concentration can be detrimental to foam stability.

2.3.5. Foam Destruction in the Presence of Oil

It has been shown that the presence of oil is detrimental to foam stability and reduces the foam's lifetime significantly (Farajzadeh et. al 2012). This is due to undissolved oil droplets forming on the interfacial surfaces of the foam.

The process of how the oil droplets destabilize the foam can be thought of in two distinct steps, first the oil must penetrate the foam liquid-air interface, and secondly the oil must spread over the foam interface (Pugh 1996).

The ability of an oil droplet to first enter the foam interface, and then to spread over the interface, is defined in Equations (5) and (6) respectively, both developed by Robsinson and Woods (1948) using coefficients defined by Harkins (1941). These equations define an entering coefficient (E) and a spreading coefficient (S). In order for the oil to penetrate the interface, E must be greater than or equal to 0. Once the oil enters the interface, S must be greater than or equal to 0 to allow the oil to spread over the film and cause it to rupture (Robsinson and Woods 1948; Harkins 1941; as cited by Pugh 1996).

$$E = \gamma_{l/g} + \gamma_{l/o} - \gamma_{o/g} \text{ ,} \tag{5}$$

$$S = \gamma_{l/g} - \gamma_{l/o} - \gamma_{o/g} \text{ ,} \tag{6}$$

where

S = Spreading Coefficient,
E = Entering Coefficient,
$\gamma_{l/g}$ = Interfacial Tension between the liquid and gas phase of the foam (N/m),
$\gamma_{l/o}$ = Interfacial Tension between the foam liquid and oil (N/m), and
$\gamma_{o/g}$ = Interfacial Tension between the oil and foam gas (N/m).

2.4. Experimental Studies

This section will first discuss the common experimental techniques that are used in evaluating surfactant based enhanced oil recovery techniques (micromodel and coreflooding). First micromodel and coreflooding will be discussed with a focus on micromodel flooding as that experimental method is the focus of this thesis. This will be followed by an overview of the laboratory scale research for the use of surfactant in enhanced oil recovery techniques in both micromodels and cores. This will be followed by a brief overview of field applications using surfactant enhanced oil recovery techniques. This section will end with a discussion on the factors chosen for this research.

Micromodel experiments can be utilized for all surfactant injection techniques discussed in this thesis. Micromodels are generally two dimensional (width and length) models made out of two layers of glass. One or both of the glass layers are etched, either using a laser or chemical process, to create the pore bodies and throats. The two layers are then bonded together with the etched sides facing inwards.

Enhanced oil recovery techniques can be designed and tested using these micromodels to obtain an understanding of the underlying pore scale physics of different oil recovery techniques. This understanding can improve the design and application of different oil recovery techniques for field applications. The models are generally first saturated with water to simulate the original state of the reservoir. Oil is then injected to displace the water, simulating the initial oil saturation of the reservoir. The micromodels are either then flooded with water to mimic the secondary oil recovery phase, or are directly subjected to the specific enhanced oil recovery technique being investigated. The visualization of the injection and reservoir fluids moving through the micromodel is one of the greatest benefits of performing a micromodel experiment, allowing transition zones and the channeling of the injection fluids to be observed. In addition to observing the pore scale physics, raw data such as oil recovery, flow rates, time to injection fluid break through, along with any additional information that is required may be measured. The greatest disadvantage of using micromodels is the lack of three dimensional flow and the often unrealistic characteristics of the model (permeability, porosity, pore size, rock properties) which can differ greatly from real reservoirs (Hematpour et. al 2012). As the micromodels are two dimensional, field scale heterogeneity is not captured in micromodel studies.

Coreflooding experiments can be utilized for all surfactant injection techniques. Coreflooding experiments utilize either synthetically manufactured cores or cores obtained from a reservoir of interest. Enhanced Oil Recovery techniques can be designed and tested using these cores to obtain an appreciation of how the technique may perform in a field application. The cores are generally first saturated with water to simulate the original state of the reservoir. Oil is then injected to displace the water, simulating the initial hydrocarbon saturation of the reservoir. The core is then either flooded with water to mimic the secondary oil recovery phase, or are directly subjected to the enhanced oil recovery technique which is desired.

The raw data which is measured in core flooding experiments include oil recovery, water cut, flow rates, time to injection fluid break through, along with any additional information that is required. The advantages of coreflooding experiments are that three-dimensional flow can be simulated (pores are connected in three dimensions), and if a core from a real reservoir is used, the core will have identical characteristics (permeability, porosity, rock properties) as the reservoir. The greatest disadvantage of using coreflooding experiments is the inability to visually observe what is occurring inside the core (in the pore space) as the fluids are injected (Bonilla 2013; Rao et. al 2006).

2.4.1. Laboratory-Scale Experiments

This section discusses the laboratory scale research conducted with both micromodels and cores. The enhanced oil recovery techniques that are covered in this discussion are the simultaneous and alternating flooding of surfactant and gas, the flooding of surfactant, and the combined flooding of alkaline, surfactant, and polymer chemicals.

2.4.1.1. Surfactant and Gas Flooding

This section will present an overview of the research work conducted so far on alternating and simultaneous surfactant-gas flooding. First the research conducted using micromodels will be discussed, followed by the coreflooding research.

Micromodel Experiments

Several researchers have investigated the simultaneous or alternating injection of surfactant and gas slugs into glass micromodels. This section will present a chronological overview of the surfactant/gas micromodel flooding research.

Chang et. al (1990) investigated surfactant alternating gas flow in a heterogeneous micromodel (permeability and porosity unstated). Waterflooding, gasflooding, pre-generated foam injection, simultaneous surfactant-gas injection, simultaneous brine-gas injection, and surfactant flooding techniques were investigated. All experiments were conducted at 32^{o}C and 9.1 MPa. The surfactant solution used was Alipal CD-128 at three different concentrations (0.1, 1.0, and 10 weight percents), while the brine used had a salinity of 1.0 weight percent of NaCl, and the oil phase was separator oil from the Malijamar field. The micromodel was first saturated with the crude oil or with the surfactant solution (for experiments in the absence of crude oil). The water-alternating-gas ratio was held constant at 1:4 for any experiments in which liquid and gas were simultaneously injected. It was found that in the absence of oil, increasing the surfactant concentration in simultaneous surfactant-gas injection produced stronger foams. When the foam, either generated in the micromodel or in the external foam generated, encountered an oil phase the foam collasped. The addition of surfactant in all cases increased total oil recovery, though magnitudes of the increase were unstated.

Hornbrook et. al (1991) investigated injecting alternating slugs of surfactant and air into an oil wet, horizontal micromodel with irregular pore sizes (unstated permeability or porosity). The conditions (temperature and pressure) used were not stated. First the micromodel was half saturated with oil with the use of a vacuum pulling oil in through one port, once the micromodel was approximately half full the vacuum was broken and no additional oil was pulled into the micromodel. Then displacing fluid was injected into a port on the opposite end of the micromodel, not filled with oil. Two experiments of injecting displacing fluid were investigated, in the first a surfactant solution (AOS 1618 at unstated concentration) was injected into the micromodel and the interface between the oil and surfactant were observed. In the second experiment, a small amount of surfactant solution was injected into the micromodel, followed by high pressure nitrogen, where the nitrogen generated a foam with the surfactant. Both the surfactant and foam displaced the oil, however the surfactant performed better at displacing the oil as the foam phase would collapse at the foam/oil interface. The magnitude of the oil recoveries achieved were not stated.

Chang et. al (1994) investigated injecting alternating slugs of surfactant or brine with carbon dioxide gas into a horizontal micromodel (unstated permeability or porosity) with structured, differing pore sizes. The conditions used were high pressures (5.3 MPa to 9.1 Mpa) and 90^{o}F (32^{o}C). The fluids used were 1 weight percent NaCl-brine, 1 weight percent Alipal CD-128 surfactant solution in brine, and carbon dioxide gas. Simultaneous surfactant-gas, simultaneuos water-gas, and gasflooding injection schemes were investigated. The micromodel was first flooded with Malijamar crude, followed by injecting surfactant-gas or water-gas slugs simultaneously, or only injecting gas. A surfactant-carbon dioxide foam phase was generated in the micromodel. It was observed that the surfactant-alternating-gas injection scheme produced the greatest oil recovery. In addition to this, higher pressures also produced higher oil recoveries.

Sagar and Castanier (1997), experimenting with a glass micromodel (permeability and porosity unstated) of irregular pore sizes and channels, conducted three experiments. All experiments used a brine with a salinity of 44,000 ppm (4.4 weight percent) The first experiment utilized crude oil as the non-wetting, a brine-surfactant phase (AOS 1618 surfactant with concentrations of 0.01 weight percent and 0.001 weight percent) as the wetting, and carbon dioxide as the gas phase. In this experiment an oil emulsion was formed in the presence of the surfactant, however no foam lamella were observed in the micromodel. In the second experiment, a kerosene phase was used as the wetting phase, brine-surfactant (Nansa-AOS surfactant at concentrations of 0.001, 0.01, 0.1, and 1.0 weight percents) as the wetting phase, and carbon dioxide as the gas phase. Again a kerosene emulsion was formed in some pores, however no foam was observed during the experiment. To investigate the lack of foam, a third experiment was conducted, utilizing a kerosene-surfactant solution (FC 740 surfactant at concentrations of 0.01, 0.1, and 1.0 weight percent) as the non wetting phase, brine as the wetting phase, and carbon dioxide as the gas phase. In this experiment, the kerosene-surfactant solution did create a kerosene-surfactant foam with the carbon dioxide gas.

Sohrabi et. al (2000) investigated injecting alternating slugs of water and hydrocarbon gas into a horizontal glass micromodel (unstated permeability or porosity) at 41 MPa and 38^{o}C. The micromodel was first flooded with water, followed by oil injection to achieve irriducible water saturation. The micromodel was then flooded with water in secondary waterflooding, followed by alternating cycles of gas and water, the slug size and water-alternating-gas ratio was not stated. After five cycles of water and gas, an incremental increase in oil recovery over waterflooding of 11.5% was observed.

Coreflooding Experiments

Research has also been performed in the simultaneous or alternating injection of surfactant and gas slugs into rock cores. This section will present a chronological overview of the surfactant/gas coreflooding research.

Xu and Rossen (2003) investigated simultaneously injecting slugs of brine or surfactant with nitrogen gas into a unfired Berea sandstone core (290 – 300 mD, 21 – 23% porosity) at room temperature and 1 MPa. The surfactants used were Bio-Terge AS-40 and Shell NEODOL 91-8. The brine solution consisted of 1.0 weight percent NaCl and 0.02 weight percent $CaCl_2$; for a total salinity of 1.02 weight percent. These experiments investigated the effect of foam on the fractional flow of water.

Farajzadeh et. al (2009) also investigated surfactant-alternating-gas injection schemes in Bentheimer sandstone cores (1200 ± 100 mD permeability, 22 ± 1% porosity). They used carbon dioxide and nitrogen gas as the gas phase, at 1 bar pressure and unstated temperature. The surfactant used was (C_{14}-C_{16})-alpha-olefin sulfonate, with a concentration of 0.5 weight percent, in a NaCl-brine of 3 weight percent salinity. The oil used was a synthetic oil, Isopar H

(ExxonMobil Chemical). The core was first saturated with brine, then saturated with oil to irriducible water saturation, followed by secondary waterflooding. Then 1 to 2 pore volumes of surfactant were injected, followed by gas injection of an unspecified volume. Foam with both nitrogen and carbon dioxide gas, with the nitrogen gas generating more foam. The water-alternating-gas injection utilizing nitrogen gas resulted in a total oil recovery of 56 ± 2% (an incremental increase of 9.0 ± 0.5% over waterflooding), which the carbon dioxide gas resulted in a total recovery of 50 ± 2% (an incremental increase of 4.0 ± 0.5%). Therefore, nitrogen gas both generated more foam and produced more oil than the carbon dioxide gas.

Salehi et. al (2013 & 2014) experimented with injecting alternating slugs of a surfactant solution and nitrogen into a sand pack core (150 mD, 29% porosity). Salehi et. al (2013) operated at a temperature of 70^{o}C and a pressure of 15.6 MPa. The surfactant solution was created by dissolving sodium dodecyl sulfate in water at an unspecified concentration. The core was first flooded with water, then flooded with oil to reach irreducible water saturation. Nitrogen gas and surfactant solution were then injected alternately at slug sizes of 0.15 PV, injecting a total of 1.2 PV of gas and liquid combined, at a water-alternating-gas ratio of 1:1. Salehi et. al (2013) also experimented with first heating the injection fluids to 120^{o}C before injecting them into the core. A foam phase of surfactant and nitrogen gas was formed in the core. The recovery factors that were achieved were 87% for the alternating injection of heated surfactant and nitrogen, 74% for the alternating injection of ambient temperature surfactant and nitrogen, 62% for the alternating injection of water and nitrogen, 56% for waterflooding, and 50% for gas flooding (Salehi et. al 2013). Salehi et. al (2014) experimented with the sodium dodecyl sulfate surfactant used in Salehi et. al (2013) at 1500 ppm (0.15 weight percent) and nitrogen gas both at 70^{o}C and 14.5 MPa. Several surfactant concentrations ranging from 100 ppm (0.01 weight percent) to 4000 ppm (0.4 weight percent) were investigated to determine the optimum concentration to minimize adsorption onto the rock wall, it was found that 1500 ppm (0.15 weight percent) was optimum. This study was designed to look at the optimum water-alternating-gas ratio between 1:1, 1:2, 1:3, 2:1, and 3:1, with slug sizes of 0.15 PV. A total of 1.2 PV was injected, consisting of 4 cycles each of surfactant injection followed by nitrogen injection (for a ratio of 1:1). The optimum ratio was found to be 1:1, with increasing surfactant slug volumes causing early breakthrough of surfactant solution and decreasing the macroscopic sweep efficiency. The macroscopic sweep efficiency decreased because the increasing surfactant volume decreased the amount of nitrogen available to create foam, and a decrease in foam decreases the macroscopic sweep efficiency. A surfactant/nitrogen foam was generated in these experiments. Likewise, increasing the nitrogen volume compared to the surfactant volume also decreases macroscopic sweep efficiency as there is not enough surfactant present to generate foam and the gas phase causes early breakthrough. Using the optimum ratio of 1:1, it was found that the oil recovery was 87%, while the oil recovery for water-alternating-gas, waterflooding, and gas flooding were 70%, 66%, and 59% respectively.

Shokrollahi et. al (2014) also investigated surfactant alternating gas injection in coreflooding of a sandstone core. Shokrollahi et. al (2014) first investigated the foam stability of anionic (surfactant sodium dodecyl), cationic (cetrimonium bromide), and nonionic (Triton X-100) surfactants and found that anionic surfactants generated the most stable foam, followed by cationic surfactants and nonionic surfactants. Two gases were also investigated, nitrogen and carbon dioxide, it was found that nitrogen generates more stable foam than carbon dioxide. Shokrollahi et. al (2014) investigated two different surfactants in coreflooding, the anioinic surfactant sodium dodecyl sulfate, and the cationic surfactant cetrimonium bromide, nitrogen gas was used as the gas phase. Coreflooding experiments were conducted at 80^{o}C and 17 MPa, with surfactant concentrations of 0.5 weight percent. Water-alternating-gas ratios of 1:0.5 and 1:1 were investigated (without secondary waterflooding), with set slug sizes of 4 cc (0.19 PV), it was not specified if liquid or gas was injected first into the core. It was found that surfactant-alternating-gas injection resulted in an ultimate recovery of 80% for the anionic surfactant sodium dodecyl sulfate, 68.5% for the cationic surfactant cetrimonium bromide, and 62% for water-alternating-gas. It was also found that for ionic surfactants, a ratio of 1:0.5 outperformed a ratio of 1:1.

Abdi et. al (2014) also investigated adding surfactants to the water phase in both waterflooding and water-alternating-gas flooding in a sandstone core with asphaltenic oil. Triton X-100 was used as the surfactant at 0.5 weight percent and carbon dioxide was used as the gas phase. A 10,000 ppm (1 weight percent) brine consisting of NaCl was used for the aqueous phase. All experiments were conducted at 25^{o}C and 6.2 MPa. Three experiments consisted of waterflooding, with one waterflooding experiment including 0.5 weight percent of Triton X-100. Another three experiments consisted of water-alternating-gas injection (without secondary waterflooding) at a ratio of 1:1, starting with water and consisting of 4 water cycles and 3 gas cycles for a total of 1.6 PV injected, for a slug size of approximately 0.22 PV. He concluded that asphaltene disposition decreases oil recovery, but the addition of surfactants lessened the decrease cause by the asphaltenes.

Moayedi et. al (2014) investigated surfactant assisted water-alternating-gas in coreflooding, using Triton X-100 and Iveysol 108 surfactants both at the CMC value and at 0.3 weight percent plus the CMC value, with nitrogen gas as the gas phase, with brine phases of 7000 ppm (0.7 weight percent) and 21,000 ppm (2.1 weight percent). The experiments were conducted at 3.4 MPa and 25°C in a sandstone core (100 mD, 20% porosity). It was found that the surfactants caused a foam phase in the core and resulting in an incremental oil recovery increase of 9%, with Triton X-100 performing the best at the high surfactant concentration. The experiments consisted of secondary waterflooding followed by alternating water (with or without surfactant) and gas injection. It was found that with the first cycle being gas increased oil recovery compared to when the first cycle was surfactant due to the core wettability. However when injecting surfactant-brine before the gas was injected generated the most foam.

2.4.1.2. Surfactant/Brine Flooding

Several researchers compared injecting brine or a surfactant solution into micromodels and rock cores. Jeong and Corapcioglu (2000), Jamaloei and Kharrat (2010), and Hematpour et. al (2012) all investigated injecting surfactant or brine solutions into micromodels. While Bryant and Douglas (1988) and Rao et. al (2006) investigated surfactant flooding in rock cores.

Micromodel Experiments

Several researchers have investigated the injection of brine or a surfactant-brine solution into glass micromodels. This section will present a chronological overview of the surfactant/brine micromodel flooding research.

Jeong et. al (2000) experimented with removing the oil phase as a contaminant and not a desirable product in a glass micromodel. The surfactant used was an anionic surfactant, sodium $C_{14\text{-}16}$ olefin sulfonate (Bio-terge AS-40), at a concentration of 2 weight percent in distilled water, while the gas phase used was unstated. Surfactant flooding, waterflooding, gasflooding, and surfactant foam flooding were all investigated, with each fluid (surfactant, foam, water, and gas being injected for 25 PV). To generate a surfactant foam, the surfactant and gas were first sent through a foam generator which was not described. They found that the surfactant foam increased the amount of oil that could be removed from the micromodel compared to surfactant flooding, which also performed better than waterflooding and gas flooding.

Jamaloei and Kharrat (2010) also investigated surfactant flooding in glass micromodels (unstated permeability and porosity). The brine had a salinity of 0.664 weight percent, while the surfactant used was a petroleum sulfonate at 0.22 weight percent. Each micromodel experiment consisted of first flooding the micromodel with brine, followed by injecting crude oil until the irriducible water concentration was reached. This was followed by injecting brine as a secondary waterflooding, followed by injecting surfactant. The micromodel could be made both oil wet and water wet through conditioning. When the micromodel was water wet, surfactant flooding produced an incremental oil recovery increase of 15.6% of oil originally in place, while for oil wet micromodels, surfactant flooding produced an incremental oil recovery increase of 9.7% of oil originally in place. This suggests that surfactant flooding outperforms waterflooding, and performs better in water-wet conditions.

Hematpour et. al (2012) investigated surfactant flooding in glass micromodels (unstated permeability and porosity). The surfactants investigated were PNX-2360 and linear alkylbenzene sulphonate (LABS), ethanol was used as a co-surfactant to stabilize te surfactant solution, while the synthetic brine the surfactant was in had a salinity of 136,000 ppm (13.6 weight percent). The experiments were conducted at ambient pressures and unstated temperatures, with three different micromodel pore-distribution patterns. The surfactant type (PNX-2360 and LABS), surfactant concentration, and co-surfactant concentration were investigated. It was found that the LABS surfactant performed slightly better than the PNX-2360 surfactant. As well, surfactant concentrations of 2.4, 3.0, and 3.8 weight percent were investigated. It was found that the surfactant concentration did not greatly affect the oil recovery, therefore it was chosen that the lower concentration of 2.4 weight percent would be optimal. It was also found that lower co-surfactant concentrations resulted in higher oil recoveries. Surfactant flooding resulted in a higher total oil recovery than waterflooding, however the magnitude of this difference in oil recovery was not stated.

Coreflooding Experiments

Research has also been performed in the surfactant/brine flooding of rock cores. This section will present a chronological overview of the surfactant/gas coreflooding research.

Bryant and Douglas (1988) experimented with injecting microbes into a berea sandstone sore (unstated permeability and porosity) and a glass micromodel (unstated permeability and porosity). One microbe produced carbon dioxide, while the other produced a surfactant. Both the core and micromodel were flooded with oil and then brine to reach residual oil. The cores were then flooded with 0.2 PV of microbial solution (concentration of 100,000 cells/mL) and 0.3 PV of molasses solution (for the microbes). The cores were then incubated at 37oC for 1 week and then flooded with brine. It was observed that the microbes could recover an average 32.2% of the residual oil in the core, for a total oil recovery of 73.6%. The surfactant producing microbes increased the oil recovery more than the carbon dioxide producing microbes, however the carbion dioxide producing microbes gave more consistant results. For the micromodel experiments, the micromodel was waterflooded after 3 days of incubation. The waterflooding of the surfactant producing microbe performed better than the carbon dioxide producing microbe, though the magnitude of the difference is not stated.

Rao et. al (2006) conducted coreflooding experiments using stock tank oil (oil at atmospheric conditions which contains little to no dissolved gases), live oil (oil that does contained dissolved gases), and brine from the Yates reservoir in the United States of America. The relationship between the ability of surfactants to alter the wettability of a rock surface and the recovery of oil was investigated. Two surfactants, the non-ionic ethoxy alcohol and anionic ethoxy sulphate, were used in the experiments. The cores were first fully saturated with Yates synthetic reservoir brine, followed by flooding with either stock tank oil or live oil, followed by flooding with Yates synthetic reservoir brine. Then the cores were flooded with Yates synthetic reservoir brine containing different concentrations of surfactants (500, 1500, 3500, and 5000 ppm; 0.05, 0.15, 0.35, and 0.50 weight percent) for 3.0 PV. The experiments were carried out at Yates reservoir conditions (28^{o}C, 4.8 MPa) and the core wettability was altered by aging the core for one week in the desired fluid. Table 2-1 provides an overview of the results obtained in these experiments. As shown in Table 2-1, surfactants generally increase oil recovery, except in the case of anionic surfactants with live oil in initially oil wet reservoirs. The oil recovery mechanisms observed were the alteration in wettability and reduction in interfacial tension.

Table 2-1. Yates Reservoir Core Flooding Results (Rao et. al 2006)

	Initially Water Wet		Initially Oil Wet			
Surfactant	Non-Ionic	Anionic	Non-Ionic		Anionic	
			Tank Oil	Live Oil	Tank Oil	Live Oil
Concentrations (ppm)	0 – 5000	0 – 3400	0 – 5000	0 – 5000	0 – 5000	0 – 5000
Optimum Concentration (ppm)	3500	3400	3500	1500	1500	0
Reason	No change in oil recovery above 3500 ppm.	Emulsion formed at 3400 ppm	Decrease in oil recovery above 3500 ppm.	Decrease in oil recovery above 1500 ppm.	Decrease in oil recovery above 1500 ppm.	Decrease in oil recovery above 0 ppm.
Initial Wettability	Water	Water	Strong Oil	Weak Water	Strong Oil	Weak Water
Final Wettability	Weak Water	Weak Water	Weak Oil	Intermediate	Weak Oil	Oil Wet
Main oil	Wettability	Wettability	Interfacial	Wettability	Interfacial	Wettability

recovery mechanism	Alteration	Alteration	Tension Reduction and Wettability Alteration	Alteration	Tension Reduction and Wettability Alteration	Alteration
Incremental oil recovery	38%	26%	5.8%	20%	5%	0%

From the results of Rao (2006), it appears that there is an increase in oil recovery as the wettability of the core becomes more neutral. Moving to a less oil wet, more water wet state is associated with an increase in oil recovery.

2.4.1.3. Combined Alkaline/Surfactant/Polymer Flooding

Several researchers have investigated the injection of alkaline, surfactant, and polymer chemicals into glass micromodels. This section will present a chronological overview of the surfactant/gas micromodel flooding research.

Romero et. al (2002) investigated injecting alternating slugs of surfactant-polymer and nitrogen gas in a horizontal glass micromodel (78,000 mD, 50% porosity) at ambient conditions. The surfactant used was C_{14}-C_{16} alpha-olefin sulfonate (AOS) (1.0 weight percent), the polymers used were polyacrylamindes (0.1 weight percent), and the brine was a Lake Maracaibo synthetic reservoir brine. The critical micelle concentrations for the surfactant solutions ranged from 0.000012 weight percent to 0.000015 weight percent, therefore the solutions were between 66,000 and 83,000 times the critical micelle concentration. A foam phase was generated outside of the micromodel in a foam generator, consisting of a small core of packed glass beads.

It was found that low molecular weight polymers resulted in a more stable foam when compared with high molecular weight polymers. Oil recovery data was not recorded.

Dong et. al (2006) investigated with alkaline flooding in water wet micromodels (permeability and porosity unstated). The chemicals used were NaOH and Na_2CO_3 alkalines and the surfactant Stepanol Me Dry (sodium lauryl sulfate). The micromodel was saturated with water and then flooded with heavy oil at 60^oC. A secondary waterflooding was carried out for 2 PV at 60^oC. After this, an alkaline flood was conducted at ambient temperature, pressures for the experiment are not stated. The alkaline flooding resulted in increased oil recovery compared to waterflooding, though the magnitude of this increase is not stated.

Jamaloei et. al (2012) investigated surfactant-polymer flooding in horizontal, oil wet glass micromodels (permeability and porosity unstated). The injection fluid had a concentration of 0.2 weight percent petroleum sulfonate surfactant, 0.0125 weight percent Xanthan (polymer), and varying salinities (0.079 weight percent to 0.79 weight percent). The micromodel was first saturated with crude, followed by polymer-surfactant solution flooding. It was found that the surfactant decreased the interfacial tension, while the viscosity decreased with increasing salinity, oil recovery was not measured.

Esmaeili et. al (2013) investigated with alkali-surfactant-polymer flooding in a glass micromodel designed with dead-end pore channels (permeability and porosity unstated). The surfactant used was sodium dodecyl sulfonate (0.2 weight percent and 0.1 weight percent), the alkaline used was sodium carbonate (1.0 weight percent and 0.5 weight percent), and the polymer used was polyacrylamide (0.12 weight percent and 0.06 weight percent). The brine used had a concentration of 1 weight percent NaCl. The micromodels were first saturated with oil, followed by the injection of the alkaline-surfactant-polymer solutions. It was found that the including dead-end pores in directions perpendicular to the direction of flow produced the highest oil recovery of all cases investigated. The addition of polymer to alkali-surfactant flooding increased oil recovery, while alkali-surfactant flooding increased oil recovery from baseline waterflooding. In cases with low polymer concentration and low salinity, increasing the surfactant and alkali concentration resulted in a decrease in oil recovery. The exact magnitude of the differences in oil production were not stated.

2.5. Field Applications

This section will discuss field applications for the various surfactant application methods. Table 2-2 provides and quick overview of all of the field applications which will be discussed in the following sections, further details on each field application can be found in the sections below.

Table 2-2. Overview of Selected Field Applications

Field Application	Method	Results
Daqing	Surfactant	Decreased watercut (by 8.7%) and increased oil recovery (4.6 – 5.4%). Net economic benefit
Yates	Surfactant Soak	Increased oil recovery
Cotton Creek	Surfactant Soak	Increased oil recovery
7th Chinese Gudong	Surfactant/Polymer Flood	Decreased watercut and increased oil recovery
7th Chinese Gudong	Alkali/Surfactant/Polymer	Increased oil production
Snorre	Foam Assisted Water-Alternating-Gas	Decreased gas-oil ratio, accelerating oil production

2.5.1. Surfactant Injection

Many papers listed surfactant flooding this as a common practice (Iglauer et. al 2010), with one describing the design (Cooper et. al 1985), however published research on the results of these field applications is lacking. One paper discussing the results of a surfactant flood at the Daqing oil field in China and another discussing the foam-assisted-water-alternating-gas flood at the Snorre field in Norway are discussed. Two additional field applications discussed here are applications in which the surfactant is injected into the production well and shut in for the surfactant to "soak" into the reservoir.

2.5.1.1. Chinese Daqing Field

The Daqing oil field is China's largest oil field, accounting for nearly 25% of China's oil production (Tang et. al 2010). As China's largest and most important field, numerous chemical enhanced oil recovery pilot tests have been conducted, including surfactant flooding, micellar-polymer flooding, alkaline flooding, alkaline/surfactant flooding, alkaline/surfactant/polymer flooding, alkaline flooding, and alkaline/surfactant/polymer-foam flooding (Pu and Xu 2009). During preliminary core studies, the incremental oil recovery increased between 4.6% and 5.4%. During field tests, the surfactant concentrations ranged between 0.5 and 2.0 weight percent (5,000 ppm to 20,000 ppm), while the incremental oil recovery increase ranged between 0.88% and 1.47%, with the higher recovery being associated with higher surfactant concentration. Overall, the net economic benefit of the surfactant pilot test was approximately $480,000 CAD, with a cost to revenue ratio of 1:3 (Yin and Pu 2008).

2.5.1.2. American Yates Field

The American Yates Field is a naturally fractured carbonate dolomite field discovered in 1962. Several enhanced oil recovery techniques have been evaluated in this reservoir, including surfactant flooding (Manrique et. al 2004). The surfactant used was a non-ionic ethoxy alcohol (Shell 91-8), diluted with produced water to concentrations between 0.31 and 0.3880 weight percent (3100 ppm and 3880 ppm, both above the critical micelle concentration). Surfactant slugs were injected into production wells to the oil-water transition zone using both single and multi-well injection strategies. The wells were then shut in for a brief period of time termed the “soak time”, after which the wells were returned to productivity (Manrique et. al 2004). The surfactant increased the recovery of oil through a reduction of interfacial tension, and wettability alteration (although to a lesser extent). The degree to which the interfacial tension or wettability were altered was not given (Manrique et. al 2004). One of the test wells was recorded as increasing the production from 35 barrels per day (5.6 sm^3/d) before the surfactant injection to 67 barrels (11 sm^3) per day after the surfactant injection with an increment of 17,000 barrels (2700 sm^3) of oil at the time of the reports publication. The field results identified surfactant injection as an economically encouraging enhanced oil recovery technique. (Manrique et. al 2004)

2.5.1.3. American Cotton Creek Field

The American Cotton Creek Field is a Carbonate Dolomite class II (low matrix porosity and permeability) field (Manrique et. al 2004). A surfactant solution at a concentration of twice the CMC of non-ionic poly-oxyethylene alcohol (POA) surfactant was injected into the production wells with amounts ranging from 500 to 1,500 bbl (80 sm^3 to 240 sm^3) of solution depending on the well perforation interval. Injection required approximately three days, followed by a shut in (soak time) of one week. Initial results were below expectations due to the loss of surfactant from adsorption to the reservoir rock. The surfactant concentration was increased to 0.15 weight percent (1500 ppm) to account for loss due to adsorption. The unspecified increase in oil recovery was attributed to wettability alteration (increased water-wet) rather than a decrease in interfacial tension. (Manrique et. al 2004)

2.5.2. Surfactant/Polymer Injection

There are several examples of surfactant/polymer flooding field applications (Bou-Mikael et. al 2000; Gurgel et. al 2008). The Chinese Gudong field was chosen for discussion because of the extensive results provided.

The Chinese Gudong 7th oil field is a sandstone reservoir located in the Yellow River delta in the north-east section of Shandong province, China (Hongyan et. al 2009) with a permeability of 3.8 Darcy and a porosity of 35% (Zhijian et. al 1998). The pilot test included 26 wells (16 production wells and 10 injection wells), along with 3 observation wells. Before the pilot test, the water cut was 98.2% and the oil recovery was 34.4%. A three slug injection strategy was designed to prevent excessive fingering and cross flow in the reservoir. The first slug consisted of a polymer solution of 0.2 weight percent and 0.05 PV (poly pre-protection), the second slug consisted of 0.17% polymer, 0.45% SLPS (main surfactant), and 0.15% #1 (secondary surfactant) and 0.3 PV, the third slug consisted of 0.15% polymer and 0.05 PV. The field results included a reduction in water cut of 13% (from 98.2% to 85.2%), and an increase in oil production by 144,000 kg/day (from 31,000 kg/day to 175000 kg/day). The oil recovery increased 4.15%. Laboratory tests compared surfactant/polymer and polymer injections and determined that surfactant/polymer injections produce more favorable results compared to polymer only injections (Hongyan et. al 2009).

2.5.3. Alkali/Surfactant/Polymer Injection

The Alkali/Surfactant/Polymer injection technique has received a great deal of interest in the past few decades for its apparent superior performance over surfactant or surfactant/polymer floods (Thomas 2007) (Wyatt et. al 2002).The Chinese Gudong field was chosen for discussion because of the extensive results provided.

A different section of the Chinese Gudong field than in Section 2.5.2 was evaluated using the alkali/surfactant/polymer technique. Before the ASP flood the reservoir was waterflooded, resulting in an oil recovery of 54.4% and a remaining oil saturation of 35.1%, with a water cut of 98.4% (Zhijian et. al 1998). The pilot test included 4 injectors, 9 producers, and 2 observation wells. The injection process was designed to consist of 5 stages. First a 0.05 PV 0.1% 3530S (polymer) slug was injected to improve mobility. Second, a chemical slug of 0.05 PV 1.5% Na_2CO_3 (alkali), 0.2%OP10 (surfactant), 0.2% CY1 (surfactant), and 0.1% 3530S (polymer) was injected. The third slug was the main slug, consisting of 0.35 PV 1.5% Na_2CO_3 (alkali), 0.2% OP10 (surfactant), 0.2% CY1 (surfactant), and 0.1% 3530S (polymer). The fourth slug consisted of 0.1 PV 0.05% 3530S (polymer). The total amount of ASP injected was designed to be 0.55 PV. This is followed by injecting Yellow River water and produced water continuously at a rate of 400 m^3/d (Zhijian et. al 1998). It was recorded that the oil extracted using the ASP technique contained heavier components. The oil produced from Well 7 increased in middle-heavy aromatic hydrocarbons from 61.1% to 76.1%. The content of non-hydrocarbon and asphalt increased from 35.4% to 41.3%. The ASP technique also increased the sweep efficiency, demonstrating an even frontal advance, resulting in 70% of the gross reservoir thickness being well swept. The residual oil saturation decreased from 35.1% to 23.2% on average, resulting in an increased oil recovery of 13.4% oil originally in place or 30% recoverable oil originally in place (Zhijianet. al 1998).

2.5.4. Surfactant Assisted Water-Alternating-Gas

The surfactant assisted water-alternating-gas technique has recieved attention recently due to its ability to create foam. One field application, the Snorre field in Norway, is discussed.

The Snorre field is one of Norway's major offshore oil fields. A foam-assisted-water-alternating-gas trial was conducted on the field between 1997 and 2000 to test the ability of foam to control gas mobility. The trial was conducted in the central and western fault blocks, with permeabilities in the range of 400 to 3,500 md. The surfactant used was an alpha-olefin-sulphonate surfactant and the gas phase was natural gas. The trial was conducted in a surfactant-alternating gas technique, with a total of 2,000 tons of surfactant being used. The trial was divided into four sections, mobility control tests in two wells, gas shut off test in one well, and an injection test in another well. If the gas-oil ratio (GOR) of a production well can be reduced on a well that is restricted due to gas (well life is associated with GOR), then the ultimate oil recovery from that well can be increased by delaying the well end-of-life. The surfactant concentration used ranged from 0.2% to 0.5%, however the CMC value of the surfactant was not specified (Blaker et al. 2002). As well the surfactant injection was split into two slugs, separated by a gas slug, however the WAG ratio was not specified. The gas shut off test created a strong foam in-situ, reducing the GOR by 50% over a period of two months and resulting in a project payback of 12 days. This increased oil production by producing more oil from lower zones in the reservoir which would have its flow restricted due to high GOR (Shabib-asl et. al 2014). The gas shut off and injector tests had to be stopped due to fracturing and gas leakages in the injector well. The gas mobility tests resulted in reducing the free back-produced gas by 33%, reducing the GOR and allowing accelerated oil production (Shabib-asl et. al 2014; Blaker, et al., 2002). The exact production/recovery increases were not specified, however the project was deemed a success as it generated 25 to 40 million USD (Skauge et. al 2002).

2.6. Experimental Factors

This section will discuss the experimental factors that were chosen for this research and their justification. The four factors that were chosen include the water-alternating-gas ratio (WAG ratio), surfactant concentration, gas type, and surfactant type. The brine solution used was a synthetic brine solution that matches the composition and salinity of Atlantic sea water, with a salinity of 35,000 ppm. No experimental research using this composition and salinity brine could be found in literature. Crude oil from the Hibernia reservoir offshore Newfoundland and Labrador, Canada, was used as the oil phase. Oil recovery experiments utilizing Hibernia crude oil have only been conducted by Moayedi et. al (2014) to date, with experiments involving coreflooding. No micromodel oil recovery experiments with 32-36^{o} API crude oil have been published to date.

All of the published studies evaluated did not make use of any statistical design of experiments software that allows for identifying interaction effects between different factors (WAG ratio and surfactant concentration, surfactant type, or gas type).

2.6.1. WAG Ratio

The Water-Alternating-Gas (WAG) ratio is the ratio of the volume of a water slug to the volume of a gas slug. Salehi et. al (2013; 2014) investigated WAG ratios of 1:1, 2:1, 3:1, 1:2, and 1:3 in a core of packed sand, using a surfactant solution and nitrogen gas. It was found that a WAG ratio of 1:1 resulted in the highest macroscopic and microscopic sweep efficiencies, leading to the highest recovery of oil. Motealleh et. al (2012) also experimented with core flooding and water/carbon dioxide injection in a WAG injection scheme. It was found that a WAG ratio of 1:1 was optimal, and that slug sizes of 20% of the pore volume were effective. Shokrollahi et. al (2014) experimented with coreflooding with surfactants and carbon dioxide and nitrogen gases in a WAG injection scheme with WAG ratios of 1:1 and 1:0.5. It was found that a WAG ratio of 1:0.5 produced the best results for these experiments. Feng et. al (2014) experimented with water-alternating-gas injection in a heterogeneous micromodel using water and reservoir gas. They investigated WAG ratios of 3:1, 2:1, 1:1, 1:2, and 1:3, finding that a WAG ratio of 1:1 produced the highest recovery of oil.

This study utilized the common range of WAG ratios (1:1 to 1:2) that have been investigated by other researchers to identify any interaction between the WAG ratio and any other factors that are being investigated (surfactant concentration, gas type, and surfactant type). It was also decided to further investigate the gap between the WAG ratios of 1:1 and 1:2. As discussed above, Shokrollahi et. al (2014) investigated a WAG ratio of 1:0.5, however no research could be found for a WAG ratio of 1:1.5, between 1:1 and 1:2. Therefore it was decided to further investigate the gap between 1:1 and 1:2 in the research to evaluate a point between these commonly studied WAG ratios.

The size of the injected slugs was taken from Motealleh et. al (2012), who found that slug sizes of 20% of the pore volume, or 0.2PV, was an efficient slug size. Therefore the slug size of 0.2PV was chosen as the baseline slug size. The total injection volume of 1.2 pore volumes for each liquid and gas phase was taken from Salehi et. al (2013), who injected the fluids until 1.2 pore volumes was injected. This is corroborated with the findings of Feng et. al (2014) that found that recovery increased with increasing cycles of water and gas. Feng et. al (2014) investigated increasing the number of cycles from one to five, with recovery steadily increasing with increasing cycle number. It was decided to use a slug size of 0.2 pore volumes, and having a total injection of 1.2 pore volumes of fluid, it was decided to inject six cycles each of liquid and gas to make up the experiment (1.2 pore volumes of both liquid and gas in 0.2 pore volume slugs). The volumes of the gas slug and total injected gas increases with WAG ratio, therefore for a WAG ratio of 1:1.5 the gas slug was 0.3 PV, giving a total injected gas volume of 1.8 PV. Likewise for a WAG ratio of 1:2 the gas slug was 0.4 PV, with a total injected gas volume of 2.4 PV. Table 2-3 provides the ratio and volume data for the WAG ratios used.

Table 2-3. Water-Alternating-Gas Ratios and Volumes

WAG Ratio	Liquid Volume (PV)	Gas Volume (PV)
1:1	0.2	0.2
1:1.5	0.2	0.3
1:2	0.2	0.4

2.6.2. Surfactant Concentration

The concentration of surfactant in a solution is either a volume or weight percent of the surfactant in the solution. Shokrollahi et. al (2014) investigated three different surfactants, keeping the surfactant concentration at 0.5 weight percent for all experiments. Moayedi et. al (2014) investigated surfactant concentrations at the CMC and at 0.3 weight percent plus the CMC. Chang et. al (1990) used one surfactant, varying the concentration from 0.1 weight percent, 1.0 weight percent, and 10.0 weight percent. Sagar and Castanier (1997) investigated three different surfactants at different concentration levels in weight percent (0.001%, 0.01%, 0.1%, and 1.0%).

It has been suggested that surfactant should be injected around the CMC value for nonionic surfactants (Gurgel et. al 2008), therefore it was decided to experiment with surfactants at and above the CMC value.

As discussed in Section 2.2.3, the behavior of the surfactants differ above and below the CMC, therefore to be able to compare different surfactants equally, it was decided to vary the concentration in proportion to the critical micelle concentration. This is a different method of varying the concentration than was used in all of the studies discussed above as Shokrollahi et. al (2014), Chang et. al (1990), and Sagar and Castanier (1997) all varied the concentration by weight percent, while Moayedi et. al (2014) used a combination weight percent and CMC varying method by investigating at CMC and a set weight percent above CMC.

This method of varying by total concentration instead of proportionally from CMC leads to the possibility of one surfactant performing better than another when varied proportionally from CMC, but underperforming when compared on a total concentration basis.

Therefore the concentration was varied by multiples of the critical micelle concentration, meaning two different surfactants at the same proportional concentration point may have different total solution concentrations. The concentration was varied from one (1) times the critical micelle concentration to ten (10) times the critical micelle concentration, with a centre point at 5.5 times the critical micelle concentration. The values of one, five-and-a-half, and ten times the critical micelle concentration were chosen to obtain a baseline at the critical micelle concentration, at which point many physiochemical properties change, and data points above the critical micelle concentration. The upper limit of ten times the critical micelle concentration was chosen arbitrarily as the upper limit as research to identify an optimal range of concentrations based on the critical micelle concentration does not exist.

The total solution concentrations used are presented in Table 2-4. As is shown in Table 2-4, if the Triton X-100 and Iveysol 106 surfactants were compared on a total concentration basis and not on a proportional concentration from CMC basis, at ten times the CMC, the Iveysol 106 concentration would have a value of twice the Triton X-100 concentration.

Table 2-4. Surfactant Concentrations

Triton X-100		**Iveysol 106**	
CMC Proportion	**Total Concentration (weight %)**	**CMC Proportion**	**Total Concentration (weight %)**
CMC x 1	0.015	CMC x 1	0.0287
CMC x 5.5	0.083	CMC x 5.5	0.158
CMC x 10	0.150	CMC x 10	0.287

2.6.3. Gas Type

In water-alternating-gas, the choice of the gas phase is very important, air, nitrogen, carbon dioxide, hydrocarbon gas (methane-decane mixture), and reservoir gas has all been used as the gas phase in micromodel and coreflooding experiments as previously discussed in Section 2.4. Table 2-5 provides an overview of the gases that have been used by other researchers.

Table 2-5. Gas Phases Previously Investigated

	Air	Carbon Dioxide	Nitrogen	Hydrocarbon	Reservoir Gas
Hornbrook et. al (1991)	X				
Chang et. al (1994)		X			
Farajzadeh et. al (2009)		X	X		
Motealleh et. al (2012)		X			
Shokrollahi et. al (2014)		X	X		
Xu and Rossen (2003)			X		
Sohrabi et. al (2000)				X	
Feng et. al (2014)					X
Moayedi et. al (2014)			X		

This study utilizes two different gas phases to investigate the gases on their own and in comparison to one another. For the first gas phase, air was chosen as the gas phase as it is both a less studied gas phase for WAG injection, and is cheap and readily available for use by industry. For the second gas phase, propane gas was chosen as the gas phase as it is readily available and can simulate a rich reservoir gas. The choice of air and propane allows for the investigation of air and propane by themselves, along with comparing air to a hydrocarbon gas. Due to the ambient conditions operated under, it is not possible to take advantage of any pseudo-miscible aspects of using a hydrocarbon gas..

2.6.4. Surfactant Type

As discussed in Section 2.4, various types of surfactants have been used previously. Rao et. al (2006) used nonionic and anionic surfactants in coreflooding experiments, while Shokrollahi et. al used nonionic, anionic, and cationic surfactants in coreflooding experiments.

Two nonionic surfactants were investigated; their choice was based on their availability to the researchers and the advantages of non-ionic surfactants over other types of surfactants. In coreflooding experiments, Rao et. al (2006) found that non-ionic surfactants produced a higher oil recovery than anionic surfactants. Using concentrations ranging from 0% to 0.35% for non-ionic surfactants, oil recoveries ranged from 56% to 94%, while oil recoveries with anionic surfactants ranged from 52% to 78%. This is due to the fact that non-ionic surfactants do not react chemically to either the reservoir rock or fluid, while anionic surfactants can react chemically with the reservoir rock or fluid to create a more acidic environment.

The two surfactants investigated were Triton X-100 and Iveysol 106. Triton X-100 has only recently been used in research, mainly by Abdi et. al (2014) and Moayedi et. al (2014), while Shokrollahi et. al (2014) used it for foam tests but did not conduct any coreflooding experiments with it.

Research using Iveysol surfactants for enhanced oil recovery has used Iveysol 108 surfactant (Moayedi et. al 2014), however no research utilizing Iveysol 106 surfactant has been published. Therefore it was decided to utilize the Iveysol 106 surfactant due to the lack of research available.

2.7. Experimental Design

Design of Experiments is a collection of various statistical design methods that assist in pre-planning, planning, and analysis stages of conducting any type of experiment. These methods work for any type of experiment where independent variables are altered to observe the change in other dependent variables. This is generally done to better understand how certain variables have an effect on other variables in a closed system. The altered variables are termed factors, while the variables being observed are termed responses.

A designed experiment consists of altering multiple factors at the same time while measuring the responses. This differs from the typical one-factor-at-a-time method of altering only one factor for every experimental run. Designed experiments are superior to the one-factor-at-a-time method as they are more efficient by requiring less experimental runs to examine the same number of factors and allow for the identification of interactions between two factors. The one-factor-at-a-time method has a disadvantage where it is impossible to identify interactions between two or more factors (Czitrom, 1999).

One subset of designed experiments is termed response surface methodologies. Optimal designs are one type of response surface methodology, and are used to create custom designs which incorporate both numerical (continuous) and categorical (discrete) values (Stat-Ease 2014). Design of Experiments software, offered by Stat-Ease, can be utilized to design experiments based on various design of experiments methods, analyze those designs for statistical error, and analyze the results of those experiments.

The Design of Experiments software uses the analysis of variance (ANOVA) method to model the relationships that may exist between the different variables that are being studied, either individually or interaction effects between two or more factors, and the responses that are being measured. This method is also capable of identifying any non-linearity in these factor(s)-response relationships utilizing centre-points. The ANOVA method measures the effect of each individual factor and any interaction effects between two or more factors by calculating the variance. This is done by dividing the sum of the squared error over the degrees of freedom. The ANOVA method predicts the upper and lower levels for the 90% confidence level for each effect being investigated; this is done by calculating the p-value which tests the null hypothesis and the significance of the regression model. If the p-value is larger than 0.10, the probability of the effect being investigated being due to error and not the altered factor(s) increases and the effect does not fit into the 90% confidence interval. Therefore if the p-value is greater than 0.10, the effect is deemed not significant, however if the p-value is less than 0.10 the effect is deemed significant.

As the p-value is only the calculated statistical measure of whether or not the observed effect is due to the altered factors or just random error, various cut-off values for the p-value can be used to determine whether the factor is significant or not significant. Values of 0.1, 0.05, and 0.01 are commonly used to determine statistical significance, corresponding to a 10%, 5% and 1% chance that the effect is due to error and not the factor being investigated (National Institute of Standards and Technology 2013). Therefore for this research, a p-value of 0.1 was chosen to determine statistical significance.

The ANOVA method is dependent on the model identified by the user as being appropriate for the data. Therefore various models (linear, two-factor interaction, quadratic, etc) should be investigated to determine which model fits the data the best. From the ANOVA method, significant factors that influence the result can be identified and a mathematical model to predict the response based on the significant factors can be identified.

Chapter 3: Experimental Methodology

A series of experiments were conducted in glass etched micromodels to investigate how various factors, including water-alternating-gas ratio, surfactant concentration, surfactant type, and gas type, influence the surfactant assisted water-alternating-gas enhanced oil recovery technique, ideally having the surfactant create a foam phase inside the porous media to take advantage of the added benefits of the foam assisted water-alternating-gas technique. A glass micromodel was chosen for the experiments, micromodel MIM DC2 from Dr. Lesley James (42% porosity, 130 μm^2 permeability) (James et al. 2009). This chapter details the experimental system and procedures used for the micromodel tests. This includes the equipment and experimental design.

3.1. Equipment

This section discusses the equipment used for the low pressure micromodel experiments. The equipment used for the interfacial tension and viscometer experiments is also discussed briefly. These two experimental setups are only discussed briefly because they were purchased as standalone systems, and therefore the manufacturer supplied procedures were followed. This section focuses on the low pressure micromodel system which was created to conducted low pressure water-alternating-gas enhanced oil recovery experiments. A schematic of the micromodel system is given in Figure 3-1 and Appendix A, along with the procedures used in Appendix B. Figure 3-2 provides an image of the micromodel to define the dimensions of the micromodel.

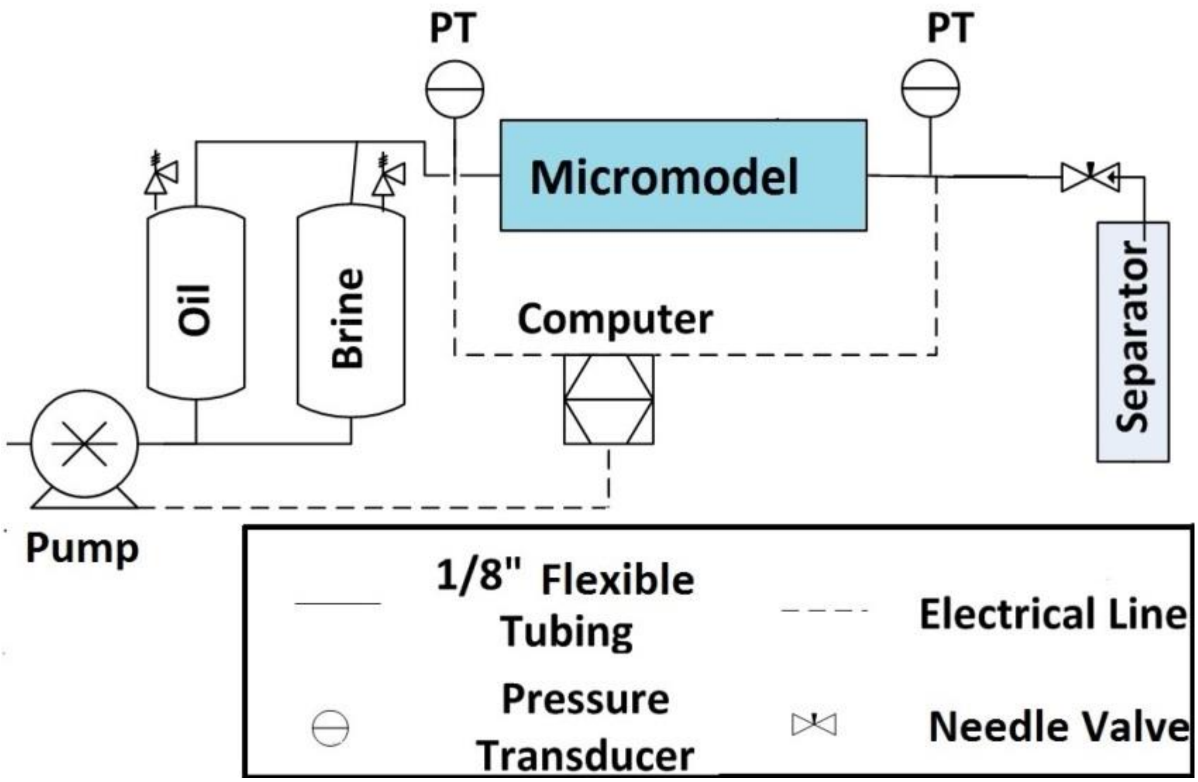

Figure 3-1. Diagram of Micromodel System (Khezrnejad et. al 2014)

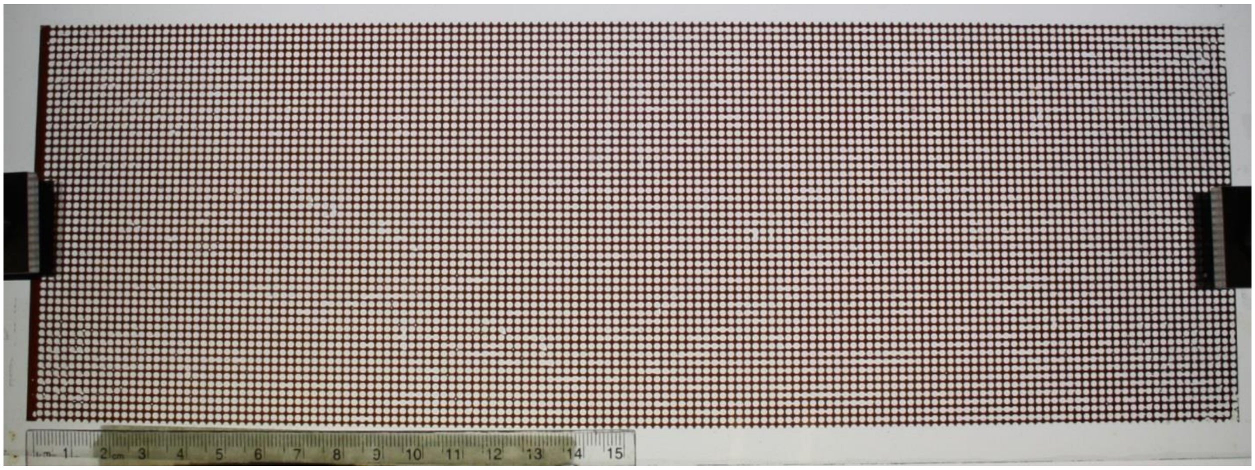

Figure 3-2. Micromodel with scale

3.1.1. Pressure and Temperature Indicators

The experimental system has two pressure indicators and two temperature indicators, located directly upstream and downstream of the micromodel. The indicators are used to monitor the conditions of the fluid within the system mainly as a safety precaution. The temperature indicators used are TC-T-1/8 NPT-G-72 thermocouples from OMEGA, with an accuracy of 1^{o}C and a range of -270^{o}C to 400^{o}C, which connect to a OM-USB-TC-AI Data Acquisition system from OMEGA with an accuracy of 0.5^{o}C. Therefore the total accuracy of the temperature monitoring system using the sum of squares method is 1.12^{o}C:

$$Error = \sqrt{(1°C)^2 + (0.5°C)^2} = 1.12°C\,.$$

The pressure indicators used are PX409-100AUSBH High Accuracy USBH Pressure Transducers from OMEGA, which connect directly to a USB port on a computer. This pressure transducer has an accuracy of 0.08% of the range of the unit, which is 0 psia to 100 psia; therefore the transducer has an accuracy of +/-0.08 psia.

3.1.2. Syringe Pump and Syringes

The syringe pump that was used is a KDS Gemini 88 Syringe Pump, which has an accuracy of ±0.35% of the dispensing rate over a dispensing range of $4.0*10^{(-7)}$ mL/hr to 6396 mL/hr. For this research we used a liquid flow rate of 1.16 mL/hr and a gas flow rate of 2.32 mL/hr, therefore the flow rates were 1.160 ± 0.004 mL for the liquid and 2.315 ± 0.003 ml/hr for the gas. This syringe pump is a dual-syringe, dual-rate pump, which allows the independent operation of two syringes at one time, with each syringe either injecting, withdrawing, or remaining stable.

The syringe pump was used with two KR Analytical 100 mL gas tight stainless steel syringes. These gas tight syringes are used to hold both the liquid and gas injection fluids. In addition to the main syringe pump syringes, 20 mL and 30 mL KDS glass syringes were utilized for the manufacture of injection fluids and the cleaning and initial preparation of the micromodel system.

3.1.3. Micro Separator

The micro separator was constructed out of a 10 mL PYREX borosilicate glass burette with a custom attachment created by Memorial University of Newfoundland's Department of Technical Services. Figure 3-3 is a diagram of the micro separator that was attached to the top of the 10 mL burette.

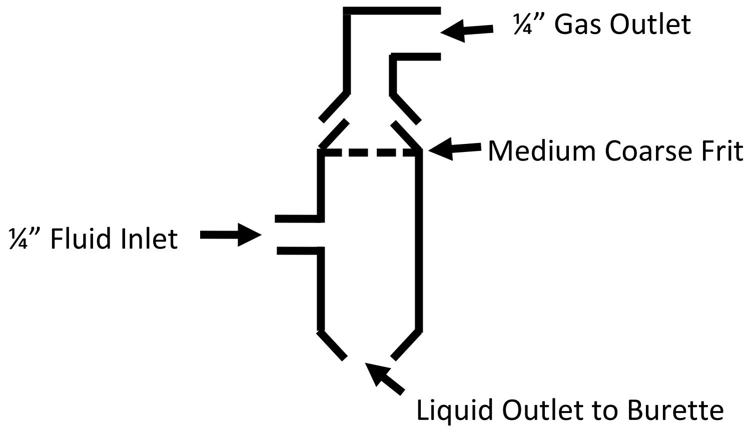

Figure 3-3. Diagram of Micro Separator

The micro separator is designed to separate the liquid effluent from the gaseous effluent, and to also provide a space in which any remaining foam or emulsions may be allowed to collapse. There is a medium coarse frit near the gas outlet to prevent any liquids from escaping in the gas outlet, and to act as a maximum height for any foam. The custom attachment allows gaseous fluids to escape the separator through the frit, while the liquid fluids are drained into the burette for measurement.

3.1.4. Brine Solution

A brine solution simulating the salinity of sea water was used for the experiments. This is because the oil and gas operations offshore Newfoundland & Labrador generally use seawater for injection water, therefore a simulated seawater accurately represents the water used in offshore oil and gas injection strategies. The simulated seawater was created utilizing Sodium Chloride (NaCl), Sodium Sulfate (Na_2SO4), Calcium Chloride ($CaCl_2$), Sodium Bicarbonate ($NaHCO_3$), Potassium Iodide (KI), and Magnesium Sulfate ($MgSO_4$) salts acquired from Fisher Scientific. These salts were added to distilled water to create a salinity mimicking the salinity of Atlantic sea water, the composition of which is given in Table 3-1. The total salinity of seawater is generally 35 parts per thousand (Anderson 2008).

Many researchers have used synthetic brines, with common values of 7,000 ppm (Jamaloei and Kharrat, 2010), 10,000 ppm (Abdi et. al 2014; Xu and Rossen 2003; and Chang and Martin 1994), and 136,000 ppm (Hematpour et. al 2012). Injection of sea water is common offshore

Newfoundland and is a motivation to investigate the effect of such saline water on oil recovery. As well, no research has been found using such saline water.

Table 3-1. Chemical Ions in Sea Water (Anderson 2008)

Chemical Ion	Concentration (parts per thousand)	Proportion of Total Salinity (%)
Chloride	19.345	55.03
Sodium	10.752	30.59
Sulfate	2.701	7.68
Magnesium	1.295	3.68
Calcium	0.416	1.18
Potassium	0.390	1.11
Bicarbonate	0.145	0.41
Bromide	0.066	0.19
Borate	0.027	0.08
Strontium	0.013	0.04
Fluoride	0.001	0.003
Other	Less than 0.001	Less than 0.001

To this base brine solution, methylene-blue was added to colour the water a blue colour. This dye assisted in distinguishing the water phase from the oil and the glass in the micromodel, without which it is very difficult to distinguish between injection fluids and glass.

3.1.5. Oil

Dead crude oil (oil at sufficiently low pressure that there is no dissolved gas in the oil) from the Hibernia field, offshore the province of Newfoundland & Labrador, Canada was used for the oil phase in all of the experiments conducted. This oil is a dead, light, sweet crude oil with a density of approximately 0.870 g/cm^3 based on Anton Paar mPD55 densometer tests.

3.1.6. Fluid Characterization

The interfacial tension experiments were conducted using a Vinci Technologies interfacial tension apparatus model IFT 700 machine. This instrument uses the pendent drop and rising bubble methods to calculate the interfacial tension between two fluid phases, and can also be used to determine the contact angle between two fluid phases and a solid surface.

The rising-bubble/pendent-drop method measures the interfacial tension between two immiscible liquid phases. The instrument is a glass container, filled with one fluid while the other fluid is introduced through a needle either at the bottom or top of the vessel. The fluid with the greatest transparency is chosen as the bulk fluid, and fills the vessel completely (in this case, water or surfactant-water solution). The other fluid (in this case, oil) is injected either into the top of the vessel (if the injected fluid is heavier than the bulk fluid, causing it to want to drop through the bulk – pendent drop method) or at the bottom of the vessel (if the injected fluid is lighter than the bulk fluid, causing it to want to rise through the bulk – rising bubble method). In this case, the oil is injected into the bottom of a vessel containing a water/surfactant solution, as the oil is less dense than the water/surfactant solution. When the bubble is formed it rises through the water, through the water-oil interface, and up through the oil column. The behavior of the rising bubble is recorded with a camera (Elsharkawy 1992).

The viscosity experiments were conducted using a Cambridge Viscosity VISCOlab PVT high pressure viscometer. This viscometer uses the oscillating piston method to calculate the viscosity of very small liquid samples, and is accurate to 1% of the range of the piston being used.

A viscometer is a device used to measure the viscosity of a fluid. One type of viscometer is the oscillating piston viscometer. In this design, a piston is enclosed in a thermally controlled chamber. Electromagnetic coils are housed outside of this chamber and create a magnetic field while causes the piston to oscillate. This oscillation causes a shear stress in the liquid which is measured via the time it takes for the piston to complete an oscillation. From the shear stress the dynamic viscosity can be measured.

3.2. Experimental Method

The set of experiments was designed using Design Expert 9 software by Stat-Ease, using an Optimal Response Surface Methodology design. This section will discuss the factors investigated and the responses measured, also providing an overview of the experiments conducted.

3.2.1. Factors

Four factors were investigated in a series of experiments that were conducted. These four factors include the Water-Alternating-Gas Ratio, the surfactant concentration, the gas type, and the surfactant type. This section will discuss each factor in detail, providing an explanation of what each factor is and the levels of the factor that were investigated.

3.2.1.1. Water-Alternating-Gas Ratio

The Water-Alternating-Gas (WAG) ratio is the ratio of the volume of a water slug to the volume of a gas slug. As discussed in Section 2.6.1, research has been conducted on WAG ratios of 3:1, 2:1, 1:1, 1:2, 1:3 and 1:0.5, which found that a WAG ratio of 1:1 was optimum for oil recovery (Salehi et. al 2013; Salehi et. al 2014; Motealleh et. al 2012; Shokrollahi et. al 2014; Feng et. al 2014).

As well, none of the published studies evaluated made use of any statistical design of experiments analysis that allows for identifying interaction effects between different factors (WAG ratio and surfactant concentration, surfactant type, or gas type). Therefore this study utilized the common range of WAG ratios (1:1 to 1:2) that have been investigated by other researchers to identify any interaction between the WAG ratio and any other factors that are being investigated (surfactant concentration, gas type, and surfactant type). It was also decided to further investigate the gap between the WAG ratios of 1:1 and 1:2. As discussed above, Shokrollahi et. al (2014) investigated a WAG ratio of 1:0.5, however no research could be found for a WAG ratio of 1:1.5, between 1:1 and 1:2. Therefore it was decided to further investigate this WAG ratio.

The size of the slugs were taken from Motealleh et. al (2012), who found that slug sizes of 0.2 PV was an efficient slug size, while the frequency of the slugs were designed to match the findings of Salehi et. al (2013) who found that injecting 1.2 pore volumes worked well, along with Feng et. al (2014) who found that increasing the cycles of water and gas increased recovery. Combining this total injected volume and slug volume found that six slugs each of liquid and gas, each slug consisting of 0.2 PV, would inject 1.2 PV each of liquid and gas. Therefore a base slug volume of 0.2 PV was chosen, while injecting six slugs each of liquid and gas. The volumes of the gas slug and total injected gas increases with WAG ratio, therefore for a WAG ratio of 1:1.5 the gas slug was 0.3 PV, with a total injected gas volume of 1.8 PV. Likewise for a WAG ratio of 1:2 the gas slug was 0.4 PV, with a total injected gas volume of 2.4 PV. Table 3-2 provides the ratio and volume data for the WAG ratios used.

Table 3-2. Water-Alternating-Gas Ratios and Volumes

WAG Ratio	Liquid Volume (PV)	Gas Volume (PV)
1:1	0.2	0.2
1:1.5	0.2	0.3
1:2	0.2	0.4

3.2.1.2. Surfactant Concentration

The concentration of surfactant in a solution is either a volume or weight percent of the surfactant in the solution. As discussed in Section 2.6.2, previous studies have either investigated the surfactant at the CMC, or varied the surfactant by weight percent in the solution (Shokrollahi et. al 2014; Moayedi et. al 2014; Chang et. al 1990, and Sagar and Castanier 1997). It has also been suggested that surfactant should be injected around the CMC value for nonionic surfactants (Gurgel et. al 2008), while Schramm (2000) suggests that surfactants must be present at a concentration higher than the CMC value to achieve the greatest effect in lowering interfactial tension or promoting foam stability. Therefore, it was decided to experiment with surfactants at and above the CMC value to take full advantage of the surfactants ability to lower interfacial tension and create a stable foam.

As discussed in Section 2.2.3, the behavior of the surfactants differ above and below the CMC, therefore to be able to compare different surfactants equally, it was decided to vary the concentration in proportion to the critical micelle concentration. This is a different method of varying the concentration than was used in all of the studies discussed above as Shokrollahi et. al (2014), Chang et. al (1990), and Sagar and Castanier (1997) all varied the concentration by weight percent while Moayedi et. al (2014) used the CMC concentration and a set weight percent above the CMC concentration.

This method of varying by total concentration instead of proportionally from CMC leads to the possibility of one surfactant performing better than another when varied proportionally from CMC, but underperforming when compared on a total concentration basis.

Therefore the concentration was varied by multiples of the critical micelle concentration, meaning two different surfactants at the same proportional concentration point may have different total solution concentrations. The concentration was varied from one (1) times the critical micelle concentration to ten (10) times the critical micelle concentration, with a centre point at five-and-a-half (5.5) times the critical micelle concentration. The values of one, five-and-a-half, and ten times the critical micelle concentration were chosen to obtain a baseline at the critical micelle concentration, and data points above the critical micelle concentration (Schramm 2000). The upper limit of ten times the critical micelle concentration was chosen arbitrarily as the upper limit as research to identify an optimal range of concentrations based on the critical micelle concentration does not exist.

The total solution concentrations used are presented in Table 3-3. As is shown in Table 3-3, if the Triton X-100 and Iveysol 106 surfactants were compared on a total concentration basis and not on a proportional concentration from CMC basis, at ten times the CMC, the Iveysol 106 concentration has a value of twice the Triton X-100 concentration.

Table 3-3. Surfactant Concentrations for Experiments

Triton X-100		Iveysol 106	
CMC Proportion	Total Concentration (weight %)	CMC Proportion	Total Concentration (weight %)
CMC x 1	0.0150	CMC x 1	0.02871
CMC x 5.5	0.0825	CMC x 5.5	0.1579
CMC x 10	0.150	CMC x 10	0.2871

All of the published studies evaluated also did not make use of any statistical design of experiments analysis that allows for identifying interaction effects between different factors (surfactant concentration and WAG ratio, surfactant type, or gas type). Therefore this study utilized a statistical design of experiments software to identify any interaction effects between surfactant concentration and the three other factors that were investigated (WAG ratio, gas type, and surfactant type).

3.2.1.3. Gas Type

In water-alternating-gas, the choice of the gas phase is very important, air, nitrogen, carbon dioxide, hydrocarbon gas (methane-decane mixture) and reservoir gas has all been used as the gas phase in micromodel and coreflooding experiments (Hornbrook et. al 1991; Chang et. al 1994; Farajzadeh et. al 2009; Motealleh et. al 2012; Shokrollahi et. al 2014; Xu and Rossen 2003, Sohrabi et. al 2000; Feng et. al 2014; and Moayedi et. al 2014).

This study utilizes two different gases to investigate the gases on their own and in comparison to one another. For the first gas phase, air was chosen as the gas phase as it is both a less studied gas phase for WAG injection, possibly due to the many safety challenges it poses at reservoir conditions. For the second gas phase, propane gas was chosen as the gas phase as it is readily available and can simulate a rich reservoir gas (richer than pure ethane or methane). The choice of air and propane allows for the investigation of air and propane by themselves, along with comparing air to a hydrocarbon gas. Due to the ambient conditions that the experiments were conducted at, it is not possible to take advantage of any pseudo-miscible aspects of using a hydrocarbon gas, however the differences in viscosity, density, and compressibility of the propane gas act as a comparison gas with air. If propane increases or decreases the oil recovery, it cannot be due to any pseudo-miscible aspects due to the ambient conditions of the experiments, therefore any difference in oil recovery must be due to the fluid characteristics of density, viscosity, or compressibility.

3.2.1.4. Surfactant Type

As discussed in Section 2.4 and Section 2.6.4, various types of surfactants have been used previously, with both ionic and nonionic surfactants being used (Rao et. al 2006; Shrokrollahi et. al 2014).

Two nonionic surfactants were investigated; their choice was based on their availability to the researchers and the benefits of non-ionic surfactants over ionic surfactants. Rao et. al (2006) found that non-ionic surfactants resulted in a higher oil recovery compared to anionic surfactants. The two surfactants investigated were Triton X-100 and Iveysol 106. Triton X-100 has only recently been used in research, mainly by Abdi et. al (2014) and Moayedi et. al (2014). Shokrollahi et. al (2014) used Triton X-100 for foam tests but did not conduct any coreflooding experiments with it as he found that Triton X-100 did not produce as much stable foam as the ionic surfactants that he was investigating.

Research using Iveysol surfactants for enhanced oil recovery is lacking, the Iveysol 108 surfactant has been used by (Moayedi et. al 2014), however no research utilizing Iveysol 106 surfactant has been published. Therefore it was decided to utilize the Iveysol 106 surfactant due to the lack of research available.

Triton X-100 has been used recently with promising results as a surfactant for oil recovery techniques, while the Iveysol line of surfactants are relatively new and are beginning to be investigated for their suitability as oil recovery surfactants. As Rao et. al (2006) identified non-ionic surfactants as performing better than anionic surfactants, and the fact that both Triton X-100 and the Iveysol line of surfactants are showing recent interest in their suitability as oil recovery surfactants, these two surfactants were chosen for investigation.

3.2.2. Responses

Two quantitative responses (oil recovery and breakthrough time) were observed and measured, by which to compare the factors discussed in Section 3.2.1. In addition to these, the qualitative response of fluid flow through the micromodel was observed and documented. The quantitative responses (oil recovery and breakthrough time) were analyzed using the analysis of variance (ANOVA) method of statistical analysis discussed in Section 2.7.

3.2.2.1. Oil Recovery

In the petroleum industry, the net present value of a project is the most important factor associated with different production methods and strategies. The net present value of a project depends on the oil recovery achieved and the time required to achieve that oil recovery. Oil recovery is a quantitative measurement of the amount of initial oil in place that is produced from a given reservoir or reservoir zone. The oil recovery data that is measured was the cumulative oil recovery with time. The oil recovery is measured through image processing, where images at set intervals throughout the experiment will be analyzed to determine the oil saturation of the micromodel. This is done by converting the colour image into a black and white image and counting the black pixels, representing oil. The image is processed first to include only the micromodel, then the brightness and contrast of the image is adjusted to ensure that when the image is turned into black and white, only the oil phase is given a black colour. Once the image brightness and contrast have been adjusted, the image is transformed into a black and white image; the black pixels can then be counted. Comparing black pixel counts at various points throughout the experiment to the black pixel count of an image taken before the test begins with the micromodel initially saturated with oil can give the oil recovery up to that point in the experiment. The error incurred by using the image analysis method is discussed in detail in Section 4.3.1.2. The image processing analysis results are corroborated with a specially designed mass balance experiment as the mass balance data collected during the experiments in the micro separator and burette was not reliable due to a number of issues which are discussed below. The mass balance experiment used involved a long, 1/8” tube extending from the outlet of the micromodel for 3 meters. Whenever a picture was taken for image processing, the length of fluids in the outlet tube were also measured. Using a waterflooding experiment, before breakthrough the only fluid in the tubing was oil. Therefore the length of fluid in the outlet tubing, containing only oil, when converted into a volume of oil would give the produced oil volume. Dividing this oil volume by the volume of oil in the micromodel allows for a determination of the oil recovery. Then the image processing oil recovery data can be corroborated to the mass balance oil recovery data.

3.2.2.2. Breakthrough Time

Breakthrough time is a quantitative measurement of the amount of time it takes for the injection fluids to work their way through the reservoir and appear at the outlet of the reservoir. A longer breakthrough time at the same injection rate is desired as producing injection fluids decreases the oil production. Breakthrough time is generally decreased by viscous fingering and gravity override (Chiang et. al 1980; Brock and Orr Jr. 1991).

3.2.2.3. Fluid Flow

The flow of the injection fluids through the porous media will be observed qualitatively to identify how the fluids move through the porous media. These observations can assist in explaining certain phenomena encountered and may lead to a better understanding of surfactant processes.

3.2.3. Experiments

The Optimal Response Surface Methodology design resulted in 23 required experiments, as outlined in Table 3-4. These 23 experiments are used to determine if any interaction effects are present between the 4 factors and how those factors affect the oil recovery and breakthrough time. Six additional experiments were conducted to completely investigate the effect which surfactants in the injection liquid have on oil recovery. These additional experiments are also outlined in Table 3-4 as experiments 24 to 29. These experiments were conducted to determine the effectiveness of surfactant assisted water-alternating-gas over normal water-alternating-gas, surfactant-brine flooding, and brine flooding. These additional experiments also investigate when or if tertiary oil recovery techniques should be implemented (whether the secondary oil recovery technique is beneficial for micromodel experiments). In experiments 1 to 26 and 29 there was no secondary waterflood before the WAG process, while experiments 27 and 28 did undergo a secondary waterflood before the WAG process.

Table 3-4. Micromodel Experiments Conducted

Run	WAG Ratio	Surfactant Concentration (X CMC)	Gas Phase	Surfactant Type	Comments
1	1:1	10	Air	Ivey-sol 106	
2	1:1	1	Propane	Ivey-sol 106	
3	1:2	1	Air	Triton X-100	
4	1:1	10	Air	Triton X-100	
5	1:1.5	5.5	Air	Triton X-100	Replicated in Experiments 16 and 22
6	1:1	5.5	Propane	Triton X-100	Replicated in Experiment 9
7	1:2	10	Air	Ivey-sol 106	
8	1:2	1	Air	Ivey-sol 106	Replicated in Experiment 10

9	1:1	5.5	Propane	Triton X-100	Replicate of Experiment 6
10	1:2	1	Air	Ivey-sol 106	Replicate of Experiment 8
11	1:2	1	Propane	Triton X-100	
12	1:1.5	10	Propane	Ivey-sol 106	
13	1:1	1	Air	Triton X-100	
14	1:1	5.5	Air	Ivey-sol 106	Replicated in Experiment 15
15	1:1	5.5	Air	Ivey-sol 106	Replicate of Experiment 14
16	1:1.5	5.5	Air	Triton X-100	Replicated in Experiments 5 and 22
17	1:1	10	Propane	Ivey-sol 106	
18	1:2	5.5	Propane	Ivey-sol 106	
19	1:2	10	Propane	Triton X-100	
20	1:2	1	Propane	Ivey-sol 106	
21	1:1.5	1	Propane	Triton X-100	
22	1:1.5	5.5	Air	Triton X-100	Replicated in Experiments 5 and 16
23	1:2	5.5	Air	Triton X-100	
24	1:1	0	Air	None	Brine-Air WAG
25	1:0	1	None	Iveysol 106	Water/Surfactant Flood
26	1:0	0	None	None	Waterflood
27	1:1	0	Air	None	Waterflooding followed by Water-Air WAG
28	1:1	1	Air	Iveysol 106	Waterflooding followed by Water/Surfactant-Air WAG
29	1:1	1	Air	Iveysol 106	Water/Surfactant WAG

3.2.4. Experimental Method

The experiments began with a clean, empty micromodel. The experiments were then conducted as follows:

- Liquid was injected up to the micromodel.

- The micromodel was vacuumed and completely filled with oil from the inlet to the micro separator.
- Gas was injected up to the water/gas injection tee.
- A liquid slug (0.2 PV) was injected into the micromodel.
- A gas slug (0.2 to 0.4 PV) was injected into the micromodel.
- Alternating liquid/gas slugs were injected until 6 slugs each of liquid and gas had been injected into the micromodel.
- Pictures were taken every 1 minute.

The core set of experiments did not consist of any primary waterflood, instead beginning with alternating slugs of liquid and gas. The additional experiments that were conducted varied slightly from the above. For experiments that did not involve a gas phase, the liquid was injected until breakthrough. Two additional experiments consisted of first performing a waterflood until breakthrough, followed then by injecting alternating liquid and gas slugs for 6 cycles of each.

3.3. Foam Stability Tests

To investigate whether or not foam was possible with the fluids used in this study, the standard test for foam in aqueous media, the bottle test, was conducted on the fluids. The standard test method taken from the withdrawn ASTM Standard D3601-88 (2007) (which was only withdrawn due to lack of interest), was used (ASTM International 2007). This test involves placing 200 mL of solution into a 500 mL bottle, shaking the bottle vigorously, and measuring the height of the foam created as a factor of time. These experiments measure the ability of the solution to create a foam and the stability of any foam generated. Eight different experiments were conducted in total, four without oil present, and four in the presence of oil. To conduct the four experiments in the presence of oil, 20 mL of oil was added to the 200 mL of surfactant solution, as was done by Moayedi et. al (2014). The eight experiments used the same solution as was used in the micromodel experiments, all eight experiments are outlined in Table 3-5. Each experiment was conducted twice.

Table 3-5. Bottle Tests Conducted

Experiment	Surfactant	Surfactant Concentration (Multiple of CMC)	Presence of Oil
1	Triton X-100	1	No
2	Triton X-100	10	No
3	Iveysol 106	1	No
4	Iveysol 106	10	No
5	Triton X-100	1	Yes
6	Triton X-100	10	Yes
7	Iveysol 106	1	Yes
8	Iveysol 106	10	Yes

3.4. Interfacial Tension Experiments

In addition to the micromodel experiments, several interfacial tensions experiments were conducted to determine the effect of surfactants on the interfacial tension. As discussed in Section 2, interfacial tension plays an important role in the recovery of oil, and therefore knowing how the surfactants affect the interfacial tension between brine-surfactant and oil can better help explain the results of the micromodel experiments. Only one response was measured in these experiments, the interfacial tension between brine and oil. Five experiments were conducted to investigate the two different surfactants experimented with at the low and high concentrations of the surfactants. Table 3-6 shows the five interfacial tension experiments that were conducted. During each experiment, an oil bubble was introduced into the bulk liquid (brine for experiment 1, brine-surfactant for experiments 2 to 8), and the interfacial tension was determined. To validate the results, more oil was introduced, increasing the size of the oil bubble, until the oil bubble broke off from the injection port. Interfacial tension measurements were made for several different sized bubbles. This process was repeated several times, introducing several oil bubbles into the bulk liquid to ensure that each new bubble gave similar results for the interfacial tension. For each experiment, the apparatus was calibrated so that the proper user input variables (densities, needle size) were correct. As well, for each bubble, the optical calibration procedure was followed, ensuring that the camera settings were appropriate for the bubble and that the computer generated boundary and needle lines used for calculation were adjusted properly.

Table 3-6. Interfacial Tension Experiments Conducted

Run	Surfactant	Surfactant Concentration (X CMC)
1	None – Distilled Water	
2	None – Brine	0
3	Triton X-100	1
4	Triton X-100	5.5
5	Triton X-100	10
6	Iveysol 106	1
7	Iveysol 106	5.5
8	Iveysol 106	10

3.5. Viscosity Experiments

In addition to the micromodel experiments, several viscosity experiments were conducted to determine the effect of surfactants on the viscosity of the surfactant-brine solutions. As discussed in Section 2, viscosity affects recovery of oil though viscous fingering. Therefore knowing how the surfactants used affect the viscosity of the brine-surfactant solution can better help explain the results of the micromodel experiments. Only one response was measured in these experiments, the viscosity of the solution. Eight experiments were conducted to investigate the two different surfactants used. Table 3-7 shows the eight viscometer experiments that were conducted. The apparatus was officially calibrated by the manufacturer before being shipped; however an experiment using distilled water was completed to verify that the apparatus was still functioning properly. Several experiments of each solution were completed to ensure that the viscosity values were repeatable.

Table 3-7. Viscometer Experiments Conducted

Run	Surfactant	Surfactant Concentration (X CMC)
1	None – Distilled Water	
2	None – Brine	0
3	Triton X-100	1
4	Triton X-100	5.5
5	Triton X-100	10
6	Iveysol 106	1
7	Iveysol 106	5.5
8	Iveysol 106	10

Chapter 4: Experimental Results and Analysis

This section presents and discusses the results obtained and observed during the experiments. First, this section presents and discusses the viscosity and interfacial tension measurements in Section 4.1 on fluid characterization. It will then present a qualitative overview of the observed fluid flow through the micromodel in Section 4.2, discussing all observations. Following this, the quantitative results for oil recovery and breakthrough time with be presented and analyzed in Sections 4.3 and 4.4 respectively. A short investigation into the optimum time during production to implement enhanced oil recovery techniques will then be presented in Section 4.5. This section will then end with an overview of the encountered difficulties and the solutions used to overcome these difficulties in Section 4.6. A full set of the experimental raw data is available in from the authors. An image of the micromodel alongside a scale is provided at the beginning of Appendix G for the reader.

4.1. Fluid Characterization

This section discusses the viscosity and interfacial tension experiments that were conducted on the surfactant and brine solutions. First the viscosity results are analyzed, followed by the interfacial tension results.

4.1.1. Viscosity

Experiments were conducted using a Cambridge Viscosity VISCOlab PVT high pressure viscometer to determine the effect of surfactants on the viscosity of the liquid phase. The viscometer has accuracy to ±1% of the range of the piston being used. As the piston used had a range of 0.2 cP to 2.0 cP, the accuracy of the measurements are within ±0.018 cP. Eight experiments were conducted, one using distilled water, one using the brine solution, and three each for Iveysol 106 and Triton X-100. Both surfactants were investigated at surfactant concentration multiples of one, five-and-a-half, and ten times the critical micelle concentration, corresponding to the low and high values of surfactant concentration used in the micromodel experiments. Figure 4-1 shows the viscosity data for the five fluids. The Cambridge Viscosity VISCOlab PVT high pressure viscometer operates by taking a viscosity measurement every few seconds. The viscometer is calibrated in the factory, and the only calibration required is to choose to appropriate piston for the expected viscosity range (0.2 cP to 2.0 cP). Distilled water was also tested to determine if the viscometer was operating correctly, as the viscosity of distilled water is known. The fluid was injected into the testing cell, and the viscometer was allowed to operate until the viscometer came to steady state with the viscosity readings not changing. Once steady readings were achieved, more fluid was injected and the readings were allowed to converge to a single value again. The data from the viscometer experiments can be found in Appendix D. The viscosity data is presented to the second decimal since the accuracy of the equipment used is 0.018 cP, therefore any data beyond the second decimal is within the error range of the equipment and unreliable as it may be due to random error and not due to a difference in the factors. From Appendix D, the standard deviation for the experiments are very small, to the third and fourth decimal place, therefore the standard deviations are not shown here since the accuracy of the viscometer is so large.

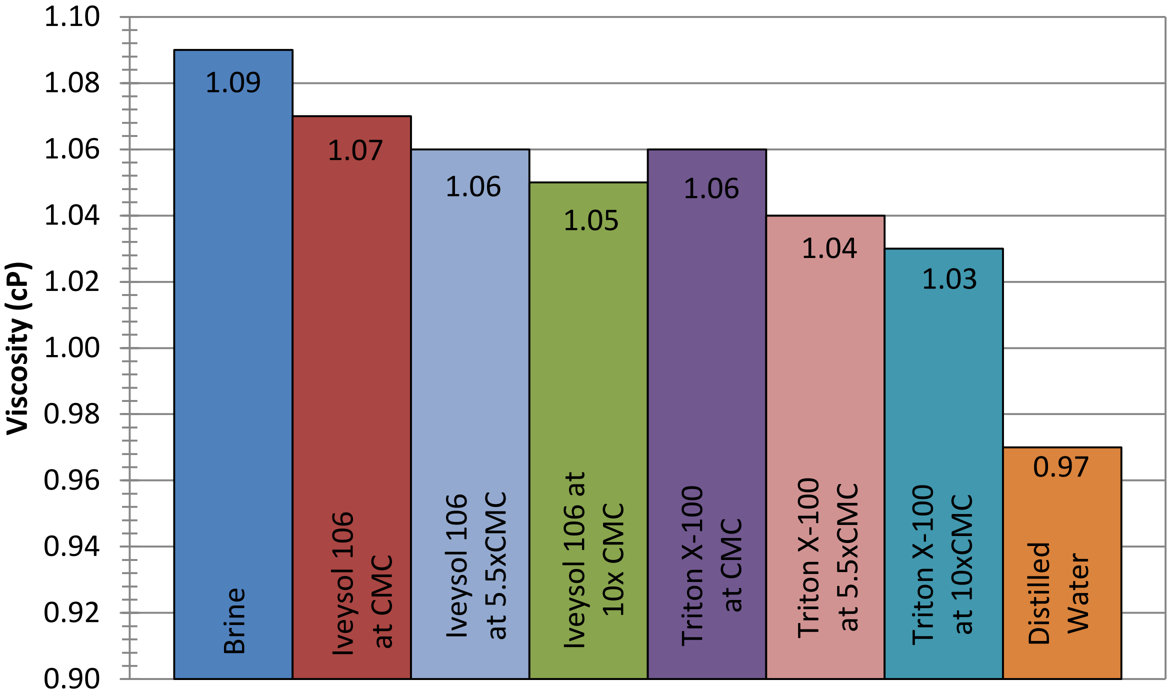

Figure 4-1. Viscosity data for brine and surfactant solutions

As shown in Figure 4-1, the accuracy range of the machine means that some of the differences in the values may be obscured by error. For example, the Triton X-100 and Iveysol 106 surfactants at the critical micelle concentration are only 0.01 cP in difference, while the error inherent in the data is 0.018 cP. Therefore this difference is within the error range of the equipment and cannot be interpreted as an actual difference in viscosity of the surfactants. However, it is shown that viscosity decreases with increasing surfactant concentration. At low surfactant concentrations (1 x CMC), it is not possible to confidently determine which surfactant reduces the viscosity more, as the results may be skewed by error, however at high surfactant concentrations (10 x CMC) it is shown that the Triton X-100 surfactant reduces the viscosity slightly more than the Iveysol 106 surfactant. The viscosities for brine (1.09 cP) and distilled water (0.97 cP) shows that the viscometer is working adequately, as literature values for distilled water at 20°C is 1.0 cP, while brine at 35,000 ppm salinity is 1.09 cP. The viscosity of distilled water of 0.97 cP is lower than the literature value of 1.0 cP.

The addition of surfactants to the brine reduced the viscosity of the injection liquid from the brine viscosity of 1.09 cP. The addition of Iveysol 106 surfactant at the critical micelle concentration reduced the viscosity to 1.07 cP, while the addition of Iveysol 106 surfactant at five-and-a-half and ten times the critical micelle concentration reduced the viscosity even further to 1.06 cP and 1.05 cP respectively. The addition of Triton X-100 surfactant at the critical micelle concentration reduced the viscosity to 1.06 cP, while the addition of Triton X-100 surfactant at five-and-a-half and ten times the critical micelle concentration reduced the viscosity further to 1.04 cP and 1.03 cP, respectively. The exact relationship between concentration and viscosity can not be determined due to the fact that the values are so close together and the ±0.018 cP error can obscure the data enough so that determining if the relationship if linear or not can not be deduced from the data. The Triton X-100 surfactant had a greater effect on reducing the viscosity than the Iveysol 106 surfactant.

4.1.2. Interfacial Tension

Experiments were conducted to determine the effect of surfactants on the interfacial tension between the oil and injection liquid phases using Vinci Technologies IFT 700 machine. Eight experiments were conducted, all between the oil phase and water solution phase; one using distilled water, one using the brine solution, and three each for Iveysol 106 and Triton X-100. Both surfactants were investigated at surfactant concentration multiples of one, five-and-a-half, and ten times the critical micelle concentration, corresponding to the values of surfactant concentration used in the micromodel experiments. Figure 4-2 shows the interfacial tension between the water solution and oil phases. The testing procedure involved filling the cell with liquid brine/surfactant solution, and then injecting a droplet of oil from the bottom of the cell. For each experiment, the apparatus was calibrated so that the proper user input variables (densities, needle size) were correct. As well, for each bubble, the optical calibration procedure was followed, ensuring the that camera settings were appropriate for the bubble and that the computer generated boundary and needle lines used for calculation were adjusted properly. The IFT machine tested the interfacial tension of the droplet continuously and recorded the data every 10 seconds. Droplets were formed and the interfacial tension was analyzed numerous times per droplet. One to three droplets were formed to ensure that the calculated interfacial tension was correct. Figure 4-2 shows the average interfacial tension, plus or minus the standard deviation of the data points collected. The data from the interfacial tension experiments can be found in Appendix E.

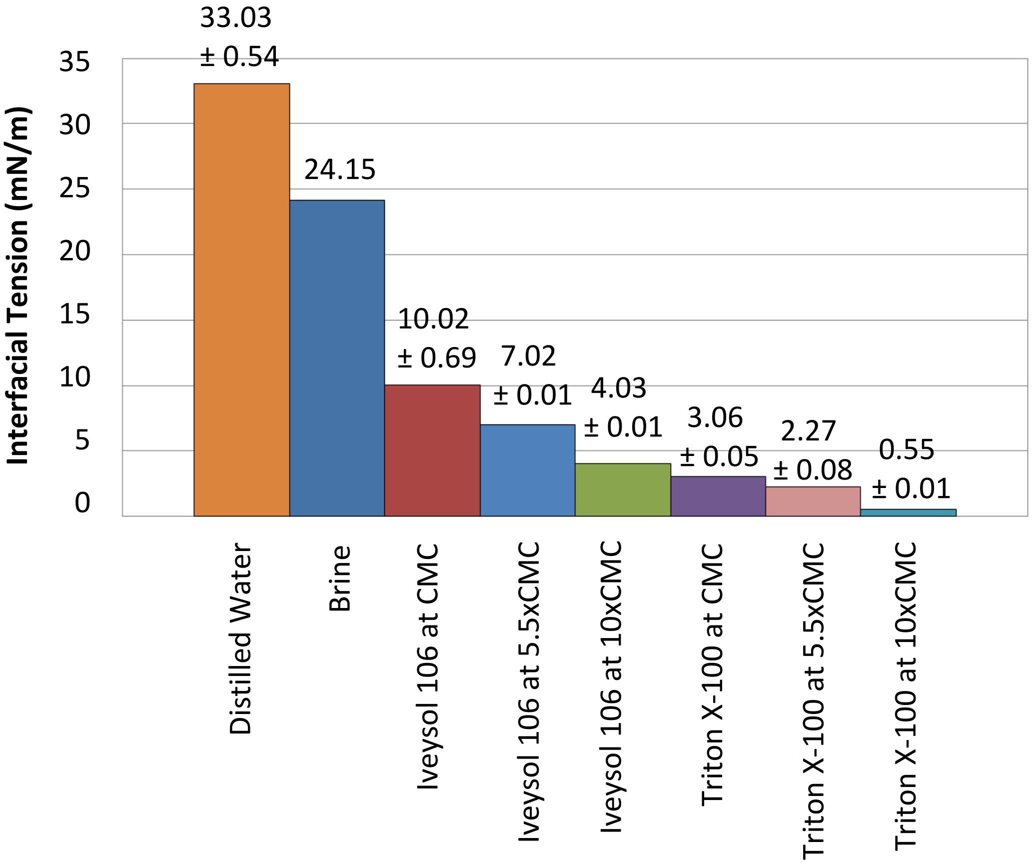

Figure 4-2. Interfacial Tension data between oil and brine and surfactant solutions

As shown in Figure 4-2, the addition of salts to distilled water reduced the interfacial tension slightly, however the addition of surfactants to the brine reduced the interfacial tension between the water solution and oil phase considerably. The interfacial tension between the brine and oil was found to be 24.15 mN/m. The addition of Iveysol 106 surfactant at the critical micelle concentration reduced the interfacial tension to 10.02 ± 0.69 mN/m, while the addition of Iveysol 106 surfactant at ten times the critical micelle concentration reduced the interfacial tension even further to 4.03 ± 0.01 mN/m. The addition of Triton X-100 surfactant at the critical micelle concentration reduced the interfacial tension to 3.06 ± 0.05 mN/m, while the addition of Triton X-100 surfactant at then times the critical micelle concentration reduced the interfacial tension further to 0.55 ± 0.01 mN/m. Both surfactants seemed to reduce the interfacial tension linearly with increasing surfactant concentration (with the surfactant concentrations being increased in proportion to the critical micelle concentration). The Triton X-100 surfactant had a greater effect on reducing the viscosity than the Iveysol 106 surfactant. This result of the interfacial tension decreasing with increasing surfactant concentration was also found by Moayedi et. al (2014), who also found that Triton X-100 decreased the interfacial tension to a greater extent than the Iveysol surfactant. Moayedi et. al used Iveysol 108 while this study used Iveysol 106, as well Moayedi et. al used a fluid with higher salinity.

4.2. Fluid Flow

The basis for conducting experiments with micromodels is to take advantage of the ability to observe the fluid flow through the micromodel. This section will discuss the different phenomenon observed and possible reasons for their occurrence, as well as the lack of certain phenomenon and possible explanations why these phenomena were not detected.

4.2.1. Foam Generation

It was attempted to generate foam in the micromodel, using different surfactant solutions and gas phases. The surfactant solution slug was injected first into the micromodel, followed by a gas slug into the same entry point of the micromodel, then another surfactant solution slug was injected, followed by another gas slug until six slugs each of liquid and gas had been injected. However, a foam was not observed either being generated or moving through the micromodel. To investigate whether or not foam was possible with the fluids used in this study, the standard test for foam in aqueous media, the bottle test, was conducted on the fluids outlined in Table 3-5. Each experiment was conducted twice, with the repeat experiment performing very similarly to the first experiment. The experiments were conducted for 210 minutes; however the repeat experiment was only performed for 120 minutes, as verification that the initial foam heights and initial foam collapse rate were the same as the previous experiment. As both experiments were similar, the results of the first experiment are presented here. The full results of both runs of each experiment, along with the average and standard deviation for the first 120 minutes are available in Appendix C.

The results of the foam stability bottle tests were analyzed two ways, first the total height of the foam with time was analyzed; the total foam height is a measure of the ability of the solution to generate foam. The second method of analysis involved recording the relative height of the foam, being a ratio of the foam height to the initial foam height; the relative foam height is a measure of the foam stability, with the solutions with higher relative foam height having a more stable foam.

First the total and relative foam heights for the experiments without oil are presented in Figure 4-3 and Figure 4-4.

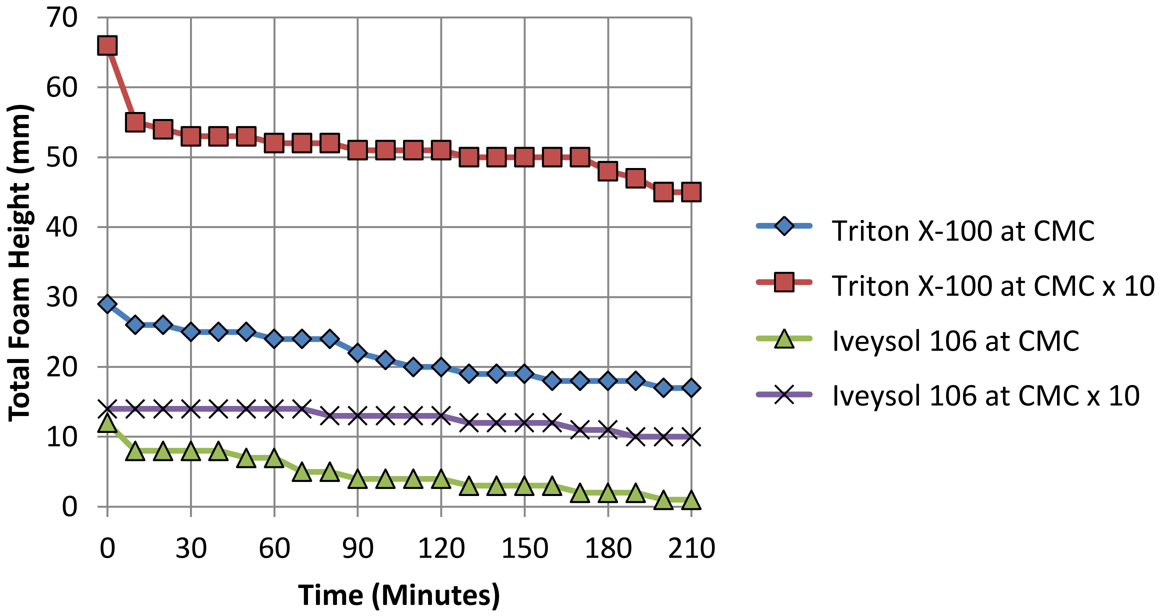

Figure 4-3. Total Foam Height for Experiments Without Oil

As shown in Figure 4-3, the Triton X-100 surfactant generated much more foam than the Iveysol 106 surfactant for all surfactant concentrations. As well, higher surfactant concentrations generated more foam.

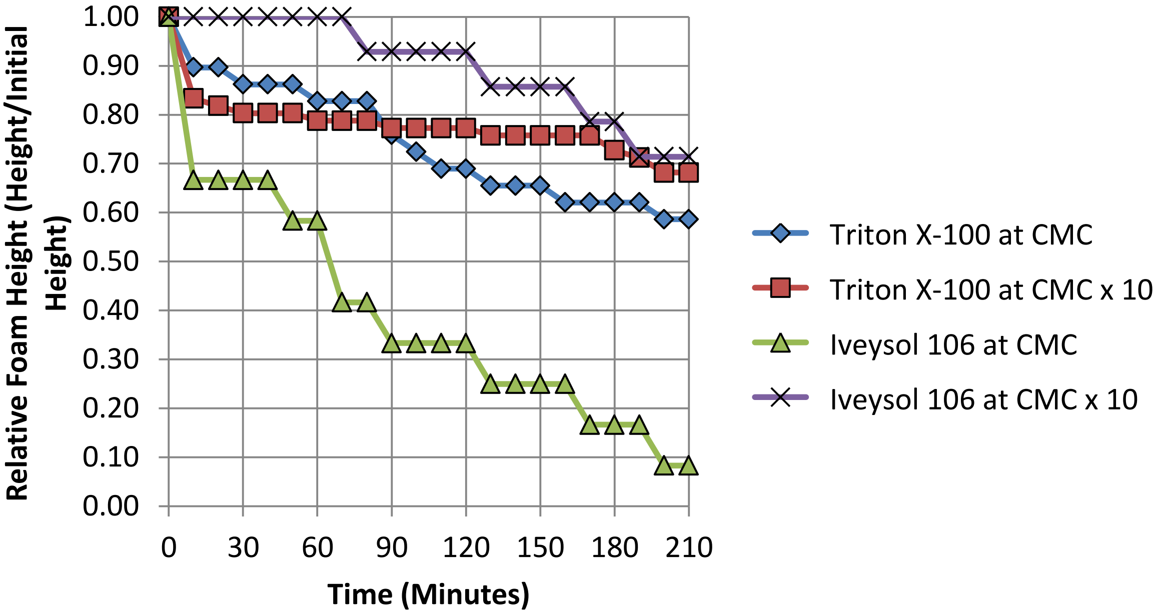

Figure 4-4. Relative Foam Height for Experiments Without Oil

When the data is given as relative foam height (Figure 4-4), the relative foam stability of each surfactant can be observed. The Triton X-100 surfactant formed a stable foam, with the foam height only dropping to 59% of the initial foam height for the low concentration and 68% for the high surfactant concentration, after 210 minutes. The Iveysol 106 surfactant generated a stable foam at the high surfactant concentration, dropping to 71% of the initial foam height after 210 minutes. However, at the low surfactant concentration for Iveysol 106, the foam height dropped to 8% of the initial foam height after 210 minutes. This would show that Iveysol 106 at a high surfactant concentration would generate a more stable foam than the Triton X-100 surfactant, however the total foam height should also be considered, as the Iveysol 106 surfactant generated much less foam than the Triton X-100 surfactant.

Without oil, the Triton X-100 surfactant outperformed the Iveysol 106 surfactant for foam height for both concentrations. The Triton X-100 surfactant also generated a stable foam at both concentrations, the Iveysol 106 surfactant generated a very unstable foam at low concentrations and a stable foam at high concentrations, however it must be taken into consideration that the Iveysol 106 high concentration foam may have been more stable, it also generated much less foam than the Triton X-100 solutions.

Next the total and relative foam heights for the experiments with oil are presented in Figure 4-5 and Figure 4-6.

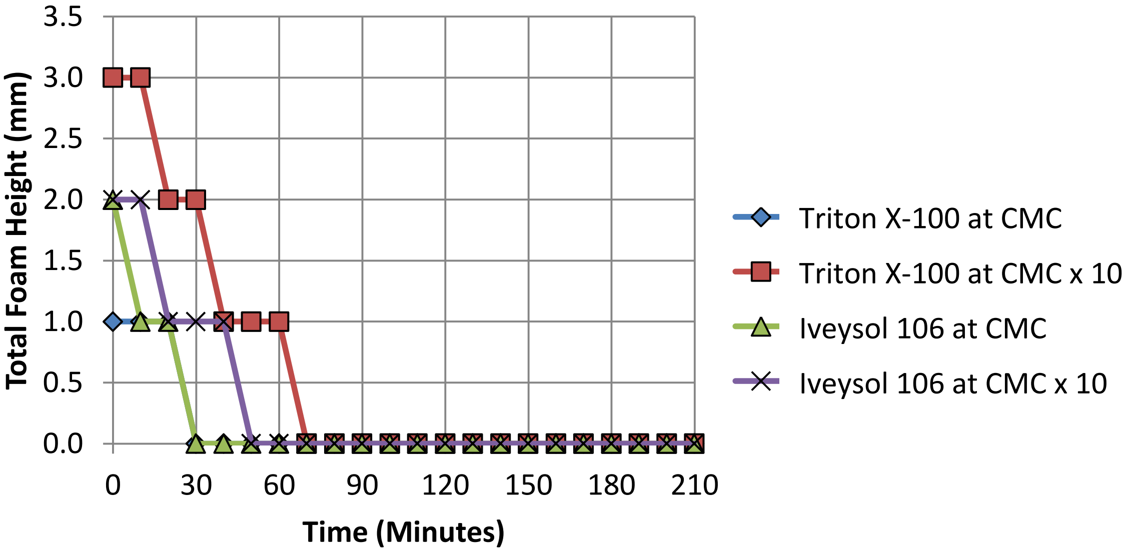

Figure 4-5. Total Foam Height for Experiments 5 to 8, With Oil

As shown in Figure 4-5, the Triton X-100 surfactant at high concentrations generated more foam than the other solutions. Interestingly, the Iveysol 106 surfactant at both concentrations outperformed the Triton X-100 surfactant at low concentration. In total, all solutions generated much less foam, and was present for a much shorter time, in the presence of oil. Thin foam layers were only a few millimeters in width, and were completely gone within 70 minutes.

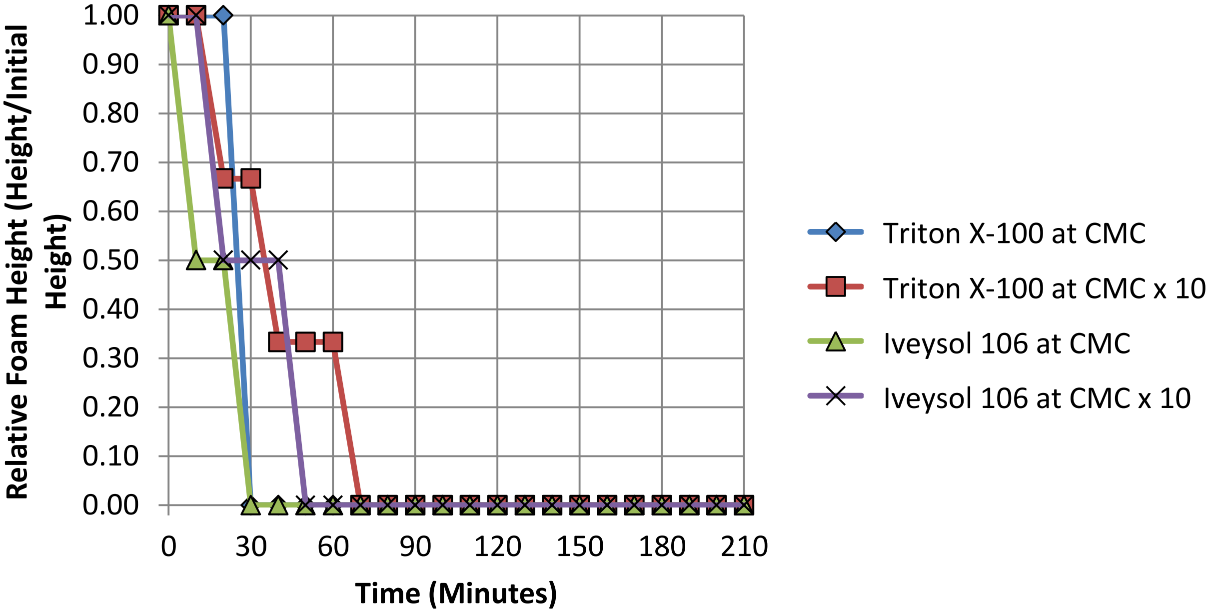

Figure 4-6. Relative Foam Height for Experiments 5 to 8, With Oil

When looking at relative foam height (Figure 4-6), the presence of oil also decreased the stability of the few millimeters of foam that was generated. The foam generated was very unstable, disappearing within 70 minutes, with all surfactant solutions being affected by the oil.

All solutions experimented with were able to generate foam, with the Triton X-100 surfactant generating more, and more stable, foam than the Iveysol 106 surfactant. Even in the presence of oil small amounts of foam were generated. Therefore the fluid compositions used were not a factor in not being able to generate foam in the micromodel. The step-wise drop in foam height was also observed by Moayedi et. al, suggesting that there is some physical mechanism behind the step-wise decrease in foam height.

Investigating this lack of foam further, several theories were considered and investigated. These theories consisted of surfactant concentration, two dimensionality of the micromodel, gas flow rate, inlet condition, and order of injection fluids.

Surfactant Concentration

It was thought that the surfactant concentrations may have been too low to be able to disperse the surfactant molecules throughout the solutions while having enough molecules to create foam films. The largest surfactant concentration used was ten (10) times the critical micelle concentration, which resulted in solutions with 0.15 weight percent of surfactant for Triton X-100 and 0.125 weight percent of surfactant for Iveysol 106. A test of Triton X-100 surfactant solution with a concentration of 0.5 weight percent of Triton X-100 was investigated. In this experiment the micromodel was placed horizontally and flooded completely with surfactant-brine solution with a surfactant concentration of 0.5 weight% Triton X-100, then air was injected into the inlet of the micromodel. As shown in Figure 4-7, even at high surfactant concentrations there was still no foam creation in the horizontal micromodel. The air simply fingered through the surfactant-brine phase.

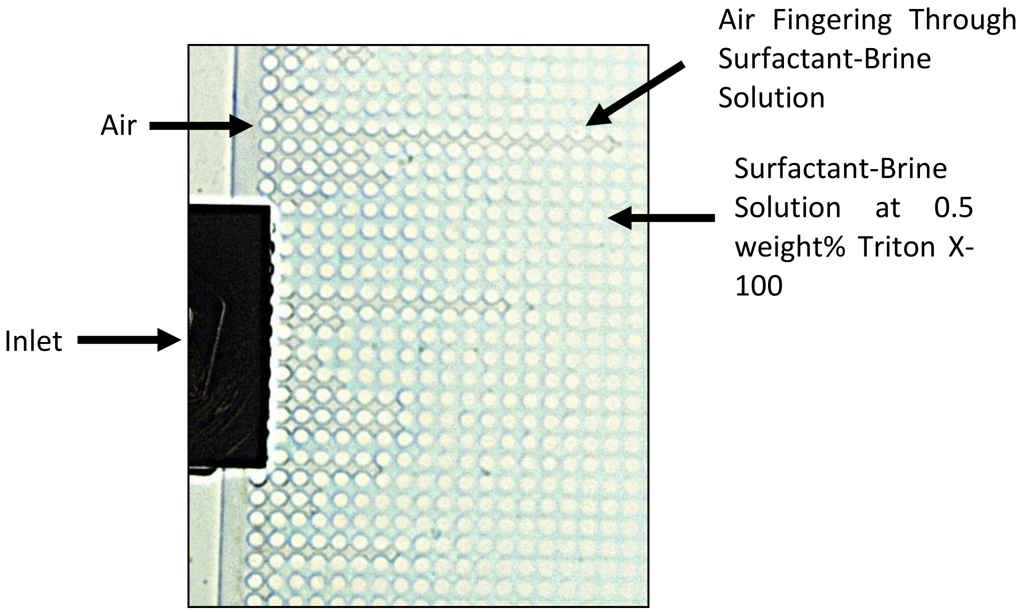

Figure 4-7. No foam creation at high surfactant concentration (0.5% Triton X-100)

Gas Flow Rate

It was also thought that the gas injection rate may have been too high to allow proper foam generation; the gas was injected at twice the rate of the liquid phase. To investigate this, gas was also injected at a rate equal to the liquid injection rate. In this experiment, similarly to the experiment discussed above, the micromodel was placed horizontally and flooded completely with surfactant-brine solution with a surfactant concentration of 0.5 weight% Triton X-100, then air was injected into the inlet of the micromodel. As shown in Figure 4-8, even at low gas injection rates, the gas phase did not create a foam phase in the horizontal micromodel.

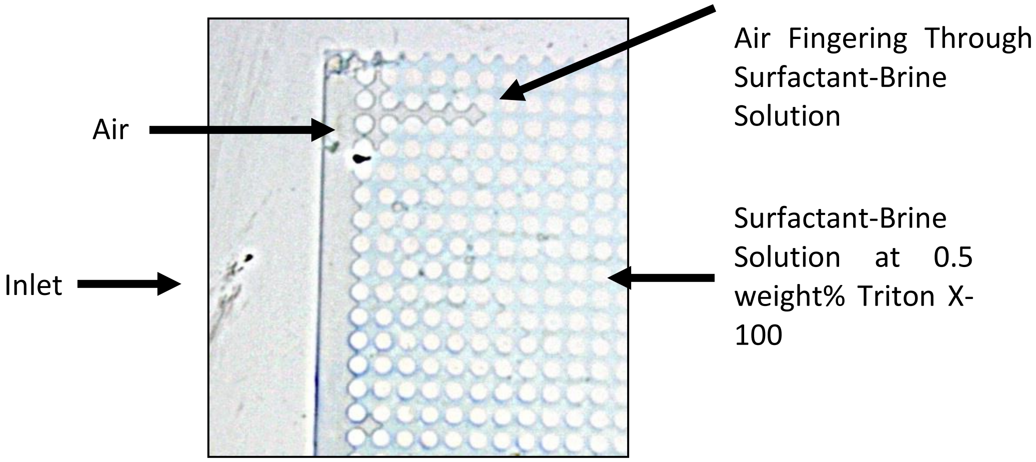

Figure 4-8. No foam creation at low gas injection rate

Two Dimensionality and Homogeneity of the Micromodel and Well Type

Another factor that was thought to have played a role in the absence of foam was the two dimensionality of the micromodel. The micromodel has a vertical depth of only one (1) pore; therefore the surfactant solution could not drain vertically, which is an important method for foam generation.

The published research suggests that the two-dimensionality of the micromodel may have played a main role in not being able to generate foam, as those researchers who were successful in generating foam have used cores (Salehi et. al 2013; Salehi et. al 2014; Shokrollahi et. al 2014; Moayedi et. al 2014; Farajadeh et. al 2009; Xu and Rossen 2003) or a miniature core as a foam generator before the micromodel (Romero et. al 2002; Chang et. al 1990). Chang et. al (1990, 1994) were able to generate a foam in situ in a micromodel of varying pore sizes at high pressures and temperatures, while Sagar and Castanier (1997) were not able to generate a foam phase in a micromodel of varying pore size operating under ambient conditions.

Hornbrook et. al (1991) was also able to generate a foam phase in a homogeneous micromodel at high pressures. This suggests that pore size distribution/irregular pore sizes and shapes of the micromodel and/or pressure of the injection fluids may play a role in the generation of foam as well.

Investigating the pore size distribution, irregular pore shapes, and the pressure of the injection fluids was not possible due to the experimental setup, an investigation into the two-dimensionality of the micromodel was conducted. Investigating the micromodel two-dimensionality, the micromodel was also placed on its side, causing the vertical depth to be several pore volumes. One end of the micromodel had a long well stretching the full width of the micromodel, while the other end had a single point well in the middle of the micromodel. A diagram of the micromodel is provided in Figure 4-9. The effect of injection well designs was also investigated, the gas was also injected into the opposite side of the micromodel, which instead of a long well, has a point well in the middle of the micromodel.

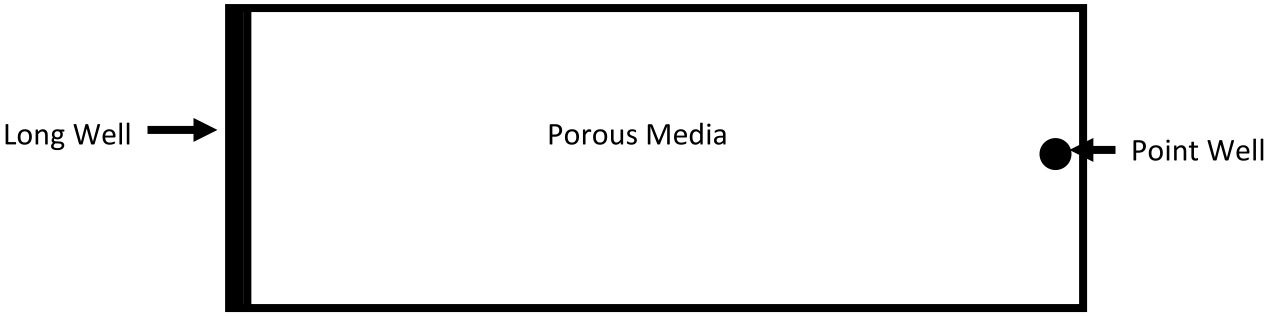

Figure 4-9. Well Configuration of the Micromodel

Investigating whether foam is formed when the micromodel is positioned on its side (giving it a vertical dimension), the micromodel was laid horizontal and flooded with Triton X-100 at

0.5 weight percent, the micromodel was then placed on its side and gas is injected into the micromodel. As shown in Figure 4-10, with the micromodel in a vertical position, there is some foam creation. However it was found that the air simply moved to the top of the long injection well and entered the micromodel near the top of the micromodel. This reduced the foam creation because the air simply traveled to the top of the micromodel and then entered into the pore system, simply moving across the top. Even with the air entering at the top of the long well, a foam structure can be seen. While foam bubbles of individual pores are uncommon in Figure 4-10, foam bubbles covering multiple pores are very common.

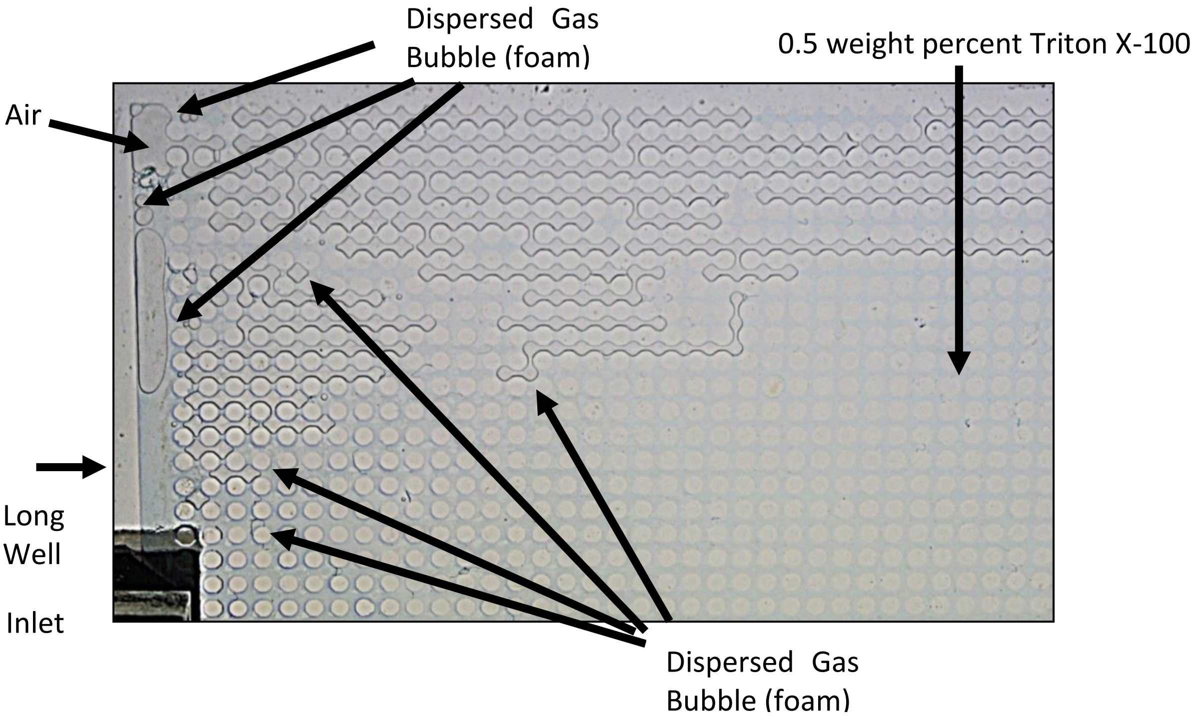

Figure 4-10. Some foam creation in vertical micromodel with long well

The effect that the long vertical well has on the creation of foam was also investigated. The air was injected into the opposite end of the micromodel, which has a point-like well located in the middle of the far end of the micromodel. Again the micromodel was completely flooded with Triton X-100 at 0.5 weight percent before being placed vertically and gas being injected. As shown in Figure 4-11, injecting the air into the point well with the micromodel held vertically created additional foam when compared to injecting the air into the long well. The foam created using the point well in the vertical micromodel consisted of additional and smaller foam bubbles compared to the long well situation. The foam structure consisted of several instances of gas bubbles ranging in size from less than one pore up to two pores, along with multiple larger gas bubbles of several pores. This additional foam generation was due to the gas entering the micromodel vertically in the middle of the micromodel, the buoyancy of the gas caused the gas to rise in the micromodel while the liquid drained downwards. This process resulted in additional and smaller gas bubbles compared to when the gas entered the micromodel already at the top of the micromodel.

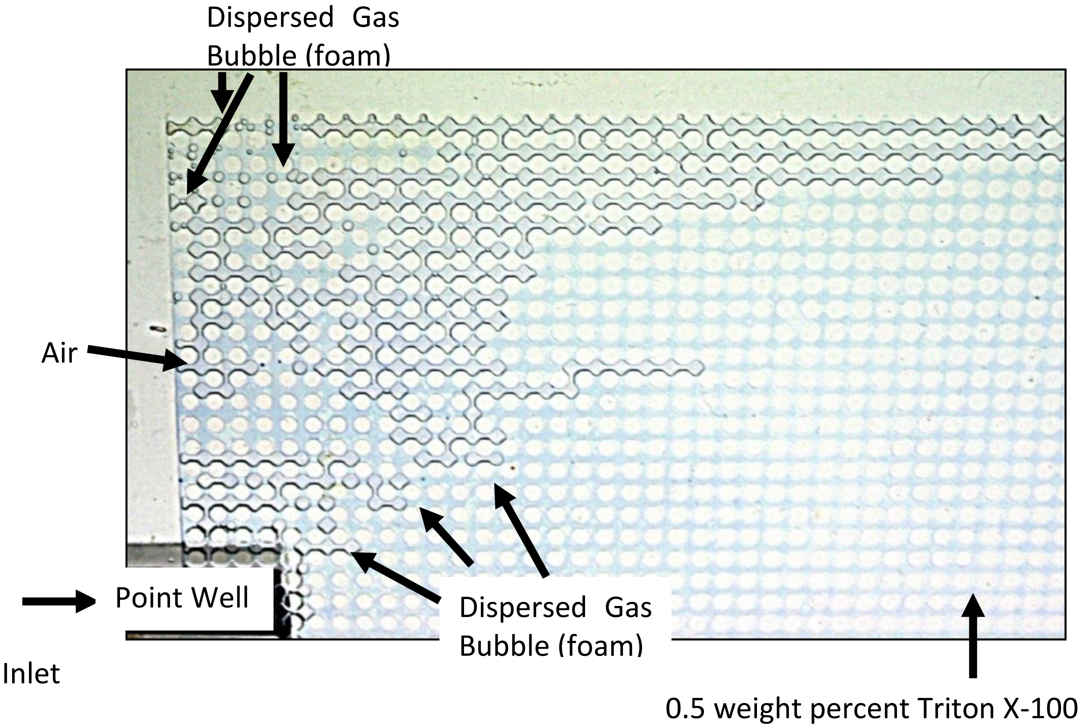

Figure 4-11. Foam creation in vertical micromodel with point well

Order of Injection Fluids

Another possibility for the lack of foam generation is the order in which the fluids are injected into the micromodel. Investigating this, the micromodel was placed horizontally and filled completely with air, then a surfactant-brine solution of Triton X-100 at 0.5 weight percent was injected into the inlet.

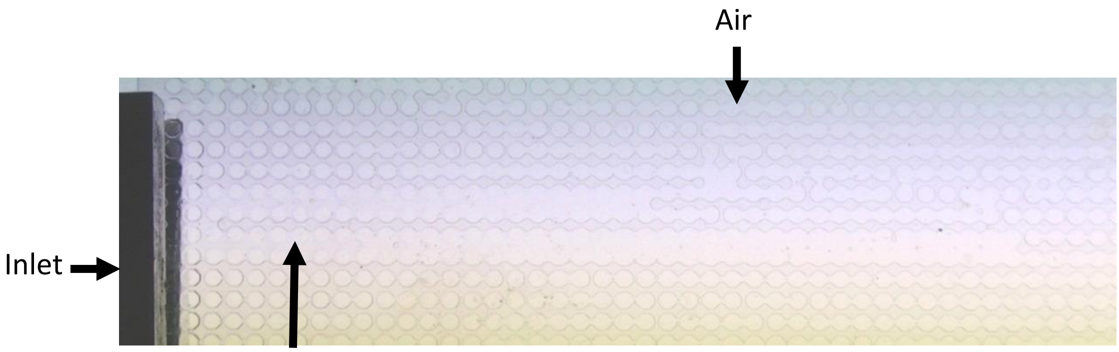

Triton X-100 0.5 Weight Percent Fingering Through the Air

Figure 4-12. No foam creation in horizontal micromodel, Triton X-100 0.5% injected into air filled micromodel

As shown in Figure 4-12, when the air filled micromodel is laid horizontally and injected with 0.5 weight percent Triton X-100 surfactant solution, the liquid fingers through the micromodel instead of generating a foam. The two dimensionality of the micromodel was also investigated when surfactant is injected into air, where the micromodel was again completely saturated with air while it was in a horizontal position. Then the micromodel was placed on its side and the 0.5 weight percent Triton X-100 surfactant solution was injected into the long well. As shown in Figure 4-13 and Figure 4-14, when the micromodel is placed vertically and Triton X-100 is injected into an air filled micromodel, the surfactant solution drains down by gravity through the long well and pore network to the bottom of the micromodel. As it drains down and moves through the pores, gas bubbles become dispersed in the liquid, creating foam. In both Figure 4-13 and Figure 4-14 several dispersed gas bubbles can be seen.

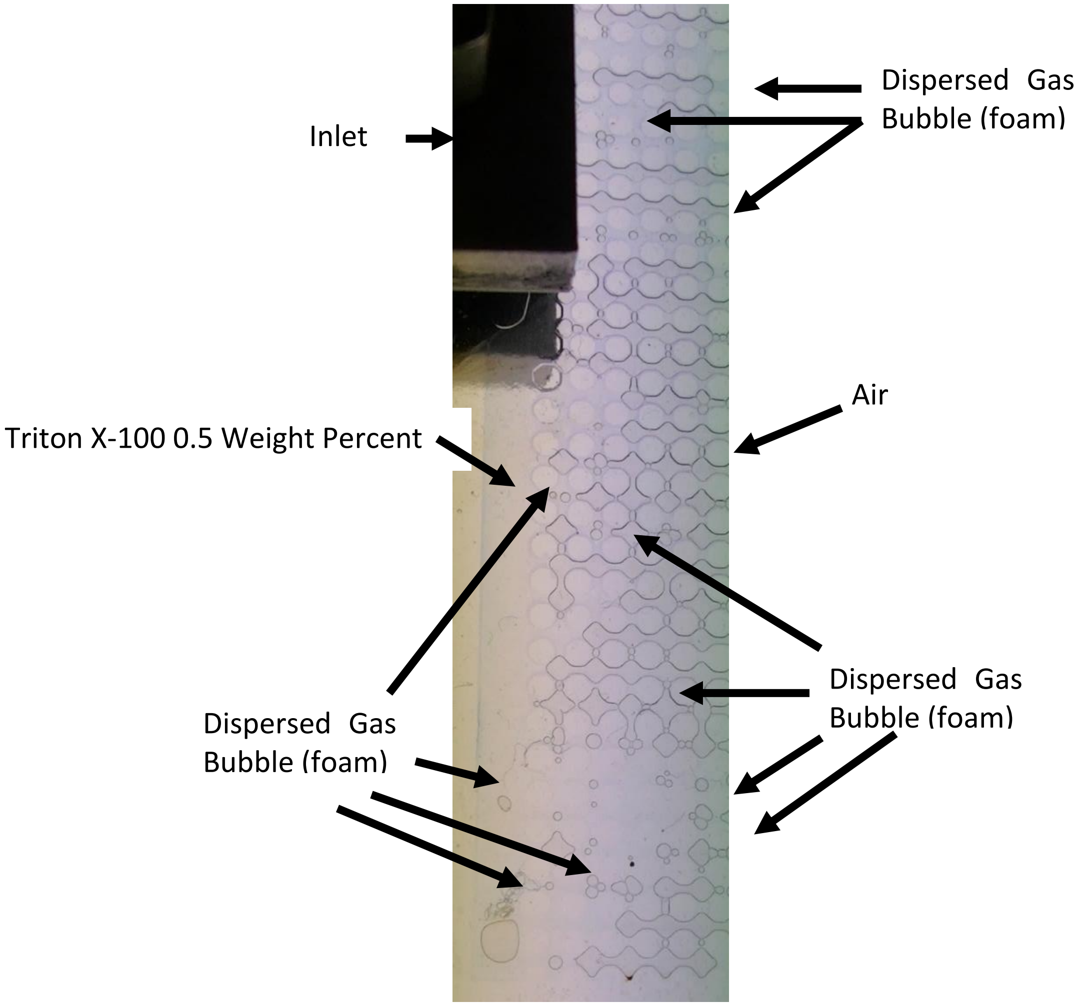

Figure 4-13. Foam creation in vertical micromodel, Triton X-100 0.5% injected into air filled micromodel from long well – View of Inlet side of Micromodel

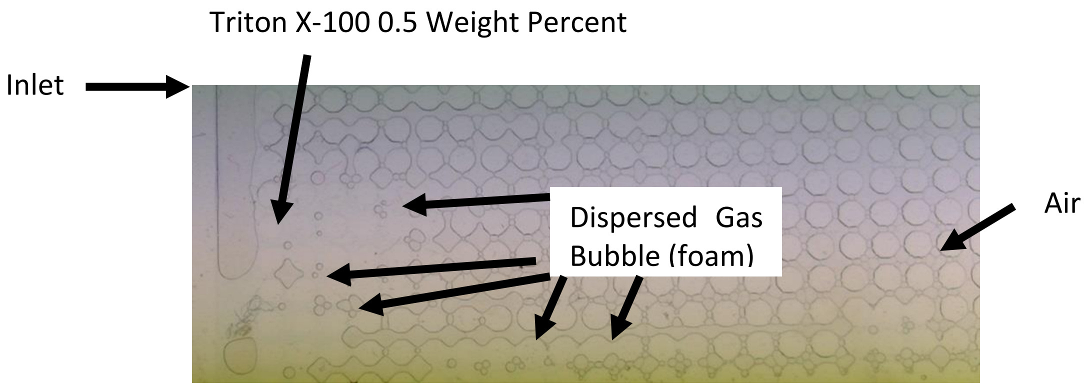

Figure 4-14. Foam creation in vertical micromodel, Triton X-100 0.5% injected into air filled micromodel from long well – View of bottom of Inlet side of Micromodel

It was investigated whether the point well would generate more foam than the long well in a vertical micromodel, as was shown above, the micromodel was again placed horizontally and saturated with air. Then it was placed vertically on its side and 0.5 weight percent Triton X-100 surfactant solution was injected through the point well. As shown in Figure 4-15, when the surfactant was injected into the point well, instead of draining down to the bottom of the micromodel as was observed with the long well, the surfactant solution advanced through the micromodel at the same elevation as the inlet. Several gas bubbles were dispersed into the liquid, mainly along the bottom of the surfactant front.

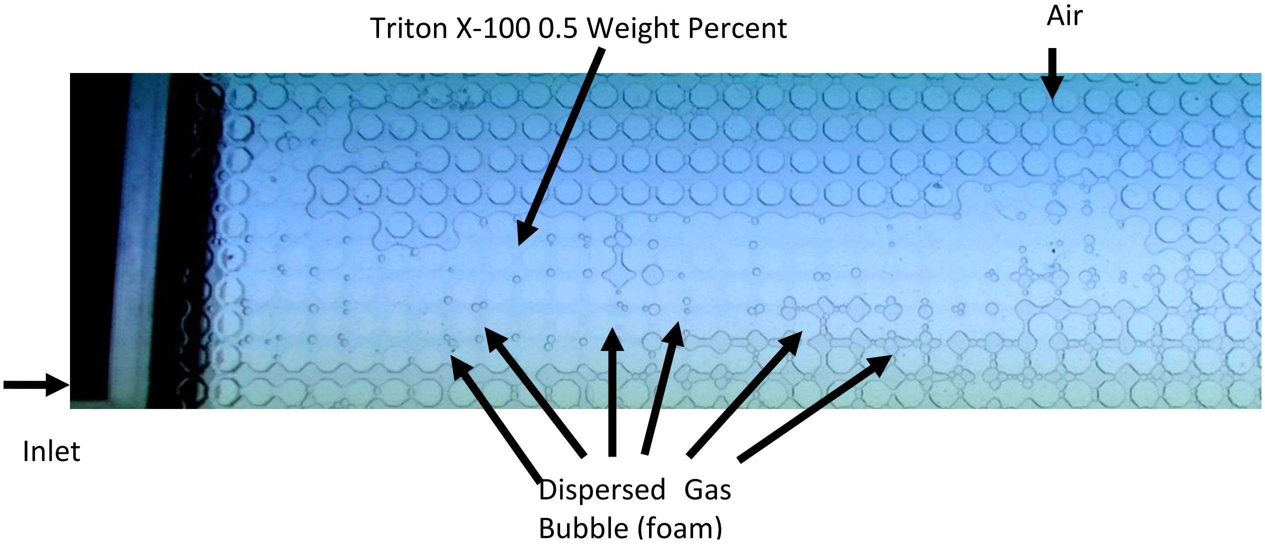

Figure 4-15. Foam creation in vertical micromodel, Triton X-100 0.5% injected into air filled micromodel from point well

As shown, injecting gas into the micromodel first and then injecting surfactant did not produce a foam when the micromodel was placed horizontally. When the micromodel was placed vertically, foam was generated. These findings agree with the experimental results of the water-alternating-gas micromodel experiments conducted, as there were 6 cycles each of liquid and gas injected, so there would have been five opportunities to generate foam in the micromodel (gas slug 1 followed by liquid slug 2, gas slug 2 followed by liquid slug 3, gas slug 3 followed by liquid slug 4, gas slug 4 followed by liquid slug 5, and gas slug 5 followed by liquid slug 6). These findings are consistant with Moayedi et. al (2014) who found that surfactant-brine being injected before gas generates the most foam compared to injecting gas before surfactant-brine.

As discussed in this section, the micromodel orientation is a major factor in the ability to create foam in-situ with the water-alternating-gas technique. The buoyancy of the gas allows it to rise in the micromodel, while the force of gravity causes the liquid to drain to the bottom of the micromodel. This rising of gas and drainage of liquid allowed for the foam generation experienced in Figures 4-8, 4-9, 4-13, 4-14, and 4-15. In addition to micromodel orientation, the well type (long well vs. point well) also influenced the creation of foam. The point well allowed the gas to enter the porous media of the micromodel in the middle, compared to entering at the top of the porous media with the long well situation. This allowed the gas to rise through the porous media, in which situation the foam is generated. With the micromodel in the horizontal orientation, it was found that raising the surfactant concentration, decreasing the gas flow rate, or injecting air before surfactant was not able to generate a foam phase.

4.2.2. Viscous Fingering

Viscous fingering was noted with the gas phase, both air and propane fingered through both the injection fluid and oil phases. Figure 4-16 shows an example from Experiment 7 (Air with a WAG ratio of 1:2, Iveysol 106 at CMC x 10) of air fingering first through the Iveysol 106 (at CMC x 10) surfactant solution phase, and then through the oil phase. Figure 4-16 shows the point in Experiment 7 after the first gas slug was injected into the micromodel, up to the point pictured in Figure 4-16, the micromodel had first been fully saturated with brine, then oil was injected to irreducible water saturation, followed by one slug of 0.2 PV of Iveysol 106 surfactant at CMC x 10. The picture is taken during the injection of the first gas slug of 0.4 PV of air. As shown in Figure 4-16, the air is fingering through the middle of the micromodel from the inlet to the outlet. Due to the low viscosity of the gas used and the inability to create foam, the gas phases regularly fingered through the liquid phases and caused breakthrough of gas at the outlet.

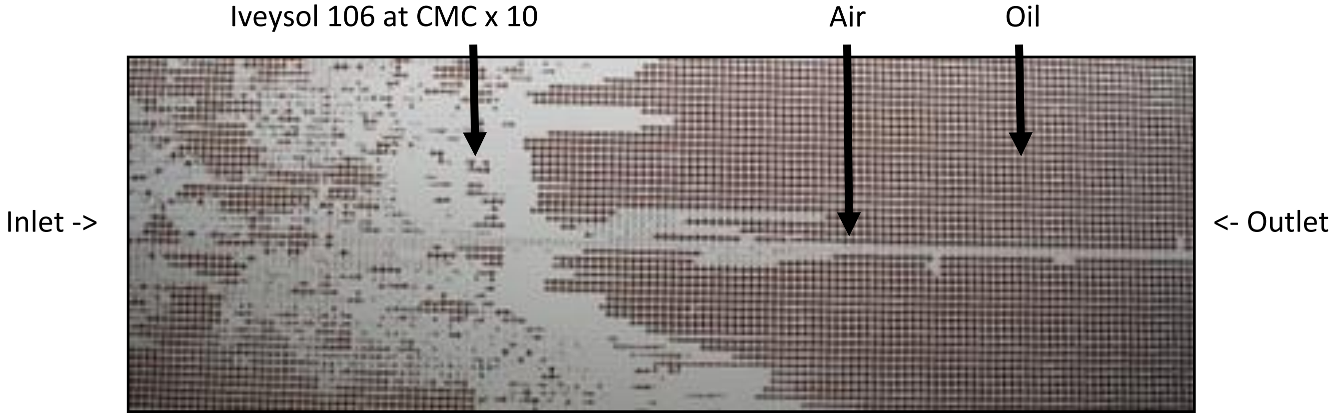

Figure 4-16. Viscous Fingering Through Micromodel (Experiment 7, Air with a WAG ratio 1:2, Iveysol 106 at CMC x 10)

4.2.3. Micromodel Wettability

The micromodel exhibited a water-wet behaviour. Figure 4-17 shows the water-wet nature of the micromodel. Figure 4-17 was taken from Experiment 28 (waterflood followed by WAG ratio of 1:1 with air, Iveysol 106 at CMC), which consisted of initially fully saturating the micromodel with brine, followed by injecting oil to reach irreducible water saturation. Then the micromodel was flooded with brine to the point of water breakthrough, at which point WAG with air and Iveysol 106 at CMC with a WAG ratio of 1:1 was initiated. Figure 4-17 was taken at a point during the injection of the 5^{th} air cycle of 0.2 PV. As shown, the water is clearly the wetting phase, adhering to the glass while the oil and air do not adhere to the glass. In Figure 4-17, the air phase clearly does not wet the glass as it is separated from the glass by a thin layer of oil and a layer of water surrounding the glass. The oil also does not wet the glass, though the refractive index of the water and glass are similar, the water can be distinguished from the glass due to the methylene blue that turns the water slightly blue, this is shown in Figure 4-18 which is a close up view of the centre glass grain in Figure 4-17. In Figure 4-18, the slight difference between glass and water colour can be seen, with the octagonal nature of the glass grain being visible. Half of the glass-water interface has been marked with a dashed line, the other half has not been marked so the difference in water and glass colour and the glass-water interface can be observed. The fact that the micromodel is water wet is further shown by the long connected water channel through the micromodel. Covering the bottom and bottom-right portion of Figure 4-17, the water phase extends over several pore volumes without any interruption. As well, the water-oil interface creates a concave interface, with the water adhering to the glass grain while the oil pushes into the middle of the pore volume between two glass grains surrounded by water.

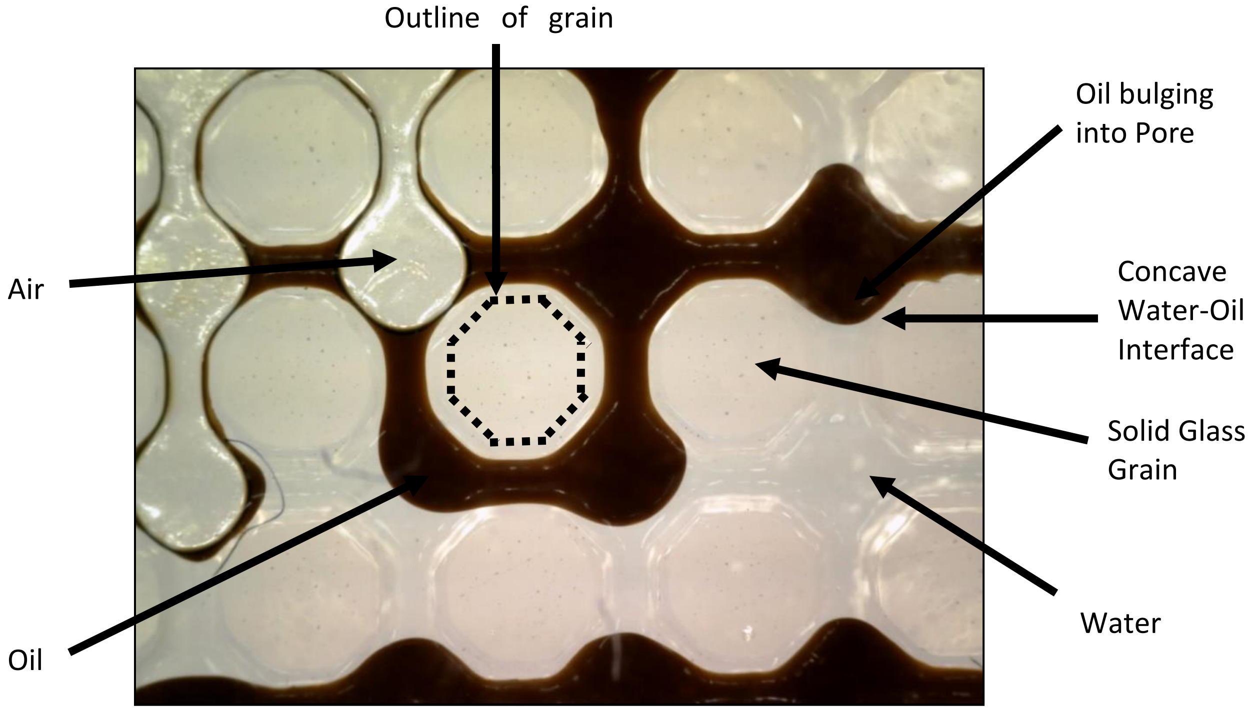

Figure 4-17. Micromodel Wettability - Experiment 28 (Waterflood followed by WAG, WAG ratio of 1:1 with air, Iveysol 106 at CMC)

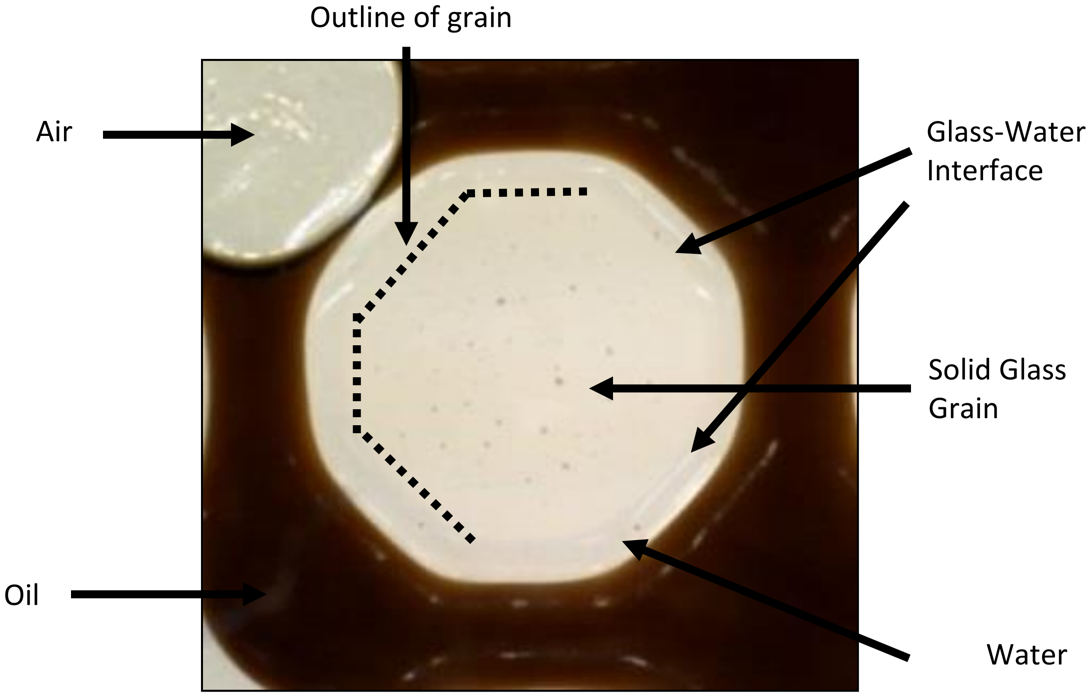

Figure 4-18. Micromodel Wettability Experiment 28 (Waterflood followed by WAG, WAG ratio of 1:1 with air, Iveysol 106 at CMC) Close View

As was discussed in Section 2.2.3, surfactants tend to change the wettability to a weak water wet system. Therefore it was not expected to observe a change in the wettability since the micromodel is already water wet.

4.2.4. Gravity Segregation

Gravity segregation was not observed. This is due to the fact that the micromodel has only one (1) pore volume in the vertical direction. This prevented gravity segregation from being possible.

4.2.5. Oil Displacement by Water Solution Phase

The main mechanism of oil displacement by the water solution phase (brine and brine-surfactant) displacing the oil phase involved water film flow along the solid glass surface and a displacement of oil by water imbibition. The water-oil meniscus advanced until it encountered and adhered to the grain wall on the opposite side of the pore throat. This mechanism of displacement resulted in an efficient displacement of oil by the water solution. Figure 4-19 shows this displacement mechanism, with the top left and bottom-left oil-filled pores in the beginning stages of the displacement and the middle-left oil filled pore in the middle of the displacement. Figure 4-19 was taken from Experiment 13 (No waterflood, WAG ratio of 1:1 with air, Triton X-100 at CMC), at a point during the injection of the 2nd gas slug.

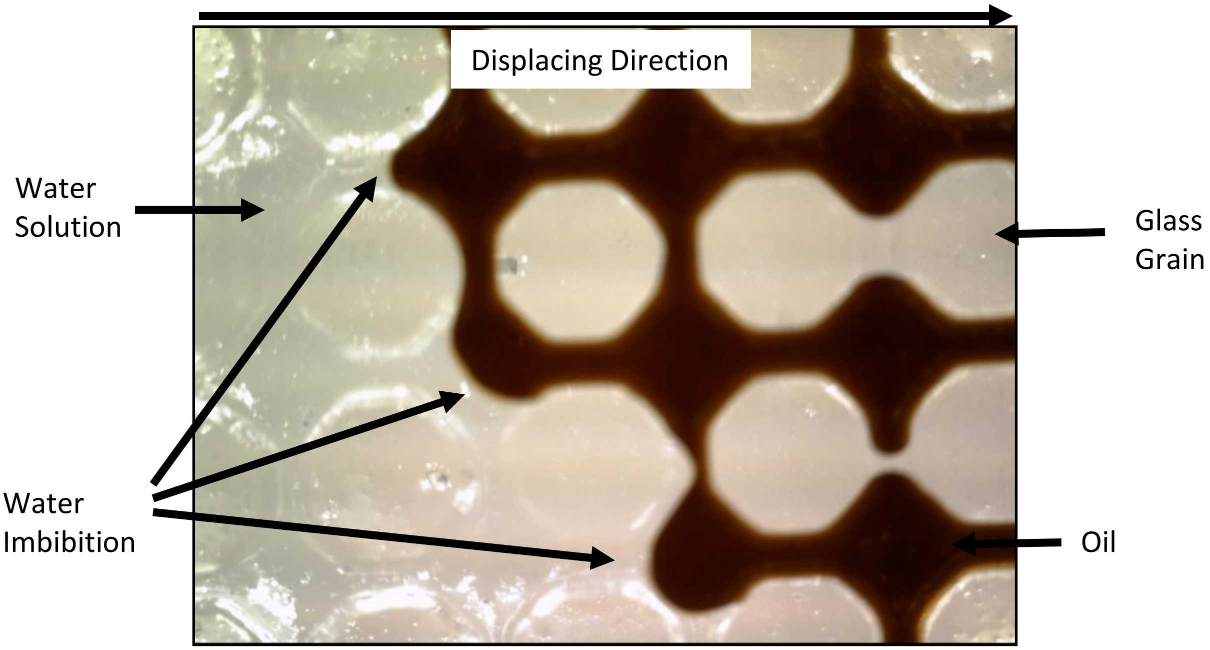

Figure 4-19. Oil Displacement by Surfactant Liquid – Experiment 13 (WAG ratio of 1:1 with air, Triton X-100 at CMC)

Generally, in the areas of the micromodel that have been swept with the water solution, the water solution completely displaces the oil, however as shown in Figure 4-20 taken from Experiment 23 (No waterflood, WAG ratio of 1:2 with air, Triton X-100 at CMC x 5.5), occasionally the aqueous phase creeps along the pore walls and fills all of the pore throats before the oil is displaced, effectively trapping the oil in the centre of the pore.

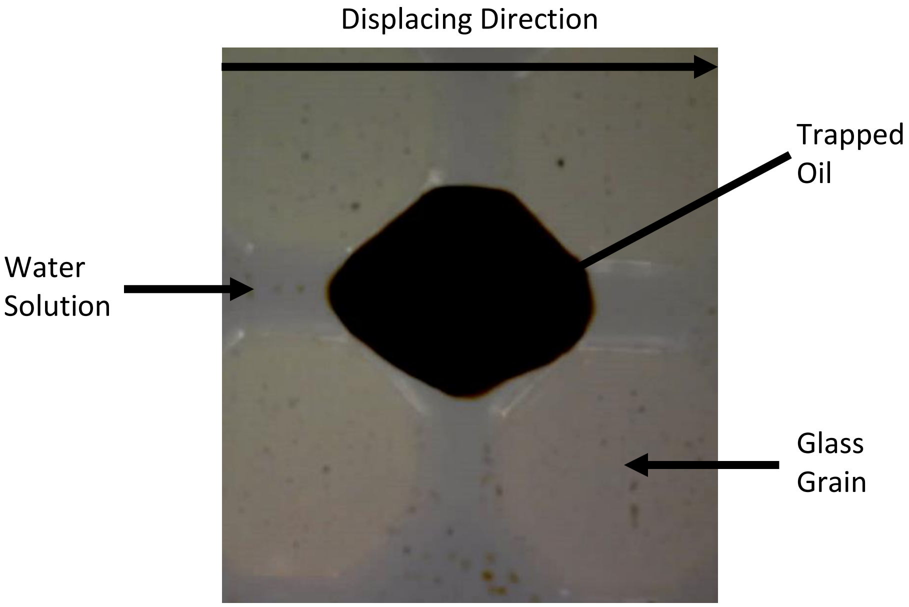

Figure 4-20. Trapped Oil – Experiment 23 (WAG ratio of 1:2 with air, Triton X-100 at CMC x 5.5)

There are several reasons why the oil may become trapped as in Figure 4-20. First, as the displacing fluid advances through the micromodel, if there are several displacing fronts moving both forward and to the side, some oil may be caught between the advancing fronts. This was observed on several occasions when the displacing fluid fingered through the oil in two or more fingers, as the fingers of displacing fluid expanded to the side they encountered each other and some oil would be trapped between the two fingers. Another reason for this trapping of oil is the ratio of viscous forces to capillary forces.

The micromodel is homogeneous, with pore body or throat sizes and pore shapes not changing significantly over the whole of the micromodel. This means that the entrance capillary pressure is similar for all the pores, as the pore aspect ratios are all the same and the pores are initially filled with oil (with some connate water). This makes the micromodel very different from real field reservoirs, where there is a distribution of pore body and throat sizes with pores able to have a wide range of shapes and sizes. Looking strictly at capillary forces, this should mean that the injection fluid should behave similarly throughout the micromodel due to the homogeneity of the pores. However some differences in the displacement efficiency can be noted throughout the micromodel as shown in Figure 4-19 and Figure 4-20. The displacement efficiency can be associated with the capillary number, which was discussed in Section 2.1.1 and presented in Equation (3). As surfactants lower the water-oil interfacial tension, the capillary forces between water and oil decrease. As discussed above in Section 4.1, the addition of surfactant to the brine lowers both the water-oil interfacial tension and the water viscosity. However the interfacial tension is reduced to a greater proportion than the viscosity, so the capillary number will increase.

Using values discussed in Section 4.1 and the equation for capillary number given in Equation (3), the capillary number can be calculated as 0.000045v, 0.00034v, and 0.0019v for brine, Triton X-100 at CMC, and Triton X-100 at 10 times CMC respectively. The flow rate will be constant between all three so they can still be compared without precisely knowing the velocity. If we look at the minimum and maximum liquid velocities for the micromodel (minimum when flow is through all pore bodies, maximum when flow is through one pore throat), the minimum liquid velocity is 0.046 m/hr, while the maximum is 6.93 m/hr. This would give the following ranges for capillary number for the above fluids: for brine $8.66\text{x}10^{-8}$ to 0.00753, for Triton X-100 at CMC $6.54\text{x}10^{-7}$ to 0.0569, and for Triton X-100 at 10xCMC $3.66\text{x}10^{-6}$ to 0.318. This shows that even though both viscosity and interfacial tension decrease with the addition of surfactants, the interfacial tension decreases at a faster rate than viscosity, causing the capillary number to increase.

At low capillary numbers, the capillary forces dominate, while at high capillary numbers the viscous forces dominate. In cases of high capillary numbers, the viscous forces push the displacing fluid into the pore. If the viscous forces are large enough, the displacing fluid may, while adhering to and creeping along the pore walls, be pushed forward and jump across the pore throats before the viscous forces have displaced all of the oil in the pore. Low capillary numbers are required for spontaneous water imbibitions, where the water phase slowly creeps along the pore walls, pushing the oil phase out of the pore until most, if not all, of the oil is removed from the water-wet pore like in Figure 4-19. As the micromodel is homogeneous, the viscous and capillary forces should not change from pore to pore, however the displacing fluid velocity may change. With one inlet and one outlet well, the path of least resistance, and therefore the path through which most of the displacing liquid flows, is directly between the inlet and outlet due to the micromodel homogeneity. Therefore the fluid moving through the middle of the micromodel will also have the greatest velocity. This velocity may be large enough to increase the capillary number to the point that the imbibition of water into the pore is overtaken by viscous forces, resulting in oil being trapped in the middle of the pores as in Figure 4-20.

Once the oil is completely surrounded by water, it is very difficult to displace the trapped oil. This is due to the fact that the displacing fluid will simply travel around the trapped oil and the viscous forces required to force enough water through the pore to displace the oil require very high flow rates, which in turn require very high pressures which may not be practical or economical.

4.2.6. Oil Displacement by Gas Phase

The gas phase rarely adhered to the pore walls, instead remaining in the middle of the pore. This is caused by the micromodel being a water-wet system, with the air wettability being less than the water wettability. The oil displacement by the gas phase followed a drainage-like immiscible displacement, with the gas non-wetting to the glass. The gas displaced the oil, forming an air-oil meniscus that advanced through the pore. Oil adhering to the water phase that surrounded the glass grain was not displaced, leaving large amounts of oil behind the front compared to the liquid displacement discussed above. The drainage-like displacement of the oil by the gas phase is shown in Figure 4-21, which is taken from Experiment 14 (No waterflood, WAG ratio of 1:1 with air, Triton X-100 at CMC), taken during the injection of the 4th liquid slug. The liquid slug was displacing the gas phase nearer to the inlet, the displaced gas phase was then displacing the oil phase at the gas front. The four images show the progression of air through an oil filled pore.

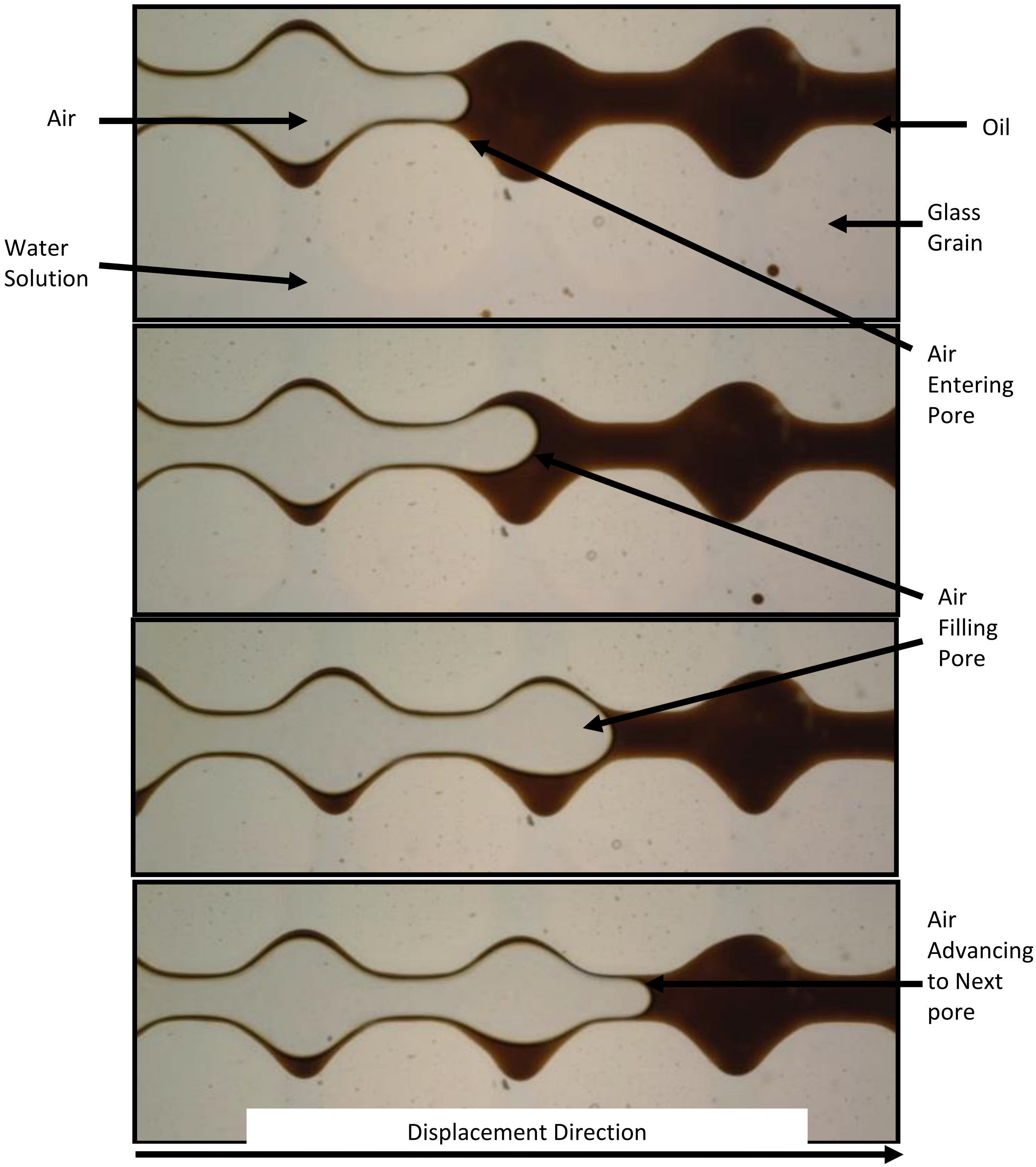

Figure 4-21. Oil Displacement by Air (Experiment 14, no waterflood, WAG ratio 1:1 with air, Triton X-100 at CMC, taken during liquid injection)

4.3. Oil Recovery

The percentage of oil recovered from the micromodel was calculated using Matlab to process images taken at set intervals throughout the experiment, including at the beginning, end, and after each slug had fully entered the micromodel. A sample of this image processing calculation is shown in Appendix F, which gives an overview of the analysis for Experiment 23. These results were then processed via Design Expert 9.0 to identify the significant factors affecting oil recovery. Table 4-1 provides the final cumulative oil recovery data for all of the experiments conducted.

Table 4-1. Oil Recovery Experimental Results

Experiment	WAG Ratio	Surfactant Concentration (CMC x)	Gas Type	Surfactant Type	Comments	Oil Recovery (%)
1	1:1	10	Air	Ivey-sol 106		59.55
2	1:1	1	Propane	Ivey-sol 106		63.90
3	1:2	1	Air	Triton X-100		60.10
4	1:1	10	Air	Triton X-100		48.88
5, 16, 22	1:1.5	5.5	Air	Triton X-100		62.64 ± 3.08
6, 9	1:1	5.5	Propane	Triton X-100		48.65 ± 9.00
7	1:2	10	Air	Ivey-sol 106		54.64
8, 10	1:2	1	Air	Ivey-sol 106		58.23 ± 6.27
11	1:2	1	Propane	Triton X-100		64.50
12	1:1.5	10	Propane	Ivey-sol 106		63.33
13	1:1	1	Air	Triton X-100		77.78
14	1:1	5.5	Air	Ivey-sol 106		67.82
15	1:1	5.5	Propane	Ivey-sol 106		62.47
17	1:1	10	Propane	Ivey-sol 106		52.72
18	1:2	5.5	Propane	Ivey-sol 106		61.82
19	1:2	10	Propane	Triton X-100		56.88
20	1:2	1	Propane	Ivey-sol 106		58.78

21	1:1.5	1	Propane	Triton X-100		58.82
23	1:2	5.5	Air	Triton X-100		68.22 ± 3.55
24	1:1	0	Air	None	Brine-Air WAG	49.47
25	1:0	1	None	Iveysol 106	Surfactant/water Flood	50.99
26	1:0	0	None	None	Waterflood	41.04
27	1:1	0	Air	None	Waterflooding followed by Water-Air WAG	48.92
28	1:1	1	Air	Iveysol 106	Waterflooding followed by Water/Surfactant-Air WAG	56.82
29	1:1	1	Air	Iveysol 106	Water/Surfactant WAG	60.23

The ANOVA method, as discussed in Section 2.7 was used to analyze the results. Comparing different model types (linear, two-factor interaction, quadratic, etc), the Two Factor Interaction model was noticed as being the best fit for the oil recovery data, with no transforms of the data required. Table 4-2 provides the ANOVA results for the oil recovery data using a two factor interaction model, meaning that there are individual factor effects and two factor interaction effects that are deemed significant. To determine if a factor or interaction is significant, the ANOVA table is calculated which calculates the experimental error by comparing the replicate experiments. Using the sum of squares method, the F-value for each factor, and for the model chosen, can be calculated and used to find the p-value. The p-value is a calculation of the probability that an identified effect is actually due to experimental error and not the factor being investigated. If the p-value calculated is less than 0.1, there is a less than 10% chance that the effect identified by the factor or interaction between the factors is due to experimental error and not the factor(s) being investigated. In this way, the factor(s) and two-factor interactions which are significant to the recovery of oil can be identified.

As shown in Table 4-2, the two factor interaction model that was chosen is deemed significant with a p-value of 0.0189, far below the threshold of 0.1, meaning that there is a less than 1.89% that the model chosen is accurate only due to experimental error. Individually, the effects of the WAG ratio (p-value of 0.6126) and surfactant type (p-value of 0.3146) are not deemed significant to oil recovery as there is a high probability (61.26% for WAG ratio and 31.46% for surfactant type) that the effects identified for these two factors are due more to error than to the factors. The effects of surfactant concentration (p-value of 0.0090) and gas type (p-value of 0.0550) are deemed significant and probably are not due to experimental error. This is because there is a 91% chance that the effect identified for surfactant concentration was not due to experimental error and a 94.5% chance that the effect for gas type was not due to experimental error.

For two factor interaction effects, the effects of WAG ratio-surfactant concentration (p-value of 0.0212), WAG-ratio-gas type (p-value of 0.0411), WAG ratio-surfactant type (p-value of 0.0634), and gas type-surfactant type (p-value of 0.0884) are all deemed significant and probably are not due to experimental error. This is because the WAG ratio-surfactant concentration effect has a 97.88% chance that the effect is not due to experimental error. Likewise the chance that the identified interaction effect is not due to experimental error for

WAG-ratio-gas type, WAG ratio-surfactant type, and gas type-surfactant type are 95.89%, 93.66%, and 91.16%, respectively.

As the model that best represents the data is a two factor interaction model, no nonlinearity in the data was identified. The lack of fit has a p-value of 0.6306 and is therefore not significant to the model, meaning that the model fits the data well as there is a 63.06% that the lack of fit is due to error.

Table 4-2. ANOVA table for Oil Recovery Data

Source	Sum of Squares	Degrees of Freedom	Mean Square	F Value	P-Value Prob>F	Significance
Model	764.61	8	95.58	3.54	0.0189	Significant
WAG Ratio	7.25	1	7.25	0.27	0.6126	Not Significant
Surfactant Concentration	247.79	1	247.79	9.17	0.0090	Significant
Gas Type	118.45	1	118.45	4.38	0.0550	Significant
Surfactant Type	29.40	1	29.40	1.09	0.3146	Not Significant
WAG Ratio-Surfactant Concentration	181.93	1	181.93	6.73	0.0212	Significant
WAG Ratio-Gas Type	136.78	1	136.78	5.06	0.0411	Significant
WAG Ratio-Surfactant Type	109.85	1	109.85	4.07	0.0634	Significant
Gas Type-Surfactant Type	90.62	1	90.62	3.35	0.0884	Significant
Lack of Fit	224.59	9	24.95	0.81	0.6306	Not Significant

The Two-Factor Interaction model that was identified as the best fit for the oil recovery trend out of four model types (linear, two-factor interaction, quadratic, and cubic). The individual effects are represented by single-factor terms (ex -4.88*C for the effect of surfactant concentration), while the interaction effects are represented by two-factor terms (ex. 2.8*W*G for the WAG ratio-gas type effect). Some factors (W for WAG Ratio and S for surfactant type) were identified as not being significant to oil recovery; however they are represented in the mathematical model as they are required for the interaction effects. The mathematical model is given in Equation (7).

$$R_{Oil} = 60.08 + 0.66 * W - 4.48 * C - 2.30 * G + 1.16 * S + 4.14 * W * C + 2.8 * W * G - 2.51 * W * S + 2.01 * G * S \quad , \qquad (7)$$

where:

W= WAG Ratio (1:1 = -1, 1:2 = 1),
C= Surfactant Concentration (1 x CMC= -1, 10 x CMC=1),
G= Gas Type (Air=-1, Propane=1), and
S= Surfactant Type (Triton=-1, Iveysol=1).

Figure 4-22 below shows the plot of model predicted values vs. actual experimental values for oil recovery. As shown, the predicted and actual values generally lay on the center diagonal line, meaning little statistical bias. There is some discrepancy between actual and predicted values, with some actual values not laying on the diagonal line. This is due to the fact that the model is not a perfect match for the oil recovery data, only the best match of the models available with an R-squared value of 0.7544 and an adjusted R-squared value of 0.5497. This means that the model explains 54.97% of the variance in the data, an ideal model would account for 100% of the variance, however out of the models available, the Two-Factor Interaction model accounted for the most variance in the data. The discrepancy between actual and predicted values for oil recovery are in the order of a few percent original oil in place.

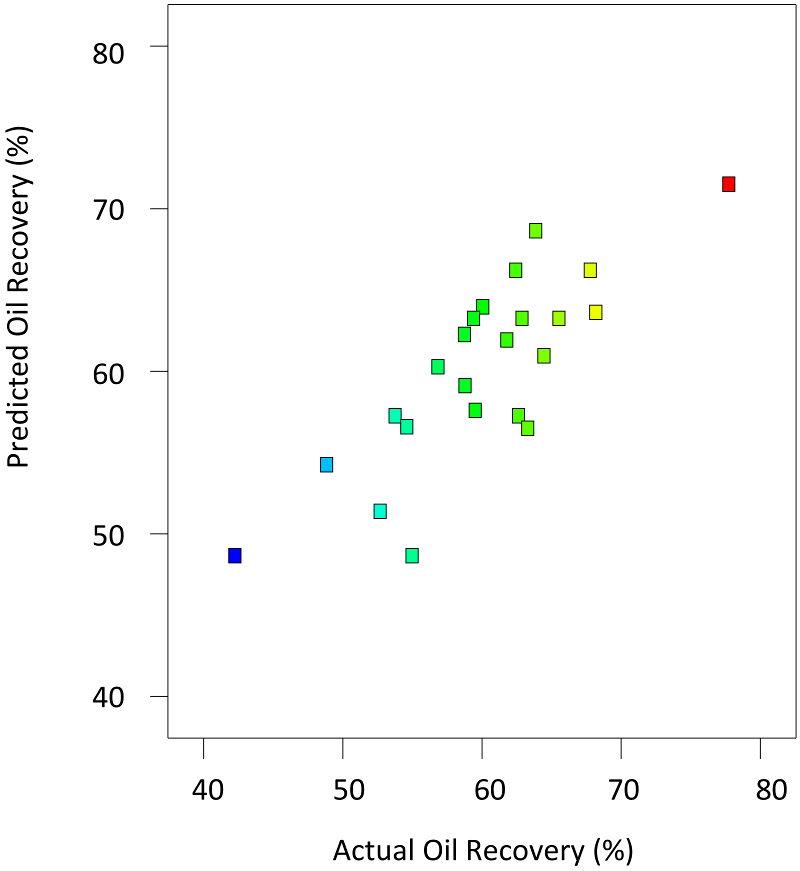

Figure 4-22. Predicted vs. Actual Values for Oil Recovery

Overall, to maximize the oil recovery, it was found that the levels of the four factors presented in Table 4-3 should be used.

Table 4-3. Optimization of Factors for Oil Recovery

Factor	**Level**
WAG Ratio	1:1
Surfactant Concentration	1 x CMC
Gas Type	Air
Surfactant Type	Iveysol 106

All of the factors investigated proved to be significant, either individually or in interaction with each other. Details of each individual effect will be discussed in Section 4.3.2, while the interaction effects between the main factors will be discussed in Section 4.3.3. As well, the baseline experiments, consisting of waterflooding, water-surfactant flooding, brine-air flooding, and brine-propane flooding will be discussed in Section 4.3.4.

4.3.1. Oil Recovery Error Analysis

The oil recovery was measured using two different methods, image processing and mass balance. The image processing method involved taking pictures of the micromodel and determining the oil saturation through counting pixels, while the mass balance method involved measuring the volume and weight of fluids produced in the micro separator. This section will discuss the error in the experimental data and examine the difficulties associated with corroborating the image analysis data with mass balance data for oil recovery. This section will be broken down into three parts, the difficulties in recording accurate mass and volume data, the image processing-mass balance corroboration and accuracy of the measurements, and an examination of the replicate experiments.

4.3.1.1. Difficulty in Accurate Mass and Volume Measurements

This section will discuss the difficulties associated with gathering accurate mass and volume data from the micromodel experiments. It was initially planned to collect produced fluids in an outlet separator, and measure the fluids both by volume in a burette, and by mass on a scale.

It was hoped to be able to corroborate this mass-volume data with the image processing data; however this proved difficult for a number of reasons. The first reason, as will be discussed in Section 4.6, is that there were several problems encountered with oil being trapped in the lines behind the injection fluids. This oil had to be drained to not affect the images collected during the experiment. This trapped oil was part of the line volume used to calculate the total oil in the system, which would be used to calculate the oil recovery. Draining this oil reduced the expected produced oil, and thereby also reduced the oil recovery.

The second difficulty encountered was that the micromodel was never fully saturated with oil due to connate water. The procedure of first flooding with brine and then oil to reach connate water saturation resulted in some water adhering to the pore walls. Connate water was expected, however quantifiable measurements of the volume of connate water proved difficult to determine. In addition to this, despite vacuuming the oil phase prior to oil flooding, small air bubbles were present in the oil. Figure 4-23 and Figure 4-24 shows connate water present in the micromodel after oil flooding. All of this again reduced the volume of oil which was initially in the micromodel.

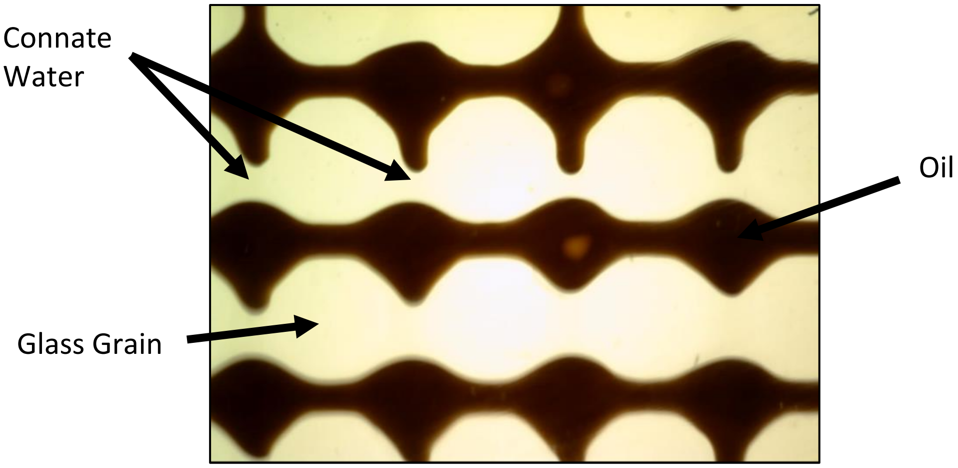

Figure 4-23 Connate Water in the Micromodel

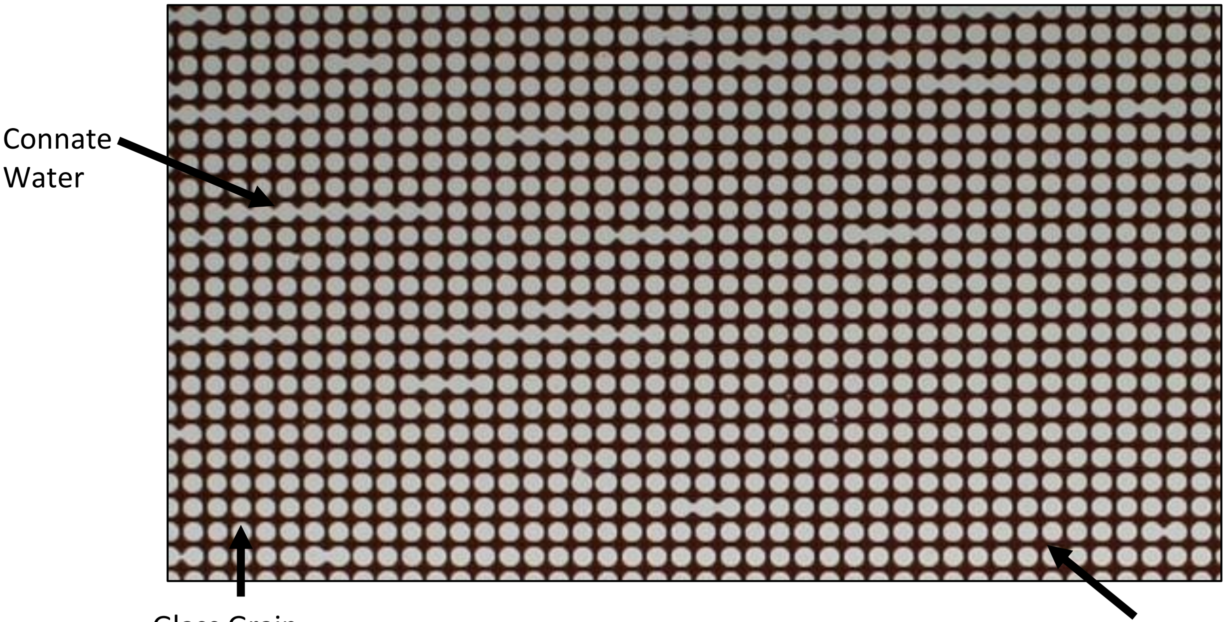

Figure 4-24 Water and Oil in the Micromodel

Connate water was expected, however the presence of connate water reduced the volume of the micromodel that was filled with oil which made it difficult to get an accurate measurement of the mass of oil that would be in the micromodel. This decrease is small compared to the effects of the other difficulties encountered, discussed below, however in addition to the other difficulties the difference between produced oil weight and volume and expected produced oil weight and volume were large. This problem interfered with the mass balance data only and not the image processing data.

The third reason that accurate mass and volume data was difficult to obtain was due to hold up and trapping of fluid. The procedure was to inject air into the micromodel outlet line to push any fluids in the lines after the micromodel into the separator. In practice this did not work as desired. The fluids were wetting to the walls of the tubing, causing a significant amount of fluid to remain in the lines. Figure 4-25 and Figure 4-26 show the fluids that were typically trapped in the lines past the micromodel. Figure 4-25 shows the ½” tubing near the micro separator, which retained a large amount of oil on the tubing walls. Figure 4-26 shows the 1/8” tubing at the micromodel outlet, which retained much less oil than the ½” tubing. For comparison these tubings should be a clear-yellow, which would appear lighter in colour, while in these figures there is so much oil adhered to the tubing walls that the tubings appear much darker.

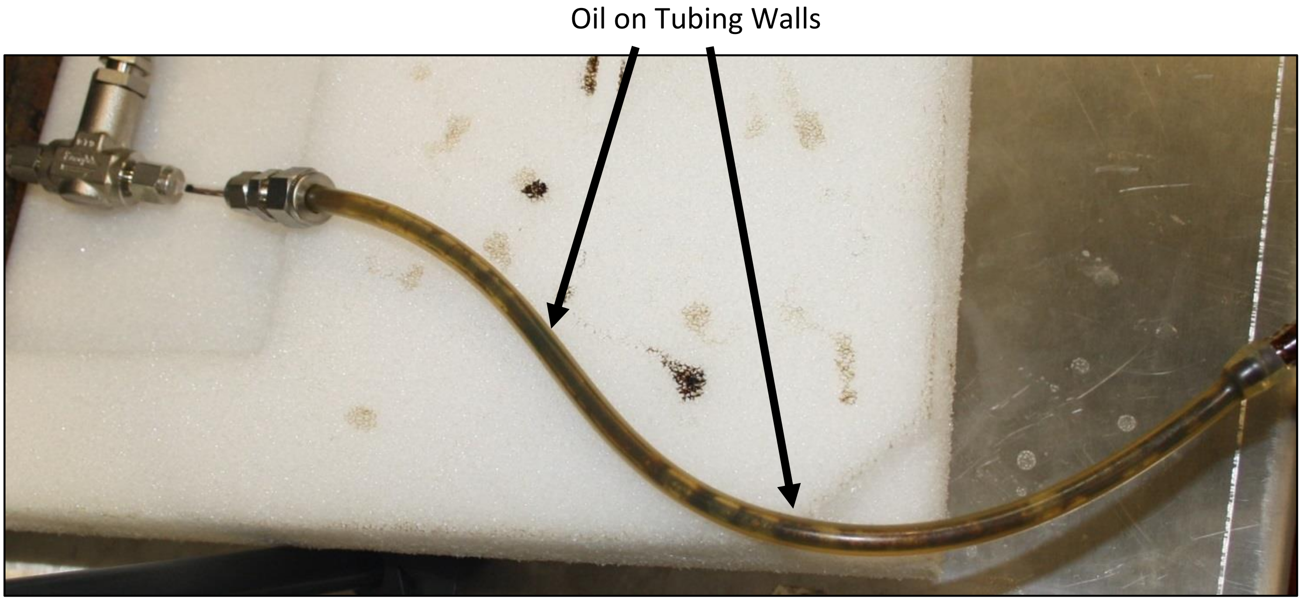

Figure 4-25 Fluids trapped at the end of the micromodel before the separator

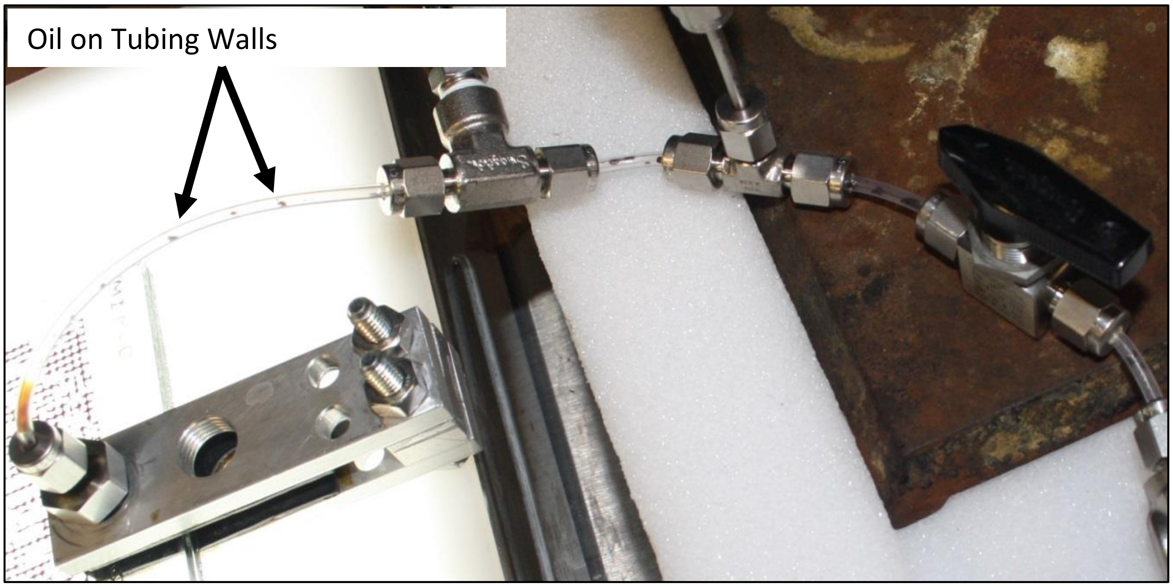

Figure 4-26 Fluids trapped at the end of the micromodel at the micromodel outlet

In addition to the oil trapped in the outlet lines, oil was also trapped on the walls of the separator, obscuring both the volume and weight measurements. The oil adhered to the separator wall, making an accurate volume calculation difficult. As well, after draining the separator to measure the weight of the produced fluids, the oil trapped on the separator walls would not drain, thereby reducing the amount of fluid that the weight measurement calculated. Figure 4-27 shows the fluids trapped on the separator walls, on the left hand side of the picture is the separator with oil trapped, and on the right hand side of the picture is what the clean separator should look like. As shown, a significant amount of oil is trapped on the separator walls.

Figure 4-27 Fluids trapped in the separator

This again reduced the amount of oil which could be measured both by volume and weight. In addition to the trapped oil, the water and oil phases were difficult to separate in the separator due to its small tube. The water and oil would not separate 100%; therefore individual measurements of oil and water volume were occasionally impossible to measure. Therefore two volumetric measurements of the oil and water were taken, one in the separator, and one in the graduated cylinder which was used to measure the mass of the fluids. The graduated cylinder only had graduations of 1 mL, this combined with some oil being trapped on the walls of the graduated cylinder made accurate measurements of the fluids difficult to obtain.

All of these difficulties resulted in a percent difference between the measured weight data and the weight data calculated from using the volume data of between 6% and 14%. The oil recovery was then calculated from the volume data measured. The percent difference between the oil recovery calculated from image processing and the oil recovery calculated from the volumetric data ranged between -4.7% to -111%. This percent difference data had a mean value of -76% and a median value of -79%, with a standard deviation of 24%. This means that the oil recovery from the volumetric calculations were consistently well below the oil recovery measured through image processing. In addition to the noted difficulties in measuring the volumetric data for the produced fluids, the dead volume (volume of oil in tubings and fittings outside of the micromodel) in the system was nearly double the volume of the micromodel, meaning a significant amount of oil produced was attributed to the dead volume and not as being recovered from the micromodel. This, combined with the difficulties mentioned above, significantly reduced the amount of produced oil which was attributed as being produced from the micromodel. Not taking into account the dead volume would over-estimate the oil recovery as the oil that is contained within the tubing and fittings is nearly double the pore volume of the micromodel, meaning that the oil recovered from the system could be greater than the pore volume of the micromodel. This could greatly affect the experimental results obtained in a mass balance exercise; therefore image processing was used to calculate the oil saturation of the micromodel by determining the number of pixels of oil in the image. The oil recovery was then determined by analyzing the decreasing oil saturation of the micromodel as the experiment progressed.

Due to these difficulties in measurement, and the large percent differences in calculated oil recoveries observed, it was found that it was not possible to corroborate the image analysis data with a mass balance analysis for every experiment. Though one experimental run had a very low difference between volumetric calculated and image processing calculated oil recoveries of -4.7%, this was deemed to be an outlier as it was the only data point above -40% which existed.

4.3.1.2. Mass Balance-Image Processing Corroboration and Accuracy

In order to corroborate the image processing data and mass balance data, an extra validation experiment was conducted. In this experiment, only the micromodel itself was saturated with oil, with the rest of the lines of the system not being saturated with oil. The outlet lines and fittings were replaced with a three meter long, 1/8” OD, 1/16” ID tube. The experiment involved flooding the micromodel with brine until breakthrough, while taking pictures and collecting volume data every 2 minutes. The volume data gathered was the length of the oil in the three meter outlet tube, as the experiment was a waterflood, all of the liquid in the outlet tube was oil until breakthrough was achieved, therefore the outlet tube was a direct measurement of produced oil. The length of oil in the tube was measured with a ruler with the smallest graduation of 1 mm, therefore it's accuracy is ±0.5 mm. Therefore the volume of the oil in 0.5 mm of tubing can be calculated by:

$$V = \pi * \left[\frac{r}{2}\right]^2 * L$$

$$V = \pi * \left[\frac{\left(\frac{1}{16}in\right) * \left(\frac{25.4\ mm}{1\ in}\right)}{2}\right]^2 * \frac{(\pm 0.5\ mm)}{\frac{1000\ mm}{1\ mL}}$$

$$V = \pm 0.00099\ mL$$

With an accuracy of oil volume of 0.00099 mL, the accuracy in the oil recovery can be found by dividing the volume accuracy by the micromodel volume. The micromodel volume was found by weighing the micromodel both fully saturated with distilled water and fully evacuated and dried, this gave a pore volume of 2.9 mL.

$$R = \frac{V_{Oil}}{V_{Micromodel}} * 100\%$$

$$R = \frac{\pm 0.00099\ mL}{2.9\ mL} * 100\%$$

$$R = \pm 0.034\%$$

Figure 4-28 below shows that the percent oil recovery obtained from both the volume data and image processing methods, while Figure 4-29 shows the percent difference between the image processing and mass balance data.

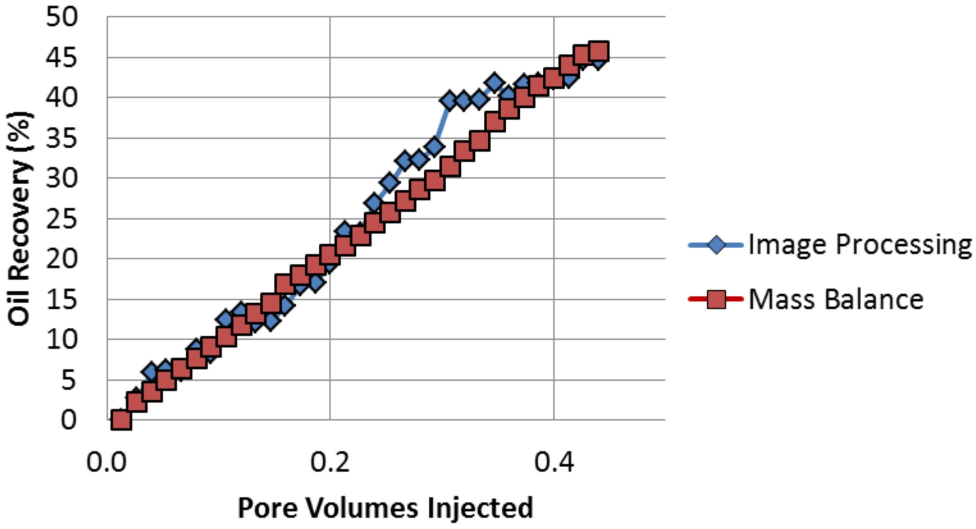

Figure 4-28. Mass Balance - Image Processing Correlation

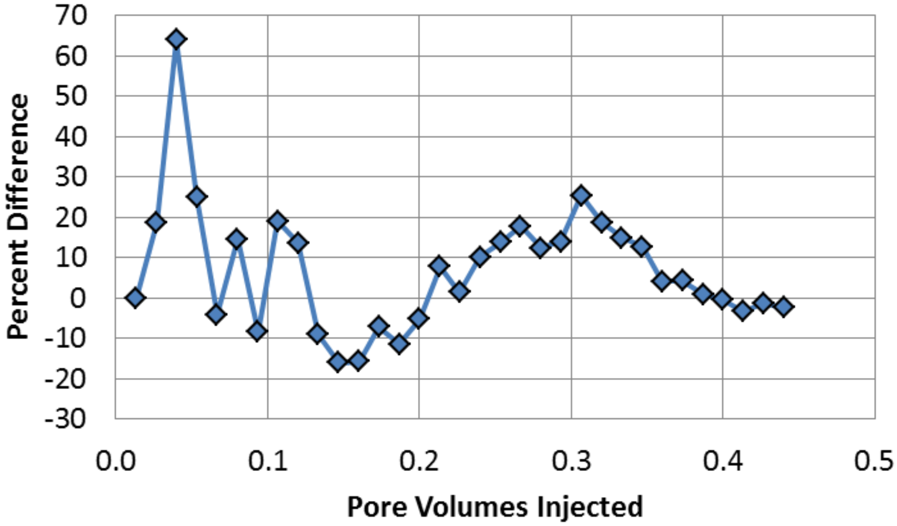

Figure 4-29. Mass Balance - Image Processing Percent Difference

As shown in the Figures 4-28 and 4-29, the percent oil recovery obtained from the image processing data is very similar to the values obtained from the mass balance, with an average percent difference of 6.9%. The percent difference is fairly large for the first few data points, however this is expected since the recoveries obtained for these points are very low and any small error in measurement translates into large percent differences when dealing with such small values. This can be seen by the percent difference decrease to near zero as time goes on. This validation experiment corroborated the image processing data with mass balance data very well, therefore only the image processing data will be shown for the oil recovery from here on as the original mass balance method did not corroborate well with the image processing data due to the reasons discussed above.

The image processing analysis also incorporates error into the oil recovery calculation. Assuming that the error is equal to the smallest measurement gradient (Taylor 1982), the error would be equal to one-half pixel for each pixel of an interface between oil and another substance. Only the oil-other substance interfaces are used as when the image is turned to black and white since only oil is turned black while all other phases are turned white. The threshold used to turn a colour pixel to a black pixel was 0.5, meaning that if the pixel was at least 50% black, the entire pixel would be turned black. This corresponds with the error of one-half pixel, as a pixel that is turned white may have been up to 50% black. The interfaces used for the error calculation included the interface between the grains and the oil, the interface between oil and any of the injection fluids (liquid or gas), and the interface between the oil and the sides of the micromodel. As the oil was displaced throughout the experiment, the number of grains that the oil had an interface with decreased, this was accounted for by prorating the grain interface error with the amount of oil remaining in the micromodel. When the micromodel was fully saturated with oil, the oil had an interface with all of the grains (6600 grains in total, micromodel was 44 grains wide by 150 grains long). As the oil was displaced, the number of grains that the oil had an interface with was prorated based on the amount of oil remaining in the micromodel based on the black pixel count, if 60% of the oil remained, it was assumed that the oil had an interface with 60% of the grains. Each grain was 11 pixels x 11 pixels, for a total grain-interface pixel count of 44 pixels, using the one-half pixel for the error; the pixel error per grain was 22 pixels.

Next the oil-water and oil-gas interfaces are accounted for; this was done by approximating the length of the interface in pixels. An example of this procedure can be found in Appendix H, as the interface length changed throughout the experiment, the interface error also varied throughout the experiment. Finally the interface between the oil and the micromodel sides was determined. It was assumed that the oil was always in contact with all sides of the micromodel, this is a conservative assumption, however the error associated with the sides of the micromodel is relatively low compared to the grain and injection fluid interfaces and therefore do not affect the total error significantly. An example of the full error analysis procedure can be found in Appendix H. From Appendix H, the average error of the image processing analysis throughout the experiment is approximately 32%. This calculated error is very large, and if this was the true error of the image processing analysis it would be expected to observe an error on that magnitude in the data. An error is observed in the data, with the measured oil recovery occasionally decreasing, which is not a physical possibility. However, the average error observed in the data (measured by the magnitude of the decreases in oil recovery) was 2.76% including outliers. Removing the outliers as error due to other reasons (lighting, etc.), the average error observed in the data was 2.0%. Both of these observed errors are significantly less than the calculated error of 32%. It is possible that the method used to calculate the error associated with the image processing analysis is incorrect, no published literature on methods to account for image processing analysis error for oil recovery experiments in micromodels could be found and this is an area recognized by the author as requiring in-depth investigation.

4.3.1.3. Replicate Experiments

The set of experimental runs conducted involved several repeat experiments, with one experiment being repeated outside of the main set of experiments. Figure 4-30 shows Experiments 5, 16, and 22, which are the repeat experiments dealing with Triton X-100 at 5.5 times CMC with air at a WAG ratio of 1:1.5. The three experiments are very similar; with the average final oil recovery of 62.64 ± 3.08%.

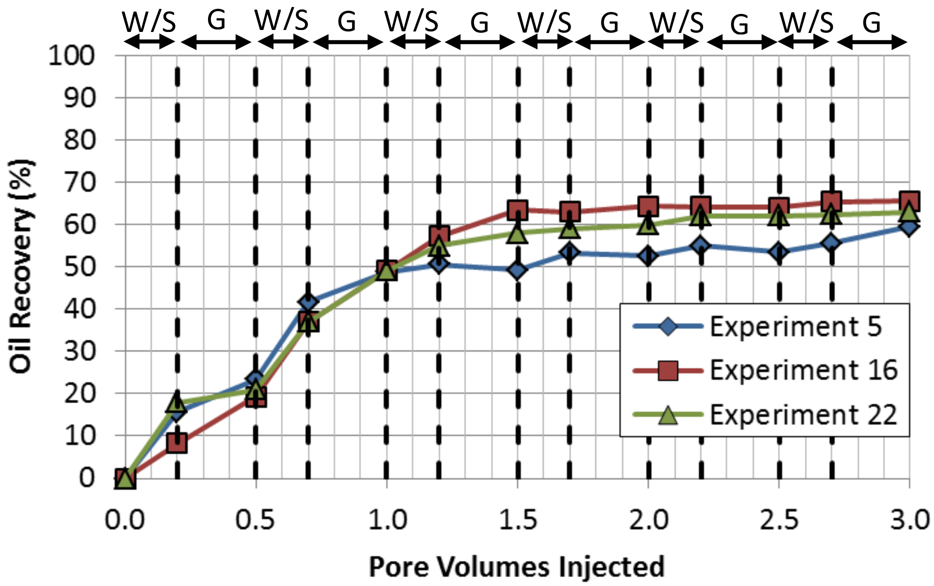

Figure 4-30. Repeat Experiments for Triton-100 5.5 times CMC with Air, WAG ratio 1:1.5

Figure 4-31 shows Experiments 8 and 10, which are the repeat experiments dealing with Iveysol 106 at 1 x CMC with air at a WAG ratio of 1:2. The two experiments behaved similarly though Experiment 8 consistently recorded a lower oil recovery than Experiment 10, with the average final oil recovery being 58.23 ± 6.27%.

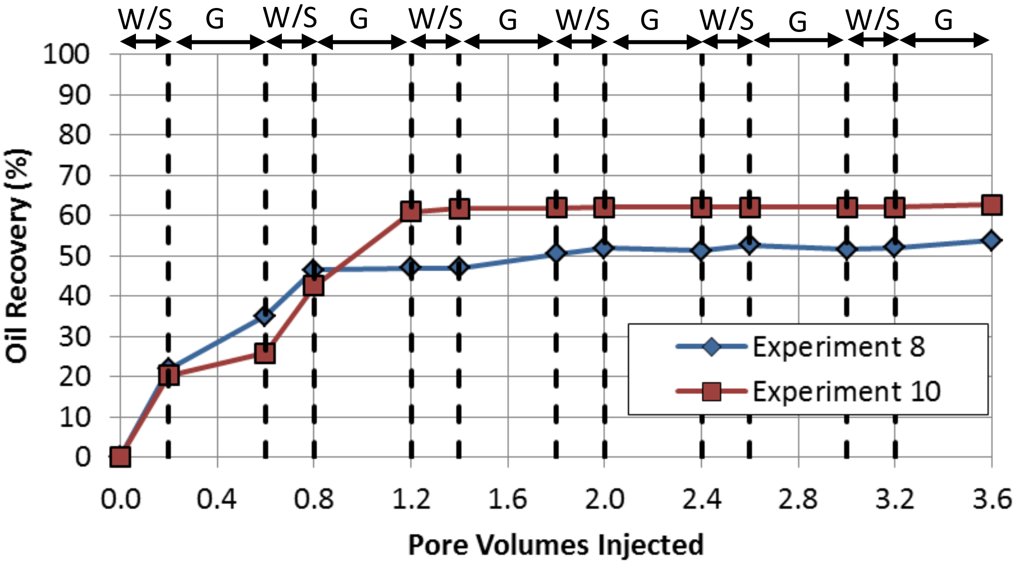

Figure 4-31. Repeat Experiments for Iveysol 106 1 x CMC with Air, WAG ratio 1:2

Figure 4-32 shows Experiment 23, which deals with Triton X-100 at 5.5 x CMC with air at a WAG ratio of 1:2. Experiment 23 was repeated as an extra reproducibility test. The two runs of Experiment 23 are very similar, with the average final oil recovery being 68.22 ± 3.55.

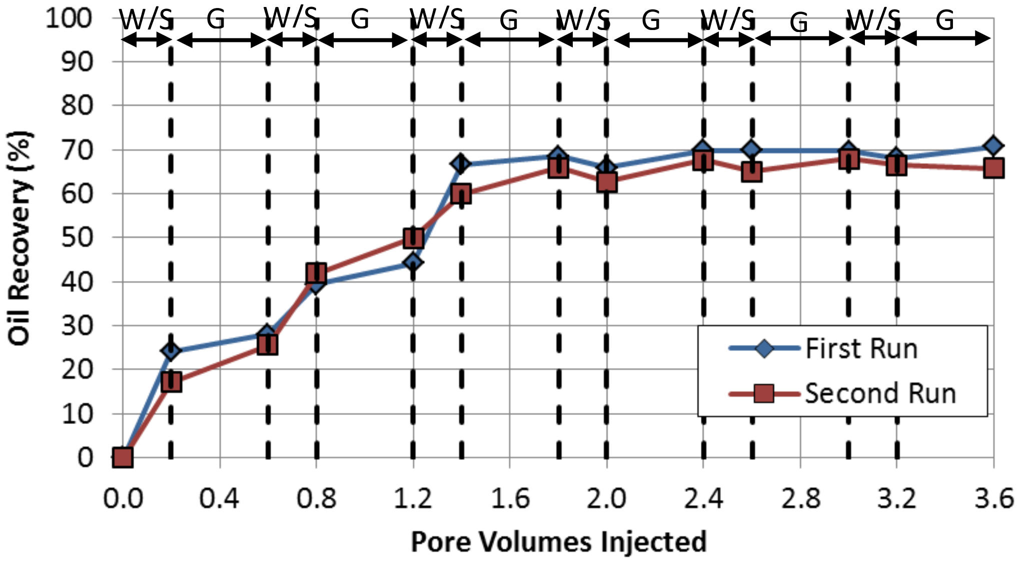

Figure 4-32. Repeat Experiments for Triton X-100 5.5 x CMC with Air, WAG ratio 1:2 (Experiment 23)

These repeat experiments consistently found standard deviations in the range of 3 to 9%, with the standard deviation of 9% most likely being an anomaly, with most standard deviations between 3% and 6%. Including all repeat experiments, the average standard deviation is 5.48%, while excluding the 9% anomaly the standard deviation is 4.3%. These reproducibility experiments show that the experiments are reproducible within a reasonable range (generally 4% to 6% difference). This set of two experiments had an ultimate oil recovery of 68 ± 3%.

The reproducibility of the experiments is also evident in the ANOVA analysis of the data. The lack of fit had a p-value of 0.6306, with p-values over 0.1 were considered not significant. The software analyzed the error of the experiment in terms of the mean square data, with the lack of fit data having a mean square of 24.95 while the pure error has a mean square of 30.74. The higher the mean square, the more significant the factor is to the model. The mean square data for both lack of fit and pure error are well below the mean square values for the investigated factors, especially the significant factors, which all have mean square values of over 80. This is further evidence that the pure error invoked by the experimental procedure and data analysis is below the detectable difference between the effects of the different factors that were investigated. This is corroborated with percent differences in the experiments of generally 4% to 6%.

.

4.3.2. Individual Factor Effects

This section will detail the individual effects of the four factors investigated (WAG ratio, surfactant concentration, gas type, and surfactant type). These individual effects do not show the full impact of the factor, as several factors may interact with each other to produce different effects. To determine the full effect of each factor the individual and interaction effects should be considered.

Several figures in Sections 4.3 and 4.4 do not contain data points. This is due to the fact that Design of Experiments software was utilized, varying four factors simultaneously. This caused instances where one factor was not varied across the full range of values for every combination of the other three factors. For example, when using Iveysol 106 surfactant with air at a WAG ratio of 1:1, surfactant concentrations of 5.5 and 10 times CMC were tested, while a surfactant concentration of 1 times CMC was not directly tested. Design of Experiments software utilized statistical analysis of all the experiments to develop the relationships between the factors and responses. In this way the 1 times CMC concentration for Iveysol was tested under different conditions (WAG ratio, gas type) and the effect determined.

4.3.2.1. WAG Ratio

The water-alternating-gas ratio was investigated using three levels ranging from 1:1 to 1:2, a low level of 1:1 (one slug of water to one slug of gas), a high level of 1:2 (one slug of water to two slugs of gas), and a center point of 1:1.5 (one slug of water to one and a half slugs of gas). The individual effect of WAG ratio was found not to be significant to the recovery of oil as evident in the ANOVA table by a p-value of 0.6126, well above the cut-off of 0.1. As shown in Figure 4-33, the oil recovery does not change significantly over the full range of WAG Ratios investigated. The change in oil recovery over the full range of WAG ratios of approximately 6% is on the same order of magnitude of the standard deviation identified earlier (5.74%, or 4.3% excluding the 9% anomaly), therefore this observed response may be due to random error and can not be attributed to the individual factor of WAG ratio. Figure 4-33 shows the trend for WAG Ratio incorporating all of the first 23 experiments. Only the first 23 experiments are incorporated into this due to the fact that the first 23 experiments are the Design of Experiments set of experiments, while experiments 24 to 29 were additional experiments outside of the main set of experiments. In Figure 4-33, all the data points sorted by WAG Ratio do not change significantly between WAG Ratios of 1.0 and 2.0. As shown, the oil recovery does not change over the full range of WAG ratios, with the 95% confidence interval trend being horizontal.

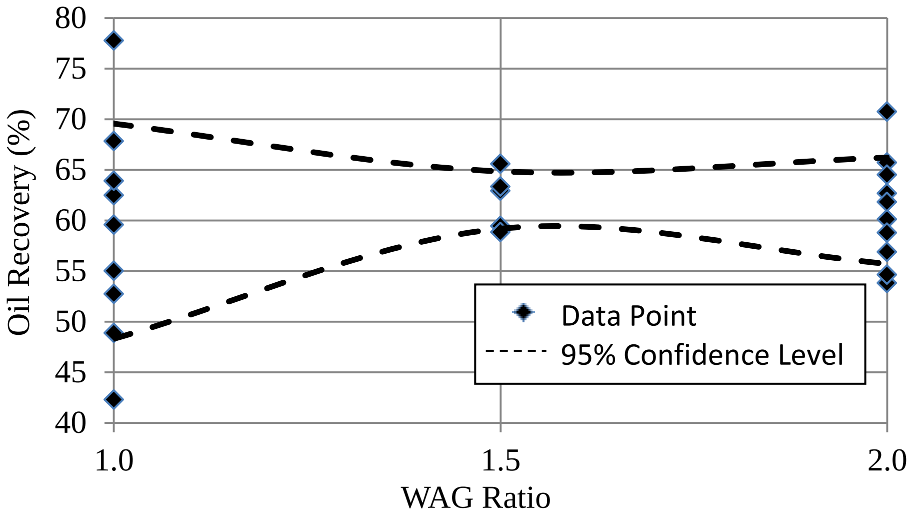

Figure 4-33. WAG Ratio vs. Oil Recovery (%) Data Points

The insignificance of WAG Ratio may be due to the observed movement of the gas phase through the micromodel. Generally, when the gas phase entered the micromodel, due to the low viscosity of the gas, the gas phase would finger through the oil phase and cause a breakthrough of the gas phase at the outlet well. Once the gas phase broke through to the outlet well, the gas traveled through this channel and no additional oil recovery was noticed after the gas phase broke through until the next water slug entered the micromodel.

4.3.2.2. Surfactant Concentration

The concentration of surfactant in the water was investigated at three levels, a low level of one times the critical micelle concentration (CMC), a high value of ten (10) times the CMC, and a center point of five-and-a-half (5.5) times the CMC. The individual effect of concentration was found to be significant on the oil recovery, as evident in the ANOVA table by a p-value of 0.09, below the cut-off value of 0.1. The change in oil recovery over the full range of surfactant concentrations of approximately 18% is greater than the standard deviation identified earlier

(5.74%, or 4.3% excluding the 9% anomaly), therefore this observed response is likely due to the individual factor of surfactant concentration and not random error. As shown in Figure 4-35, the oil recovery decreases as the concentration of the surfactant is increased.

Figure 4-34 shows the average trend for increasing surfactant concentration, using the averages for WAG Ratio, gas type, and surfactant type incorporating all of the first 23 experiments. Only the first 23 experiments are incorporated into this due to the fact that the first 23 experiments are the Design of Experiments set of experiments, while experiments 24 to 29 were additional experiments outside of the main set of experiments.

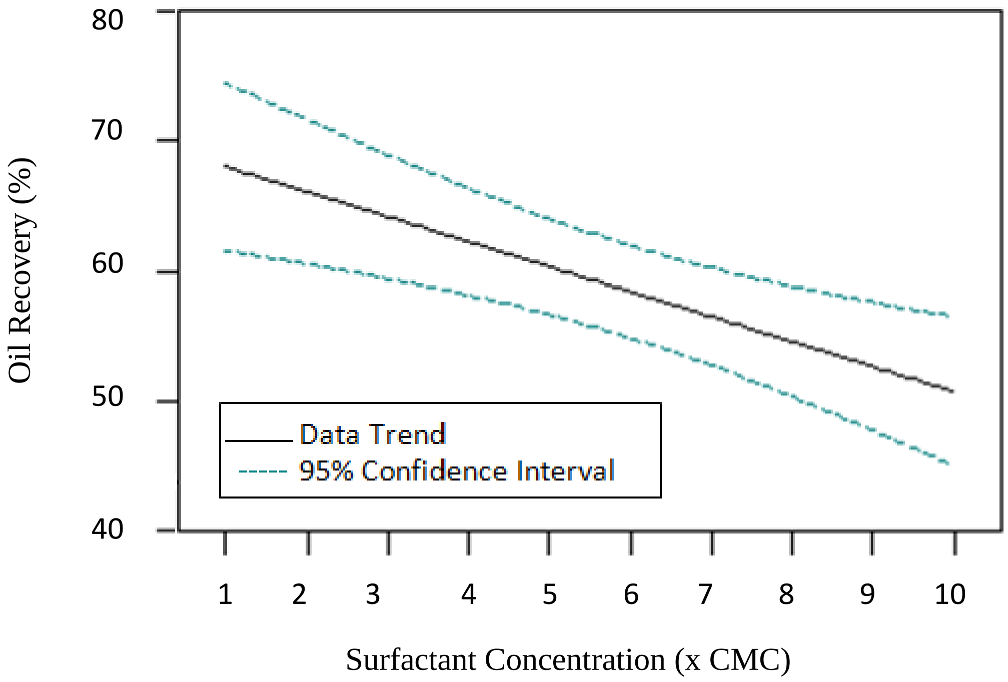

Figure 4-34. Multiple of CMC vs. Oil Recovery (%)

It was expected that increased surfactant concentration would produce increased oil recovery, however in the micromodel the opposite effect was observed, with the oil recovery decreasing approximnately 18% between surfactant concentrations of 1 x CMC and 10 x CMC. This may be due to the fact that in the absence of creating foam, the increase in mobility ratio caused by the surfactant decreases the sweep efficiency and causes the injection fluids to bypass some of the oil in the micromodel. A comparison between two experimental runs can show this. Experiment 7 and experiment 10 both consisted of injecting Iveysol 106 with air at a WAG ratio of 1:2. Experiment 7 had a surfactant concentration of ten times CMC, while Experiment 10 had a surfactant concentration of one times CMC. Experiment 7 had a cumulative oil recovery of 54.64%, while experiment 10 had a cumulative oil recovery of 62.67%. Figure 4-35 shows a comparison of experiments 7 and 10, showing unswept oil in Experiment 7.

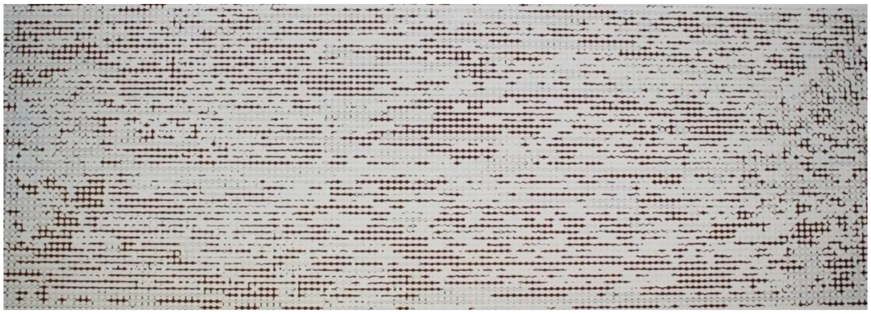

1 x CMC Iveysol 106 Surfactant

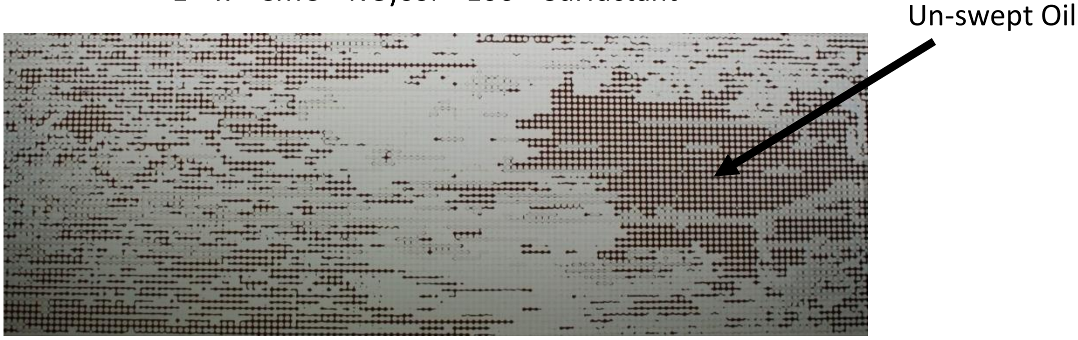

10 x CMC Iveysol 106 Surfactant Solution

Figure 4-35. Comparison of 1 x CMC and 10 x CMC Iveysol 106 Solution (Experiments 10-top, 10-bottom), WAG ratio of 1:2 with air.

The mobility ratio presented in Section 2.1.1 is the ratio of the mobility of an injected fluid to the mobility of the displaced fluid which is oil in this case, and is given in Equation (4). While the surfactants decrease the viscosity of the injection fluid, thereby increasing the mobility slightly, the decrease in interfacial tension caused by the surfactants also increases the injection fluid relative permeability (Sheng 2011; Shen et. al 2006).

$$M = \frac{K_{ri}}{K_{ro}} \frac{\mu_o}{\mu_i} \qquad , \tag{4}$$

where:

μ_o = Oil Viscosity,
μ_i = Injected Fluid Viscosity,
K_ro = Oil Relative Permeability, and
K_ri = Injected Fluid Relative Permeability.

The small decrease in injected fluid viscosity, coupled with the increase in injected fluid relative permeability that is caused by decreasing the interfacial tension, increases the mobility ratio, thereby making it easier for the surfactant solution to bypass areas of oil, which happened in Experiment 7. Several other cases of increased surfactant concentration causing unswept areas of oil are given in Appendix F. These unswept oil areas reduce the cumulative oil recovery of the experiment when the surfactant concentration is increased. It appears that the disadvantage to sweep efficiency caused by an increase in mobility ratio overshadows the advantage of decreasing the interfacial tension between the surfactant and oil fluids.

4.3.2.3. Gas Type

Two different gases were investigated, air and propane. The individual effect of gas type was found to be significant to the recovery of oil, as evident in the ANOVA table by a p-value of 0.055, less than the cut-off value of 0.1. As shown in Figure 4-36, the oil recovery is higher for tests involving air as the gas phase than the tests with propane as the gas phase. The change in oil recovery over the full range of WAG ratios of approximately 10% is greater than the standard deviation identified earlier (5.74%, or 4.3% excluding the 9% anomaly), therefore this observed response is likely due to the individual factor of gas type and not random error. Figure 4-36 shows the trend between air and propane, while using the average values for WAG Ratio, surfactant concentration, and surfactant type incorporating all of the first 23 experiments. Only the first 23 experiments are incorporated into this due to the fact that the first 23 experiments are the Design of Experiments set of experiments, while experiments 24 to 29 were additional experiments outside of the main set of experiments. As shown, the oil recovery for air of approximately 65% was greater than the oil recovery for propane of approximately 55%.

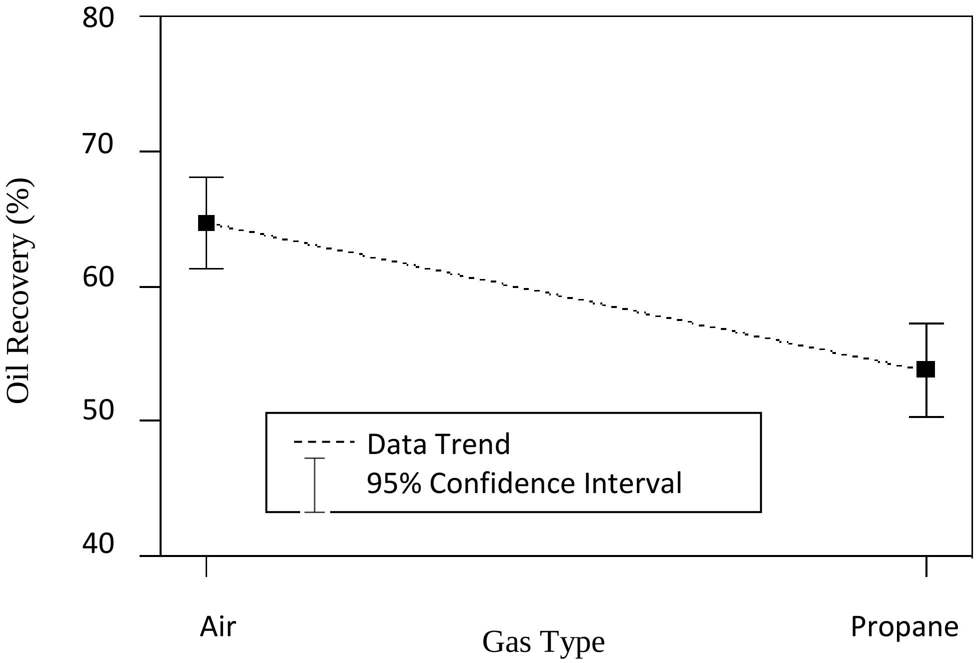

Figure 4-36. Gas Type vs. Oil Recovery (%)

As shown in Figure 4-36, the oil recovery decreases from approximately 65% for air to approximately 55% for propane. The lower oil recovery for propane compared to air may be due to the viscosities of the fluid, and therefore the fingering potential of the fluids. Air has a dynamic viscosity of $17.83\ x\ 10^{-6}\frac{N\,s}{m^2}$ (Dixon 2007), while propane has a dynamic viscosity of $7.655\ x\ 10^{-6}\frac{N\,s}{m^2}$ (Vogel et. al 1998), this would have caused the mobility ratio of the propane to be over double the mobility ratio of the air, assuming that the relative permeabilities of air and propane are nearly the same, as shown by the following calculation.

Mobility Ratio of air

$$M_{air} = \frac{K_{r-air}}{K_{ro}}\frac{\mu_o}{\mu_{air}}$$

$$K_{ro} = \frac{K_{r-air}}{M_{air}}\frac{\mu_o}{\mu_{air}}$$

Mobility Ratio of propane

$$M_{propane} = \frac{K_{r-propane}}{K_{ro}}\frac{\mu_o}{\mu_{propane}}$$

$$K_{ro} = \frac{K_{r-propane}}{M_{propane}}\frac{\mu_o}{\mu_{propane}}$$

$$K_{ro} = \frac{K_{r-air}}{M_{air}}\frac{\mu_o}{\mu_{air}} = \frac{K_{r-propane}}{M_{propane}}\frac{\mu_o}{\mu_{propane}} \quad ,$$

$$\frac{K_{r-air}}{M_{air}\mu_{air}} = \frac{K_{r-propane}}{M_{propane}\mu_{propane}} \quad ,$$

$$\frac{M_{propane}}{M_{air}}\frac{K_{r-air}}{K_{r-propane}} = \frac{\mu_{air}}{\mu_{propane}} \quad .$$

Assuming that the relative permeabilities are nearly the same:

$$\frac{M_{propane}}{M_{air}} = \frac{17.83x10^{-6}\frac{N\,s}{m^2}}{7.655x10^{-6}\frac{N\,s}{m^2}} \quad ,$$

$$\frac{M_{propane}}{M_{air}} = 2.33 \quad .$$

This increase in mobility ratio for propane vs. air causes the propane to bypass areas of oil, decreasing the sweep efficiency. This can be seen in a comparison between two experiments, Experiments 1 and 17. Both experiments consisted of Iveysol 106 surfactant at 10 x CMC with a WAG ratio of 1:1. Experiment 1 used air, while Experiment 17 used propane. As both experiments are at the high surfactant concentration, it is expected that there will be areas of unswept oil due to the surfactant. Experiment 1 had a cumulative oil recovery of 59.55%, while Experiment 17 had a cumulative oil recovery of 52.72%. Figure 4-37 shows the comparison between Experiments 1 and 17.

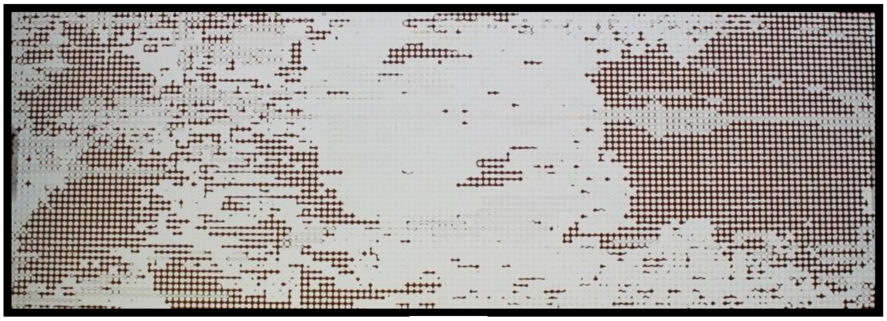

Air

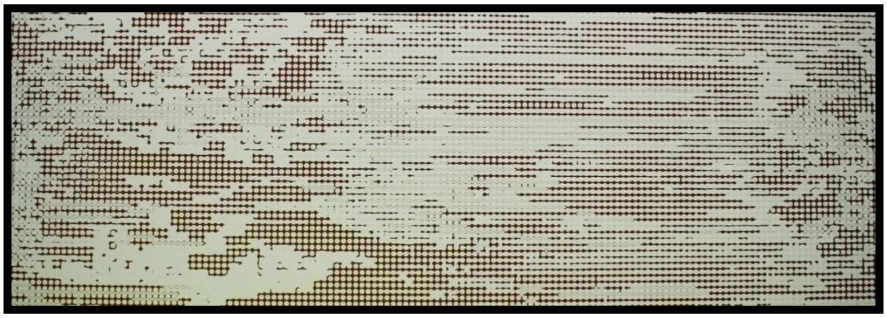

Propane

Figure 4-37. Comparison of air and propane (Experiments 1-top, 17-bottom) at the end of the experiment, WAG ratio of 1:1 with Iveysol 106 at 10 x CMC.

While both figures look alike, with the air figure seeming to leave the most oil behind, the air leaves large areas unswept, possibly due to the high concentration of surfactant. However, the propane in fact leaves most oil behind, though in smaller areas, as is evident by the air recovery of an extra 6.83% of total oil. Another example of this is Experiments 10 and 20, which consisted of injecting Iveysol 106 surfactant at 1 x CMC with a WAG ratio of 1:1.. Experiment 10 used air, while Experiment 20 used propane. Experiment 10 had a cumulative oil recovery of 62.7%, while Experiment 20 had a cumulative oil recovery of 58.8%. As shown in Figure 4-38, the propane leaves slightly more areas unswept than the air, resulting in the air recovering an extra 3.9% of total oil.

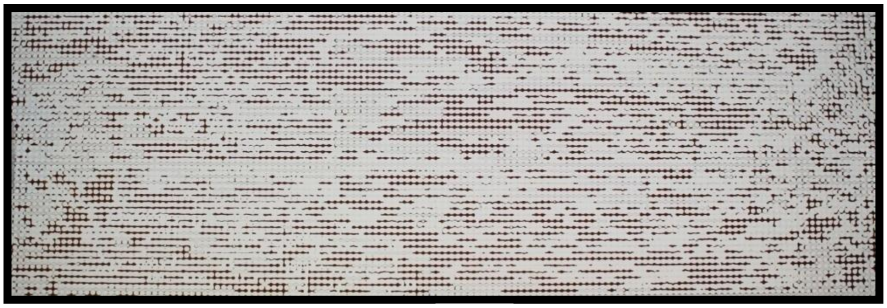

Air

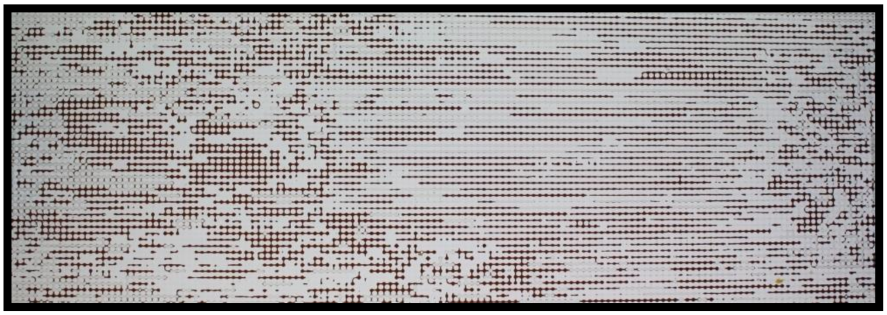

Propane

Figure 4-38. Comparison of air and propane (Experiments 10 at top, 20 at bottom) at the end of the experiment, WAG ratio of 1:2 with Iveysol 106 CMC.

4.3.2.4. Surfactant Type

Two different surfactants were investigated, Triton X-100 and Iveysol 106. The individual effect of surfactant type was found not to be significant on oil recovery, as evident in the ANOVA table by a p-value of 0.3146, above the cut-off value of 0.1. As can be Figure 4-39, the oil recovery does not change significantly between the two surfactants. The change in oil recovery over the full range of WAG ratios of approximately 5% is on the same order of magnitude of the standard deviation identified earlier (5.74%, or 4.3% excluding the 9% anomaly), therefore this observed response may be due to random error and can not be attributed to the individual factor of surfactant type. Figure 4-39 shows the difference between surfactant type using the average values for WAG Ratio, surfactant concentration, and gas type incorporating all of the first 23 experiments. Only the first 23 experiments are incorporated into this due to the fact that the first 23 experiments are the Design of Experiments set of experiments, while experiments 24 to 29 were additional experiments outside of the main set of experiments.

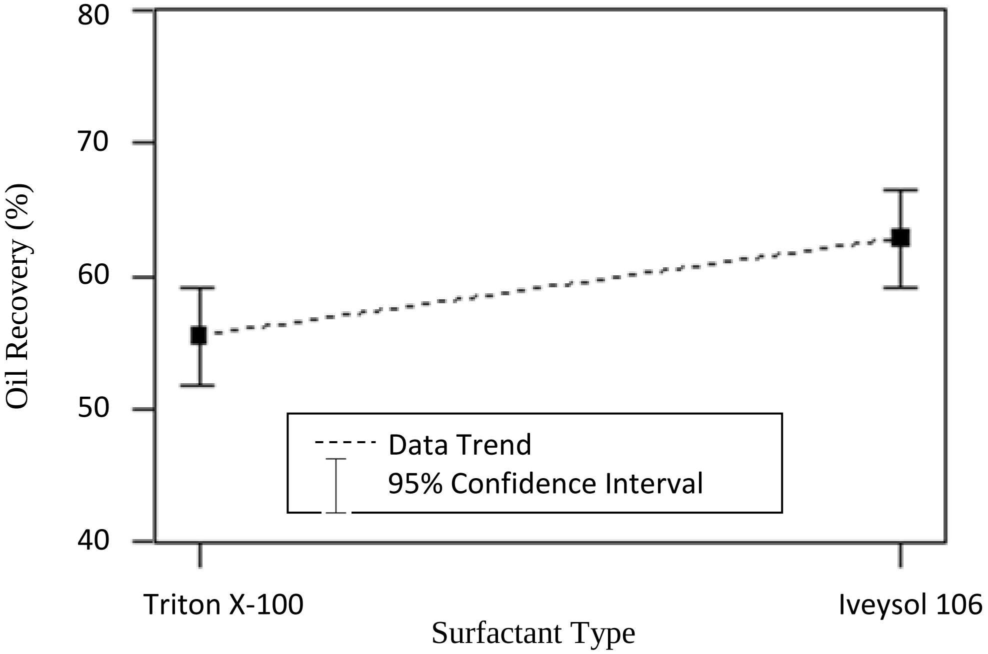

Figure 4-39. Surfactant Type vs. Oil Recovery (%)

As shown in Figure 4-39, the Iveysol 106 surfactant produces a very small increase in oil recovery when compared to the Triton X-100 surfactant of approximately 5%. However this difference of 5% is on the same order of magnitude as the standard deviation of 5.74% and therefore this factor is not statistically significant as the observed trend may be due to error.

4.3.3. Two Factor Interaction Effects

This section will deal with the two-factor interaction effects that were determined to be significant between the four main factors. Interaction effects of three or more factors are deemed unlikely and not presented here. The two-factor interaction effects that were determined to be significant to the recovery of oil are the WAG Ratio-Concentration, WAG Ratio-Gas Type, WAG Ratio-Surfactant Type, and Gas Type-Surfactant Type interaction effects. All other interaction effects were not found to be significant to the recovery of oil.

4.3.3.1. WAG Ratio-Concentration Interaction Effect

While the WAG ratio was found to not to have a significant individual effect on oil recovery, when combined with changes in the surfactant concentration, the combined WAG ratio-Concentration effect was found to be significant, as evident in the ANOVA table by a p-value of 0.0212, below the cut-off value of 0.1. The changes in oil recovery over the full range of WAG ratios and surfactant concentrations are generally above the standard deviation identified earlier (5.74%, or 4.3% excluding the 9% anomaly), therefore this observed response is likely due to the interaction of the WAG ratio and surfactant concentration and not due to random error.

As shown in Figure 4-40, at the high WAG ratio level (1:2), the oil recovery is not changed over the whole range of surfactant concentrations. However, at lower WAG ratios, oil recovery decreases with increasing surfactant concentration. As well, at low surfactant concentrations, oil recovery decreases with increasing WAG ratio, while at high surfactant concentrations the oil recovery increases with increasing WAG ratio.

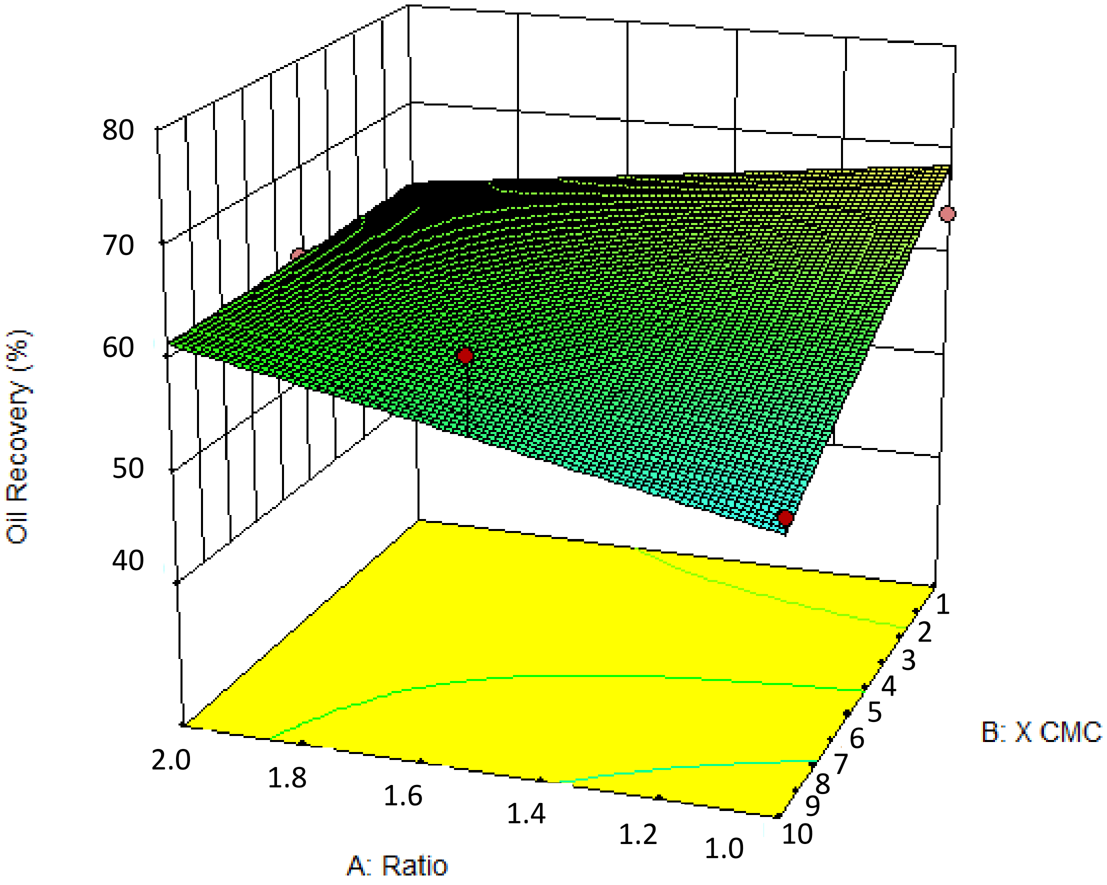

Figure 4-40. WAG Ratio-Surfactant Concentration vs. Oil Recovery for Air (%)

At the high level of WAG ratio, the surfactant concentration does not play a significant role in oil recovery, however at lower levels of WAG ratio; the surfactant concentration has an effect on oil recovery, decreasing oil recovery as surfactant concentration increases. This suggests that large WAG ratios may be able to overshadow the effect of surfactant concentration. As the largest WAG ratio investigated was 1:2, it is not known if the interaction surface may continue on past the boundaries of the figure, for example if the trend of increasing recovery with increasing WAG ratio at high surfactant concentrations continues past WAG ratios of 1:2, or if the trend stops there.

Increasing WAG Ratios produces an increase in oil recovery at high surfactant concentrations, while increasing WAG ratios produce a decrease in oil recovery at low surfactant concentrations. The oil recovery observed at a WAG ratio of 1:2 is constant over the concentration range at approximately 62%. The high oil recovery of low WAG ratio (1:1) of just below 70% and low surfactant concentration (1 x CMC) of just above 50% shows that at low WAG ratios, oil recovery decreases with increasing surfactant concentration. In addition to this, the oil recovery at low WAG ratio, low surfactant concentration is above the high WAG ratio constant oil recovery of approximately 62%, therefore at low surfactant concentrations oil recovery decreases with WAG ratio. The opposite trend is seen for high surfactant concentrations, with the low WAG ratio, high surfactant concentration oil recovery of just over 50% being below the constant high WAG ratio oil recovery of 62%, therefore at high surfactant concentrations oil recovery increases with increasing WAG ratio.

This effect of WAG ratios at different surfactant concentrations may be due to the ability of the gas phase and surfactant to finger through the oil. At low surfactant concentrations, the gas phase is causing breakthrough and taking away the ability of the surfactant to increase oil recovery, while at high surfactant concentrations, the fingering ability of the surfactant fluid is greater than the effect of altering the gas and liquid phases to prevent fingering at low WAG ratios.

4.3.3.2. WAG Ratio-Gas Type Interaction Effect

When combined with the Gas Type, the resulting WAG Ratio-Gas Type interaction effect was found to be significant on oil recovery, as evident in the ANOVA table by a p-value of 0.0411, below the cut-off value of 0.1. As shown in Figure 4-41, at the high WAG ratio level (1:2), the oil recovery is not changed between the different gas phases since at a WAG ratio of 2.0 the oil recovery for both air and propane are identical. However, at lower WAG Ratios, oil recovery is lower for propane compared with air. The changes in oil recovery over the full range of WAG ratios and gas type of between 8 and 10% are above the standard deviation identified earlier (5.74%, or 4.3% excluding the 9% anomaly), therefore this observed response is likely due to the interaction of the WAG ratio and gas type and not due to random error. Figure 4-41 shows the trend for WAG Ratio-Gas Type while using the average values for surfactant concentration and surfactant type incorporating all of the first 23 experiments. Only the first 23 experiments are incorporated into this due to the fact that the first 23 experiments are the Design of Experiments set of experiments, while Experiments 24 to 29 were additional experiments outside of the main set of experiments.

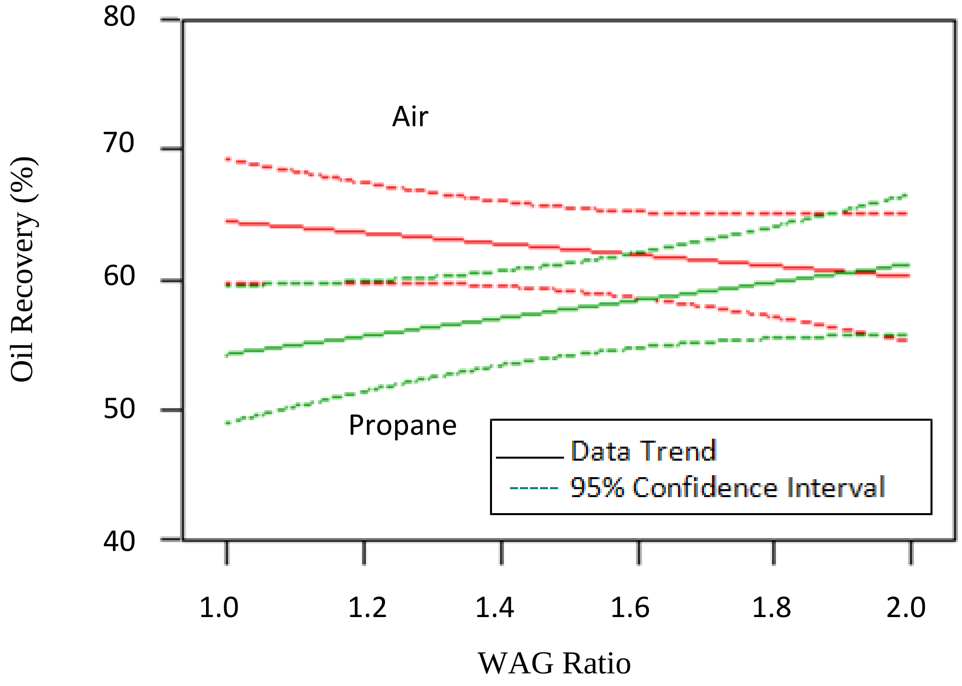

Figure 4-41. WAG Ratio-Gas Type vs. Oil Recovery (%)

As shown in Figure 4-41, at low WAG ratios, the oil recovery for both air and propane are nearly identical at 60%. However, over the full range of WAG ratios, for air the oil recovery decreases with increasing WAG ratio, while for propane increasing the WAG ratio increases the oil recovery.

4.3.3.3. WAG Ratio-Surfactant Type Interaction Effect

When WAG ratio was combined with the surfactant type, the resulting WAG ratio-surfactant type interaction effect was found to be significant on oil recovery, as evident in the ANOVA table by a p-value of 0.0634, below the cut-off value of 0.1. The changes in oil recovery over the full range of WAG ratios and surfactant type of approximately 8% is above the standard deviation identified earlier (5.74%, or 4.3% excluding the 9% anomaly), therefore this observed response is likely due to the interaction of the WAG ratio and surfactant type and not due to random error. However this change of 8% is close to the standard deviation, therefore this response is statistically more uncertain compared to the other interaction effects identified in this section. Figure 4-42 shows the trend for WAG Ratio-Surfactant Type while using the average values for surfactant concentration and gas type incorporating all of the first 23 experiments. Only the first 23 experiments are incorporated into this due to the fact that the first 23 experiments are the Design of Experiments set of experiments, while Experiments 24 to 29 were additional experiments outside of the main set of experiments.

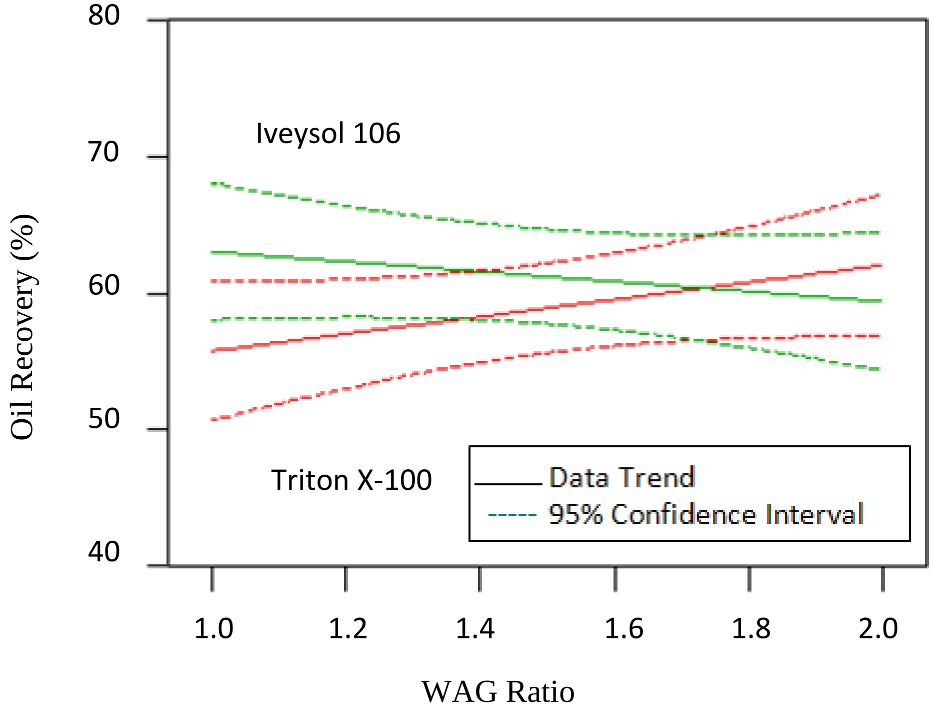

Figure 4-42. WAG Ratio-Surfactant Type vs. Oil Recovery (%)

As shown in Figure 4-42, at the high WAG ratio level (1:2), the oil recovery is not changed between the different surfactants used as the oil recoveries are very similar at approximately

60%. However, at lower WAG ratios, oil recovery is lower for the Triton X-100 surfactant compared with the Iveysol 106 surfactant. The trends for each surfactant are also different, with oil recovery decreasing with increasing WAG Ratio for Iveysol 106, while oil recovery increases with increasing WAG ratio for Triton X-100.

4.3.3.4. Gas Type-Surfactant Type Interaction Effect

The Gas Type-Surfactant Type combined interaction effect was the only interaction effect that did not include WAG Ratio that was determined to be significant on oil recovery, as evident in the ANOVA table by a p-value of 0.0884, below the cut-off value of 0.1. The change in oil recovery over the full range of air type while using Triton X-100 is approximately 10%, above the standard deviation identified earlier (5.74%, or 4.3% excluding the 9% anomaly), therefore this observed response is likely due to the interaction of the gas type and surfactant type and not due to random error. Figure 4-43 shows the trend for Gas Type-Surfactant Type while using the average values for WAG ratio and surfactant concentration incorporating all of the first 23. Only the first 23 experiments are incorporated into this due to the fact that the first 23 experiments are the Design of Experiments set of experiments, while Experiments 24 to 29 were additional experiments outside of the main set of experiments.

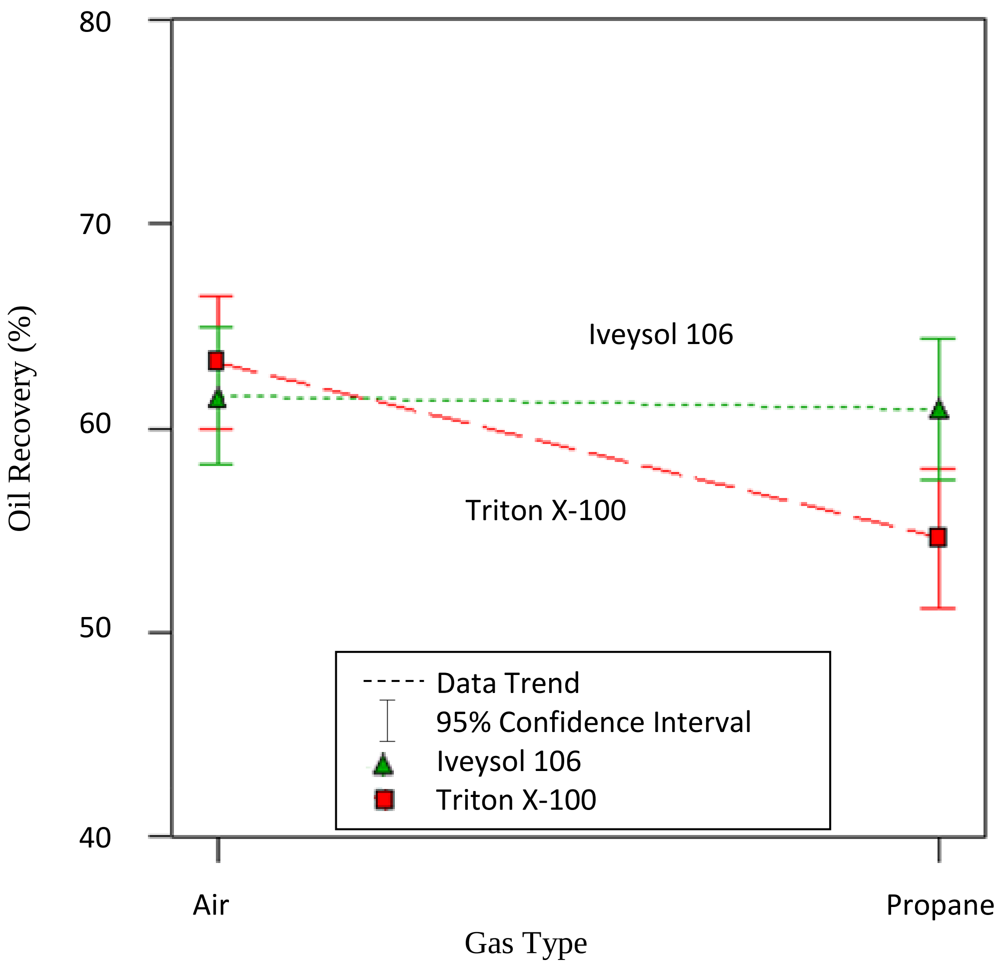

Figure 4-43. Gas Type-Surfactant Type vs. Oil Recovery (%)

As shown in Figure 4-43, the oil recovery using Triton X-100 is very gas dependent, with a lower oil recovery for propane gas compared to air of nearly 10%, while the oil recovery for Iveysol 106 is unchanged with the type of gas used. The Triton X-100 out-performs the Iveysol 106 surfactant slightly when air is the gas phase used, however when propane is used instead of air, the Iveysol 106 surfactant out-performs the Triton X-100 surfactant significantly. The effect on oil recovery of the Iveysol 106 surfactant seems to be completely independent of the gas phase used as the oil recovery does not change between gas types. This trend is also shown in Figure 4-44 below.

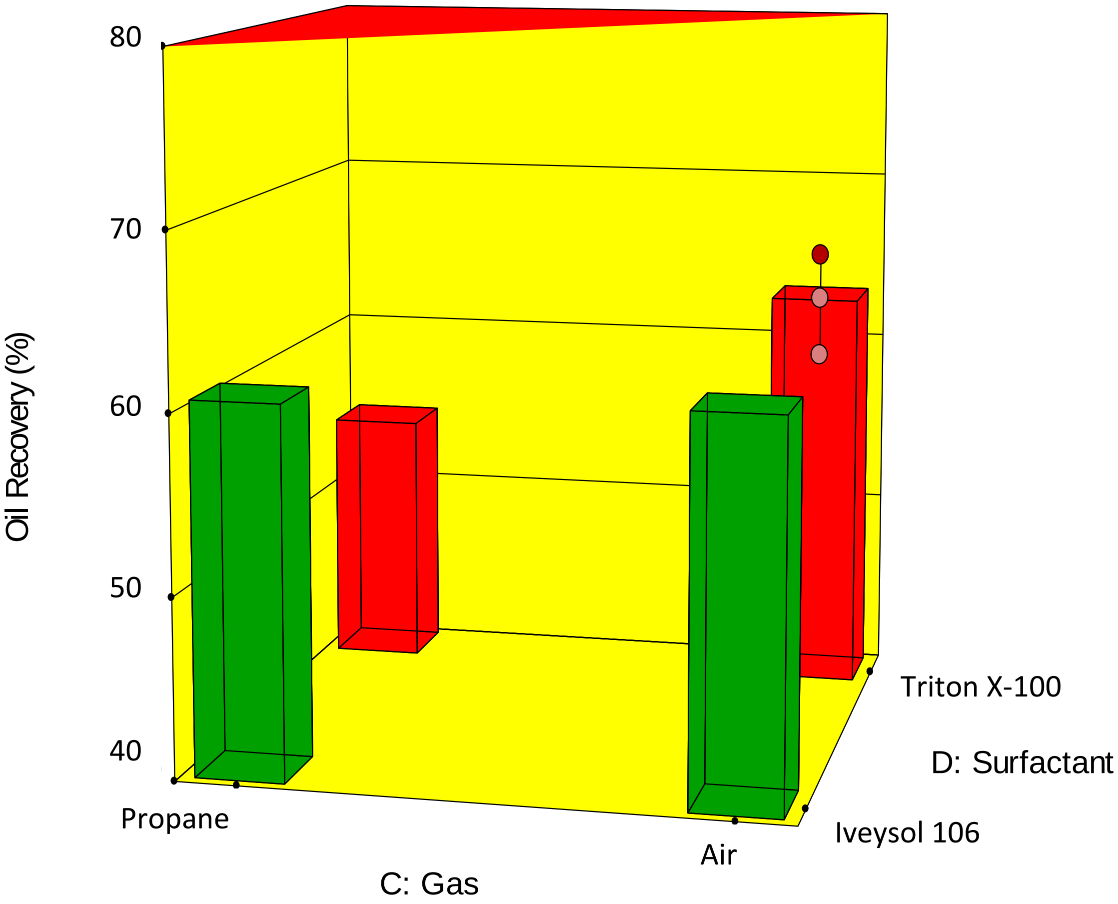

Figure 4-44. Gas Type-Surfactant Type vs. Oil Recovery (%) Comparison

4.3.4. Additional Experiments

Four additional experiments were conducted outside of the Design of Experiments set of experiments. These consisted of a waterflooding only, water-surfactant flooding only, brine-air water-alternating-gas flooding, and surfactant assisted water-alternating-gas flooding. For the water-surfactant flooding and surfactant assisted water-alternating-gas flooding the surfactant used was Iveysol 106 at 1 x CMC as this was the surfactant type and concentration identified in the beginning of Section 4.3 as the optimal surfactant type and concentration for oil recovery.

These experiments will be discussed in this section to determine if surfactant and/or water-alternating-gas improves the oil recovery compared to waterflooding only.

4.3.4.1. Waterflooding vs. Water-Surfactant Flooding

Two experiments were conducted to determine the effect of adding surfactant to the water phase in a waterflooding experiment. Both experiments consisted of injecting 1.0 pore volumes of liquid into the micromodel. One experiment had brine as the liquid phase, while the other experiment had an Iveysol 106 surfactant solution at the critical micelle concentration. For both experiments the liquid was injected past breakthrough, after breakthrough was achieved, the oil recovery did not increase for the duration of the experiment. Figure 4-45 shows the comparison of oil recovery between waterflooding and surfactant-water flooding. The difference between waterflooding and water-surfactant flooding of approximately 10% is above the standard deviation identified earlier (5.74%, or 4.3% excluding the 9% anomaly), therefore this observed response is likely due to the effect of surfactants and not due to random error.

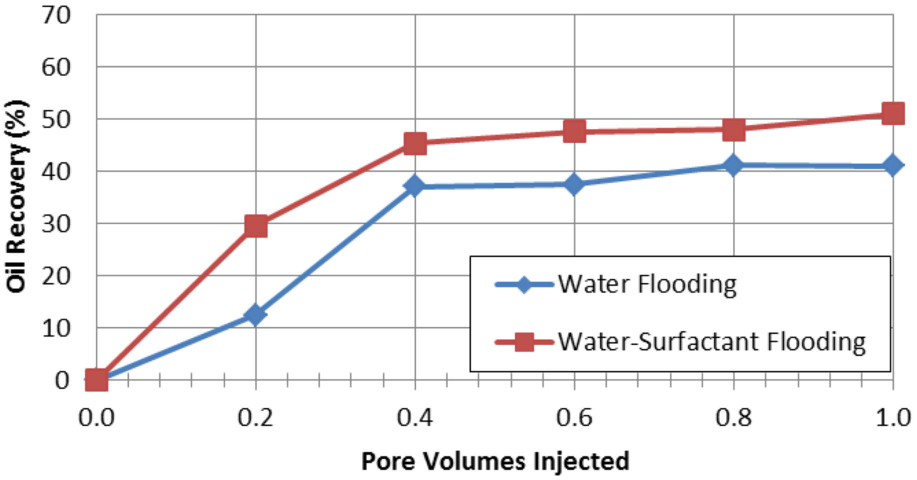

Figure 4-45. Oil Recovery vs. Injected Volume for Waterflooding (Experiment 26) and Water-Surfactant Flooding (Experiment 25)

As shown in Figure 4-45, the surfactant-water flooding produces a significant increase in oil recovery over waterflooding. The surfactant-water flooding produced an additional 10% of the original oil in place compared to the waterflooding experiment. The surfactant-water flooding also produced a higher oil recovery for all pore volumes injected compared to waterflooding. This increase in oil recovery may be due to the decrease in interfacial tension between the oil and liquid phases.

4.3.4.2. Water Flooding vs. Water-Alternating-Gas Flooding

Two experiments were conducted to determine if water-alternating-gas resulted in an increase in oil recovery compared to waterflooding only. The waterflooding experiment was the same experiment discussed in Section 4.3.4.1. The brine-air experiment consisted of 6 slugs each of brine and air injected alternatively (0.2 PV slugs). Figure 4-46 shows the comparison between only using waterflooding and using water-alternating-gas flooding.

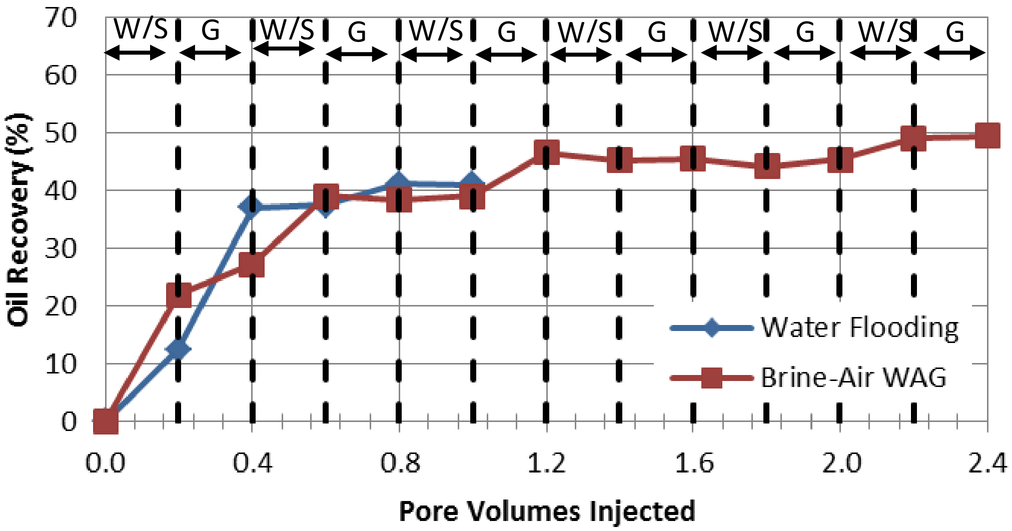

Figure 4-46. Oil Recovery vs. Injected Volume for Waterflooding (Experiment 26) and WAG Flooding (Experiment 24)

The waterflooding experiment was stopped after 1.0 pore volumes were injected, this is because it was noticed that once the water had broken through to the outlet well, all of the water simply followed in the water channels, not producing any extra oil. The experiment was run for 66 minutes after breakthrough, with no additional oil being recovered after breakthrough. As shown in Figure 4-46 that the water-alternating-gas option is able to produce nearly 8.5 percent more of the original oil in place compared to only waterflooding. Below 1.2 injected pore volumes, the waterflooding performs better in some instances than the WAG flooding. This is due to the alternating gas slugs which channeled through the micromodel quickly, and after achieving breakthrough did not produce any additional oil until the next water slug was injected. It is shown that in 0-0.2 PV and 0.4-0.6 PV when the water slug was moving through the micromodel, the recovery of oil proceeded at a greater rate when compared to injecting the same amount of water in the waterflooding experiment. This may be due to the gas breaking up the water slugs in the WAG process, allowing the next water slug to seek different channels through the micromodel than the preceding water slug, thereby displacing additional oil.

4.3.4.3. Water-Alternating-Gas Flooding vs. Surfactant Water-Alternating-Gas Flooding

Two experiments were conducted to determine if surfactant assisted water-alternating-gas resulted in an increase in oil recovery compared to water-alternating-gas flooding. The water-alternating-gas flooding experiment was conducted with air and is the same experiment discussed in Section 4.3.4.1. The brine-air experiment consisted of 6 slugs each of brine and air injected alternatively (0.2 PV slugs). The surfactant assisted water-alternating-gas experiment chosen for comparison was the Iveysol 106 at 1 x CMC and air, with a WAG ratio of 1:1. Figure 4-47 shows the comparison between using surfactant assisted water-alternating-gas flooding and water-alternating-gas flooding. The difference between waterflooding and water-surfactant flooding of approximately 10% is above the standard deviation identified earlier (5.74%, or 4.3% excluding the 9% anomaly), therefore this observed response is likely due to the effect of surfactants and not due to random error.

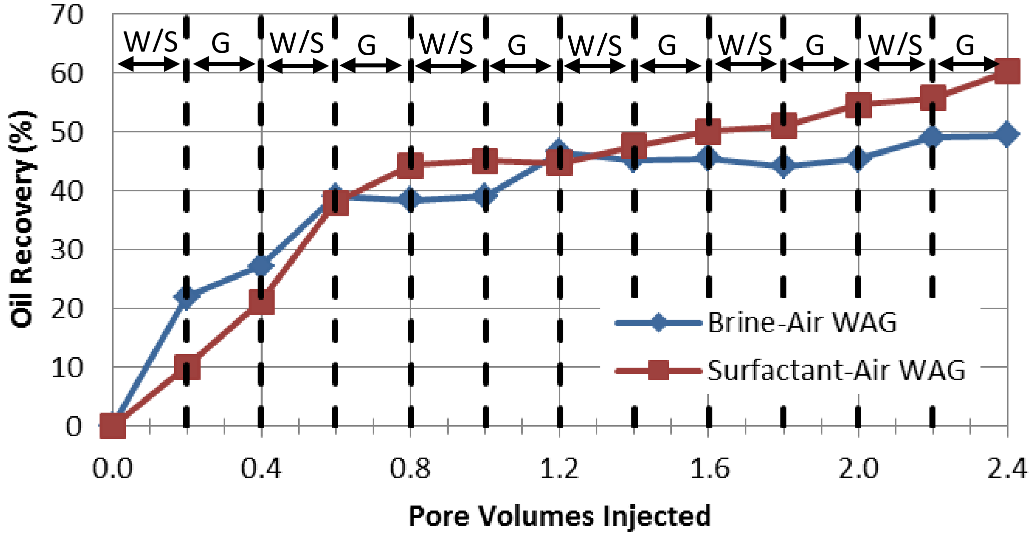

Figure 4-47. Oil Recovery vs. Injected Volume for Surfactant-WAG (Experiment 29) and WAG Flooding (Experiment 24)

Both experiments were conducted until 2.4 pore volumes total were injected into the micromodel. As shown in Figure 4-47, the surfactant assisted water-alternating-gas option outperforms the water-alternating-gas option significantly. This is evidence that even without being able to produce a foam phase, the surfactant is still able to contribute greatly to oil recovery.

4.4. Breakthrough Time

The breakthrough time was measured by identifying the time elapsed from when the test began (first liquid slug entered micromodel) to when the first injection fluid entered the exit well from the micromodel. These results were then processed via Design Expert 9 to identify the significant factors affecting the breakthrough time. Table 4-4 provides the breakthrough time for each experiment.

Table 4-4. Breakthrough Time Experimental Results

Experiment	WAG Ratio	Surfactant Concentration (CMC x)	Gas Type	Surfactant Type	Comments	Breakthrough Time (Seconds)
1	1:1	10	Air	Ivey-sol 106		2940
2	1:1	1	Propane	Ivey-sol 106		4560
3	1:2	1	Air	Triton X-100		1560
4	1:1	10	Air	Triton X-100		2580
5, 16, 22	1:1.5	5.5	Air	Triton X-100		2500 ± 1268
6, 9	1:1	5.5	Propane	Triton X-100		4350 ± 2078
7	1:2	10	Air	Ivey-sol 106		1680
8, 10	1:2	1	Air	Ivey-sol 106		3180 ± 1442
11	1:2	1	Propane	Triton X-100		2820
12	1:1.5	10	Propane	Ivey-sol 106		2640
13	1:1	1	Air	Triton X-100		2460
14, 15	1:1	5.5	Air	Ivey-sol 106		4170 ± 1146
17	1:1	10	Propane	Ivey-sol 106		3840
18	1:2	5.5	Propane	Ivey-sol 106		3300
19	1:2	10	Propane	Triton X-100		3060
20	1:2	1	Propane	Ivey-sol 106		2940
21	1:1.5	1	Propane	Triton X-100		3000
23	1:2	5.5	Air	Triton X-100		1500 ± 170
24	1:1	0	Air	None	Brine-Air WAG	3300
25	1:0	1	None	Iveysol 106	Surfactant/water Flood	2580
26	1:0	0	None	None	Waterflood	3600
29	1:1	1	Air	Iveysol 106	Water/Surfactant WAG	2160

As shown in Table 4-4, the standard deviation ranges from 170 seconds up to 2078 seconds. Including all the replicate experiments, the standard deviation was determined using the Design of Experiments software as 965 seconds. Using the ANOVA method in the Design Expert 9 software identified the Linear model as being the suggested model for breakthrough time. Table 4-5 provides the ANOVA results for the breakthrough time data using a linear model, meaning that there are only individual factor effects and no interaction effects were deemed significant. If the p-value calculated is less than 0.1, there is a less than 10% chance that the effect identified by the factor or interaction between the factors is due to error and not the factor(s). As shown in Table 4-5, the linear model that was chosen is deemed significant with a p-value of 0.0315, far below the threshold of 0.1. Individually, the effects of the WAG ratio and gas type are deemed significant to breakthrough time and probably are not due to error. The individual effects of surfactant concentration and surfactant type was deemed not significant, with a high probably that the effect identified was more due to error than to the factor. As the model that best represents the data is a linear model, there are no interaction effects or non-linearity in the data that were identified. The lack of fit has a p-value of 0.9942 and is therefore not significant to the model, meaning that the model fits the data well.

Table 4-5. ANOVA table for Breakthrough Time Data

Source	Sum of Squares ($x10^5$)	Degrees of Freedom	Mean Square ($x10^5$)	F Value	P-Value Prob>F	Significance
Model	120.2	4	30.05	3.38	0.0315	Significant
WAG Ratio	66.52	1	66.52	7.48	0.0136	Significant
Surfactant Concentration	9.960	1	9.960	1.12	0.3041	Not Significant
Gas Type	33.55	1	33.55	3.77	0.0680	Significant
Surfactant Type	19.01	1	19.01	2.14	0.1611	Not Significant
Residual	160.2	18	8.898			
Lack of Fit	50.89	13	3.914	0.18	0.9942	Not Significant
Pure Error	109.3	5	21.86			
Cor Total	280.4	22				

Figure 4-48 below shows the plot of predicted vs. actual values for breakthrough time in seconds. As shown, the predicted and actual values are around the center diagonal line, meaning that the chosen linear model predicts the breakthrough time, with predicted values matching actual values. The model does not perfectly match the data, with an R-squared value of 0.4287 and an adjusted R-squared value of 0.3017. This means that the model explains 30.17% of the variance in the data, an ideal model would account for 100% of the variance, however out of the models available, the Linear model accounted for the most variance in the data.

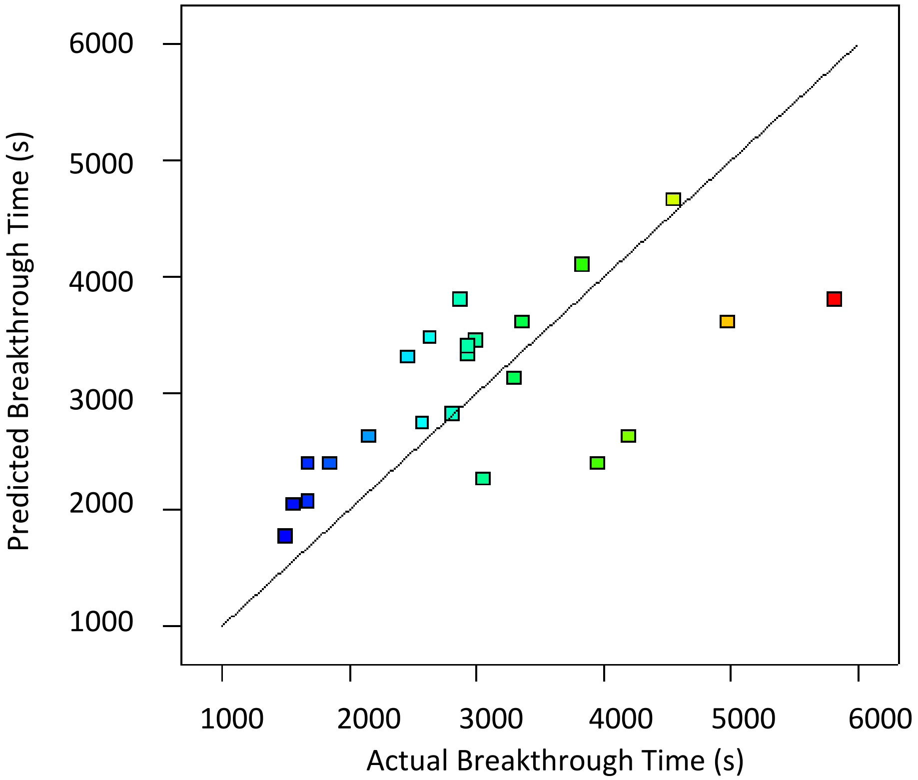

Figure 4-48. Predicted vs. Actual Values for Breakthrough Time

The Design Expert 8 software was also able to create a mathematical model for breakthrough time with variables of WAG ratio, gas type, and surfactant type. The mathematical model is given in Equation (8).

$$t_{breakthrough} = 3086.08 - 566.67 * W + 399.92 * G \quad , \tag{8}$$

where:

W= WAG Ratio (1:1 = -1, 1:2 = 1) and
G= Gas Type (Air=-1, Propane=1).

Overall, to maximize the breakthrough time, it was found that the levels of the four factors presented in Table 4-6 should be used.

Table 4-6. Optimization of Factors for Breakthrough Time

Factor	Level
WAG Ratio	1:1
Gas Type	Propane

4.4.1. Individual Factor Effects

Two of the main factors were determined to be significant to the breakthrough time, WAG ratio and gas type, while surfactant concentration and surfactant type was determined to not be significant. Surfactant concentration had a p-value of 0.3041 while surfactant type had a p-value of 0.1611, both above the cut-off value of 0.1. This is expected since the gas phase was observed to always be the phase that caused breakthrough, and the WAG Ratio and Gas Type are the only factors affecting the gas phase. This section will give details about each significant individual factor investigated.

4.4.1.1. WAG Ratio

The WAG Ratio was determined to be individually significant for breakthrough time, which is evident from the ANOVA table by a p-value of 0.0136, below the cut-off value of 0.1. In Figure 4-49, the breakthrough time decreases significantly with WAG Ratio, decreasing by approximately 1100 seconds. The change in breakthrough time over the full range of WAG ratios of approximately 1100 seconds is above the standard deviation of 965 seconds, therefore this observed response is likely due to the individual factor of WAG ratio and not random error. Figure 4-49 shows the trend between WAG ratios, while using the average values for surfactant concentration, surfactant type and gas type incorporating all of the first 23 experiments Only the first 23 experiments are incorporated into this due to the fact that the first 23 experiments are the Design of Experiments set of experiments, while Experiments 24 to 29 were additional experiments outside of the main set of experiments.

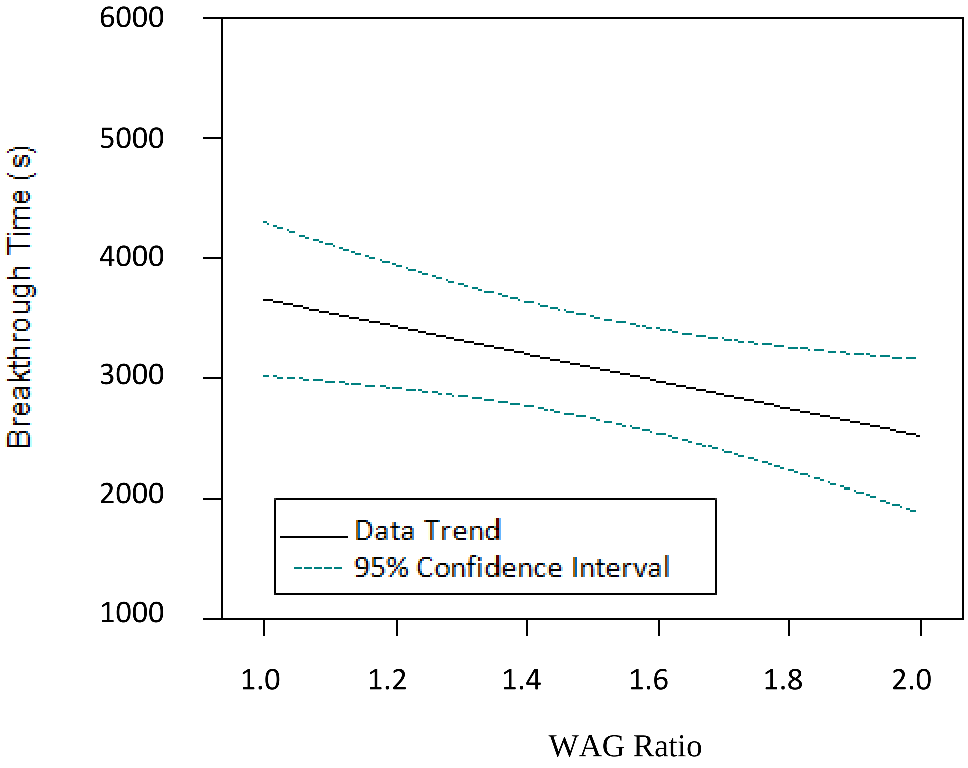

Figure 4-49. WAG Ratio vs. Breakthrough Time

As shown in Figure 4-49, the breakthrough time decreases by approximately 1100 seconds from a WAG ratio of 1.0 to a WAG ratio of 2.0. This response was expected as the larger the WAG Ratio, the more gas is injected into the micromodel. Since the gas was injected at twice the flowrate of the liquid phase, more gas injection at a higher flow rate would push the gas through the micromodel at a higher rate than if liquid was being injected, thereby decreasing the breakthrough time. The optimal WAG ratio for breakthrough time (1:1) corresponds with the optimal WAG ratio for oil recovery as discussed in Section 4.3, making a WAG ratio of 1:1 the desired WAG ratio in all instances.

4.4.1.2. Gas Type

The Gas Type was determined to be individually significant for breakthrough time, as evident from the ANOVA table by a p-value of 0.0680, below the cut-off value of 0.1. The change in breakthrough time over the full range of WAG ratios is near the standard deviation of 965 seconds, therefore this observed response may be due to random error and not the individual factor of gas type, however statistical analysis determined that gas type was likely a significant factor.

Figure 4-50 shows the trend between air and propane, while using the average values for WAG Ratio, surfactant concentration, and surfactant type incorporating all of the first 23 experiments. Only the first 23 experiments are incorporated into this due to the fact that the first 23 experiments are the Design of Experiments set of experiments, while Experiments 24 to 29 were additional experiments outside of the main set of experiments.

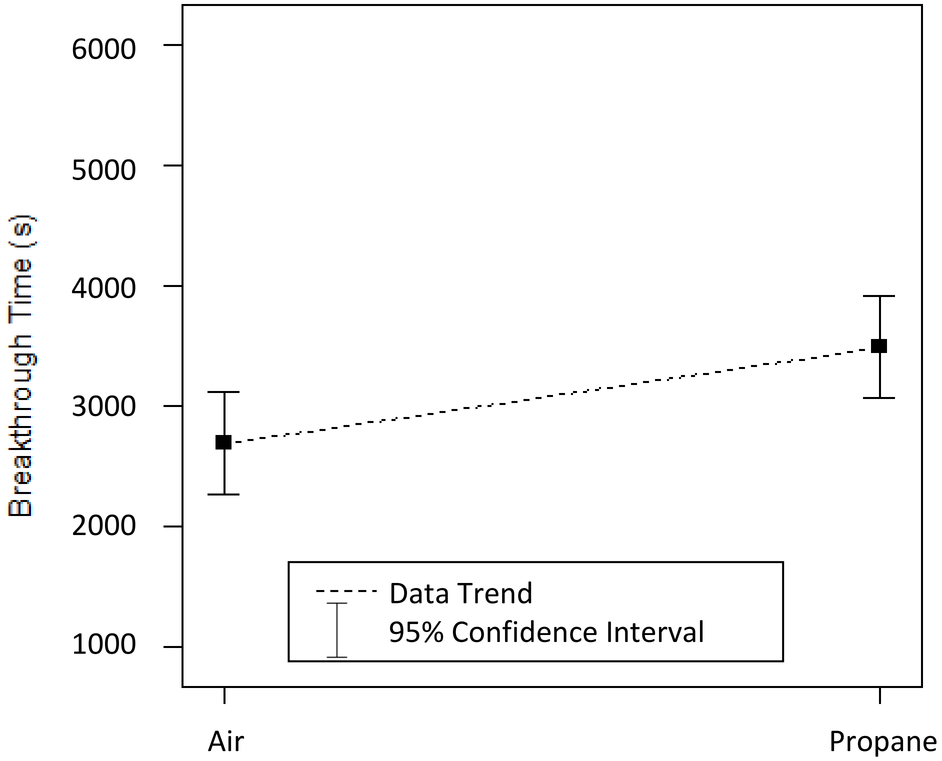

Figure 4-50. Gas Type vs. Breakthrough Time

In Figure 4-50, it is shown that breakthrough time is lower with air than for propane. This is an interesting effect since the lower viscosity of propane would suggest that it should finger through the micromodel more easily than the air, and thereby cause an earlier breakthrough, however the opposite of this was observed, with the air causing an earlier breakthrough time compared to the propane. This may be due to a characteristic of the gases that were not investigated, namely the compressibility of the gas. Air has a compressibility of 0.9996 (Air Liquide, 2013), while propane has a compressibility of 0.98194 (Air Liquide, 2013), both at 15^{o}C and 1 atm. Lower compressibilities mean that the gas is easier to compress, therefore propane is slightly more compressible than air. This was noted during the experiments, as when the syringe pump was set to inject the gas phase, it took longer for the propane to begin moving through the lines than for the air. The extra time it took the propane to begin flowing through the lines resulted in the propane having a larger breakthrough time than the air, even though it’s viscosity is lower. This is due to the fact that the breakthrough time was measured from the time that the first liquid slug entered the micromodel until the point when either liquid or gas appeared in the outlet line, as this time includes the time taken for the gases to begin flowing through the times, it is understandable that the propane would have a larger breakthrough time than the air.

An example of this is shown in comparing Experiments 3 and 11. Both experiments consisted of injecting Iveysol 106 at 10 x CMC at a WAG ratio of 1:1. Experiment 3 used air as the gas phase, while experiment 11 used propane as the gas phase. In Experiment 3, the syringe pump began injecting the air at 7:45 AM, with the air making it through the lines and entering the micromodel at 8:12 AM. In Experiment 11, the syringe pump began injecting propane at 7:25 AM, with the propane making it through the lines and entering the micromodel at 8:21 AM. The time it took for the air to push the liquid out of the lines and enter the micromodel was 27 minutes, while the time it took for the propane to push the liquid out of the lines and enter the micromodel was 56 minutes.

Investigating the time elasped from the point that the gas enters the micromodel until the point of gas breakthrough provides a different result. For Experiment 3, air breakthrough occured after an elasped time of 17 minutes. For Experiment 11, propane breakthrough occurred after an elasped time of 13 minutes. Therefore looking at the elasped time from the point when the gas enters the micromodel until breakthrough, it can be seen that the propane gas moves through the micromodel more quickly than the air, which is expected due to the mobility ratio of the gases. The recorded breakthrough times for the gas phase factor is skewed by the compressibility of the gases, causing the propane gas to take longer to move through the lines and enter the micromodel, delaying breakthrough due to the existance of "dead time", when no liquid movement occurred between the point when the syringe pump was switched to gas injection and the point when the gas began moving through the lines.

Considering this, air is the optimal gas type for breakthrough time. This also corresponds with the optimal gas type for oil recovery as discussed in Section 4.3. This makes air the desired gas type in all instances.

4.4.2. Additional Experiments

The four additional experiments discussed in Section 4.3.4 were also used to compare the breakthrough time with different oil recovery techniques. These experiments will be discussed in this section to determine if surfactant and/or water-alternating-gas improves the breakthrough time compared to waterflooding only.

Two experiments consisted of liquid flooding only, with one experiment having pure waterflooding (Experiment 26) while the other experiment had Iveysol 106 surfactant solution at the critical micelle concentration added to the water (Experiment 25). In both experiments, 1.0 pore volumes of liquid was injected into the micromodel. For both experiments the liquid was injected past breakthrough, after breakthrough was achieved, the oil recovery did not increase for the duration of the experiment.

Another two experiments consisted of water-alternating-gas flooding, with air as the gas phase, with each experiment injecting six cycles each of liquid and gas, with each cycle consisting of 0.2 pore volumes. One experiment used water as the liquid phase (Experiment 24), while the other experiment used Iveysol 106 surfactant solution at the critical micelle concentration (Experiment 29). Iveysol 106 surfactant at the critical micelle concentration was chosen for the surfactant as this was the surfactant type and concentration identified in Table 4-6 as providing the best breakthrough time results. Air was chosen over propane as air provides better oil recovery, and these experiments were used as additional experiments for the oil recovery data as well, and due to the fact that the compressibility of the propane skews its real breakthrough time. Figure 4-51 provides the breakthrough data for all the additional experiments. Two values appear on top of each column, the bracketed value is the oil recovery observed and discussed in Section 4.3.4, while the other value is the observed breakthrough time.

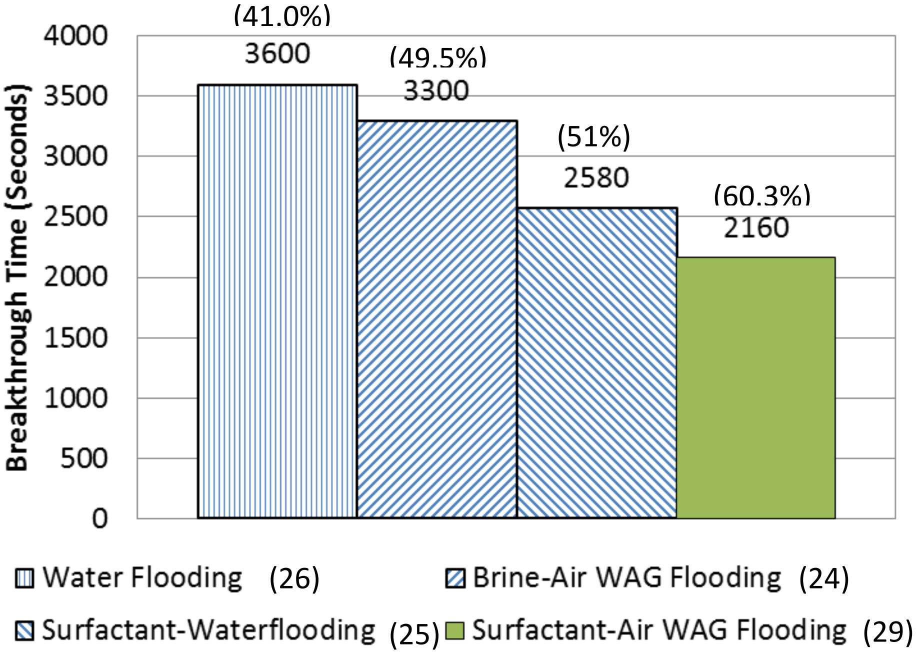

Figure 4-51. Breakthrough Time for Additional Experiments

As shown in Figure 4-51, the waterflooding experiment has the greatest breakthrough time with breakthrough occurring at 3600 seconds. This is followed closely by brine-air WAG with a breakthrough time of 3300 seconds. The addition of surfactants decreases the breakthrough time significantly, with surfactant waterflooding having a breakthrough time of 2580 seconds, down from 3480 seconds for waterflooding without surfactants. Surfactant-air WAG had the lowest breakthrough time, with breakthrough occurring at 2160 seconds, down from 3420 seconds for brine-air WAG. The largest decrease in breakthrough time is seen when adding surfactant to the waterflooding. This is due to the combined decrease in viscosity and increase in relative permeability caused by the addition of surfactants into the water phase. Interestingly, the decrease in breakthrough time between waterflooding and brine-air flooding is close to the decrease in breakthrough time between surfactant-waterflooding and surfactant-air WAG, with the surfactant-waterflooding / surfactant-air WAG decrease being slightly more than the waterflooding / brine-air WAG decrease due to the present of surfactants.

Most of the differences between the values fall within the standard deviation of 966 seconds, therefore the exact order of the decreasing breakthrough times can not be determined. However the main trends discussed above are observable. The addition of surfactants decreases breakthrough time, between waterflooding and surfactant-waterflood there is a decrease of approximately 1100 seconds (greater than the standard deviation of 966 seconds), and between brine-air WAG flooding and surfactant-air WAG flooding there is a decrease of approximately 2200 seconds (greater than the standard deviation of 966 seconds). Therefore it is clear that the addition of surfactants decreases the breakthrough time. As well, the trend of WAG reducing the breakthrough time compared to pure liquid flooding can be observed, between waterflooding and brine-air waterflooding there is a decrease of approximately 1000 seconds (greater than the standard deviation of 966 seconds). Therefore it is clear that WAG reduces breakthrough time compared to pure liquid flooding.

The opposite trend is observed when looking at the oil recovery. In the figure, with decreasing breakthrough times there is increasing oil recoveries. This is due to the increase in oil recovery caused by both surfactants and the water-alternating-gas technique, while these two factors (surfactants and water-alternating-gas) decrease breakthrough time. Earlier in this section, when analyzing the breakthrough time-oil recovery results when the addition of surfactants and use of the water-alternating-gas technique was fixed, it was noted that the breakthrough time trend corresponded with the oil recovery trend, however when investigating the addition of surfactants and use of water-alternating-gas the breakthrough time trend is opposite to the oil recovery trend.

4.5. Timing of Enhanced Oil Recovery

An important consideration in the production of oil is when to implement various oil recovery techniques. Secondary oil recovery traditionally consists of flooding the reservoir with water until oil production decreases below economically sustainable production rates. Once this occurs, production companies incorporate tertiary oil recovery techniques. The tertiary oil recovery techniques investigated in this thesis include both water-alternating-gas and surfactant assisted water-alternating-gas techniques. A common problem encountered is when or if tertiary recovery techniques should be implemented. As has been discussed in the preceding sections, the experiments conducted did not include separate primary, secondary, or tertiary production phases. Instead, the secondary recovery technique of waterflooding and the tertiary recovery techniques or water-alternating-gas and surfactant assisted water-alternating-gas were all applied in the primary recovery phase. As the micromodel was at ambient pressure, there was no pressure in the micromodel to facilitate the traditional primary recovery phase.

As has also been discussed in the preceding sections, comparing all three techniques showed that the surfactant assisted water-alternating-gas technique produced an increase in oil recovery compared to water-alternating-gas, which produced an increase in oil recovery compared to waterflooding.

In order to investigate whether tertiary recovery techniques should be applied with secondary recovery techniques or in place of them, two additional experiments were conducted. These additional experiments consisted of first flooding with water until breakthrough, and then implementing either water-alternating-gas or surfactant assisted water-alternating-gas techniques that were performed the same as the main set of experiments, with 6 cycles each of liquid and gas slugs of 0.2 PV each. A comparison of water-alternating-gas flooding and waterflooding followed by water-alternating-gas is show in Figure 4-52.

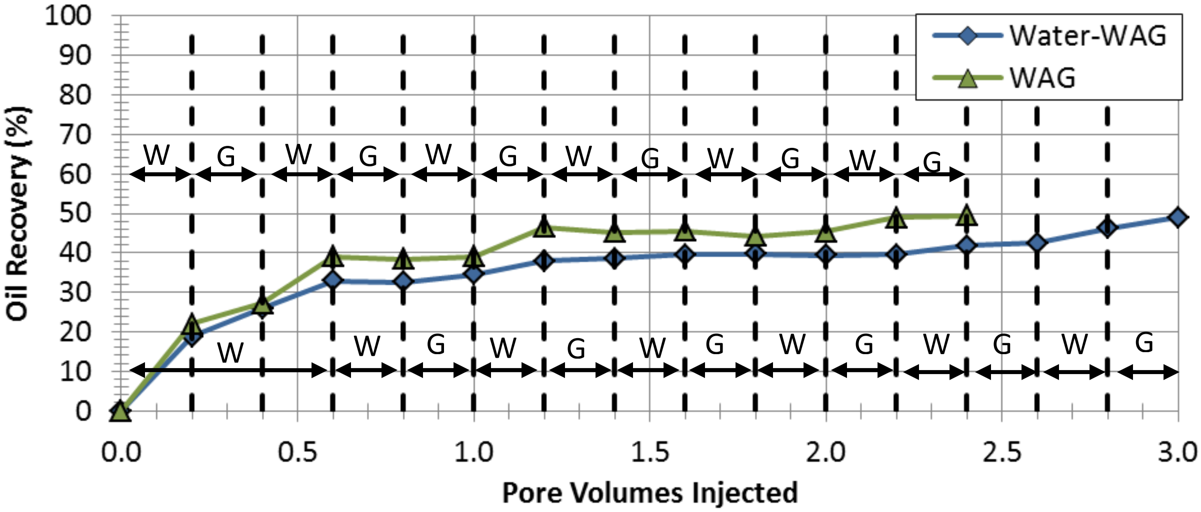

Figure 4-52. Tertiary Recovery: Water-Alternating-Gas (Experiment 24) vs. Waterflooding Followed by Water-Alternating-Gas (Experiment 27)

As shown in Figure 4-52, first flooding the micromodel with water does not significantly change the final oil recovery. Both waterflooding – water-alternating-gas flooding and water-alternating-gas flooding experiments produced a similar oil recovery of approximately 50%, with the water-alternating-gas flooding achieving this oil recovery sooner than the waterflooding – water-alternating-gas flooding. Conducting water-alternating-gas without the initial waterflooding phase produces a higher oil recovery for the same amount of pore volumes injected. The water-alternating-gas without initial waterflooding attained the final oil recovery before the case with water-alternating-gas with the initial waterflooding.

A comparison of surfactant assisted water-alternating-gas flooding and waterflooding followed by surfactant assisted water-alternating-gas flooding is given in Figure 4-53. The surfactant used in both cases was Iveysol 106 at 1 x CMC as this was the optimum surfactant type and concentration found in Section 4.3.

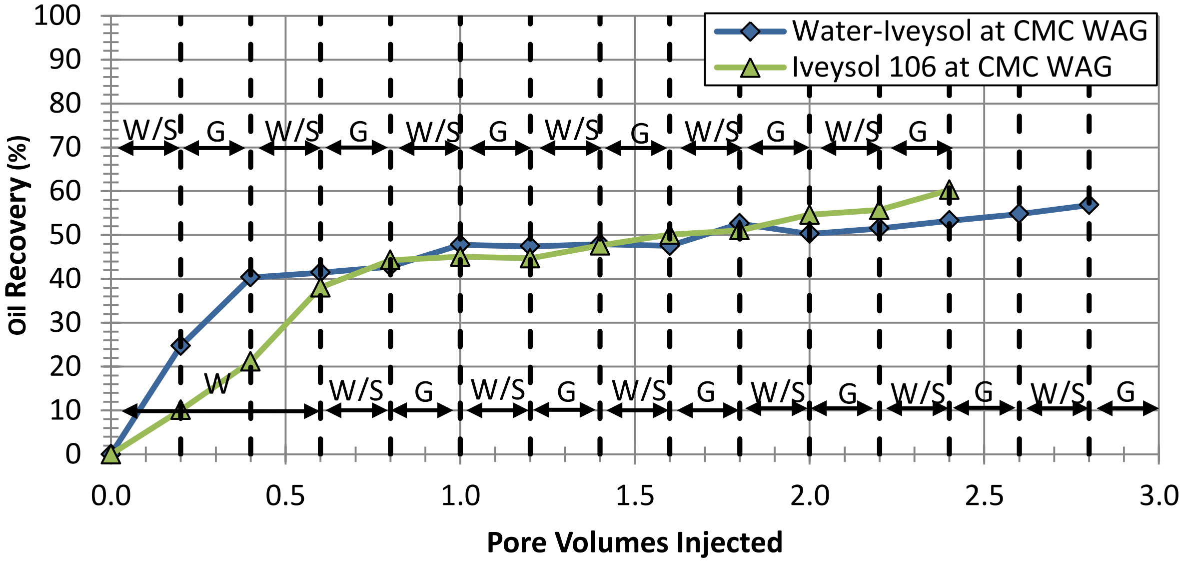

Figure 4-53. Tertiary Recovery: Surfactant Assisted Water-Alternating-Gas (Experiment 29) vs. Waterflooding followed by Surfactant Assisted Water-Alternating-Gas (Experiment 28)

As shown in Figure 4-53, waterflooding the porous media before beginning surfactant assisted water-alternating-gas was found to be beneficial in the beginning. The waterflooding/surfactant assisted water-alternating-gas phase had a higher recovery than the surfactant assisted water-alternating-gas phase for all pore volumes injected up to 1.4 pore volumes. This may be due to the fact that the surfactant assisted water-alternating-gas, with gas being injected into a system with lower liquid viscosity, can finger through the fluid more easily, causing early breakthrough and not recovering as much oil as compared to waterflooding. However, as more pore volumes are injected, the difference in oil recovery between the two experiments decreases, until the surfactant assisted water-alternating-gas begins to outperform the waterflooding/surfactant assisted water-alternating-gas past 1.4 pore volumes injected, with both experiments reaching approximately 60% oil recovery, with the surfactant assisted water-alternating-gas experiment reaching this oil recovery sooner than the waterflooding/surfactant assisted water-alternating-gas experiment.

4.6. Problems Encountered and Solutions Used

Several difficulties were encountered throughout the process of conducting the experiments. These difficulties mainly involved the trapping of oil in the system fittings and lines, and the over-pressurization of the gas phase by the syringe pump. General difficulties, including leaks, are not discussed here and were remedied by proper system setup and maintenance.

4.6.1. Oil Trapped in Fittings

Oil was regularly trapped in the fittings during the initial oil saturation of the micromodel. This oil was occasionally released at the interface of the liquid and gas slugs which were injected into the system. Generally, between the first liquid and gas slug, oil appeared as the gas slug moved through the lines towards the micromodel. When this was not detected and remedied, it would inject oil into the micromodel, causing the results of the experiment to be void. This was remedied by removing the oil from the micromodel inlet connection. Since the system was operated at ambient temperature and pressure, the micromodel inlet connection was removed when the oil reached the inlet, and the oil in the line was allowed to drain, thereby preventing the oil from entering the micromodel.

4.6.2. Oil Trapped in Water/Gas Junction

The method for injecting water and gas alternatively required a junction between these two fluids. As the tee was made of stainless steel and therefore not transparent, it was impossible to determine exactly when the gas phase had reached the middle of the tee. If the gas phase did not reach the middle of the tee, oil would be trapped in the tee gas branch. Since the experiment involved injecting water first, this would cause the first gas slug to be preceded by an oil slug. This was remedied by better timing of the gas flow to completely displace the oil in the tee gas branch, and if any oil did remain trapped it was dealt with by draining the oil the same way the oil is drained in Section 4.6.2.

4.6.3. Gas Over-Pressurization

As air and propane are both compressible fluids, the syringe pump had the potential to over-pressurize the gas in the system. If the gas became over-pressurized, it had the ability to increase the gas flow rate and move very quickly through the system, causing premature breakthrough and very quick fluid movements. This was remedied by stopping the syringe pump before the injection time calculated for the full gas slug. Once the pump was stopped, the pressure developed in the gas caused the gas to continue to flow through the system for a period of time. With careful observation, it was possible to time the shutting down of the pump correctly to still inject the full gas slug.

4.6.4. Water Colour

Initially, the brine-surfactant solution was used in trial tests, however it was noticed that this solution was very difficult to distinguish from the glass of the micromodel. The gas phase was easily distinguishable; however the liquid phase blended in with the glass. To overcome this difficulty, the injection liquid was dyed a blue colour with methylene-blue before the surfactant was added to the brine. This colouring made it possible to distinguish between injection fluid and glass.

Chapter 5: Conclusions

Using a glass micromodel, four factors were investigated: (1) the water-alternating-gas ratio (volumetric ratio of water slug to gas slug) was varied from 1:1 to 1:2 with a centre point at 1:1.5; (2) the surfactant concentration (varied proportionally from the CMC) was varied from one times the CMC to 10 times the CMC, with a centre point at 5.5 times the CMC; (3) gas type (air and propane gas was used), and (4) surfactant type (Triton X-100 and Iveysol 106 were used).

Three responses were observed and measured: oil recovery, breakthrough time, and fluid flow. This set of 23 experiments were designed using the Stat-Ease Design of Experiments 9.0 software, utilizing the Optimal Design option of Response Surface Methodology. Six (6) additional experiments were conducted outside of this set of 23, including a waterflooding, water-surfactant flooding, brine-air water-alternating-gas, Iveysol 1 x CMC-Air water-alternating gas, and two experiments where the micromodel was initially flooded with brine (brine-air water-alternating-gas and Iveysol 1 x CMC water-alternating-gas). In addition to these micromodel experiments, five interfacial tension and five viscometer experiments were also conducted to fully explain the results obtained from the micromodel experiments.

The interfacial tension experiments investigated the interfacial tension between the injection liquid and oil phases. It was found that the surfactants reduced the interfacial tension between the injection liquid and oil phase, with higher concentrations reducing the interfacial tension more than low concentrations. Triton X-100 was found to reduce the interfacial tension more than Iveysol 106.

The viscometer experiments investigated the effect which the surfactants have on the viscosity of the injection liquid. It was found that the surfactants reduced the viscosity of the injection liquid, with higher concentrations reducing the viscosity more than low concentrations. Triton X-100 was found to reduce the viscosity more than Iveysol 106.

In observing the fluid flow through the porous media, several notes on the fluid flow were made. It was observed that the gas phases both fingered through the oil phase, causing breakthrough of gas in the outlet well. It was also observed that foam was not generated by the water-alternating-gas technique in the micromodel. To further investigate the lack of foam generation, several experiments were conducted to determine why no foam was generated.

For oil recovery, it was found that individually, gas type and surfactant concentration were significant, while WAG Ratio and surfactant type were not individually significant. It was also found that air produced a higher recovery of oil compared to propane, which may be due to the lower viscosity of propane causing the propane gas to finger through the micromodel more than the air. It was also found that lower surfactant concentrations produced larger oil recoveries, possibly due to the surfactant reducing the liquid viscosity, making it easier for the liquid to finger through the oil. Several interaction effects were discovered between the four main factors. The WAG Ratio-Surfactant Concentration interaction effect was found to be significant, with the oil recovery not changing for large WAG Ratios, while it increased with decreasing concentration for lower WAG Ratios. The oil recovery also varied with varying WAG Ratios at set concentration levels. For high concentration levels, oil recovery increases with WAG Ratio, while at low concentration levels, oil recovery decreases with WAG Ratio.

The WAG Ratio-Gas Type interaction effect was also found to be significant. With air, the oil recovery did not change significantly over the full range of WAG Ratios. However with propane, the oil recovery increased with increasing WAG Ratio but never attained the level of oil recovery with air.

The WAG Ratio-Surfactant Type interaction effect was also found to be significant. With Iveysol 106, the oil recovery did not change significantly over the full range of WAG Ratios. However with Triton X-100, the oil recovery increased with increasing WAG Ratio but never attained the level of oil recovery of Iveysol 106.

The last interaction effect identified for oil recovery was the Gas Type-Surfactant Type interaction effect. The oil recovery of Iveysol 106 did not change significantly between air or propane experiments, while the oil recovery of Triton X-100 decreased between air and propane experiments. Overall, the optimized situation for oil recovery involved using a WAG Ratio of 1:1, a surfactant concentration of one (1) times the CMC value, air as the gas phase, and Iveysol 106 as the surfactant.

In the additional experiments conducted, it was found that a water-alternating-gas injection method produced a greater recovery than waterflooding only. It was also found that water-surfactant flooding outperformed waterflooding, which was expected as the surfactants reduced the interfacial tension, increasing oil recovery. In the final comparison experiment, the surfactant assisted water-alternating-gas method outperformed the water-alternating-gas method, which was also expected as the surfactants should have an added benefit to oil recovery compared to water alone.

For breakthrough time, it was found that individually WAG Ratio and gas type were significant. Increasing the WAG Ratio decreased the breakthrough time, while for gas type, it was found that breakthrough time was larger for propane gas than it was for air. This may be due to the propane holding up in the micromodel more as it more soluble with the oil phase than the air is.

To optimize both oil recovery and breakthrough time, it is best to use a WAG Ratio of 1:1, a surfactant concentration of one (1) times the CMC value, air as the gas phase, and Iveysol 106 as the surfactant. The WAG ratio results were expected, as more gas is injected into the system, at a higher flow rate than the liquid, it was expected that the gas would breakthrough sooner. The gas type results were also expected, as propane has a lower viscosity than air, its ability to finger through the system was greater than air, causing early breakthrough. What was surprising was the lack of significance of the surfactant. It was expected that surfactants, and higher surfactant concentrations, would reduce breakthrough time through reductions in viscosity, which would lead to earlier breakthrough.

In the additional experiments conducted, it was found that injection method directly affected breakthrough time. Waterflooding had the highest breakthrough time, followed by water-surfactant flooding, water-alternating-gas, and finally surfactant assisted water-alternating-gas.

Two additional experiments were conducted to determine the optimum timing of enhanced oil recovery techniques, namely whether or not waterflooding before conducted enhanced oil recovery techniques is beneficial. For water-alternating-gas, it was found that beginning with water-alternating-gas and not waterflooding was beneficial, as the water-alternating-gas method would reach higher recoveries for each pore volume injected. However, both methods seem to approach the same oil recovery, just with the waterflooding first method delayed by the length of the waterflood. For surfactant assisted water-alternating-gas, it was found that waterflooding first increased oil recovery up to a point but ultimately the case with no initial waterflooding produced greater oil recovery sooner. Again it appears that both methods approach the same oil recovery near the end, just with the waterflooding first method delayed by the length of the waterflood. These method-timing results may not be applicable to the full field scale, as the pores are all the same size with no third dimension.

Chapter 6: Recommendations

Several potential areas of research were noted by the author during the course of this work. These thoughts have been made into a series of recommendations for future work in this area.

Recommendations for further research into the effects of surfactants on enhanced oil recovery:

- Investigate additional surfactants.
- Investigate different surfactant concentrations.
- Investigate additional gas types, especially natural gas.
- Perform coreflooding experiments with the same fluids and at the same conditions as the micromodel experiments for comparison.
- Perform both coreflooding and micromodel experiments at reservoir temperatures and pressures.
- Investigate additional factors such as salinity, flow rate, slug size, dip angle, oil density and viscosity, etc.
- Perform a series of experiments with and without primary waterflooding.
- Perform a series of experiments with and without primary gasflooding.
- Perform experiments in heterogeneous micromodels.
- Perform a series of experiments with the micromodel placed such that it has a vertical dimension.

Recommendations for further research into the image processing of micromodels:

- Develop a method to account for the slope of the pore sides.
- Further develop a method to accurately calculate the error of image processing, fully and accurately accounting for all interfaces.
- Develop an automated method for calculating oil recovery from an image so that additional data points throughout the experiment are available.

References

AAPG. (2014, November 11). *Wettability*. Retrieved April 1, 2015, from AAPG Wiki: http://wiki.aapg.org/Wettability

Abdi, M., M. S., Habibniyal, B., & Kord, S. (2014). Improving Oil Recovery during Water Injection and WAG Processes in Asphaltenic Oil Reservoirs by using Nonionic Surfactants. *International Journal of Science & Emerging Technologies*, 302-308.

Air Liquide. (2013). *Gas Encyclopedia - Air*. Retrieved November 19, 2014, from Air Liquide: http://encyclopedia.airliquide.com/Encyclopedia.asp?GasID=73

Air Liquide. (2013). *Gas Encyclopedia - Propane*. Retrieved November 19, 2014, from Air Liquide: http://encyclopedia.airliquide.com/Encyclopedia.asp?GasID=53#GeneralData

Al-Mossawy, M. I., Demiral, B., & Raja, D. A. (2011). Foam Dynamics in Porous Media and its Applciations in Enhanced Oil Recovery. *International Journal of Research and Reviews in Applied Science*, 351-359.

Anderson, G. (2008, October 8). *Seawater Composition*. Retrieved April 2, 2014, from Marine Science: http://www.marinebio.net/marinescience/02ocean/swcomposition.htm

ASTM International. (2007). ASTM D3601-88(2007 Standard Test Method for FOam in Aqueous Media (Bottle Test).

Aveyard, R., & Clint, J. H. (1996). Foam and thin film breakdown processes. *Current Opinion in Colloid & Interface Science*, 764-770.

Bird, J. (2001). *Newnes Engineering Science Pocket Book.* Routledge.

Blaker, T., Aarra, M. G., Skauge, A., Rasmussen, L., Celius, H. K., Martinsen, H. A., et al. (2002). Foam for Gar Mobility Control in the Snorre Field: The FAWAG Project. *Society of Petroleum Engineers*, 317-323.

Bonilla, F. a. (2013). Surfactant Flooding Evaluation for Enhanced Oil Recovery in Sandstones Reservoirs. *17th European Symposium on Improved Oil Recovery.* St. Petersburg, Russia.

Bou-Mikael, S., Asmadi, F., Marwoto, D., & Cease, C. (2000). Minas Surfactant Field Trial Tests Two Newly Designed Surfactants with High EOR Potential. *SPE Asia Pacific Oil and Gas Conference and Exhibition.* Brisbane, Australia: Society of Petroleum Engineers.

Brock, D., & Orr Jr., F. (1991). Flow Visualization of Viscous Fingering in Heterogeneous Porous Media. *66th Annual Technical Conference and Exhibition of the Society of Petroleum Engineers.* Dallas.

Bryant, R. S., & Douglas, J. (1988). Evaluation of Microbial Systems in Porous Media for EOR. *SPE Reservoir Engineering*, 489-495.

Chambers, K., & Radke, C. (1990). Capillary Phenomena in Foam Flow Through Porous Media. In N. R. Morrow, *Interfacial Phenomena in Petroleum Recovery.* New York: Marcel Dekker.

Chang, S., Owusu, L., & French, S. (1990). The Effect of Microscopic Heterogeneity on CO2-Foam Mobility: Part 2 - Mechanistic Foam Simulation. *SPE/DOE Seventh Symposium on Enhanced Oil Recovery.* Tulsa: Society of Petroleum Engineers.

Chang, S.-H., Martin, F., & Grigg, R. (1994). Effect of Pressure on C)2 Foam Displacements: A Micromodel Visualization Study. *SPE/DOE Improved Oil Recovery Symposium.* Tulsa: Society of Petroleum Engineers.

Chatzis, I., Morrow, N. R., & Lim, H. T. (1983). Magntiude and Detailed Sturcture of Residual Oil Saturation. *Society of Petroleum Engineers*, 311-326.

Chen, M., Yortsos, Y., & Rossen, W. (2005). Insights on Foam Generation in Porous Media from Pore-Network Studies. *Colloids Surfaces A: Physiochem Eng. Aspects*, 181-189.

Chiang, J. C., Sawyal, S. K., Castanier, L. M., Brigham, W. E., & Sufi, A. (1980). Foam As a Mobility Control Agent In Steam Injection Processes. *50th Annual California Regional Meeting of the Society of Petroleum Engineers of AIME.* Los Angeles: Society of Petroleum Engineers.

Cooper, M., Southworth, R., Walsh, D., & Morgan, J. (1985). Field Experience in the Bothamsall Surfactant Flood Project. *Offshore Europe.* Aberdeen, United Kingdom: Society of Petroleum Engineers.

Czitrom, V. (1999). Teacher's Corner: One-Factor-at-a-Time Versus Designed Experiments. *The American Statistician*, 126-131.

Dixon, J. C. (2007). *The Shock Absorber Handbook.* West Sussex: John Wiley & Sons Ltd.

Dong, H., Hong, Y., & Rui, W. (2006). The Effect of Wettability on Oil Recovery of Alkaline/Surfactant/Polymer Flooding. *2006 SPE Annual Technical Conference.* San Antonio: Society of Petroleum Engineers.

Elsharkawy, A. (1992). Measureing Minimum Miscibility Pressure: Slim-Tube or Rising-Bubble Method? *SPE/DOE Eighth Symposium on Enhanced Oil Recovery* (pp. 107-116). Tulsa, Oklahoma, U.S.A.: Society of Petroleum Engineers.

Esmaeili, M., Heydarian, A., & Helalizadeh, A. (2013). An Experimental Study of Alkali-surfactant-polymer Flooding through Glass Micromodels Including Dead-end Pores. *Iranian Journal of Oil & Gas Science and Technology*, 48-56.

European Textile Services Association. (n.d.). *Surfactants*. Retrieved February 20, 2013, from Environmental Assessment of Laundry Detergents: http://www.eco-forum.dk/detergents/index_files/Page718.htm

Falls, A., Hirasaki, G., Gauglitz, T., Miller, P. D., & Ratulowski, J. (1988). Development of a Mechanistic Foam Simulator: The Population Balance and Generation by Snap-Off. *SPERE*, 884-892.

Farajzadeh, R., Andrianov, A., & Zitha, P. (2009). Foam Assisted Enhanced Oil Recovery at Miscible and Immiscible Conditions. *Kuwait International Conference and Exhibition.* Kuwait City: Society of Petroleum Engineers.

Farajzadeh, R., Andrianov, A., Krastev, R., Hirasaki, G., & Rossen, W. (2012). Foam-oil interaction in porous media: Implications for foam assisted enhanced oil recovery. *Advances in Colloid and Interface Science*, 1-13.

Feng, Q.-x., Di, L.-c., Tang, G.-q., Chen, Z.-y., Wang, X.-l., & Zou, J.-x. (2014). A visual Micro-model Study: The Mechanism of Water Alternative Gas Displacement in Porous Media. *SPE/DOE Fourteeth Symposium on Improved Oil Recovery.* Tulsa: Society of Petroleum Engineers.

Gurgel, A., Moura, M., Dantas, T., Neto, E. B., & Neto, A. D. (2008). A Review On Chemical Flooding Methods Applied In Enhanced Oil Recovery. *Brazilian Journal of Petroleum and Gas*, 83-95.

Harkins, W. D. (1941). A General Thermodynamic Thoery of the Spreading of Liquids to Form Duplex Films and of Liquids or SOlid to Form Monolayers. *The Journal of Chemical Physics*, 552-568.

Hematpour, H., Arabjamloei, R., Nematzadeh, M., Esmaili, H., & Mardi, M. (2012). An Experimental Investigation of Surfactant Flooding Efficiency in Low Viscosity Oil Using a Glass Micromodel. *Energy Sources, Part A: Recovery, Utilization, and Environmental Effects*, 1745-1758.

Hirasaki, G. (1991). Thermodynamics of thin films and three-phase contact regions. In N. R. Morrow, *Interfacial Phenomena in Petroleum Recovery* (pp. 23-76).

Hongyan, W., Xulong, C., Jichao, Z., & Aimei, Z. (2009). Development and application of dilute surfactant-polymer flooding system for Shengli oilfield. *Journal of Petroleum Science and Engineering*, 45-50.

Hornbrook, J., Castanier, L., & Pettit, P. (1991). Observation of Foam/Oil Interactions in a New, High-Resolution Micromodel. *SPE Annual Technical Conference and Exhibition.* Dallas: Society of Petroleum Engineers.

Huh, D., & Handy, L. (1989). Comparison of Steady and Unsteady-State Flow of Gas and Foaming Solution in Porous Media. *SPERE*, 77-84.

Iglauer, S., Wu, Y., Shuler, P., Tang, Y., & Goddard, W. A. (2010). New surfactant classes for enhanced oil recovery and their tertiary oil recovery potential. *Journal of Petroleum Science and Engineering*, 23-29.

Israelachvilli, J. N. (1991). *Intermolecular and Surface Forces.* London: Academic Press.

Jamaloei, B. Y., & Kharrat, R. (2010). Analysis of Microscopic Displacement Mechanisms of Dilute Surfactant Flooding in Oil-wet and Water-wet Porous Media. *Transport in Porous Media*, 1-19.

Jamaloei, B. Y., Kharrat, R., & Asghari, K. (2012). The influence of salinity on the viscous instability in viscous-modified low-interfacial tension flow during surfactant-polymer flooding in heavy oil reservoirs. *Fuel*, 174-185.

James, L. (2009). Mass Transfer Mechanisms during the Solvent Recovery of Heavy Oil (Ph.D). University of Waterloo, Canada.

Jeong, S.-W., & Corapcioglu, M. Y. (2000). Micromodel Study of Surfactant Foam Remediation of Residual Trichloroehtylene. *Environ. Sci. Technol.*, 3456-3461.

Johnson, C. (1957). Evaluation of Surfactants for Oil Field Flooding. *Journal of the American Oil Chemists' Society*, 209-214.

Khezrnejad, A., James, L. A., & and Johansen, T. E. (2014). Water Enhancement Using Nanoparticles in Water Alternating Gas (WAG) Micromodel Experiments. *SPE Annual Technical Conference and Exhibition.* Amsterdam: SPE.

Kovscek, A., & Radke, C. (1993). *Fundamentals of Foam Transport in Porous Media.* Berkeley: University of California - Berkeley.

Krumrine, P. F. (1983). Surfactant, Polymer and Alkali Interactions in Chemical Flooding Processes. *SPE International Symposium on Oilfield and Geothermal Chemistry* (pp. 79-86). Denver: SPE.

Laplace, P. S. (1805). *Traité de Mécanique Céleste, volume 4.* Paris: Courcier.

Li, Q. (2006). *Foam Generation and Propagation in Homogeneous and Heterogeneous Porous Media.* Austin: University of Texas at Austin.

Manrique, E., Gurfinkel, M., & Muci, V. (2004). Enhanced Oil Recovery Field Experiences in Carbonate Reservoirs in the United States. *25th Annual Workshop & Symposium Collaborative Project on Enhanced Oil Recovery Internation Energy Agency.* Stavanger, Norway: Center for Energy and Technology of the Americas.

Melrose, J., & Brandner, C. (1974). Role of Capillary Forces in Determining Microscopic Displacement Efficiency for Oil Recovery by Waterflooding. *The Journal of Canadian Petroleum*, 54-62.

Moayedi, M., James, L., & Mahmoodi, M. (2014). An Experimental Study on Optimization of SAG Process Utilizing Nonionic Surfactants and Sodium Lignosulfonate. *International Symposium of the Society of Core Analysts.* Avignon.

Motealleh, M., Kharrat, R., Gandomkar, A., Khanamiri, H., Nematzadeh, M., & Ghazanfari, M. (2012). An Experimental Study on the Applicability of Water-alternating-CO2 Injection in the Secondary and Tertiary Recovery in One Iranian Reservoir. *Petroleum Science and Technology*, 2571-2581.

Muskat, M. (1949). Calculation of Initial Fluid Distribution in Oil Reservoirs. *Transactions of the AIME*, 119-127.

National Institute of Standards and Technology. (2013, 10 30). *NIST/SEMATECH e-Handbook of Statistical Methods.* Retrieved 08 20, 2014, from Engineering Statistics Handbook: http://www.itl.nist.gov/div898/handbook/index.htm

Oil Chem Technologies. (2010). *Enhanced Oil Recovery*. Retrieved February 25, 2013, from Oil Chem Technologies: http://www.oil-chem.com/smartsf.htm

Pu, H., & Xu, Q. (2009). An Update and Perspective on Field-Scale Chemical Floods in Daqing Oilfield, China. *SPE Middle East Oil & Gas Show and Conference.* Kingdom of Bahrain: Society of Petroleum Engineers.

Pugh, R. (1996). Foaming, foam films, antifoaming and defoaming. *Advanced in Colloid and Interface Sciences*, 67-142.

Ransohoff, P., & Radke, C. (1988). Mechanisms of Foam Generation in Glass-Bead Packs. *SPERE*, 573-585.

Ransohoff, T., Gauglitz, P., & Radke, C. (1987). Snap-off of gas bubbles in smoothly constricted noncircular capillaries. *AlChE*, 753-765.

Rao, D., & Girard, M. (1994). A New Technique for Reservoir Wettability Characterization. *45th Annual Technical Meeting of the Petroleum Society of CIM.* Calgary, Alberta, Canada: Petroleum Society of CIM.

Rao, D., & Lee, J. (2000). Evaluation of Minimum Miscibiltiy Pressure and Composition for Terra Nova Offshore Project Using the New Vanishing Interfacial Tension Technique. *SPE/DOE Improved Oil Symposium.* Tulsa, Oklahoma, U.S.A.: Society of Petroleum Engineers.

Rao, D., & Lee, J. (2003). Determination of gas-oil miscibility conditions by interfacial tension measurements. *Colloid and Interface Science*, 474-482.

Rao, D., Ayirala, S., Abe, A., & Xu, W. (2006). Impact of Low-Cost Dilute Surfactants on Wettability and Relative Permeability. *SPE/DOE Symposium on Improved Oil Recovery.* Tulsa, Oklahoma, U.S.A.: Society of Petroleum Engineers.

Reusch, W. (2013, May 5). *Molecular Shape*. Retrieved October 24, 2014, from Michigan State University Department of Chemistry: http://www2.chemistry.msu.edu/faculty/reusch/VirtTxtJml/intro3.htm

Robsinson, J., & Woods, W. (1948). A method of selecting foam inhibitors. *Journal of the Society of Chemical Industry*, 361-365.

Romero, C., Alvarez, J., & Muller, A. (2002). Micromodel Studies of Polymer-Enhanced Foam Flow Through Porous Media. *SPE/DOE Improved Oil Recovery Symposium.* Tulsa: Society of Petroleum Engineers.

Roof, J. (1970). Snap-Off of Oil Droplets in Water-Wet Pores. *Transactions*, 85-90.

Rossen, W. (1990). Theory of Mobilization Pressure Gradient of Flowing Foams in porous Media. *Journal of Colloid Interface Science*, 1-16.

Sagar, N. S., & Castanier, L. M. (1997). *Oil-Foam Interaction in a Micromodel.* Tulsa: U.S. Department of Energy.

Salehi, M. M., Safarzadeh, M. A., & Alireza, E. S. (2013). Experimental Study of surfactant alternating gas injection versus water alternating gas and water flooding enhanced oil recovery methods. *Journal of Petroleum and Gas Engineering*, 160-172.

Salehi, M. M., Safarzadeh, M. A., Sahraei, E., & Nejad, S. A. (2014). Comparison of oil removal in surfactant alternating gas with water alternating gas, waterflooding and gas flooding in secondary oil recovery process. *Journal of Petroleum Science and Engineering*, 86-93.

Schramm, L. L. (2000). *Surfactants: Fundamentals and Applications in the Petroleum Industry.* Cambridge, United Knigdom: Cambridge University Press.

Shabib-asl, A., Ayoub, M., Alta'ee, A., Bin Mohd Saaid, I., & Valentium, P. P. (2014). Comprehensive Review of Foam Application during Foam Assisted Water Alternating Gas (FAWAG) Method. *Research Journal of Applied Sciences, Engineering and Technology*, 1896-1904.

Shen, P., Zhu, B., & Li, X. W. (2006). The Influence of Interfacial Tension on Water/Oil Two-Phase Relative Permeability. *2006 SPE/DOE Symposium on Improved Oil Recovery.* Tulsa: Society of Petroleum Engineers.

Sheng, J. (2011). *Modern Chemical Enhanced Oil Recovery.* Burlington: Gulf Professional Publishing.

Shokrollahi, A., Ghazanfari, M. H., & Badakhshan, A. (2014). Aplication of Foam Floods for Enhancing Heavy Oil Recovery Through Stability Analysis and Core Flood Experiments. *The Canadian Journal of Chemical Engineering*, 1975-1987.

SimScience. (n.d.). *Membranes - Advanced Level*. Retrieved March 2, 2013, from SimScience: http://simscience.org/membranes/advanced/essay/surfactants-reduce.html

Skauge, A., Aarra, M., Surguchev, L., Martinsen, H., & Rasmussen, L. (2002). Foam-Assisted WAG: Experience from the Snorre Field. *SPE/DOE Improved Oil Recovery Symposium.* Tulsa: Society of Petroleum Engineers.

Sohrabi, M., Henderson, G., Tehrani, D., & Danesh, A. (2000). Visualization of Oil Recovery by Water ALternating Gas (WAG) Injection Using High Pressure Micromodels - Water-Wet System. *Society of Petroleum Engineers.* Dallas: Society of Petroleum Engineers.

Som, I., Bhatia, K., & Yasir, M. (2012). Status of surfactants as penetration enhancers in transdermal drug delivery. *Journal of Pharmacy & BioAllied Sciences*, 2-9.

Somasundaran, P., & Hanna, H. (1979). Adsorption of Sulfonates on Reservoir Rocks. *Society of Petroleum Engineering Journal*, 221-232.

Somasundaran, P., & Zhang, L. (2006). Adsorption of surfactants on minerals for wettability control in improved oil recovery processes. *Journal of Petroleum Science and Engineering*, 198-212.

Stat-Ease. (2014). *Handbook for Experimenters.* Retrieved May 20, 2014, from Stat-Ease: http://www.statease.com/pubs/handbk_for_exp_sv.pdf

Tang, X., Zhang, B., Höök, M., & Feng, L. (2010). Forecast of oil reserves and production in Daqing oilfield of China. *Energy*, 3097-3102.

Tanzil, D., Hirasaki, G., & Miller, C. (2002). Conditions for Foam Generation in Homogeneous Porous Media. *SPE/DOE Symposium on Improved Oil Recovery.* Tulsa: Society of Petroleum Engineers.

Taylor, J. (1982). *An Introduction to Error Analysis.* Mill Valley: University Science Books.

Thomas, S. (2007). Enhanced Oil Recovery - An Overview. *Oil & Gas Science and Technology*, 9-19.

Tracy, C., Xie, L., & Ly, I. (n.d.). *Cohesive and Adhesive Forces*. Retrieved April 10, 2013, from University of California Davis - ChemWiki: The Dynamic Chemistry Textbook: http://chemwiki.ucdavis.edu/Physical_Chemistry/Physical_Properties_of_Matter/Intermolecular_Forces/Cohesive_And_Adhesive_Forces

Van Duijn, C., Molenaar, J., & De Neef, M. (1995). Effect of Capillary Forces on Immiscible Two-Phase Flow in Heterogeneous Porous Media. *Transport Porous Media*, 71-93.

Vogel, E., Küchenmeister, C., Bich, E., & Laesecke, A. (1998). Reference Correlation of the Viscosity of Propane. *Journal of Physical and Chemical Reference Data*, 947-970.

Wyatt, K., Pitts, M. J., & Surkalo, H. (2002). Mature Waterfloods Renew Oil Production by Alkaline-Surfactant-Polymer Flooding. *SPE Eastern Regional Meeting.* Lexington, Kentucky, U.S.A.: Society of Petroleum Engineers.

Xu, Q., & Rossen, W. (2003). Experimental Study of Gas njection in Surfactant-Alternating-Gas Foam Process. *Society of Petroleum Engineers.* Denver: Society of Petroleum Engineers.

Yin, D., & Pu, H. (2008). A Numerical Simulation Study on Surfactant Flooding and it's Field Application in Daqing Oilfield. *Society of Petroleum Engineers Europec/EAGE Annual Conference and Exhibition.* Rome: Society of Petroleum Engineers.

Yortsos, Y., & Chang, J. (1990). Capillary Effects in Steady-State Flow in Heterogeneous Cores. *Transport Porous Media*, 399-420.

Zhijian, Q., Yigen, Z., Xiansong, Z., & Jialin, D. (1998). A Successful ASP flooding Pilot in Gudong Oil Field. *SPE/DOE Improved Oil Recovery Symposium.* Tulsa, Oklahoma, U.S.A.: Society of Petroleum Engineers.

Appendix A: Micromodel System Schematic

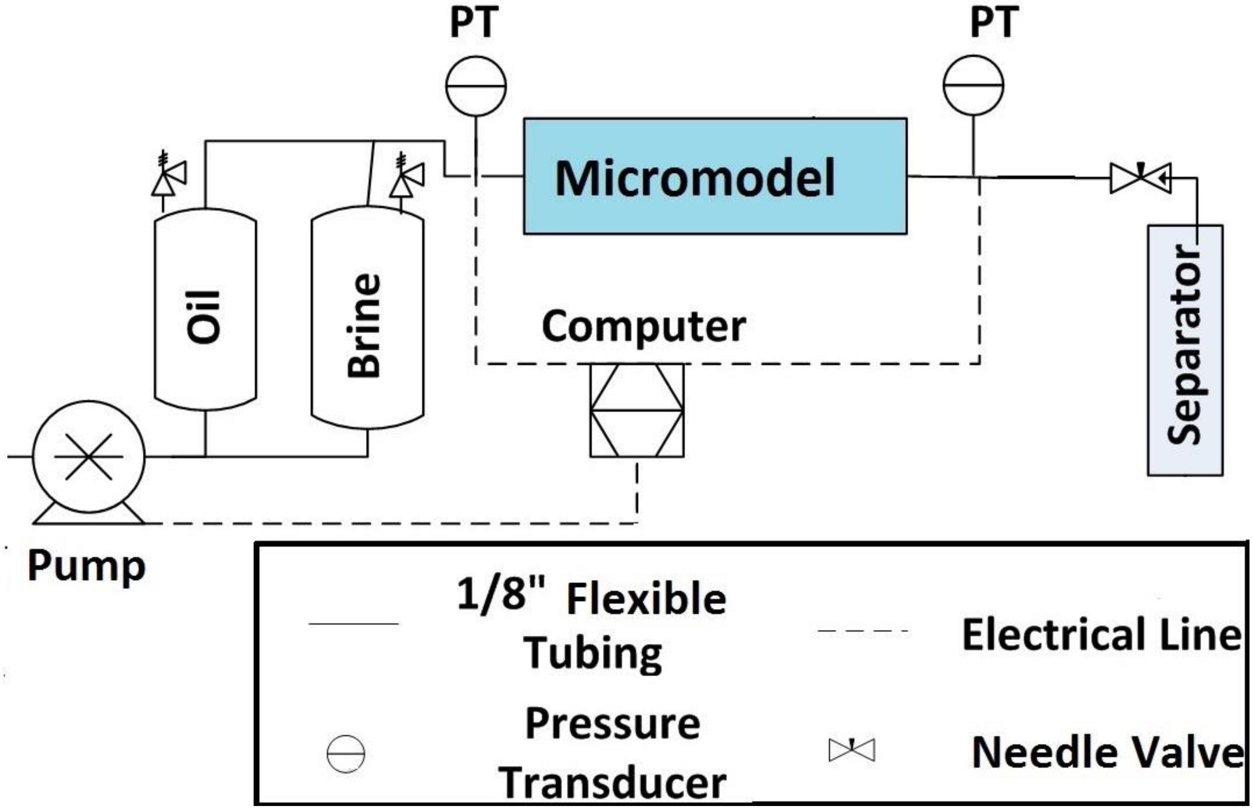

Figure A-1. Schematic for Micromodel System (Khezrnejad et. al 2014)

Appendix B: Micromodel System Procedures

This section describes the experimental procedure in detail, describing valves that are opened and closed, operation of the syringe pump, and the collection of data.

The micromodel experiment consisted of injecting six (6) slugs each of liquid and gas consecutively into the micromodel, always starting with the a water slug. A basic slug size of 0.2 PV, or 20% of the pore volume of the micromodel, was used. According to Bedrikovetsky (1993), the use of slugs of between 20% and 40% of the pore volume (0.2 to 0.4 PV), has been recommended in several experimental studies for water-alternating-gas techniques. Therefore a basic slug volume of 0.2 PV was chosen, with the gas phase slug increasing to 0.4 PV as was discussed in Section 3.2.1.1.

As discussed in Section 2.2.2, for the foam to be stable the gas mobility should be greater than the liquid mobility. Therefore the gas phase was injected at twice the flow rate of the liquid phase to give the gas phase a higher mobility. The liquid flow rate was set at 0.0193 mL/min. This flow rate allows for the 0.2 PV slug of liquid to be injected into the micromodel in 30 minutes.

Sample Preparation

Before the experiments can be conducted, the fluids and micromodel must be prepared.

Injection Liquid:

The process for preparing the liquid phase for experimentation involves two main steps, creating the synthetic brine solution, and adding the surfactant.

Synthetic Brine:

1. Place a clean beaker on the mass balance.
2. Tare the mass balance to 0.
3. Add a set amount of water, measure by:
    a. Observing the mass in the beaker.
4. Remove the beaker from the mass balance and place on a stirrer. Add a magnetic stirrer to the beaker.
    a. Ensure the mixing speed dial is between 200 and 300, keep stirring throughout step 5.
5. Add the required salts, one salt at a time:
    a. Place a weigh paper on the mass balance.
    b. Tare the mass balance to 0.
    c. Using a scoop, add the desired salt to the weigh paper until the desired mass is acheived.

    - d. Add the salt to the beaker solution.
    - e. Repeat steps a to d for each desired salt.
6. If coloured synthetic brine is desired, add methylene blue powder to the beaker while sitrring until desired colour is achieved.
7. If methylene blue is being used, ensure the beaker is well covered from light.

NOTE: If additives other than salts and surfactants are being used, follow the procedures outlined to create those solutions.

Surfactant Solution:

1. Place a beaker back on the mass balance.
2. Tare the mass balance to 0.
3. Draw surfactant solution into a small syringe.
4. Add the required amount of surfactant to the beaker, measure by observing the increase in mass.
5. Add the required amount of synthetic brine solution to the beaker, measure by observing the increase in mass.
6. Remove the beaker from the mass balance and place on a stirrer.
7. Place a magnetic stirring bar into the beaker and mix for 3 minutes.
    - a. Ensure the mixing speed dial is between 200 and 300.

NOTE: Mixer speeds above 300 have the potential to create foam if surfactant additives are being used. Mixer speeds should be kept below 300 to avoid the creation of foam.

System Preparation

Add Injection Liquid:

1. Using a completely evacuated and clean syringe, draw enough liquid from the beaker into the syringe.
2. Clean any liquid left over on the outside of the syringe.
3. Attach the liquid syringe to the liquid injection line.
4. Push liquid from the syringe until the liquid passes the micromodel inlet valve.

Add Injection Gas:

To prepare the gas phase for experimentation:

1. If air is being used, ensure the gas phase fill line is open to the atmosphere.
2. If propane gas is being used, ensure the gas phase fill line is connected to a propane container and any attached valves or regulators are in the open position.
3. Close the gas injection valve.
4. Draw gas into the syringe using the pump operations. Draw in a minimum of 20 mL of gas.

5. Close the valves on the gas phase fill line.
6. Open the gas injection valve.
7. Completely empty the syringe into the system.
8. Close the gas injection valve.
9. Open the gas fill line valve.
10. Draw gas into the syringe using the pump operations. Draw in a minimum of 20 mL of gas.

Micro Model:

To prepare the micromodel for flooding:

1. Ensure the micromodel has been cleaned and that the injection liquid and injection gas preparation steps have been completed.
2. Place a flexible ventilation snake over the outlet.
3. Turn on the flexible ventilation snake.
4. Open the inlet and outlet valves upstream and downstream of the micromodel.
5. Close the gas injection valve.
6. Completely fill a syringe with brine.
7. Attach the syringe to the temporary cleaning line.

8. Open the gas injection valve for flow between the temporary cleaning line and the micromodel.
9. Inject the system with brine until the brine passes the micromodel inlet valve.
10. Attach a vacuum pump to the outlet line.
11. Close the micromodel inlet valve.
12. Vacuum the system for several minutes.
13. Open the micromodel inlet valve and allow brine to completely flood the micromodel.
14. Disconnect the vacuum pump from the outlet line.
15. Inject the brine until the brine has passed the micromodel outlet valve.
16. Completely fill a syringe with oil.
17. Close the micromodel inlet valve.
18. Disconnect the brine syringe from the temporary cleaning line.
19. Attach the oil syringe to the temporary cleaning line.
20. Open the micromodel inlet valve for flow between the temporary fill line and the micromodel.
21. Place the microseparator into an empty waste beaker.
22. Clean the separator burette.
23. Inject oil until the oil flows into the microseparator.
24. Ensure lines are completely filled with oil.
25. Open the gas injection valve for flow between the gas syringe and the micromodel.
26. Inject the gas phase until the gas phase reaches the gas injection valve.

27. Place the microseparator onto the separator burette.
28. Close all valves.
29. Turn off the flexible ventilation snake.

Experimentation

This section describes the procedures for conducting the experiments once all preparations have been completed. This section details the injection of fluids and the monitoring of the experiments.

Injection of Liquid:

To inject a slug of liquid:

1. Ensure the gsa injection valve is in the closed position.
2. Open the micromodel inlet valve and liquid injection valve.
3. Input speed settings into the sump for syringe 2.
4. Allow the pump to run for the set period of time.
5. Stop the pump for syringe 2.
6. Closed the liquid injection valve.

Injection of Gas:

To inject a slug of gas:

1. Open the gas injection valve.
2. Input speed settings into the pump for syringe 1.
3. Allow the syringe to run for the set period of time
4. Stop the pump for syringe 1.
5. Close the gas injection valve.

System Shutdown:

Once the system has been operated for the set period of injection/time, the following should be done to shut down the system and prepare it for cleaning:

1. Turn off the pump.
2. Depressurize the system by keeping the micromodel outlet valve open, allowing the system to reach ambient pressure.
3. Using a syringe with a Luer Lock/Swagelok adaptor, attach to the temporary cleaning line and push air through until all the liquid is in the separator.

System Cleaning:

Once the system has been shut down, the following should be done to clean the system to prepare it for another experiment:

1. Fill a syringe with distilled water.
2. Attach the syringe to the temporary cleaning line using a Luer Lock/Swagelok adaptor.
3. Disconnect the liquid syringe and place in a waste beaker.
4. Open the gas injection valve for flow between the temporary cleaning line and the micromodel, push distilled water through until most of the liquid has been removed from the lines.
5. Close the micromodel inlet valve and open the water injection valve.
6. Push distilled water through until most of the liquid has been removed from the lines and micromodel.
7. Close all valves.
8. Detach the syringe from the temporary cleaning line and fill with toluene. Re-attach to the temporary cleaning line.
9. Open the gas injection valve for flow between the temporary cleaning line and the micromodel; push toluene through until the oil has been removed from the lines.

10. Detach the syringe and fill with acetone, re-attach and clean with acetone.
11. Push distilled water through until most of the liquid has been removed.
12. Push air through until most of the liquid has been removed from the lines and micromodel.
13. Attach the vacuum pump to line 18.
14. Turn on the vacuum pump.
15. Clean the separator burette.

Appendix C: Foam Stability Experimental Results

This section presents the total foam height and relative foam height for all eight bottle test experiments, for both the first and second run of each experiment. The results are presented based on surfactant used and the presence of oil, with Triton X-100 without oil (Experiment 1 and 2), being presented first, followed by Iveysol 106 without oil (Experiment 3 and 4) being presented next. This is followed by Triton X-100 with oil (Experiment 5 and 6), followed by Iveysol 106 with oil (Experiment 7 and 8).

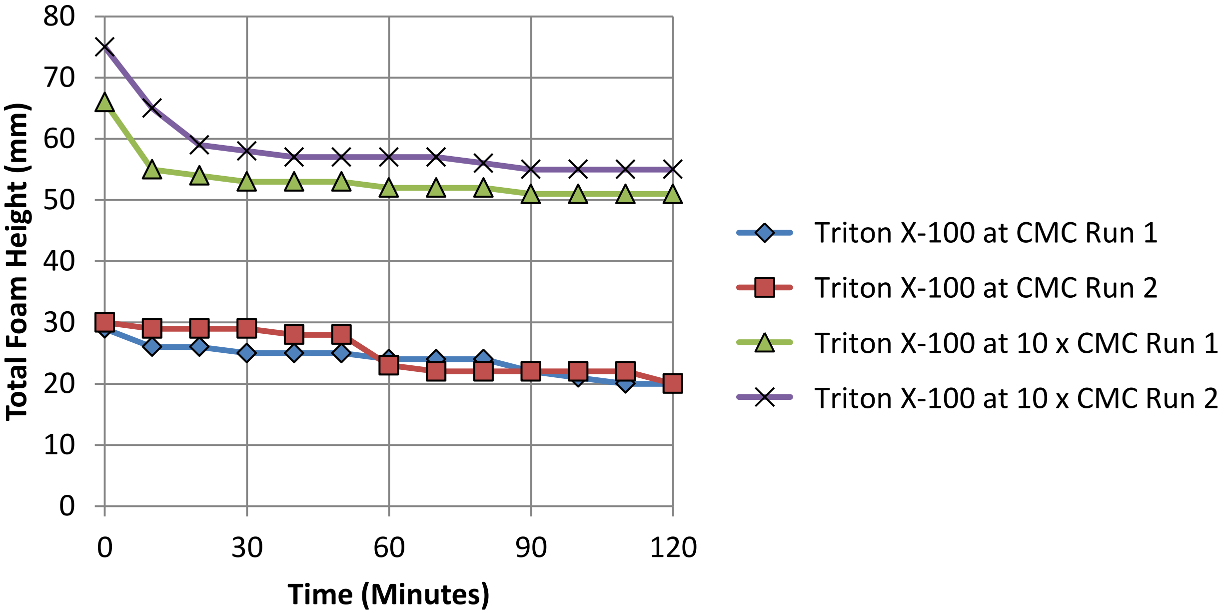

Figure C-1. Total Foam Height for Experiments 1 and 2, Without Oil, Both Runs

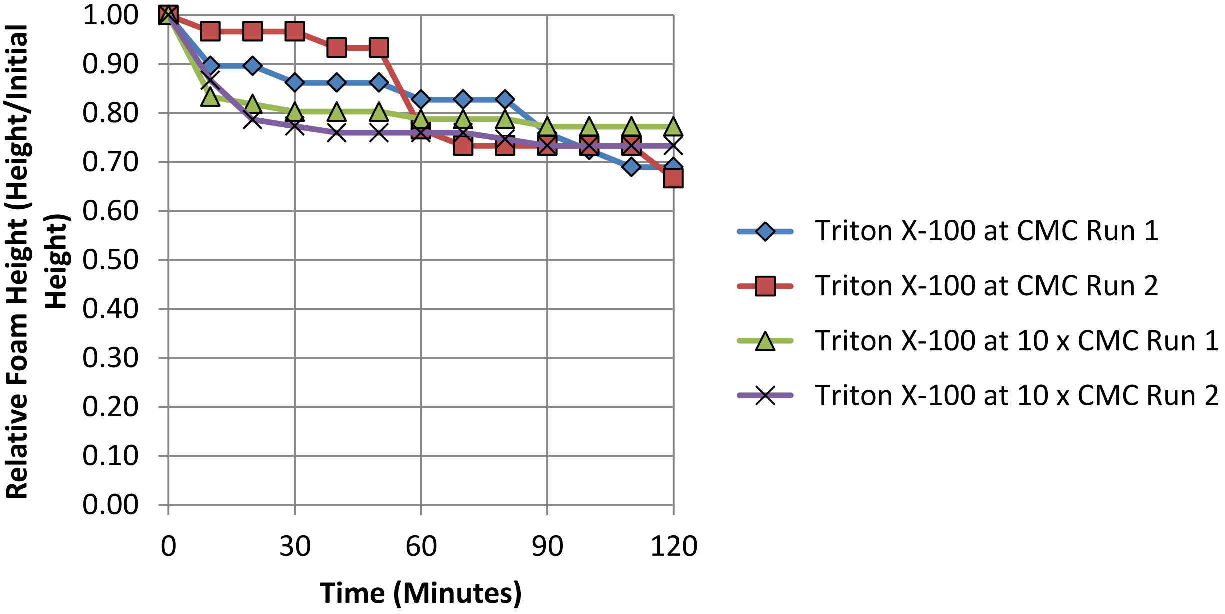

Figure C-2. Relative Foam Height for Experiments 1 and 2, Without Oil, Both Runs

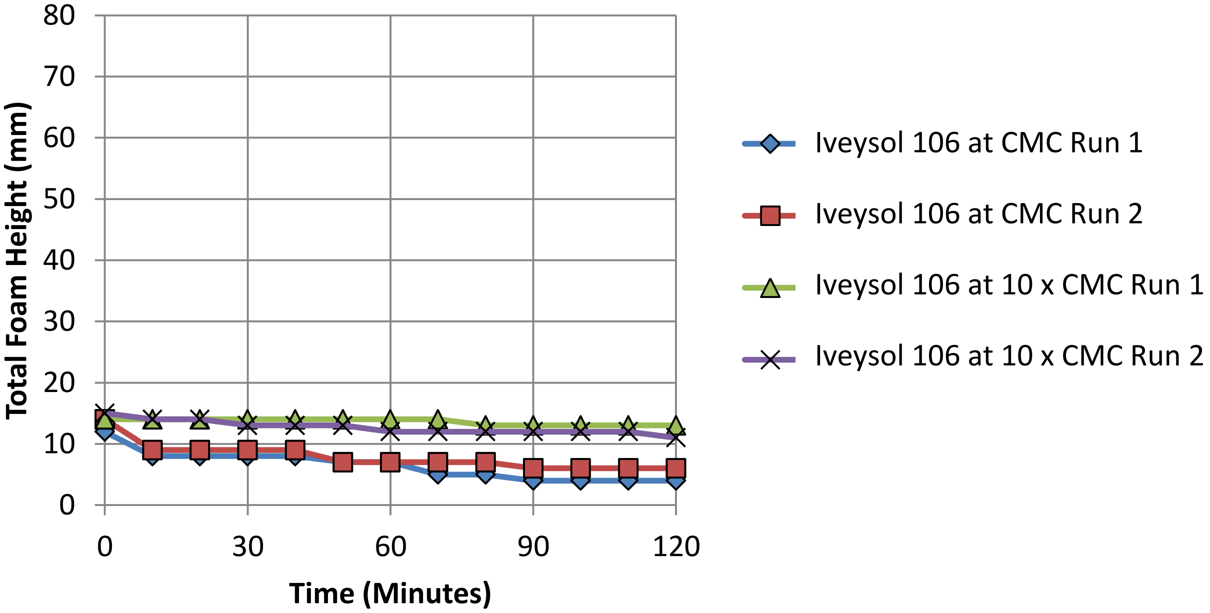

Figure C-3. Total Foam Height for Experiments 3 and 4, Without Oil, Both Runs

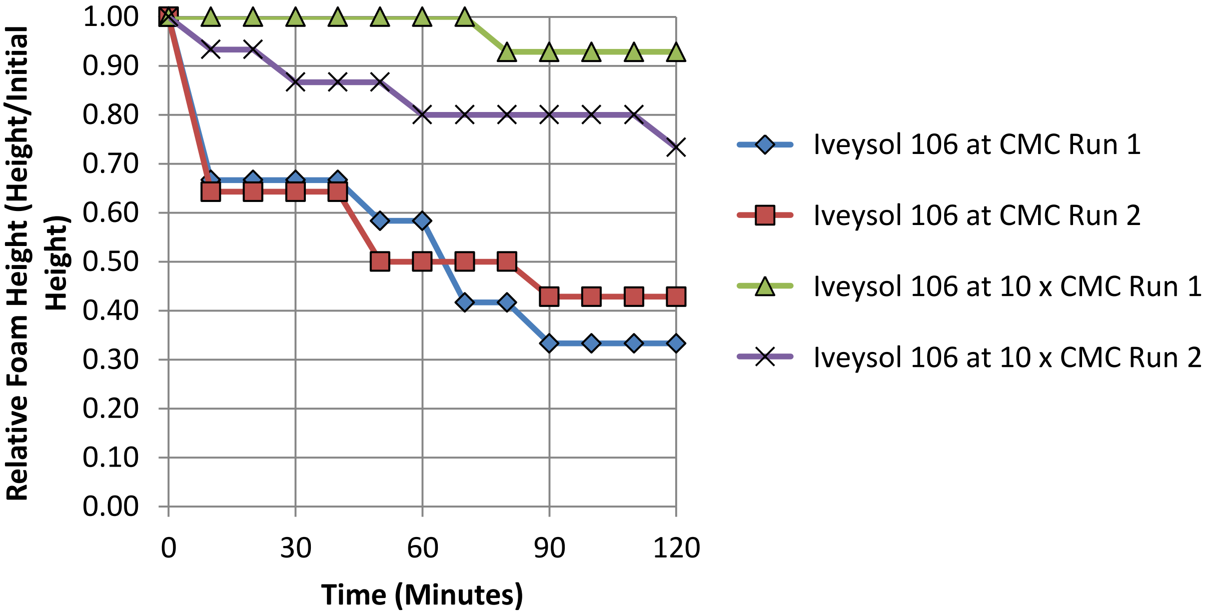

Figure C-4. Relative Foam Height for Experiments 3 and 4, Without Oil, Both Runs

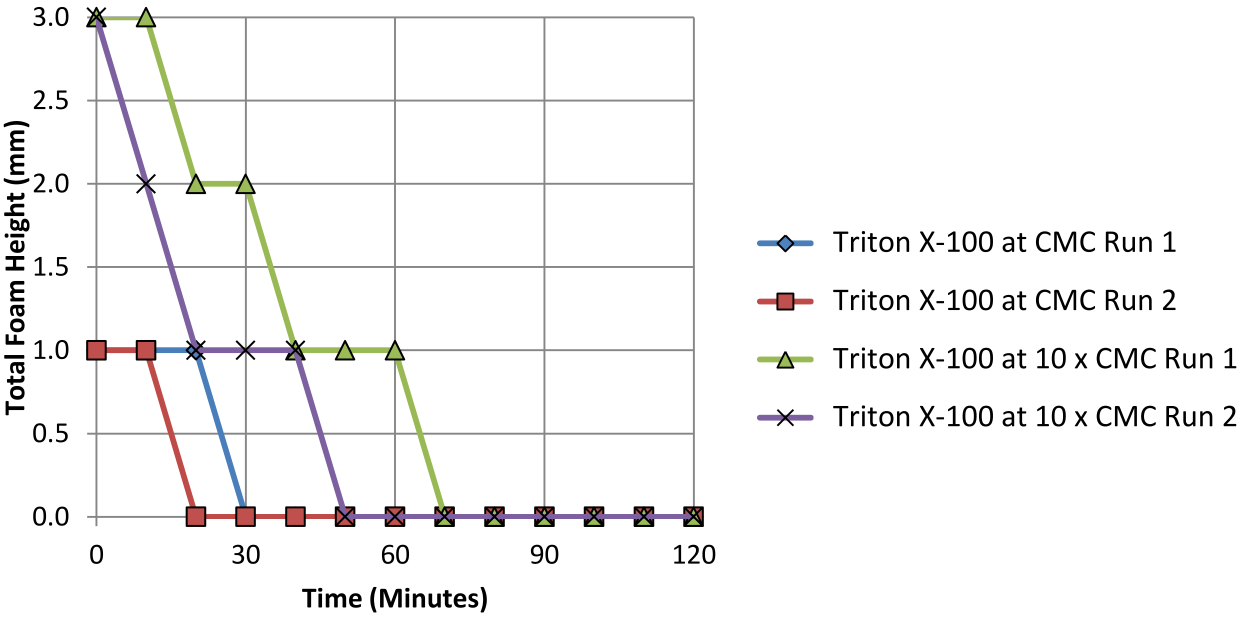

Figure C-5. Total Foam Height for Experiments 5 and 6, With Oil, Both Runs

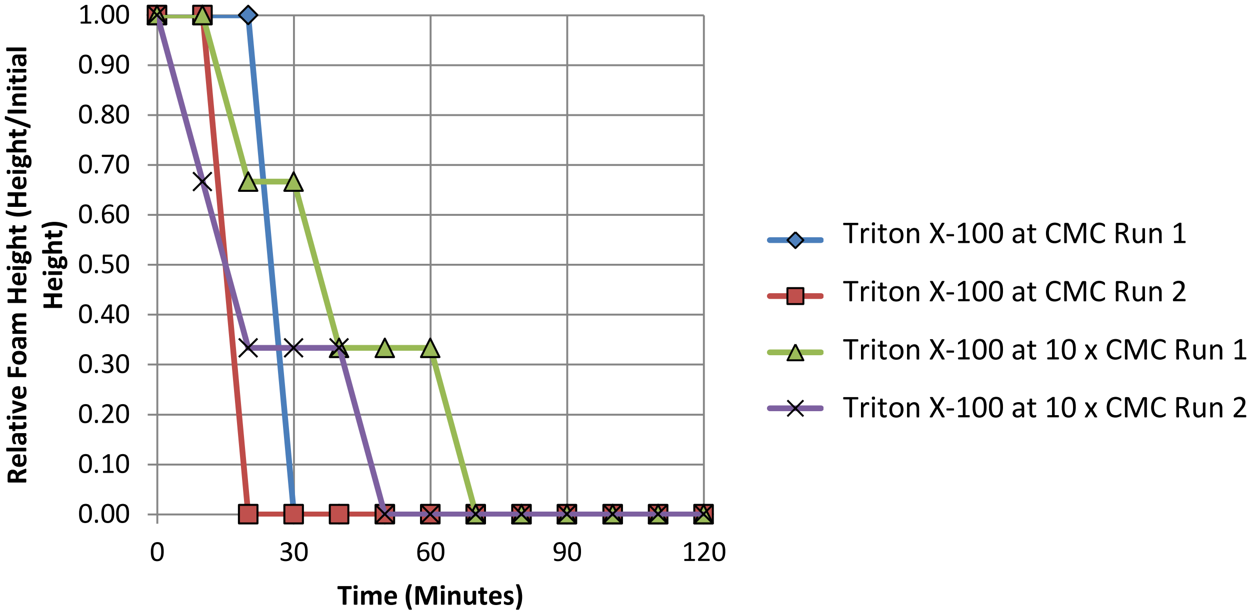

Figure C-6. Relative Foam Height for Experiments 5 and 6, With Oil, Both Runs

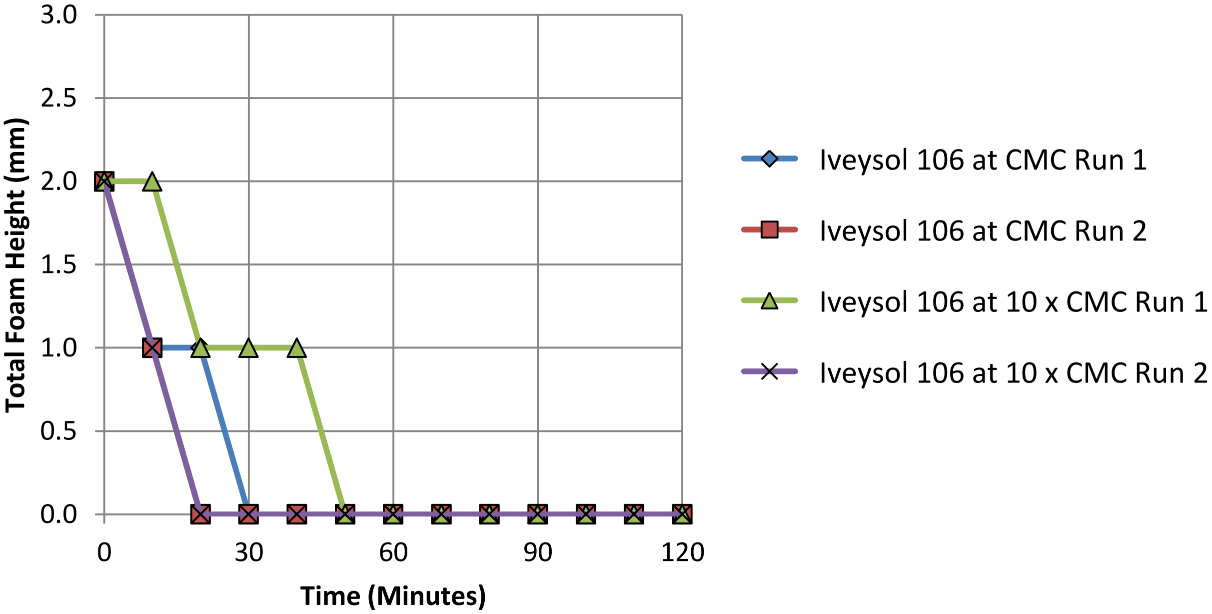

Figure C-7. Total Foam Height for Experiments 7 and 8, With Oil, Both Runs

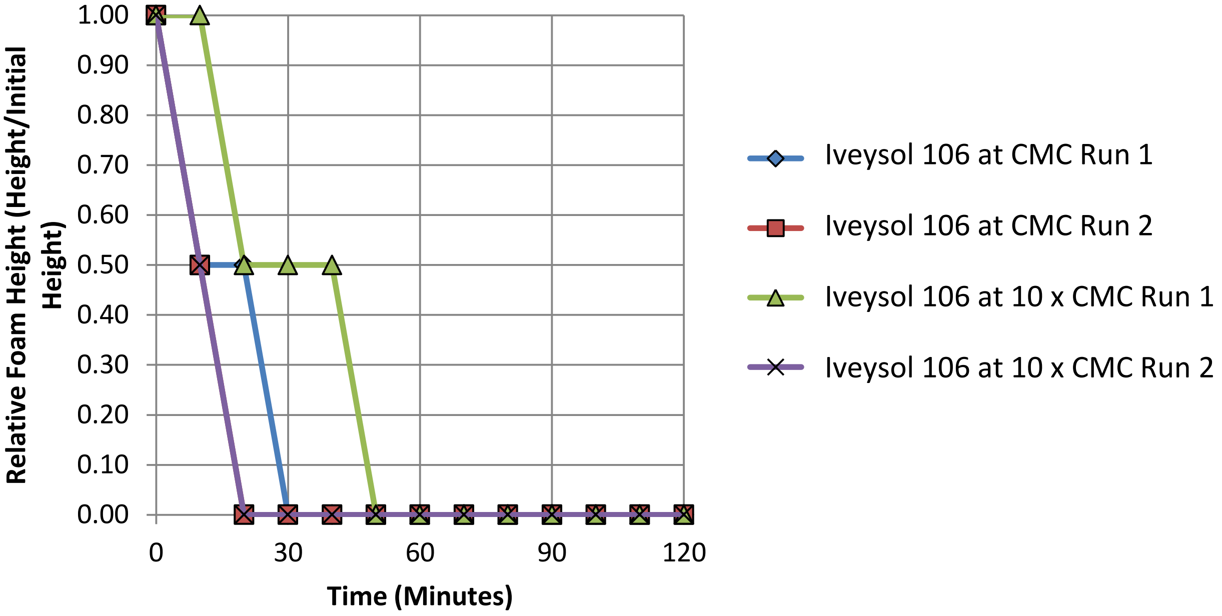

Figure C-8. Relative Foam Height for Experiments 7 and 8, With Oil, Both Runs

Appendix D: Viscometer Data

Each fluid was tested in the viscometer up to three times. The trend of decreasing viscosity with increasing surfactant concentration is shown by looking at the Triton X-100 data. Therefore in testing the Iveysol 106 data only one experiment was conducted in the mid-range surfactant concentration of 5.5 times CMC to verify that its viscosity fell between the viscosity for the high and low surfactant concentration viscosities.

The individual tests and the average and standard deviations are shown in Table D-1. Viscosity measurements were taken continuously, therefore the individual tests show the average viscosity reading for period at the end of the test when the readings were stable. The standard deviations between the tests are well within the ±0.018 cP accuracy. As well, with an accuracy only to the third decimal place (and really covering up to the second decimal place), it was decided to only display results to the second decimal place as any more precise results are not meaningful as the accuracy of the viscometer is large enough to cover any results to the third decimal place.

Table D-1. Viscometer Test Results

Fluid	Viscosity (cP)				
	Test 1	Test 2	Test 3	Average	Standard Deviation
Triton X-100 at CMC	1.0322	1.0345		1.0334 ± 0.0016	1.03
Triton X-100 at 5.5 x CMC	1.0360	1.0360	1.0411	1.0377 ± 0.0029	1.04
Triton X-100 at 10 x CMC	1.0478	1.0593	1.0595	1.0555± 0.0025	1.06
Iveysol 106 at CMC	1.0789	1.0694	1.0732	1.0738 ± 0.0048	1.07
Iveysol 106 at 5.5 x CMC	1.06			1.06	1.06
Iveysol 106 at 10 x CMC	1.0554	1.0506		1.053 ± 0.0034	1.05
Brine	1.0948			1.0948	1.09
Distilled Water	0.9733	0.9753		0.9743 ± 0.0014	0.97

Appendix E: Interfacial Tension Data

Each fluid was tested in the interfacial tension machine for up to three drops. The individual tests and the average and standard deviations are shown in Table D-1. The results are shown only to the second decimal. Interfacial tension measurements were taken continuously; therefore the individual test results show the average measurements for individual drops.

Table E-1. Interfacial Tension Test Results

Fluid	Interfacial Tension (mN/m)				
	Test 1	Test 2	Test 3	Average	Standard Deviation
Triton X-100 at CMC	3.024	3.041	3.112	3.0591 ± 0.0465	3.06 ± 0.05
Triton X-100 at 5.5 x CMC	2.3408	2.1900	2.2888	2.2732 ± 0.07658	2.27 ± 0.08
Triton X-100 at 10 x CMC	0.5390	0.5650	0.5575	0.5538± 0.0133	0.55 ± 0.01
Iveysol 106 at CMC	9.531	10.51		10.0191 ± 0.6909	10.02 ± 0.69
Iveysol 106 at 5.5 x CMC	7.0345	7.0112	7.215	7.0224 ± 0.0117	7.02 ± 0.01
Iveysol 106 at 10 x CMC	4.0209	4.0366		4.0288 ± 0.0110	4.03 ± 0.01
Brine	24.15			24.15	24.15 ± 0.00
Distilled Water	33.4192	32.6507		33.0300 ± 0.5364	33.03 ± 0.54

Appendix F: Oil Recovery Data for Core Set Experiments

This section includes the entire cumulative oil production image processing data for all of the 23 experiments in the core set of experiments. It is presented in six figures, with the experiments first divided by gas type (air data shown first followed by propane data), and then divided by WAG ratio (1:1 shown first, followed by 1:1.5 and 1:2). Some data points seem to show a decrease in oil recovery; however any decreases in oil recovery are small with an average decrease of 2/76%, with some outliers showing a large decrease, without these outliers the average of any decrease is 2%. This error is on the same order of magnitude as the calculated image processing error of ±1.5% of oil recovery as discussed in Section 4.3.1.2, which is a low estimate. These decreases are not meaningful and the data within the thesis has been adjusted to smooth out any decreases in oil recovery, however the full, unaltered data is shown in the following figures.

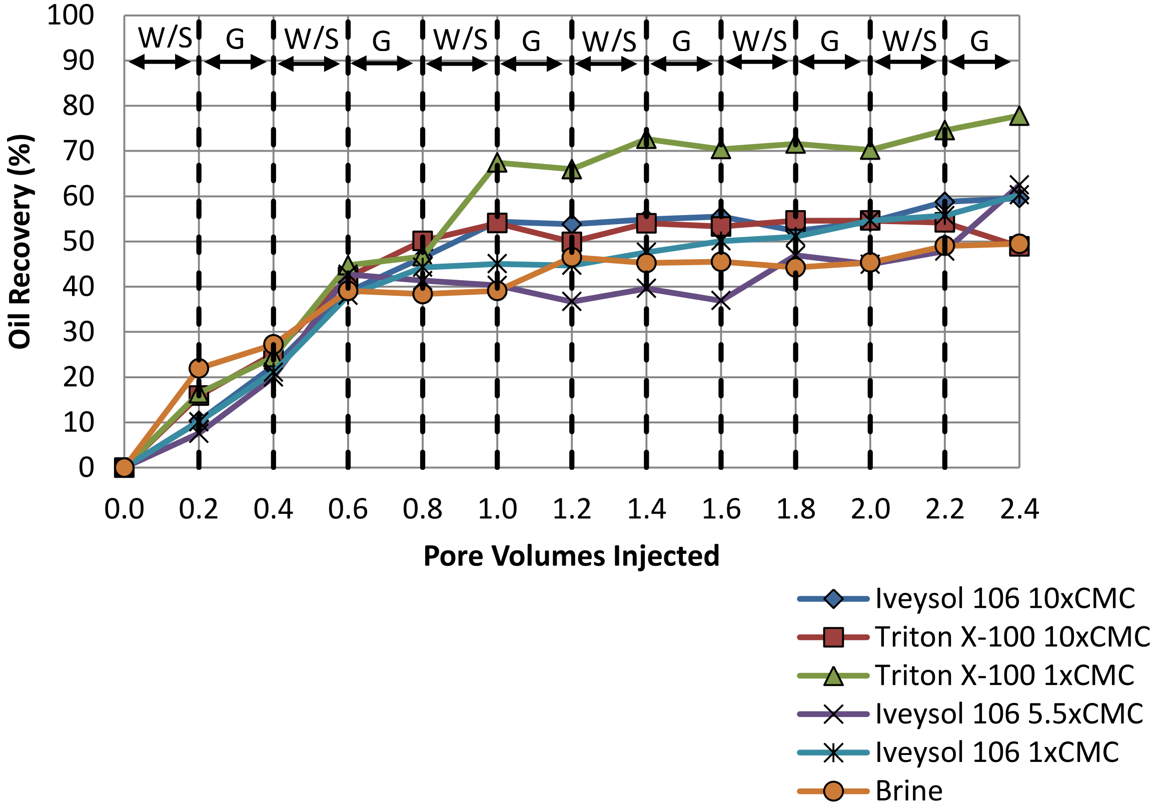

Figure D-1. Cumulative Oil Recovery vs. Pore Volumes Injected for all experiments with air at a WAG ratio of 1:1

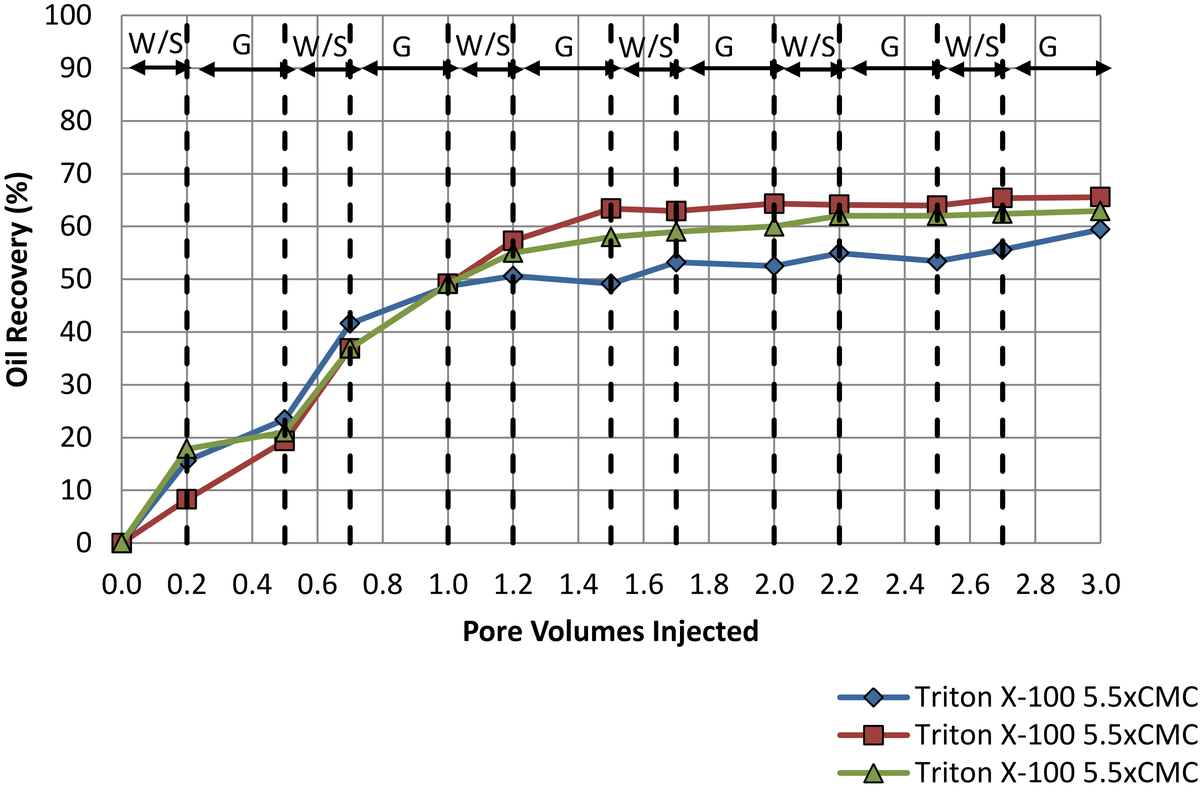

Figure D-2. Cumulative Oil Recovery vs. Pore Volumes Injected for all experiments with air at a WAG ratio of 1:1.5

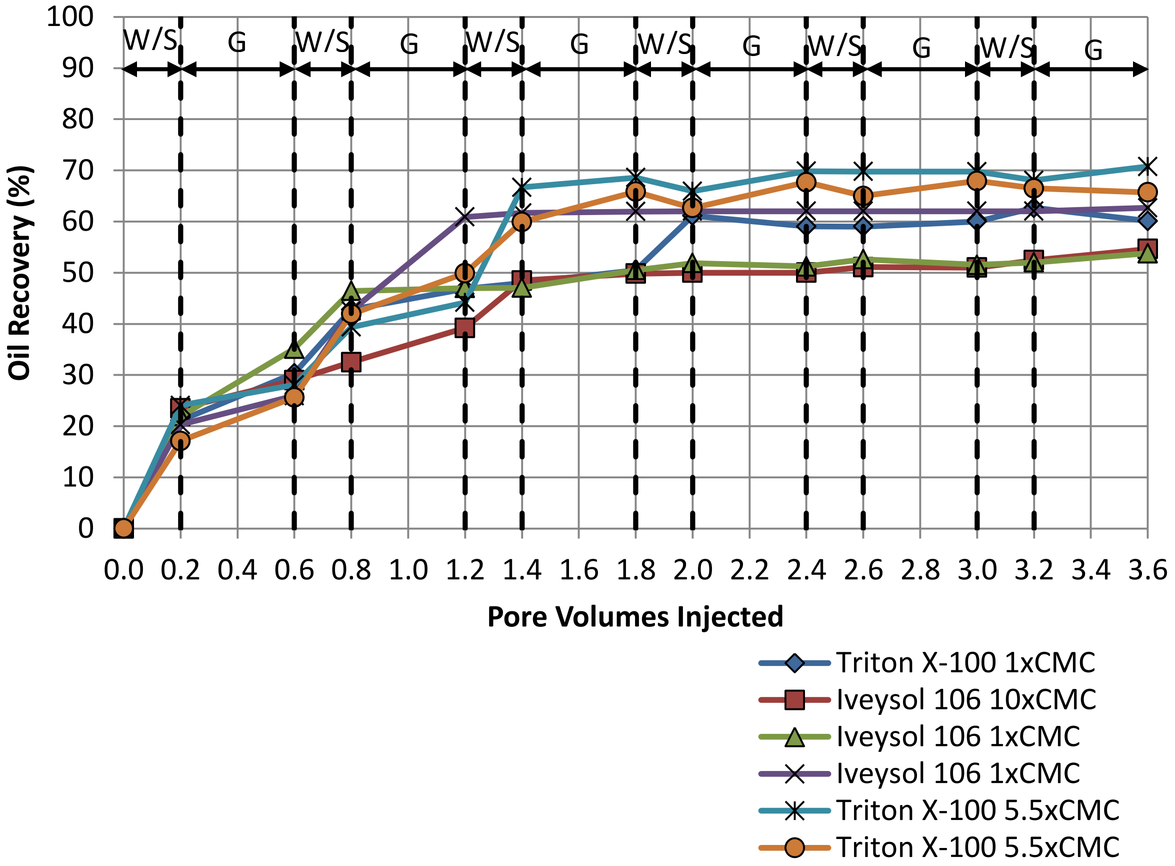

Figure D-3. Cumulative Oil Recovery vs. Pore Volumes Injected for all experiments with air at a WAG ratio of 1:2

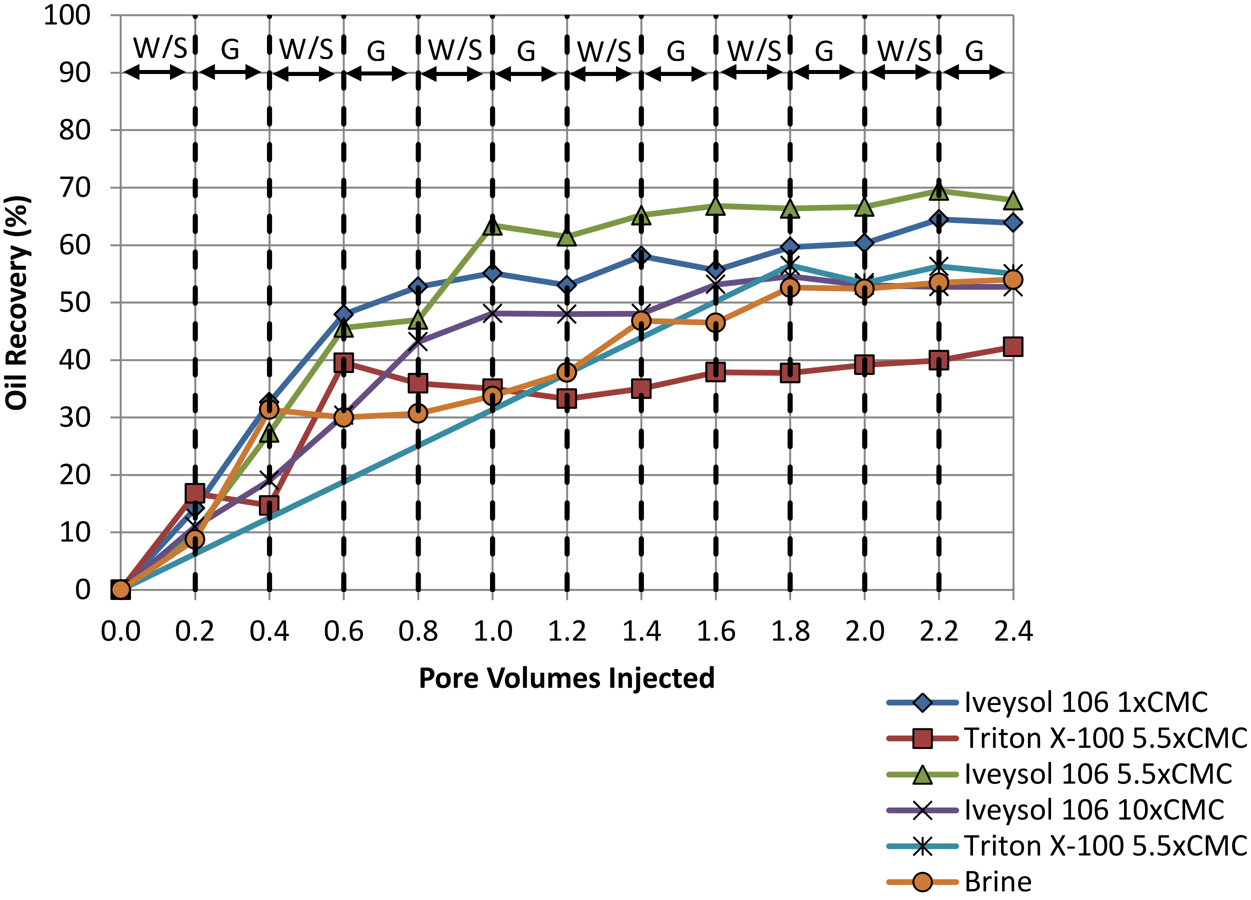

Figure D-4. Cumulative Oil Recovery vs. Pore Volumes Injected for all experiments with propane at a WAG ratio of 1:1

In Figure D-4, the Triton X-100 5.5 x CMC data is missing points for pore volumes 0.2 to 1.8 due to lighting issues.

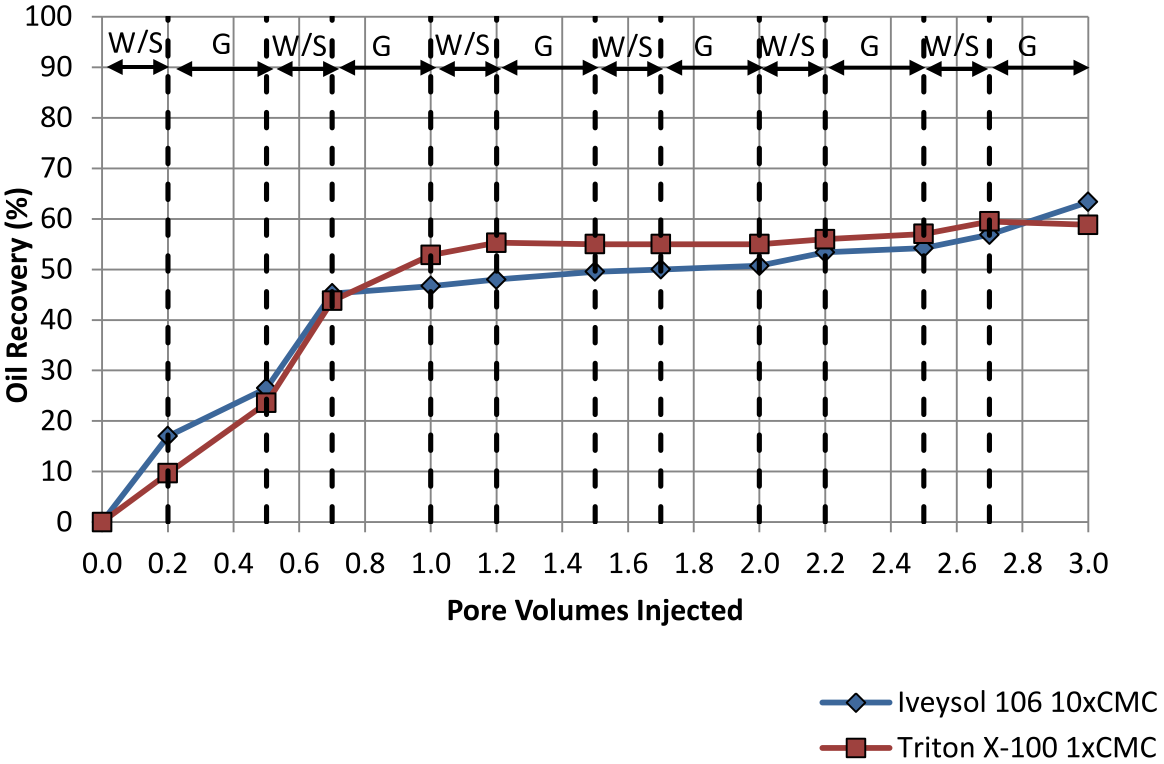

Figure D-5. Cumulative Oil Recovery vs. Pore Volumes Injected for all experiments with propane at a WAG ratio of 1:1.5

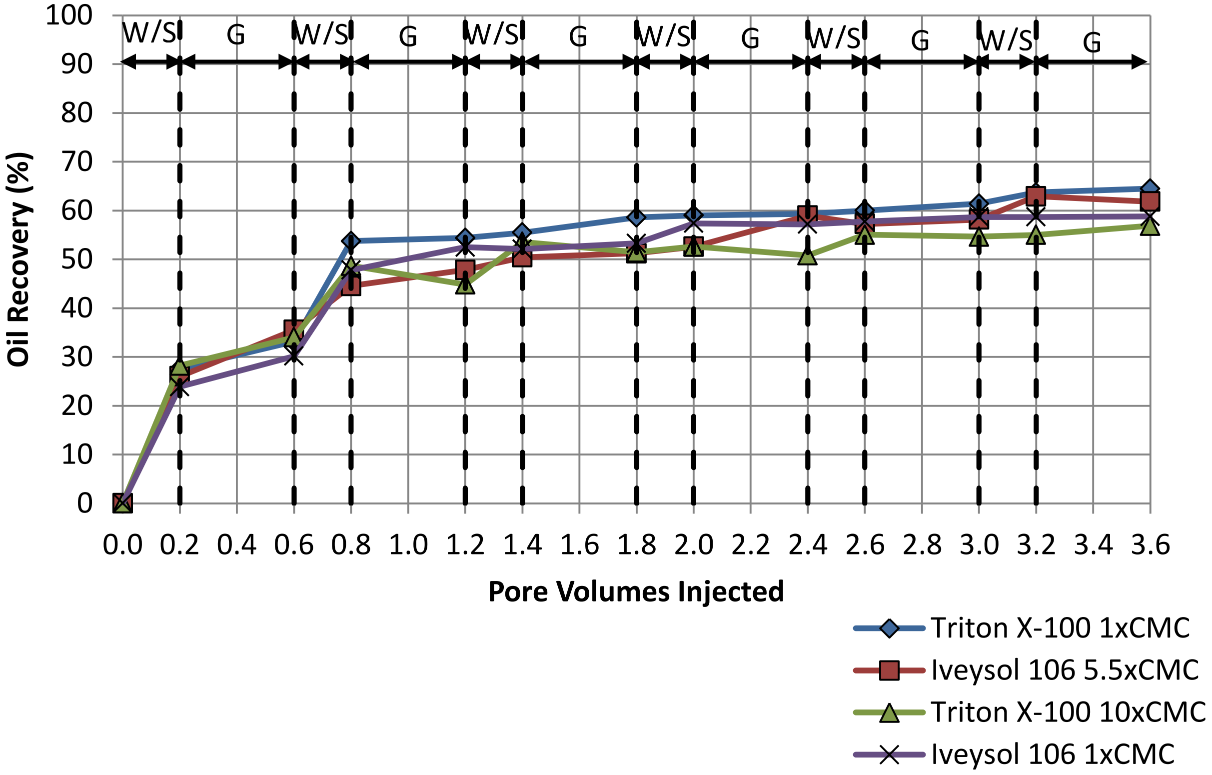

Figure D-6. Cumulative Oil Recovery vs. Pore Volumes Injected for all experiments with propane at a WAG ratio of 1:2

Appendix G: Overview of Experiment 23

This appendix will provide an overview of the first run of Experiment 23 (No waterflood, WAG ratio of 1:2 with air, Triton X-100 at CMC x 5.5). First, an image of the micromodel with an accompanying scale (in centimeters) is provided to define the dimensions of the micromdeol. After this the images taken at specific points are shown below.

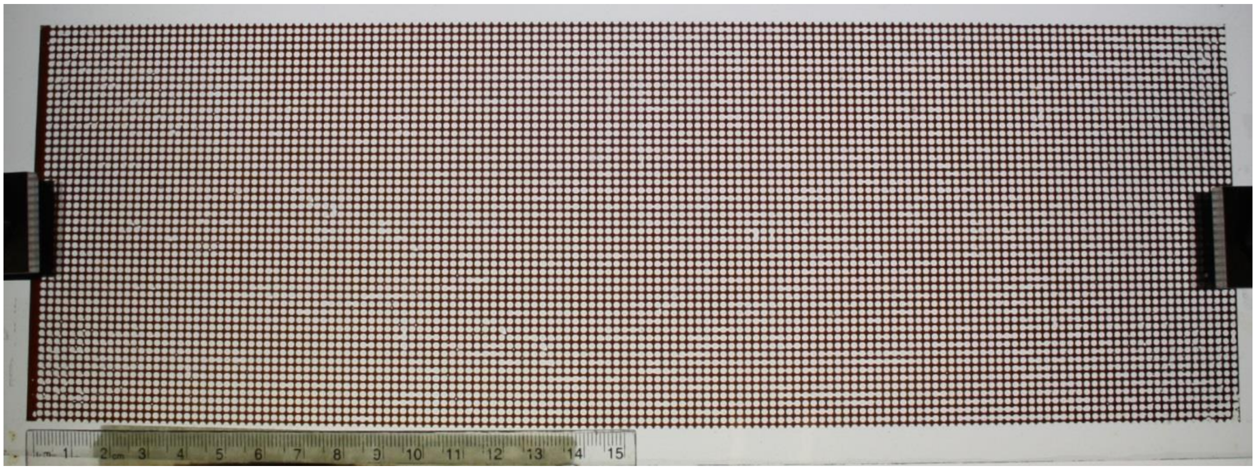

Figure E-1. Micromodel After First Liquid Slug, Just Before First Gas Slug

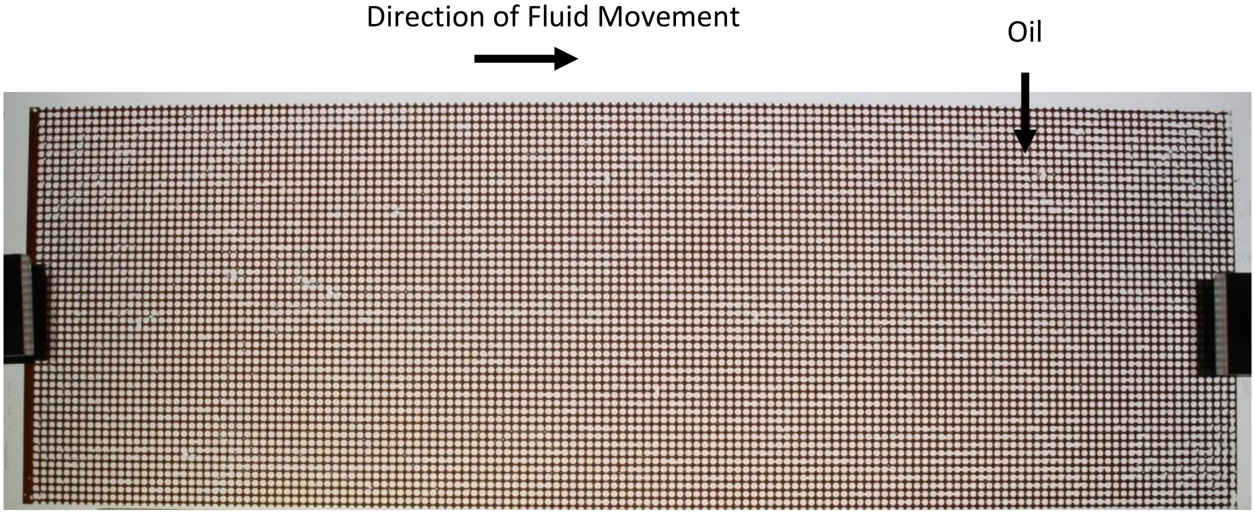

Figure E-2. Micromodel Fully Saturated with Oil

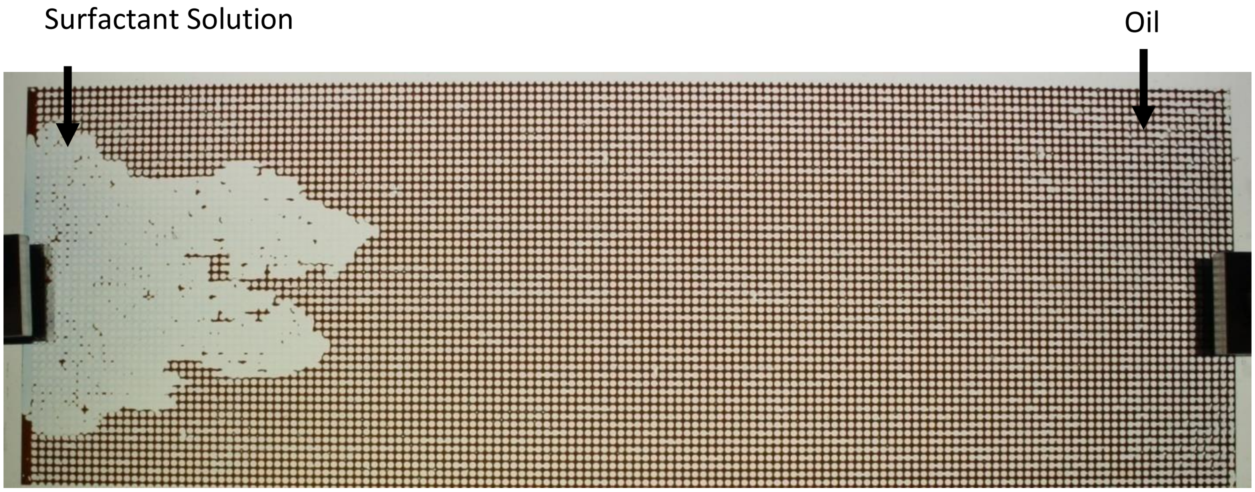

Figure E-3. Micromodel After First Liquid Slug, Just Before First Gas Slug

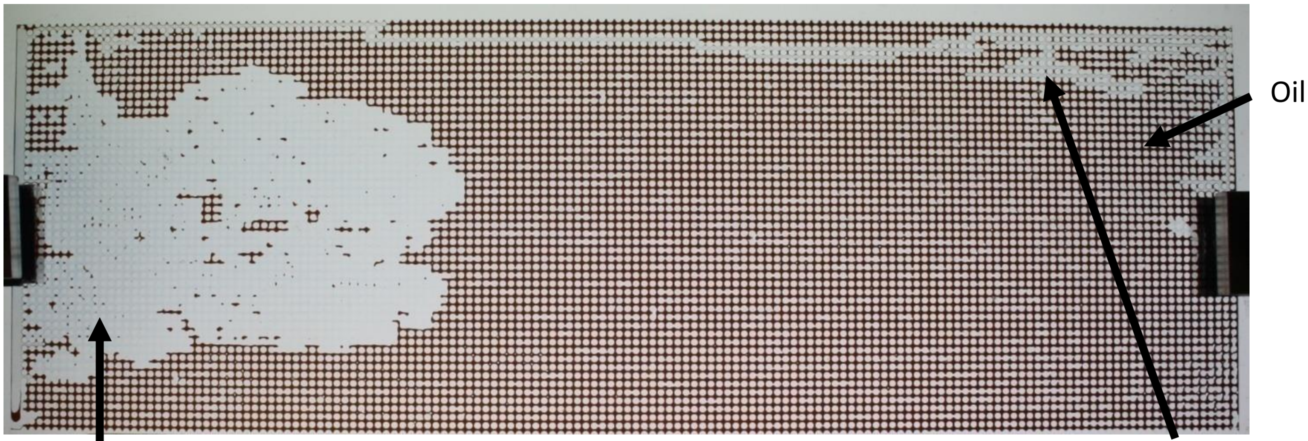

Figure E-4. Micromodel After First Gas Slug, Just Before Second Liquid Slug

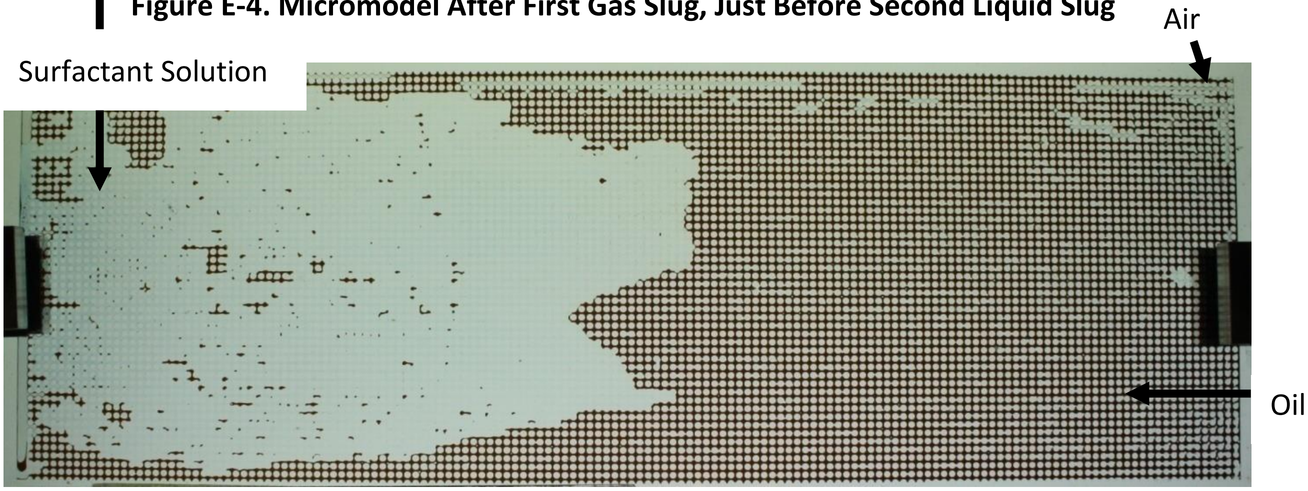

Figure E-5. Micromodel After Second Liquid Slug, Just Before Second Gas Slug

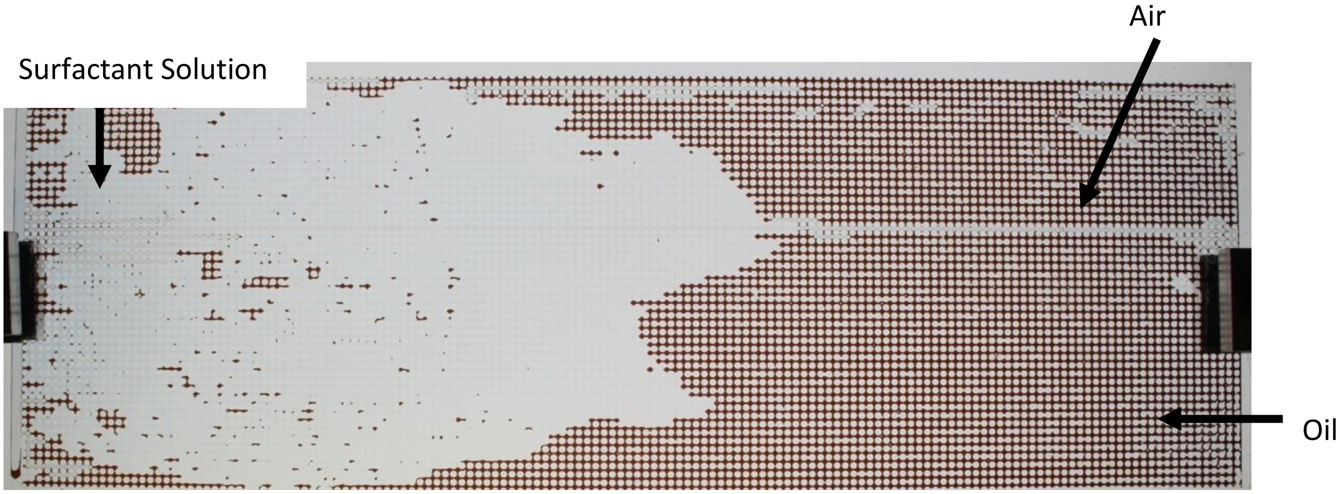

Figure E-6. Micromodel After Second Gas Slug, Just Before Third Liquid Slug

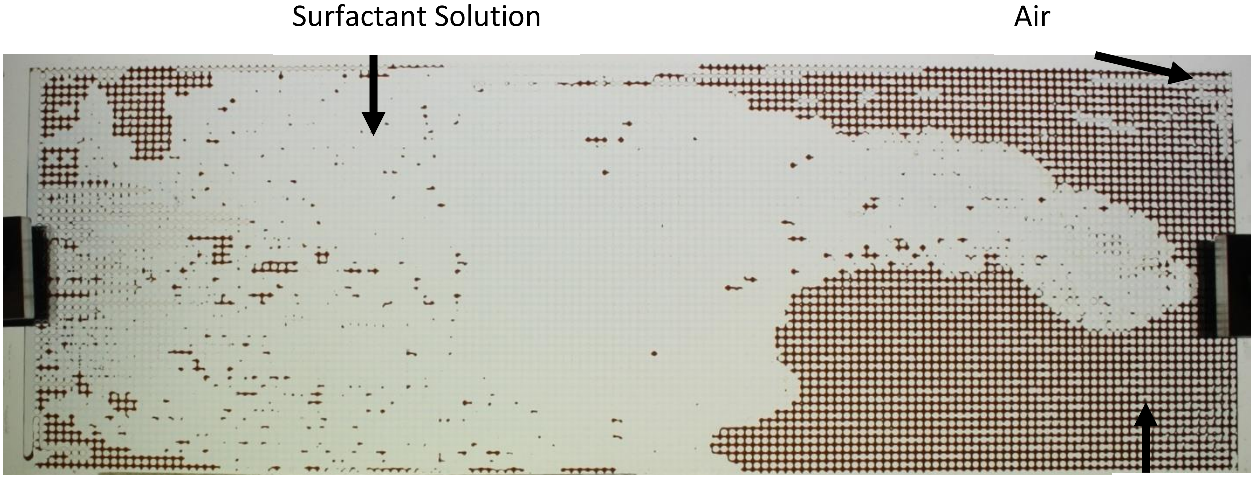

Figure E-7. Micromodel After Third Liquid Slug, Just Before Third Gas Slug

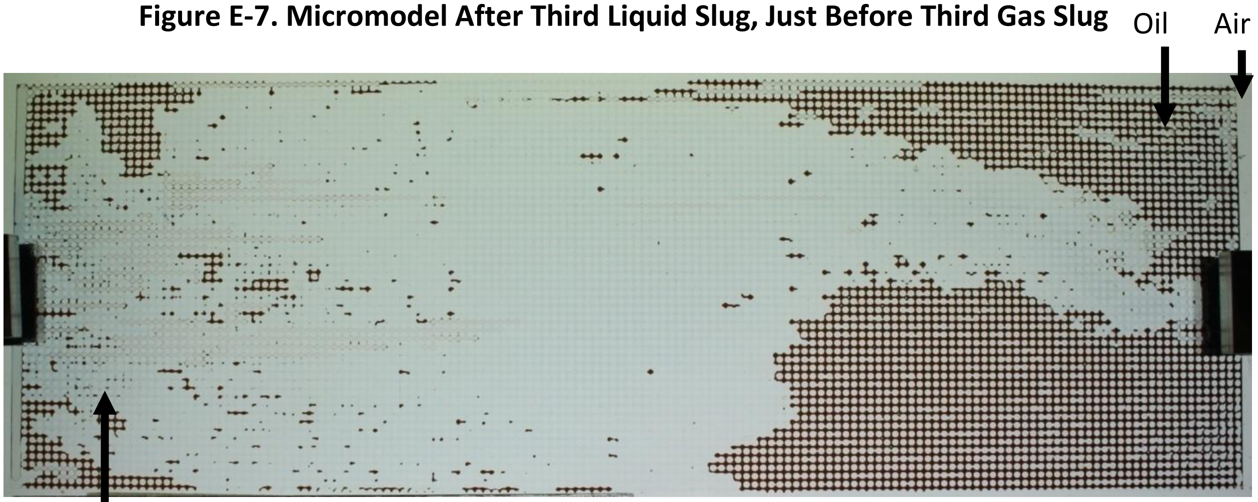

Figure E-8. Micromodel After Third Gas Slug, Just Before Fourth Liquid Slug

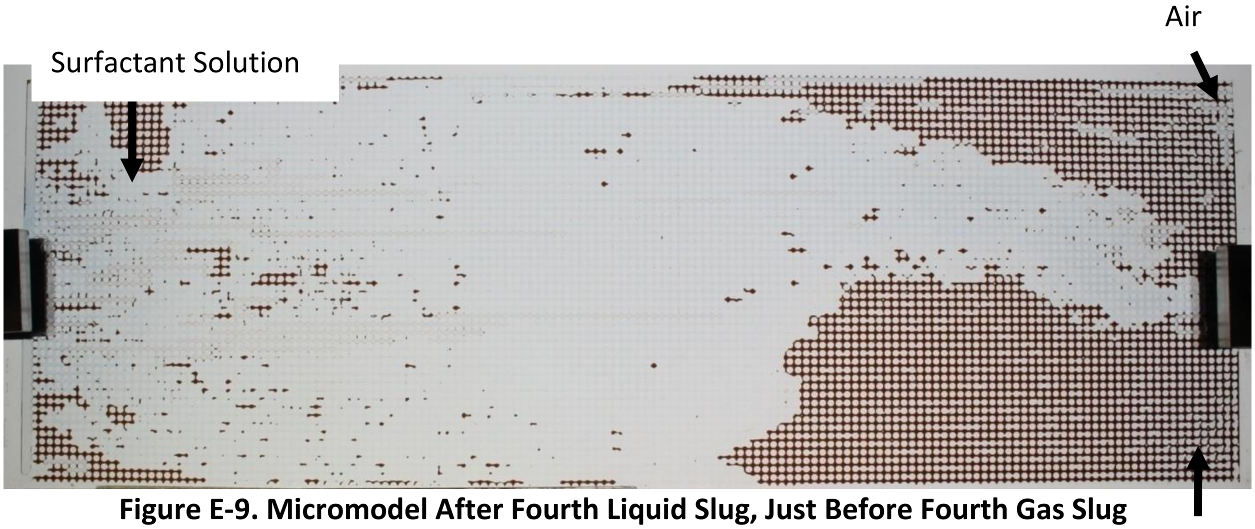

Figure E-9. Micromodel After Fourth Liquid Slug, Just Before Fourth Gas Slug

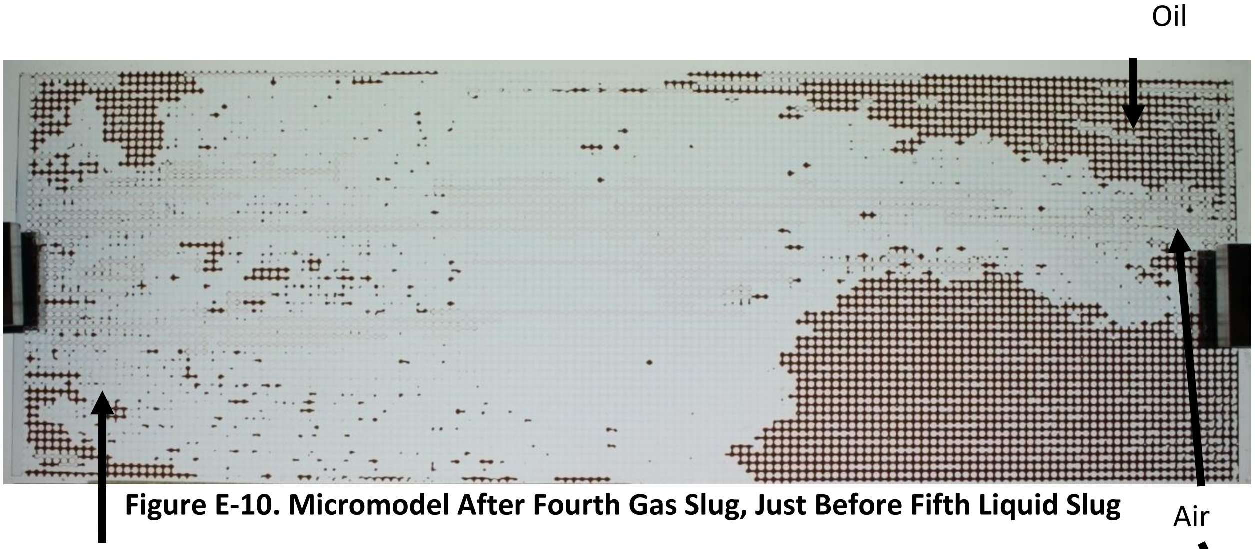

Figure E-10. Micromodel After Fourth Gas Slug, Just Before Fifth Liquid Slug

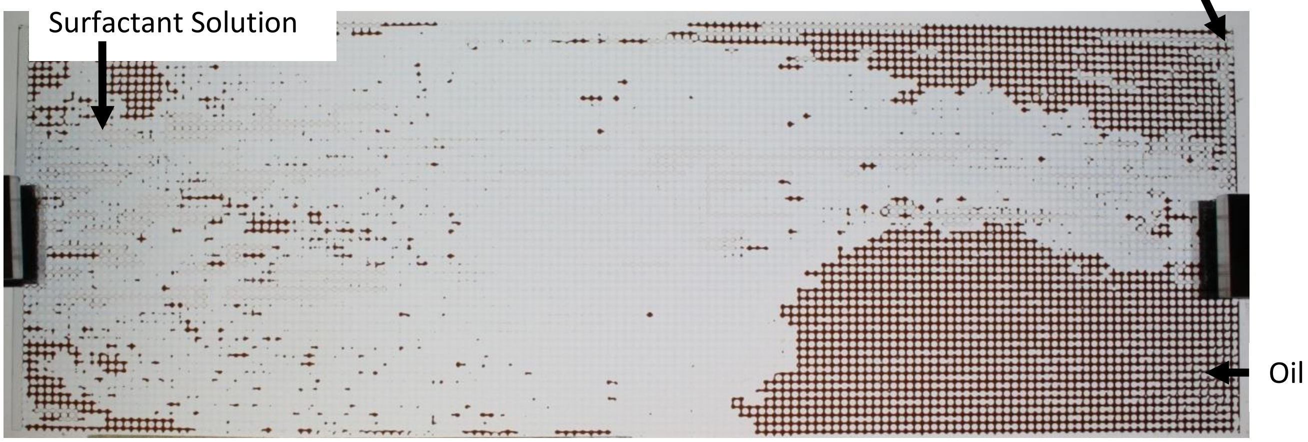

Figure E-11. Micromodel After Fifth Liquid Slug, Just Before Fifth Gas Slug

Figure E-12. Micromodel After Fifth Gas Slug, Just Before Sixth Liquid Slug

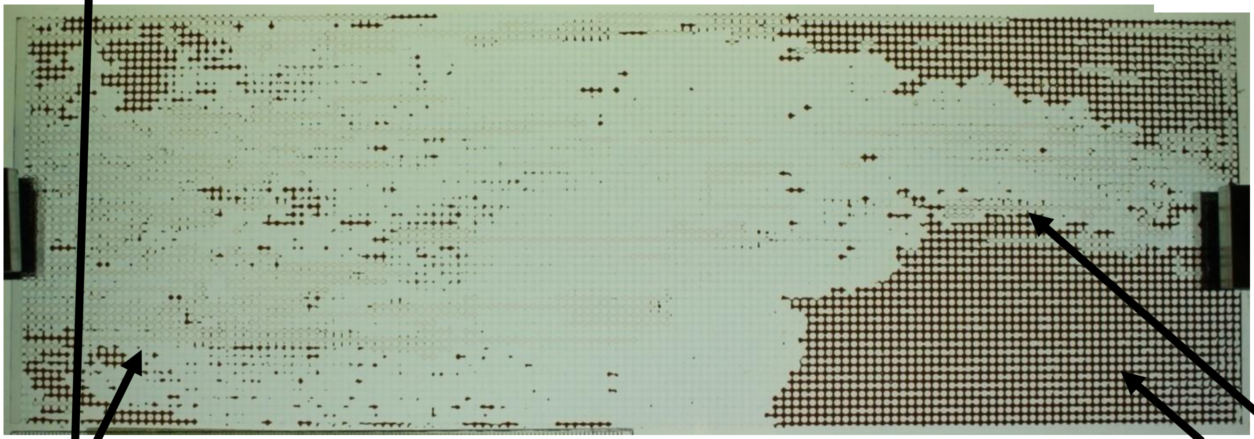

Figure E-13. Micromodel After Sixth Liquid Slug, Just Before Sixth Gas Slug

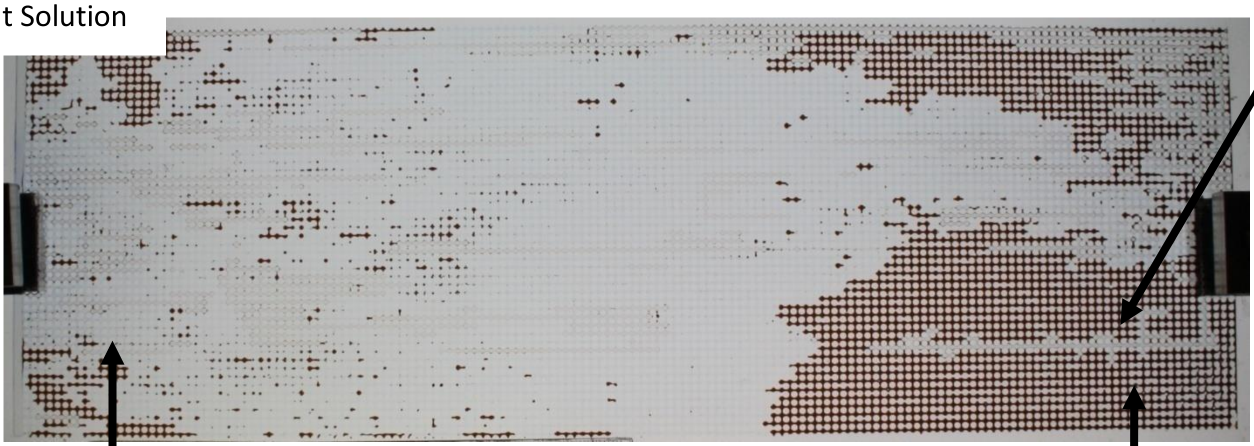

Figure E-14. Micromodel After Sixth Gas Slug, At End of Test

These pictures were then converted to black and white pictures, and the black pixels (representing oil) in each picture were counted. Three of the black and white pictures are shown here, corresponding to the beginning, middle, and end of the experiment. The oil recovery measured here is areal recovery, as will be discussed in Appendix H.

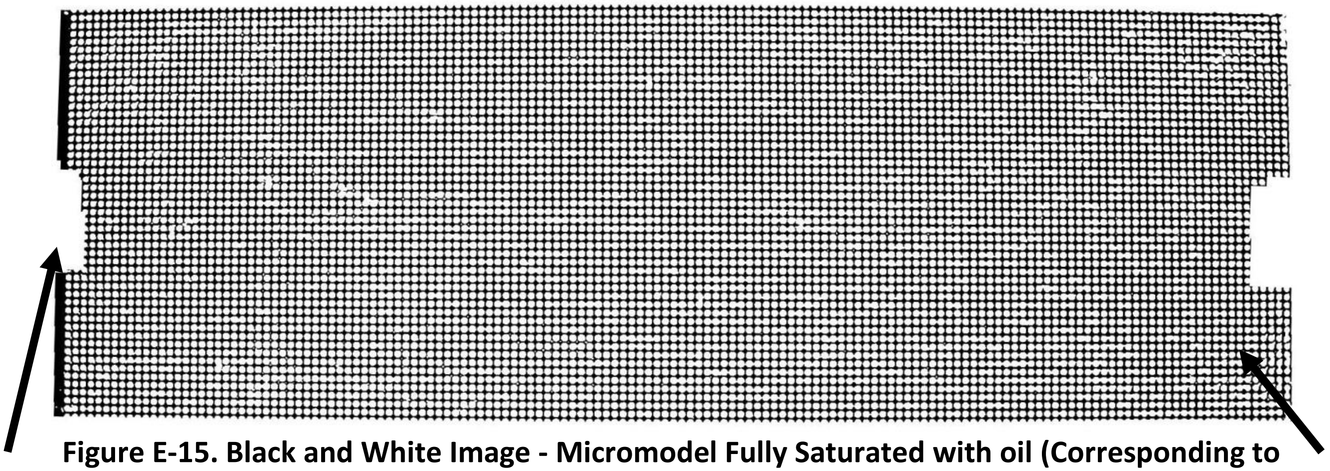

Figure E-15. Black and White Image - Micromodel Fully Saturated with oil (Corresponding to Figure E-1) (484530 Black Pixels)

Figure E-16. Black and White Image - Micromodel After Third Liquid Slug, Before Third Gas Slug (Corresponding to Figure E-6) (161470 Black Pixels)

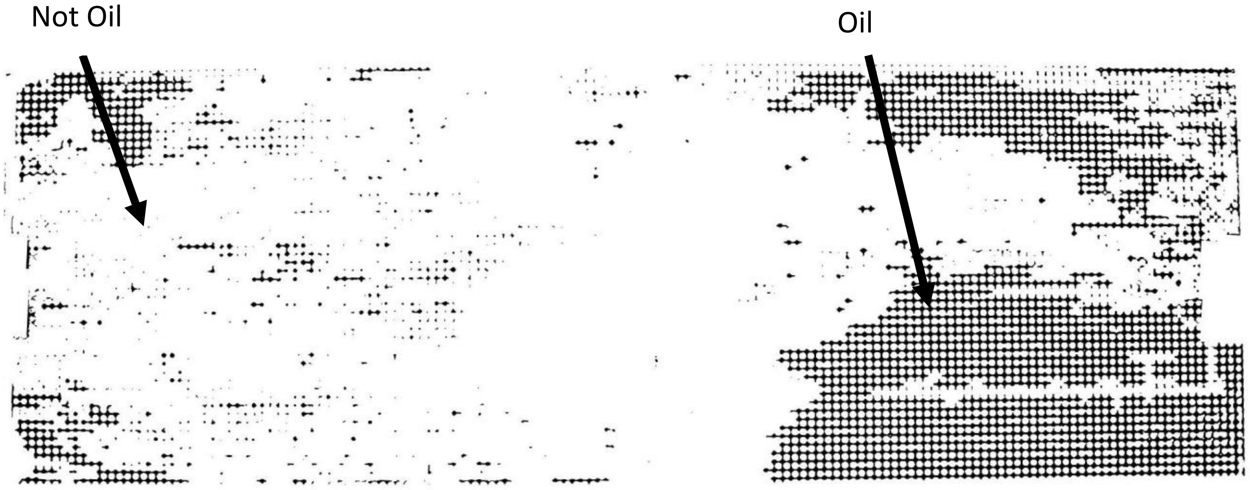

Figure E-17. Black and White Image - Micromodel At End of Experiment (Corresponding to Figure E-13) (141788 Black Pixels)

Using these black pixel counts from the beginning of the experiment and various points throughout the experiment, the oil recovery can be calculated as follows.

$$R = \frac{(Original\ Black\ Pixel\ Count) - (Current\ Black\ Pixel\ Count)}{(Original\ Black\ Pixel\ Count)} * 100\% \qquad .$$

For the beginning of the experiment:

$$R = \frac{(484530) - (484530)}{(484530)} * 100\% \qquad ,$$

$$R = 0\% \qquad .$$

For the middle of the experiment:

$$R = \frac{(484530) - (161470)}{(484530)} * 100\% \qquad ,$$

$$R = 66.67\% \qquad .$$

For the end of the experiment:

$$R = \frac{(484530) - (141788)}{(484530)} * 100\% \qquad ,$$

$$R = 70.34\% \qquad .$$

As shown from the calculations above, the oil recovery does not change significantly during the last half of the experiment. The large increases in oil recovery occur during the first few slugs

Appendix H: Image Processing Error Analysis Calculation

The image processing error analysis was calculated using Experiment 23, which was also analyzed in Appendix G. This method of finding oil recovery will calculate the areal recovery of the experiment. This is due to the oil saturation being measured from looking directly down onto the top of the micromodel. This assumes that the pore bodies and pore throats have a perfectly vertical slope, which is not the case. The difference between the assumed and real situation is shown in Figure H-1.

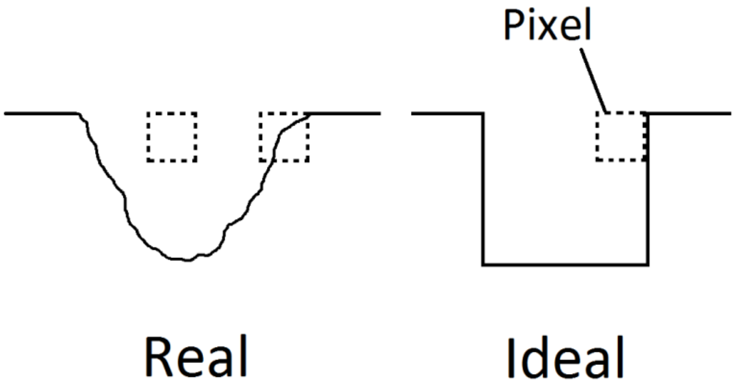

Figure H-1. Micromodel Pore Dimensions, Real and Ideal

Figure H-1 shows the difference between the ideal case and reality. In reality, the micromodel was etched in a chemical process which makes the walls of the pores have a slope. The image processing method assumes the ideal case; therefore a pixel taken in the middle of the pore would represent more oil than a picture taken at the side of the pore due to the difference depth. This adds another layer of error into image processing analysis, however for this thesis the ideal case was assumed for simplicity.

The images were converted into black and white images using a 50% threshold, meaning if the pixel was at least 50% black, it was turned into a black pixel. Based on this, and the convention of using half of the smallest measurement for error analysis (Taylor 1982), the error was calculated based on half a pixel for each interface pixel in the image.

First the total black pixels of the image were determined for four images taken at different times during the experiment, at the beginning, after the 1st liquid and gas slugs had passed through the micromodel, after the 3rd liquid slug had passed through the micromodel, and at the end of the experiment. These values are given in the summary table at the end of this section.

The first interface analyzed was the oil-grain interface error. The micromodel consisted of 6600 grains (44 grains wide, 150 grains long), with each grain being 11 pixels by 11 pixels. This gave a total grain-oil interface of 44 grains, 22 grains of error based on the one-half pixel of error for every pixel of interface assumption. At the beginning of the experiment the micromodel was fully saturated with oil, so all 6600 grains had an interface of 44 pixels with the oil phase. As the oil was displaced the number of grains that the oil had an interface with decreased, this was accounted for by prorating the number of grains based on the remaining oil. If only 60% of the oil remained, it was assumed that the oil had an interface with 3960 grains (60% of 6600 grains). Using this above method, Table H-1 can be populated.

Table H-1. Image Processing Error Calculation – Grain Interfaces

Period of Experiment	Total Black Pixels	Number of Grain Interfaces	Grain Interface (pixels)	Grain Interface Error (pixels)
Beginning	484530	6600	290400	145200
After First Liquid and Gas Slugs	348592	4748	208926	104463
After Third Liquid Slug	161470	2199	96776	48388
End	141788	1931	84980	42490

The next interface analyzed was the injection fluid interface, the interface between the oil and either the injection liquid or injection gas. This was found by tracing the length of the oil-injection fluid interface to determine the length of the interface in pixels. Figures H-2 to H-4 show the micromodel at different times during Experiment 3, the thin line shows the trace of the injection fluids interface used to determine the error.

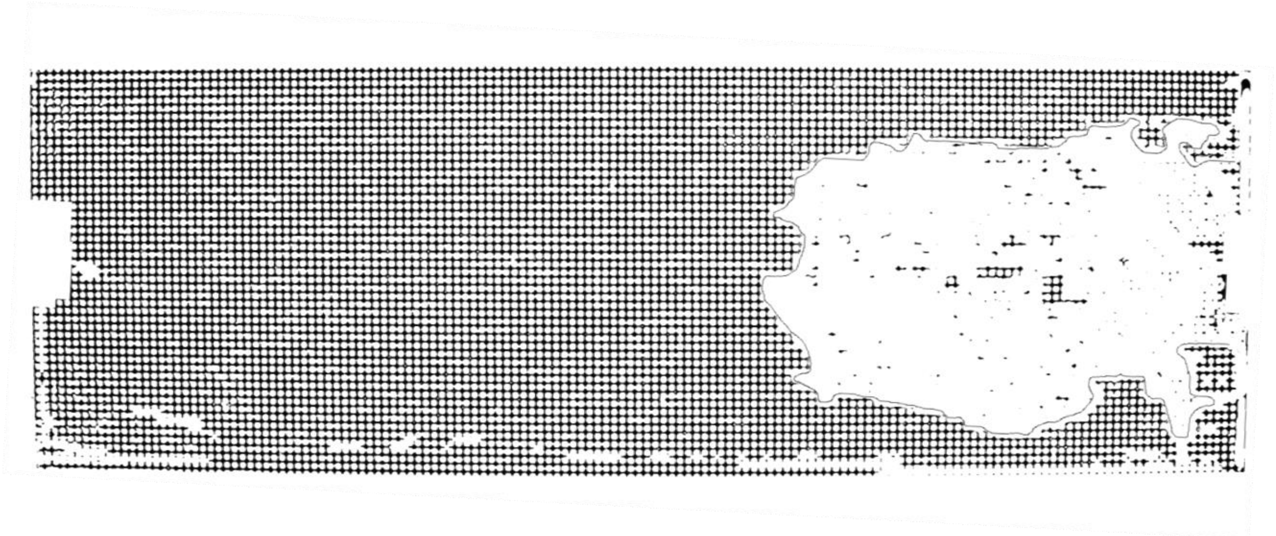

Figure H-2. Black and White Image of Experiment 23 after first Liquid and Gas Slugs showing Interface

Figure H-3. Black and White Image of Experiment 23 after third Liquid Slug showing Interface

Figure H-4. Black and White Image of Experiment 23 at End of Test showing Interface

The final interface analyzed was the interface between the oil and the sides of the micromodel. The length of the micromodel sides was measured in pixels and was assumed to be constant throughout the experiment. This assumption is conservative as the oil at the micromodel sides may be displaced by injection fluid, however the side interface error is relatively low (accounting for a maximum of 6% of the total error), therefore this assumption does not significantly change the error calculation. Using the above errors, Table H-2 can be populated.

Table H-2. Image Processing Error Calculation – Injection Fluid and Side Interfaces

Period of Experiment	Injection Fluid Interface Length (pixels)	Injection Fluid Interface Error (pixels)	Side Interface Length (pixels)	Side Interface Error (pixels)
Beginning	0	0	5536	2768
After First Liquid and Gas Slugs	2701	1351	5536	2768
After Third Liquid Slug	3457	1729	5536	2768
End	5021	2511	5536	2768

Using the pixel error in Tables H-1 and H-2, the total number of error pixels can be determined. This value is then divided by the total number of black pixels in the image to determine the error inherent in the image processing analysis method for each image. Table H-3 provides the error for each point throughout the experiment.

Table H-3. Image Processing Error Calculation

Period of Experiment	Total Black Pixels	Grain Interface Error (pixels)	Injection Fluid Interface Error (pixels)	Side Interface Error (pixels)	Total Pixels of Error	Error
Beginning	484530	145200	0	2768	147968	30.5%
After First Liquid and Gas Slugs	348592	104463	1351	2768	108582	31.1%
After Third Liquid Slug	161470	48388	1729	2768	52885	32.8%
End	141788	42490	2511	2768	47748	33.7%

The image processing error remains consistent between 30% and 34% throughout the experiment, with an average of 32%.